THE UNIVERSITY
of EDINBURGH

Cerebral blood flow and intracranial pulsatility in cerebral small vessel disease

Yulu Shi

Doctor of Philosophy

Deanery of Clinical Sciences

University of Edinburgh

2017

Declaration

1. The data presented in Chapter 5 in this thesis were obtained in a study carried out by the small vessel disease study group in the Brain Research Imaging Centre. I played a major role in the execution of the study, and the data analysis and interpretation are entirely by own work. Any contributions from colleagues in the collaboration, such as diagrams, patient recruitment, and image processing, are explicitly referenced in the text.

2. I declare that the thesis has been composed by myself and that the work has not be submitted for any other degree or professional qualification. I confirm that the work submitted is my own, except where work which has formed part of jointly-authored publications has been included. Wherever "I" was used in the thesis indicated work that was done by myself and "we" indicated work that was collaborated with other contributors. My contribution and those of the other authors to this work have been explicitly indicated below and in relevant chapters. I confirm that appropriate credit has been given within this thesis where reference has been made to the work of others.

Parts of Chapter 1 and Chapter 7 were previously published in *Stroke and Vascular Neurology* as *Update on Cerebral Small Vessel Disease: a dynamic and whole-brain disease* by myself and my supervisor Prof Joanna M Wardlaw. This review was based on a lecture given by Prof Wardlaw at the Chinese Stroke Association Inaugural Conference in 2015, Beijing. I drafted the review which was then approved by Prof Wardlaw.

The work presented in Chapter 2A was previously published in *Journal of Cerebral blood flow and Metabolism* as *Cerebral blood flow in small vessel disease: A systematic review and meta-analysis* by Yulu Shi (myself), Dr Michael J Thrippleton (my supervisor), Dr Steven D Makin, Prof Ian Marshall (my supervisor), Dr Mirjam I. Geerlings, Dr Anton JM de Craen, Prof Mark van Buchem, and Prof Joanna M Wardlaw (my supervisor). This study was originally conceived by Prof Joanna M Wardlaw, Dr Steven D Makin and I refined the study protocol. I carried out the study design, data collection and analysis, and drafted the manuscript.

The work presented in Chapter 2B was published in *Clinical Science* as *Intracranial pulsatility in patients with cerebral small vessel disease: a systematic review* by Yulu Shi (myself), Dr Michael Thrippleton (my supervisor), Prof Ian Marshall (my supervisor), and Prof Joanna Wardlaw (my supervisor) after I submitted this thesis. This study was conceived and designed by myself. I carried out the literature search, data collection and analysis, and drafted the manuscript. My supervisors helped me revise the searching strategy and the draft, and discussed the results throughout my data analysis and writing.

Signature

Date

Acknowledgements

First, I would like to express my sincere gratitude to my supervisors Prof Joanna Wardlaw, Prof Ian Marshall and Dr Michael Thrippleton for the continuous support and guidance of my PhD, for their patience and immense knowledge. In particular, I would like to thank Prof Joanna Wardlaw for inspiring me to want to become a clinical scientist like her with her genuine enthusiasm and dedication.

I would like to thank the China Scholarship Council for funding my PhD, and the Chief Scientist Office of Scotland (grant ETM/326), the Wellcome Trust-University of Edinburgh Institutional Strategic Support Fund, the Fondation Leducq Network for the Study of Perivascular Spaces in Small Vessel Disease (ref no. 16 CVD 05), and the European Union Horizon 2020, PHC-03-15, project No 666881, 'SVDs@Target' for funding the studies that I have undertaken in this thesis.

I am grateful to the small vessel disease research team including Dr Gordon Blair, Dr Fergus Doubal, Dr Michael Thrippleton, Iona Hamilton, and all the BRIC radiographers, without whose wonderful teamwork I could not have been able to finish the studies and my PhD. It was fantastic to be surrounded by and work with such a group of people.

I thank Dr David Alexander Dickie for helping me with the image processing and Dr Francesca Chappell for the statistical analyses. The administration team, Moira Henderson, Kirsten Schuler, and Britany Bovenzi are also thanked for their great help. I thank Dominic Job and Aidan Hutchison for solving all my IT problems.

Away from work, a special gratitude to my PhD "self-support" group mates Yvonne Chun, Gordon Blair, Daisy Mollison, Ellen Backhouse and Marion Boulanger, and

my dear friends Peng Xue, Zhujun Zhang, Yu Zhang and Tian Li, for listening to my moaning and sharing their happiness and niceties of their lives; to all my friends scattered around the world, for their thoughts, wishes, phone calls, texts, visits, and being there whenever I needed a friend. Without them, I would not have had such a happy PhDhood.

Last but not the least, I want to express my appreciation to my dearest parents, my grandfather, my brother and sister and my little nephew who just came to the world, for their good health, love, understanding and never failing faith in me.

Abstract

Cerebral small vessel disease (SVD) is associated with increased risks of stroke and dementia, however the mechanisms remain unclear. Low cerebral blood flow (CBF) has long been suggested and accepted, but clinical evidence is conflicting. On the other hand, growing evidence suggests that increased intracranial pulsatility due to vascular stiffening might be an alternative mechanism. Pulse-gated phase-contrast MRI is an imaging technique that allows measuring of CBF contemporaneously with pulsatility in multiple vessels and cerebrospinal fluid (CSF) spaces. The overall aim of this thesis was to provide an overview of existing clinical evidence on both hypotheses, to test the reproducibility of CBF and pulsatility measures in phase-contrast MRI, and to explore the relationship between CBF and intracranial pulsatility and SVD features in a group of patients with minor stroke and SVD changes on brain imaging.

I first systematically reviewed and meta-analysed clinical studies that have assessed CBF or intracranial pulsatility in SVD patients. There were 38 studies (n=4006) on CBF and 27 (n=3356) on intracranial pulsatility. Most were cross-sectional, and longitudinal studies were scarce. There were large heterogeneities in patient characteristics and indices used particularly for measuring and calculating pulsatility. Methods to reduce bias such as blinding and the expertise of structural image readers were generally poorly reported, and many studies did not account for the impact of confounding factors (e.g. age, vascular risk factors and disease severity) on CBF or pulsatility. Evidence for falling CBF predating SVD was not supported by longitudinal studies; high pulsatility in one large artery such as internal carotid

arteries (ICA) or middle cerebral arteries might be related to SVD, but studies that measured arteries, veins and CSF in the same patients were very limited and the reliability of some pulsatility measures, especially in CSF, needs to be tested.

In order to test the reproducibility of the CBF and intracranial pulsatility measures, I repeated 2D phase-contrast MRI scans of vessels and CSF on healthy volunteers during two visits. I also compared the ICA pulsatility index derived from the MRI flow waveform to that from the Doppler ultrasound velocity waveform in patients with minor stroke and SVD features. In 10 heathy volunteers (age 35.2±9.78 years), the reproducibility of CBF and vascular pulsatility indices was good, with within-subject coefficients of variability (CV) less than 10%; whereas CSF flow and pulsatility measures were generally less reproducible (CV>20%). In 56 patients (age 67.8±8.27 years), the ICA pulsatility indices in Doppler ultrasound and MRI were acceptably well-correlated ($r=0.5$, $p<0.001$) considering the differences in the two techniques.

We carried out a cross-sectional study aiming to recruit 60 patients with minor stroke and SVD features. We measured CBF and intracranial pulsatility using phase-contrast MRI, as well as aortic augmentation index (AIx) using a SphygmoCor device. I first investigated the relationship between intracranial measures, and systemic blood pressure or aortic AIx, and then focused on how the intracranial haemodynamic measures related to two main SVD features (white matter hyperintensities (WMH) and perivascular spaces (PVS)). We obtained usable data from 56/60 patients (age 67.8±8.27 years), reflecting a range of SVD burdens. After the adjustment for age, gender, and history of hypertension, higher pulsatility in the venous sinuses was associated with lower diastolic blood pressure and lower mean

arterial pressure (e.g. diastolic blood pressure on straight sinus pulsatility index (PI): β=-0.005, P=0.029), but not with aortic AIx. Higher aortic AIx was associated with low ICA PI (β=-0.011, P=0.040). Increased pulsatility in the venous sinuses, not low CBF, was associated with greater WMH volume (e.g. superior sagittal sinus PI: β=1.29, P=0.005) and more basal ganglia PVS (e.g. odds ratio=1.379 per 0.1 increase in superior sagittal sinus PI) after the adjustment for age, gender and blood pressure.

The thesis is the first to summarise the literature on CBF and intracranial pulsatility in SVD patients, addressed the major limitations of current clinical studies of SVD, and also assessed CBF and intracranial pulsatility contemporaneously in well-characterised patients with SVD features. The overall results of the thesis challenge the traditional hypothesis of the cause and effect between low CBF and SVD, and suggest that increased cerebrovascular pulsatility, which might be due to intrinsic cerebral small vessel pathologies rather than just aortic stiffness, is important for SVD. More importantly, this pilot study also provides a reliable methodology for measuring intracranial pulsatility using phase-contrast MRI for future longitudinal or larger multicentre studies, and shows that intracranial pulsatility could be used as a secondary outcome in clinical trials of SVD. However, future research is required to elucidate the implication of venous pulsatility and to fully explore the passage of pulse wave transmission in the brain. Overall, this thesis advances knowledge and suggest potential targets for future SVD studies in terms of mechanisms, prevention and treatment.

Lay summary

Stroke and dementia are amongst the largest threats to our ageing society. A disease that affects small vessels in the brain is responsible for nearly half of dementia and 1/5 of all strokes. As current technology is still not developed enough to directly visualise these vessels, the small vessel disease (SVD) is mainly diagnosed from lesions visible with brain imaging. There have been various theories on how these SVD lesions happen: the diseased small vessels might reduce the amount of blood entering the brain, or become stiffer which might be harmful for both vessels and brain tissues.

In this thesis, I first reviewed all papers that measured brain blood flow or brain vascular health in patients who had SVD. I found that these studies were mostly not powerful enough to support their theories. They were generally rather small, or overlooked the fact that patients' SVD might be largely due to age. They also measured the brain vessel health, or SVD differently, which makes a combined analysis very difficult.

Then we carried out a new study, with the aim of setting up a standardised method for measuring blood flow and vascular function using a brain scanner. We tested these methods on healthy volunteers and made sure these measures are reliable.

We then recruited 60 patients who had mini stroke and SVD changes in their brains. We measured the blood flow and brain vascular function using the tested methods, and also assessed their SVD burden. Eventually we obtained complete data on 56 patients (40 male; age 67.95±8.69 years). We found that patients who had a worse brain vascular function had more severe SVD. This relationship still existed after we

considered the impact of age, gender and blood pressure. How this brain vascular dysfunction happened was still unknown, but was related to lower blood pressure in our study. However, we did not find low total blood flow being associated with SVD.

Our results suggest that vascular dysfunction that is related to stiffer vessel walls might be able to explain how SVD develops. Our current and next step is to measure brain blood flow and the vascular function in SVD patients in the long term and in more patients, and to examine whether any drugs could improve brain vascular function and be used to treat and prevent SVD.

Table of Contents

List of Abbreviations

ACEI: angiotensin converting enzyme inhibitor

AD: Alzheimer's disease

AIx: augmentation index

ANOVA: analysis of variance

ARB: angiotensin receptor blocker

ASL: arterial spin labelling

BBB: blood brain barrier

BP: blood pressure

BTD: brain tissue displacement

CAA: cerebral amyloid angiopathy

cAMP: cyclic adenosine monophosphate

CBF: cerebral blood flow

CBFv: cerebral blood flow velocity

cGMP: cyclic guanosine monophosphate

CMB: cerebral microbleeds

CSF: cerebrospinal fluid

CT: computed tomography

CV: coefficients of variability

CVR: cerebral vascular reactivity

DWI: diffusion-weighted imaging

DTI: diffusion tensor imaging

DWMH: deep white matter hyperintensities

ECG: electrocardiogram

FLAIR: fluid-attenuated inversion recovery

GRE: gradient-recalled echo

ICA: internal carotid arteries

ICV: intracranial volume

IMT: intima-media thickness

ISF: interstitial fluid

IST-3: the Third International Stroke Trial

MAP: mean arterial pressure

MCA: middle cerebral artery

MID: multi-infarct dementia

MOOSE guidelines: Meta-analysis Of Observational Studies in Epidemiology guidelines

MRI: magnetic resonance imaging

OR: odds ratio(s)

PCA: posterior cerebral artery

PDE-5: phosphodiesterase – 5

PET: positron emission tomography

PI: pulsatility index

PROSPER trial: the Prospective Study of the Elderly at Risk trial

PVS: perivascular spaces

PVWMH: periventricular white matter hyperintensities

ROI: region(s) of interest

SD: standard deviation

SMART-MR study: the Second Manifestations of ARTerial disease-magnetic resonance study

SMD: standardised mean differences

SPECT: single-photon emission computed tomography

SPS3: Secondary Prevention of Small Subcortical Strokes

STRIVE: STandards for Reporting and Imaging of Small Vessel Disease

STROBE: the Strengthening the Reporting of Observational Studies in Epidemiology

SWI: susceptibility-weighted imaging

SVD: small vessel disease

T1W: T1-weighted

T2W: T2-weighted

TCD: transcranial Doppler

TIA: transient ischaemic attack

TOAST: the Trial of Org 10172 in Acute Stroke Treatment

WMH: white matter hyperintensities

List of Figures

List of Tables

Chapter 1: Introduction

As people live longer, stroke and dementia have become a great burden to the aging society. Worldwide, 47 million people were estimated to be living with dementia, and the number is expected to increase to 132 million by 2050.[1] Every year, 15 million people had a stroke, from which 5 million died and another 5 million are left disabled.[2] Up to 45% of dementias (alone or in addition to Alzheimer's disease (AD)), 25% of ischaemic strokes and a large proportion of haemorrhagic strokes are associated with a type of cerebrovascular disease, small vessel disease (SVD).[3, 4] In addition, silent burden of SVD on brain imaging is very commonly seen in the elderly and could substantially worsen cognitive function and cause psychiatric and physical disabilities.[4-6]

Theoretically, SVD are pathologies in perforating cerebral arterioles, capillaries, and venules. As currently, it is difficult to visualise small vessels *in vivo*, SVD is mostly diagnosed on brain imaging. Generally and in this thesis, the term "SVD" refers to a series of imaging changes in white matter and subcortical grey matter that are thought to result from the small vessel pathologies.(***Figure 1***) These features include recent small subcortical infarcts, lacunes, white matter hyperintensities (WMH), prominent perivascular spaces (PVS), cerebral microbleeds (CMB) and atrophy.[7](***Figure 2***)

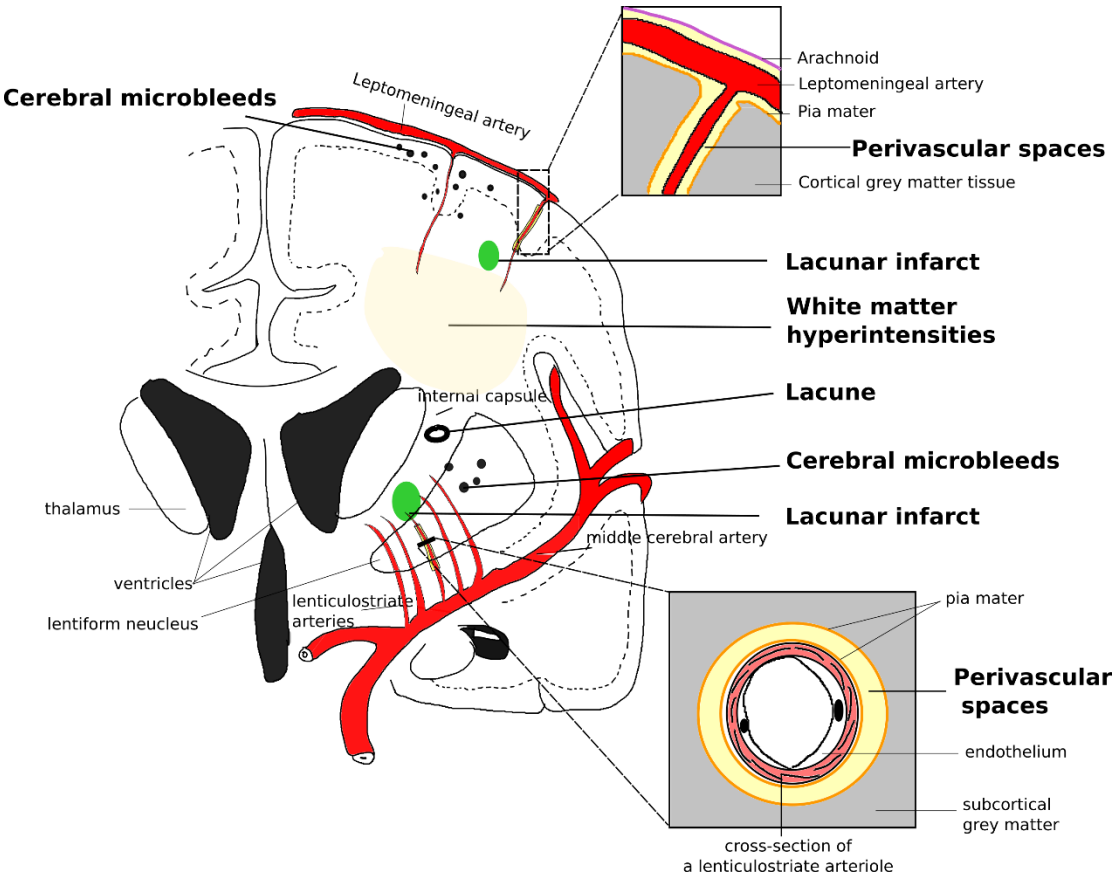

Figure 1 Key features of small vessel disease, including lacunar infarct, lacunes, white matter hyperintensities, enlarged perivascular spaces, and cerebral microbleeds. These features could be seen in the centrum semiovale, basal ganglia and sometimes in the brain stem. For brevity, only lesions in the centrum semiovale and basal ganglia are illustrated here. This figure is adapted from a figure in Prof Joanna M Wardlaw's presentation in Chinese Stroke Association Inaugural Conference (2015, Beijing) with permission.

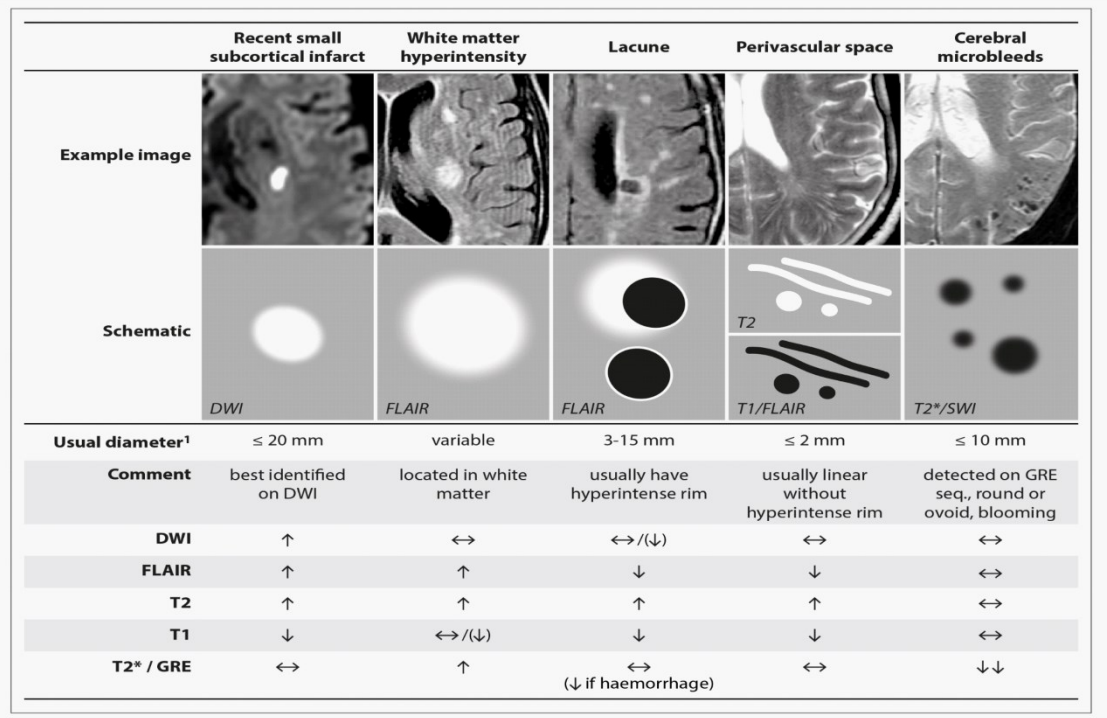

	Recent small subcortical infarct	White matter hyperintensity	Lacune	Perivascular space	Cerebral microbleeds
Usual diameter[1]	≤ 20 mm	variable	3-15 mm	≤ 2 mm	≤ 10 mm
Comment	best identified on DWI	located in white matter	usually have hyperintense rim	usually linear without hyperintense rim	detected on GRE seq., round or ovoid, blooming
DWI	↑	↔	↔/(↓)	↔	↔
FLAIR	↑	↑	↓	↓	↔
T2	↑	↑	↑	↑	↔
T1	↓	↔/(↓)	↓	↓	↔
T2* / GRE	↔	↑	↔ (↓ if haemorrhage)	↔	↓↓

Figure 2 STRIVE: STandards for Reporting and Imaging of Small Vessel Disease: example findings (upper), schematic representations (middle) and a summary of imaging characteristics (lower) of MRI features for changes related to small vessel disease (SVD).[7] The typical imaging features of SVD include recent small subcortical infarcts, white matter hyperintensities (WMH), lacunes, perivascular spaces (PVS), and cerebral microbleeds (CMB). A recent small subcortical infarct is an oval or tubular lesion of less than 20mm in diameter and appears hyperintense on diffusion-weighted imaging (DWI), T2-weighted (T2W), fluid-attenuated inversion recovery (FLAIR) sequences. WMH are punctuate or confluent lesions symmetrically distributed in the subcortical areas with hyperintense signals on T2W and FLAIR. A lacune is a round or oval subcortical lesion of usually 3-15 mm in diameter with fluid-filled signals on MRI, which is hyperintense on T2W but hypointense on T1W and FLAIR. It is consistent with a previous acute subcortical infarct or haemorrhage. A haemorrhagic lacune is hypointense on gradient-recalled echo (GRE) and susceptibility-weighted imaging (SWI). PVS are fluid-filled spaces that run along the course of a vessel. Thus on MRI, visible PVS are linear or oval fluid signals of usually less than 2 mm in diameter. CMB are small (generally 2–5 mm in diameter, but sometimes up to 10 mm) areas of signal void with associated blooming on GRE or SWI sequences.[7] This figure is a copy from a previous paper [7] with permission from the author Prof Joanna M Wardlaw.

The importance of SVD has not been recognised until the generalised use of MRI in clinical routine and research during the last three decades. In older studies, vascular dementia was often referred to as "multiple-infarct dementia" or "post-stroke dementia".[3] The Hachinski's ischaemic score was designed to distinguish vascular dementia and AD, which is based on the history of vascular risk factors, and presence and clinical characteristics of strokes.[8] However, these terms and the Hachinski's scale are imprecise and misleading, since a large proportion of patients with vascular dementia did not have a previous stroke. In vascular dementia, those who had SVD lesions without overt acute symptoms are even more common than those who had a stroke.[3] SVD also appears in other types of dementia, such as AD. Almost half of patients with clinical probable AD had mixed pathology.[9]

SVD could also present with acute symptoms, which is known as the lacunar stroke, or small-vessel-disease stroke if using the Trial of Org 10172 in Acute Stroke Treatment (TOAST) classification. Lacunar stroke is largely under-researched. Few if any other clinical trials particularly targeted lacunar stroke or treated it separately, apart from the Secondary Prevention of Small Subcortical Strokes (SPS3) trial which showed that long-term dual antiplatelet therapy was harmful to patients with lacunar stroke.[10]

Despite the important association between SVD and dementia and stroke, the underlying mechanisms of SVD remain unknown, which greatly limits the prevention and treatment of SVD. Various mechanisms have been suggested. The advances in imaging techniques have also brought new insights into mechanisms of SVD. In this chapter, I will first describe the main imaging features and the historical perspectives of SVD. Then I will talk about emerging theories and evidence on SVD

mechanisms. As this thesis focuses on "ischaemic" SVD, I will mainly focus on lacunar infarct, WMH, and PVS.

What is small vessel disease?

Lacunar infarct

Lacunar ischaemic stroke is defined as a stroke that is attributable to a recent small subcortical infarct less than 1.5 (or, some say, 2) cm diameter in white matter, basal ganglia, pons or brainstem, and is consistent with a lacunar clinical syndrome.[11] It is also worth noting that a lacunar clinical syndrome could be due to either ischaemia or a small haemorrhage.[12] On MRI, an acute lacunar infarct is shown as hyperintense on diffusion-weighted imaging (DWI) with a lowered apparent diffusion coefficient value, hyperintense on T2-weighted (T2W) and fluid-attenuated inversion recovery (FLAIR), hypointense on T1-weighted (T1W), and hypoattenuated on CT.(***Figure 2***)

Since Fisher's autopsy study in patients who had a history of hypertension and stroke, lacunar infarct has been generally thought to result from occlusion of deep perforating arteries.[13] However, this phenomenon was rarely seen on imaging. In contrast, an imaging study on lacunar stroke discovered that some lacunar stroke lesions were not at the end of but surrounding the occluded artery, and there was also signal indicating thrombus in the arteriole lumen and blood products in and around the vessel wall. This finding suggested that some lacunar infarct lesions might be due to a leakage of the vessel wall rather than the traditional understanding of an occluded arteriole.[14] A recent imaging study supported that patients with lacunar stroke had diffused blood brain barrier (BBB) impairment compared with those with

cortical stroke.[15] These results indicated that lacunar infarct might be more complex than the simple paradigm described in Fisher's original study.

Lacune

The French term "lacune" originally refers to small round holes in brain subcortical areas.[16] In the 1960s, C. Miller Fisher used this term to describe those subcortical cavitated lesions on brain autopsy which he thought were healed lacunar infarcts.[13] Therefore in SVD research, it is very common that terms like "lacunar infarction", "lacunar stroke" and "silent brain infarct" were used to refer to the cerebrospinal fluid (CSF)-filled cavities on brain MRI or autopsy.[17] In fact, lacunes are not always "ischaemic". They can also be the residual lesion of a small haemorrhage.[18] Also, it is common that many non-cavitated lacunar ischaemic strokes were not counted as 'lacunar infarcts'.

Lacunes of presumed vascular origin are round or ovoid, subcortical, fluid-filled cavities, with a diameter of 3-15 mm.(***Figure 2***) These can occur without any prior symptoms, but can also result from a previous acute small subcortical infarct or haemorrhage.[7] PVS could also mimic lacunes when they are more than 3 mm in diameter.[19] Large PVS might have also been miscounted as lacunes in many studies.[20] Although many lacunes might have lacked acute symptoms, when present in larger numbers, they are associated with dementia, cognitive impairment, gait disturbance and an increased risk of stroke.[21-23] In the general elderly population, the prevalence of lacunes ranges from 8% to 28% (mean age = 50-75 years).[22]

White matter hyperintensities

WMH of presumed vascular origin are very common in older individuals and regarded as the typical sign of SVD. Symptoms of WMH develop insidiously, such as cognitive impairment, dementia, and depression;[4] but the presence of WMH is associated with triple the risk of stroke, double the risk of dementia and higher risk of death.[24] WMH are usually symmetrically and bilaterally distributed in the white matter including pons and brain stem, and also occur in deep grey matter. They appear hyperintense to the normal brain on T2W or FLAIR MRI, and can be patchy or confluent depending on their stage in development and severity.***(Figure 2)***

Imaging-pathology studies on WMH were very limited and mostly were carried out when MRI was not very well developed. Thus the underlying pathology of WMH was not fully understood.[25] Demyelination, loss of oligodendrocytes and axonal damage were often reported. Diffusion tensor imaging (DTI) studies provided indirect evidence for axonal damage and impaired white matter integrity in WMH.[26] Indeed, recent evidence indicates that WMH are rather heterogeneous, perhaps reflecting different disease stages. Reduced density of glia and vacuolation were observed in severe WMH suggesting end-stage disease.[27] Autopsy MRI studies also found oedema that suggests leakage of fluid from the impaired BBB in and around WMH.[28, 29] Although these 'white' lesions have until now been treated as if they were all the same, different degrees of 'whiteness' might indicate different 'stages of formation' - some very white WMH are probably at the end stage of disease and irreversible once demyelination or axonal damage have happened; some perhaps less white lesions might be reversible if they are mainly interstitial fluid imbalances

before permanent tissue damage has occurred.[25] These observations remain to be confirmed in larger studies.

Perivascular spaces

PVS are the extension of the subarachnoid spaces that surround cerebral microvessels.[30] They are fluid-filled spaces that follow the course of a vessel through the brain parenchyma.[30](***Figure 1***) PVS are usually microscopic and not detected on CT or conventional MRIs. When enlarged, PVS are commonly seen as hyperintense on T2W MRI, either punctuate with a diameter less than 3 mm if imaged perpendicular to the course of the vessel, or linear if imaged parallel to the course of the vessel.[31]***(Figure 2)*** PVS are most frequent in the inferior parts of the basal ganglia and centrum semiovale but can also occur in the brainstem. Though 3 mm has generally been considered as the cut-off diameter for distinguishing PVS from lacunes,[19] occasional PVS could be larger and even cause a mass effect.[7] PVS usually do not have a hyperintense rim on T2W or FLAIR images unless passing through a WMH area, which can help the discrimination between PVS and lacunes.

Whether enlarged PVS should be regarded as 'lesions' is still controversial, as their clinical significance remains unclear. Although a few PVS can be normal,[32] the numbers of PVS increased with advancing age and other features of SVD.[20, 33-35] In some studies, more PVS were associated with increased risk of dementia or worse cognitive function or hypertension.[19, 36, 37] The mechanisms underlying enlarged PVS are not well understood. In normal ageing and other neurological diseases like multiple sclerosis, PVS are associated with inflammatory markers.[38] In SVD, it might be a sign of an impaired BBB.[15] There is also a hypothesis that visible PVS are

associated with blockage of drainage of interstitial fluid (ISF),[39] which might be attributed to increased vessel stiffness, as arterial pulsatility is thought to be a key driver of ISF drainage.[40]

What causes SVD?

Traditional risk factors

Increasing age is significantly associated with SVD features. Modifiable risk factors including hypertension, hypercholesterolaemia, smoking and diabetes mellitus are also thought to be key risk factors in the pathogenesis of SVD, particularly hypertension. However, the relationship between these risk factors and SVD is complex. Lipohyalinosis, the typical vascular pathology of SVD, has long been thought to result from hypertension. The theory is supported by clinical evidence showing that hypertension is more prevalent in patients with WMH and that higher blood pressure was associated with more severe WMH.[41] A recent study showed that vascular risk factors and large artery disease explained only 2% of the variance in WMH, leaving 98% of the variance unexplained, providing further evidence that WMH are mostly non-athromatous.[42] This finding may give a clue as to why risk factor modifications so far have very limited effects on preventing WMH progression.

Low cerebral blood flow

The narrowing of small vessel lumen seen in the pathology studies led to the suggestion that low blood flow might be the cause of WMH, and that complete occlusion of the vessel would cause an acute lacunar infarct.[4] The “chronic

hypoperfusion" hypothesis was supported by some animal studies which showed that white matter tract and glial cells were vulnerable to global ischaemia.[43, 44] Many animal models of SVD are also based on chronic occlusion or stenosis of carotid arteries which is thought to reduce CBF. However, there is limited and rather conflicting evidence in human studies. No direct association between carotid artery stenosis and lacunar stroke or WMH has been found in humans.[45, 46] Furthermore, the relationship between CBF and WMH is not consistent across clinical studies. In some cross-sectional studies, low CBF was significantly related to more WMH, whereas in other studies, no such relationship was found.[47, 48] These studies had different study designs, sample sizes and locations where low CBF was detected and most were cross-sectional. There are few longitudinal studies. Thus it is unclear whether there is a causal relationship between low CBF and WMH in humans.

Endothelium dysfunction

Common small vessel pathologies and BBB impairment were found in both clinically evident and covert SVD features, suggesting that SVD should be regarded as a whole-brain disease rather than be treated separately as individual conditions. An early endothelial failure has been suggested as a main precipitator of SVD,[11] as the endothelium is the main component of the BBB. The impaired endothelium would enable plasma fluid components and blood cells to enter the vessel wall, leading to the disintegration of the vessel wall and fibrin deposition. If this happens at arterioles where there is smooth muscle, the components deposited in the arteriolar wall could result in both dilation and narrowing of the vessel lumen and vessel wall thickening, which would eventually precipitate inflammation, platelet adhesion,

luminal occlusion and thus a traditional infarct. Whereas at the capillary level where there is no smooth muscle between the endothelium and brain tissue, the leaky BBB would cause direct damage to the tissue, such as oedema and demyelination in white matter tracts.(***Figure 3***)

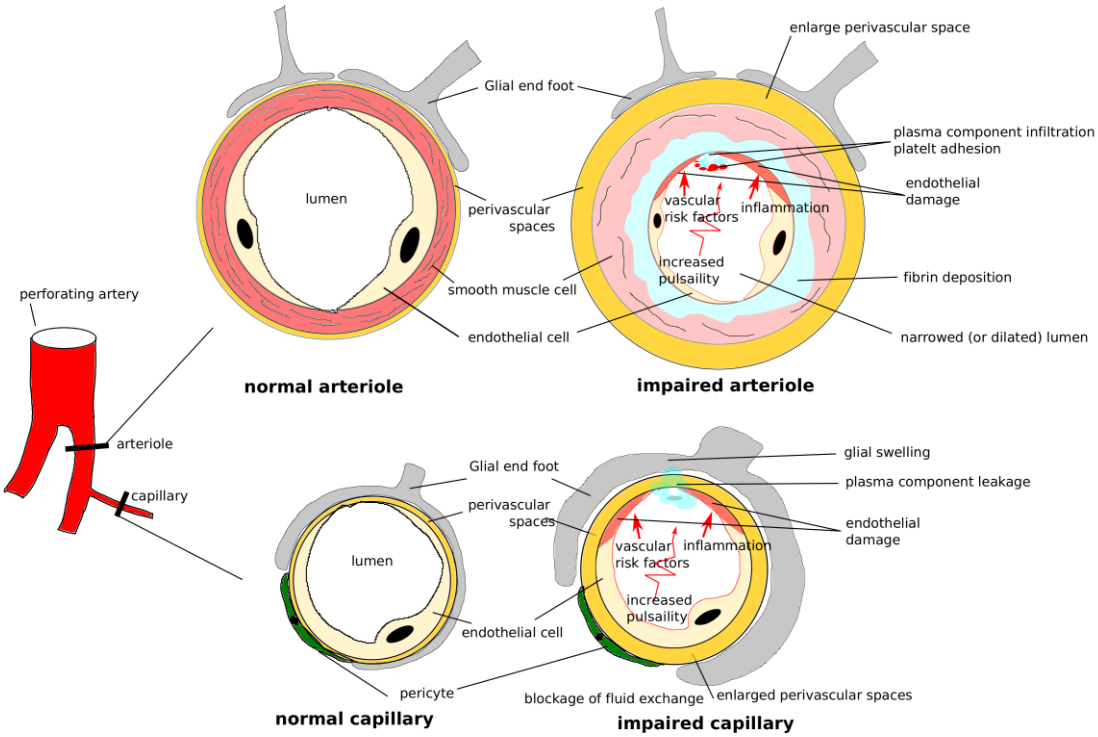

Figure 3 Example of endothelial damage at the arteriole and capillary level. In the arterioles, the blood component would infiltrate into the tunica media (smooth muscle) and induce fibrin deposition and vessel wall disintegration, causing segmental narrowing or dilation of the vessel lumen. The impaired endothelial cells could also trigger platelet adhesion and aggregation. Eventually, these multiple factors would cause occlusion of the arteriole lumen and a traditional infarct. With the fibrin deposition in the vessel wall, the vessels would stiffen and be less able to compensate the cardiac pulsatile energy, thus increasing the pulsatility in the vessels and in turn exacerbating the endothelial damage. At the capillary level where there is no smooth muscle, but only pericytes and the basement membrane, between the endothelium and brain tissue, the impaired endothelial cells result in a leaky blood brain barrier, thus causing direct damage to the tissue, such as glial oedema and demyelination in white matter tracts. At both arteriole and capillary levels, the increased pulsatility might damage the fluid exchange between the interstitial spaces

and the perivascular spaces, leading to enlarged perivascular spaces and possibly impaired metabolite clearance from the brain cells.

Increased vascular pulsatility

But how does the endothelial function fail? It is likely that the cause of endothelial dysfunction is multi-factorial. Various factors have been suggested, including increasing age,[49] inflammation[50, 51] and salt intake[11, 52]. The impaired endothelium would cause the infiltration of the blood component into the tunica media (smooth muscle) and induce fibrin deposition and vessel wall disintegration, causing segmental narrowing or dilating of the vessel lumen and vessel stiffening.(***Figure 3***)

It is hypothesized that stiffened vessels should be less able to dampen the pressure and pulsatility, leading to more pulsatile energies dissipating in the brain, which in turn could exacerbate and cause more endothelial damage. Growing evidence has shown that increased vascular pulsatility is related to endothelial dysfunction.[53] At the microvascular level, high pulsatile flow along with increased sheer stress reduced the expression of endothelial tight junction markers, thus deteriorating the BBB.[54] Studies on endothelial cells in other organs showed that high pulsatility could also induce endothelial inflammatory responses, such as via activating the toll-like receptor 2 /NF-κB pathway.[55] Furthermore, increased pulsatility could hamper the perivascular clearance pathway. In experimental models, the normal arterial pulse has been identified as a key factor in facilitating fluid drainage from the interstitium to the PVS and thence to the extracerebral CSF and venous system.[40] PVS become enlarged and visible on MRI in patients with hypertension, and are associated with

other SVD features like WMH and lacunar stroke,[7, 33] and with inflammation.[56] Some clinical studies have observed high pulsatility in large cerebral arteries, such as the internal carotid artery (ICA) or middle cerebral arteries (MCA), was associated with WMH,[57-59] but so far no clinical studies have assessed the relationship with PVS.

However, there is also suggestion that increased aortic stiffness might be the source of the high intracranial pulsatility and in turn be the cause of SVD.[53, 59] It is hypothesized that as the aorta becomes stiffer with older age or hypertension and is less able to buffer the high cardiac pulsatile energy, the impedance difference between high resistance peripheral arteries and central arteries becomes smaller, thus the excessive cardiac pulsatile energy would be more easily transmitted into "high-flow and low-resistance" organs such as the brain and the kidney. Various studies have shown the association between aortic stiffness and WMH,[60, 61] but most of the data supporting this theory is based on "healthy" populations. And very few studies have directly compared the aortic stiffness and intracranial pulsatility.

Moreover, in studies that measured intracranial pulsatility, most only assessed one (or at most two) main artery by ultrasound. Cerebral veins and CSF are also thought to be important compartments for compensating arterial pulse pressure,[62] since the sum of the brain volume, CSF, and intracranial blood is constrained within the skull.[63] Few studies have assessed pulsatility in the cerebral arteries, veins, and CSF contemporaneously in the same subjects,[64] and none has investigated how pulsatility in these multiple components related to aortic stiffness.

Pulse-gated phase-contrast MRI is an imaging technique that is able to detect flow and pulsatility in the major cerebral vessels and CSF spaces. Previous studies showed

higher pulsatility in cerebral veins in patients with vascular dementia compared to healthy elderly controls,[64] and altered CSF pulsatility in the aqueduct in patients with age-related depression compared to age-matched healthy volunteers.[65] No studies have compared vascular and CSF pulsatility contemporaneously with CBF, with SVD features, especially with PVS, or in patients with stroke in whom SVD is common.

Aim of the thesis

The aim of this thesis is to provide an overview of clinical evidence on CBF and intracranial pulsatility in subjects with SVD features, and then to set up a reliable method of CBF and pulsatility measurement and analysis. We will test this method in a pilot study with a group of typical patients who have SVD imaging changes, investigate the relationship between CBF and intracranial pulsatility, and SVD features, and explore how systemic measures such as blood pressure (BP) and aortic stiffness relate to intracranial haemodynamic measures.

Chapter 2A: Cerebral blood flow in small vessel disease: a systematic review and meta-analysis

The content of chapter 2A is a systematic review on cerebral blood flow in patients with small vessel disease, which has already been published in 2016. It is also part of the two systematic reviews in this thesis that I have undertaken for an overview of existing clinical evidence on changes of intracranial haemodynamic in small vessel disease. This chapter will be presented as the original publication, but supplementary materials will be added into the published manuscript for the comprehensiveness. Since the original search of the systematic review was undertaken before December 2015, I updated the search from December 2015 to September 2017 while writing up this thesis. As the new studies were generally small and are not suitable for meta-analysis, they were listed in a table following the original paper.

Although I was the first author of this paper, various colleagues have contributed to the work of this systematic review. Authors' contributions are listed as following: Dr Stephen D Makin (S.D.M.) and Prof Joanna M Wardlaw (J.M.W.) conceived the idea of the study. Yulu Shi (Y.S.) and J.M.W. designed the study. Y.S. did the data search and extracted data and statistical analyses. Dr Anton J. M. de Craen (A.J.M.D.C.) (now deceased), Dr Mark A van Buchem (M.A.VB.), and Dr Mirjam I Geerlings (M.I.G.) provided unpublished data for two longitudinal studies. J.M.W. cross-checked the data. Y.S. drafted the report and designed the tables and figures. J.M.W., M.J.T., S.M., I.M., A.J.M.D.C., M.A.VB., and M.I.G. revised the report. All authors approved the manuscript.

Cerebral blood flow in small vessel disease: a systematic review and meta-analysis

Introduction

White matter hyperintensities (WMHs) are commonly seen on brain magnetic resonance imaging (MRI) in older people and are considered as one of the core neuroimaging findings of cerebral small vessel disease (SVD). They are defined as patchy or confluent hyperintensities on T2-weighted or FLAIR images, without cavitation, in subcortical white or deep grey matter regions.[7] WMHs are associated with increasing age and vascular risk factors such as hypertension and diabetes.[66] Although the aetiology is not completely understood, chronic hypoperfusion is thought to be a key mechanism,[67] perhaps resulting from narrowing of the arteriolar lumena secondary to lipohyalinosis and arteriolosclerosis. Based on this theory, mechanically-induced hypoperfusion models, for example partial or complete carotid artery occlusion, are used to create pathology that appears to mimic human SVD. However, no direct association between carotid artery stenosis and lacunar stroke or WMH has been found in human studies.[45]

Additionally, the relationship between CBF and WMH is not consistent across human studies. In some cross-sectional studies, low CBF was significantly related to more WMHs, whereas in other studies, no such relationship was found.[47, 48] These studies had different study designs, sample sizes and locations where low CBF was detected and most were cross-sectional. There are few longitudinal studies. Thus it is unclear whether there is causal relationship between low CBF and WMHs in humans, or whether there is region specificity.

We sought to establish if WMH were related to changes in CBF levels, or whether differences in CBF might be related to potential confounders such as age and tissue loss. We systematically reviewed the available longitudinal and cross-sectional studies in humans, performed a meta-analysis of cross-sectional studies to assess the overall effect size of CBF differences by WMH burden in different brain regions, assessed study quality and performed sensitivity analyses on important confounders.

Methods

We performed this review according to the MOOSE guidelines[68] and a pre-specified protocol. We conducted a literature search of MEDLINE and EMBASE from 1946 up to December 2015, using the Ovid Web Gateway. We used exploded headings related to *Small Vessel Disease* (i.e. small vessel disease, white matter hyperintensities, white matter lesion, leukoaraiosis, lacune, lacunar infarct) and *Cerebral Blood Flow* (i.e. cerebral blood flow, brain blood flow, brain perfusion, cerebral hypoperfusion) with the Boolean operator AND. English and non-English literature were sought. Additional records were identified by hand searching from January 1990-December 2015 of *Stroke* and *Journal of Cerebral Blood Flow & Metabolism*. We also checked references cited in reviews and primary papers.

Eligibility criteria

We sought longitudinal and cross-sectional primary research studies assessing CBF in subjects with cerebral SVD.[7] Studies measuring cerebral blood flow velocity (CBFv) using Doppler ultrasound techniques were also considered eligible. We

excluded studies targeting unilateral or bilateral severe carotid stenosis or occlusion, studies in children, animal studies, duplicate publications, conference abstracts, and cross-sectional studies from which we could not extract either absolute values of CBF or correlation/regression coefficients.

Data extraction and analysis

We screened all potentially relevant full papers and extracted data using a standardised form. All data were cross-checked by a second reviewer (JMW). From those that met the inclusion criteria, we extracted data on study population characteristics, study design, SVD and CBF measurement techniques and units. We assessed the study quality using a checklist devised on the basis of the Strengthening the Reporting of Observational Studies in Epidemiology (STROBE) statement (www.equator-network.org) and a checklist in a previous paper,[69] including factors such as study population and bias control. ***(Table 1)***

Table 1 The 9-point study quality checklist applied to all included studies

Clearly reported study population (stroke, aging cohort, etc)?	yes/no (1/0)
Clearly defined inclusion criteria?	yes/no (1/0)
Prospective study?	yes/no (1/0)
Reported drop-out (how the final sample was reached)?	yes/no (1/0)
Adjusted/matched for risk factors (including age)?	yes/no (1/0)
Reported number of & expertise of observers of SVD image?	yes/no (1/0)
Observers blinded to clinical data?	yes/no (1/0)
Clearly defined SVD?	yes/no (1/0)
Clearly described CBF measurement?	yes/no (1/0)
Overall score	/9

This table was devised using influences from the STROBE statement and a previous study[69].

For cross-sectional studies which reported means and standard deviations (SDs) of CBF, we extracted data on CBF in disease and control groups or according to SVD burden. Means and SDs were extracted from text or tables where available, or from graphs where necessary. For cross-sectional studies where only qualitative data for the association between CBF and WMH were available, we included the studies in the review but not in the meta-analysis: we noted the statistical methods, coefficients, P values and other covariates included in the regression.

For longitudinal studies, we also listed follow-up durations and primary results extracted from the papers, and contacted the authors to request unpublished data on baseline and follow-up CBF and WMH volume.

Data transformation and analysis

All studies reporting means and SDs were included for meta-analysis. For studies that divided patients into more than two grades of WMH severity, we combined the means and SDs of groups to create a single pair-wise comparison using formulae from the Cochrane handbook (http://handbook.cochrane.org). We condensed data into new groups "negative to mild WMHs" indicating none to mild including multiple punctuate WMHs (eg. Fazekas deep WMH score 0 to1), and "moderate to severe WMHs" as beginning to large confluent WMHs (eg. Fazekas deep WMH score 2 to 3). (***Equation 1***)

Equation 1 Equations for calculating combined means and SDs

	Group 1 (e.g. males)	Group 2 (e.g. females)	Combined groups
Sample size	N_1	N_2	$N_1 + N_2$
Mean	M_1	M_2	$\frac{N_1 M_1 + N_2 M_2}{N_1 + N_2}$
SD	SD_1	SD_2	$\sqrt{\frac{(N_1 - 1)SD_1^2 + (N_2 - 1)SD_2^2 + \frac{N_1 N_2}{N_1 + N_2}(M_1^2 + M_2^2 - 2M_1 M_2)}{N_1 + N_2 - 1}}$

As most studies measured CBF in several regions of interest (ROIs), such as different grey matter and white matter regions, we conducted subgroup analysis by brain region. Due to various units of CBF being used in different papers, we calculated the standardised mean differences (SMD) and 95% confidence intervals (CI) for comparisons using a random-effect model. Sensitivity analyses were carried out for subjects with/without dementia and by age matching between study groups, as both strongly influence CBF. Meta-analyses were conducted using the Cochrane Collaboration's Review Manager (Revman Version 5.3). We assessed for heterogeneity by calculating the I^2 statistic and publication bias using a funnel plot.

Results

A total of 2843 publications were initially identified, of which 75 were potentially eligible and were selected for further review. We ultimately included 38 articles and excluded: conference abstracts (6), those where we were unable to access the full text

(6) or that had no analysable data (18), duplicate publications including the same participant population (3), and studies of severe carotid stenosis or occlusion (4).***(Figure 4)*** Note that although presence of arterial diseases was an inclusion criterion of Second Manifestations of ARTerial disease-magnetic resonance (SMART-MR) study, carotid arterial stenosis or occlusion was not one of the criteria: here patients with carotid artery stenosis were included, but they only represented a small proportion of participants, thus we included the study[70] in our review. The 38 studies included a total of 4006 participants: 4/38 were longitudinal and 34/38 were cross-sectional.

Some papers are from the same studies: van der Veen et al.[70] and Bisschops et al.[71] from the SMART-MR study; Ten Dam et al.[72] and van Es et al.[73] from the Prospective Study of the Elderly at Risk (PROSPER) trial; Vernooij et al.[74] and Claus et al.[75] from the Rotterdam Scan Study. We were careful to count each participant only once in any analysis.

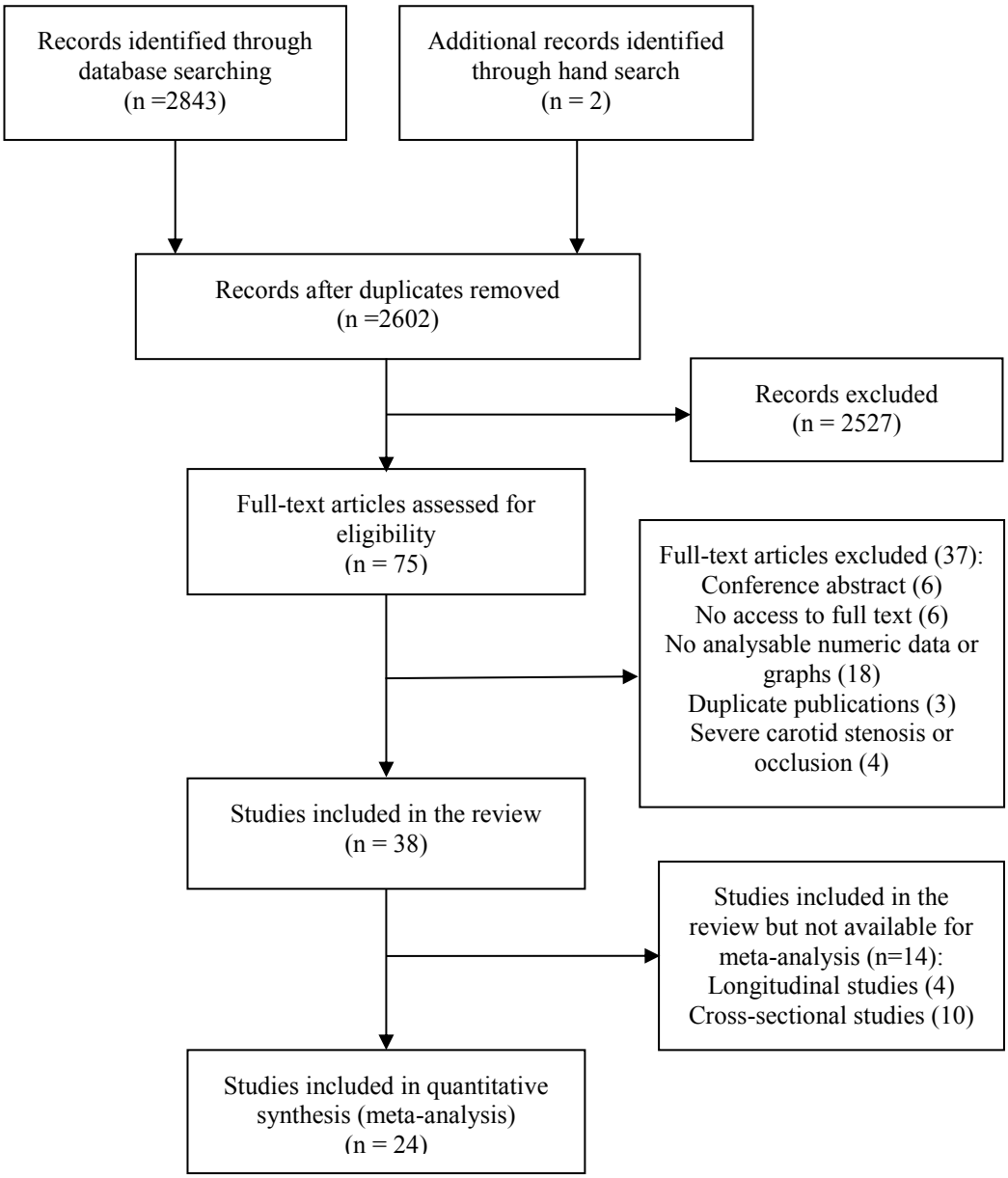

Figure 4 PRISMA diagram of literature search

Characteristics of included studies

Cross-sectional studies

34 cross-sectional studies were included.***(Table 2)*** 24/34 were suitable for meta-analysis. 6/24 studies used patients with dementia plus WMH as disease groups. Of these six studies, two included AD,[76, 77] the other four focused on vascular dementia including subcortical vascular dementia,[78] multi-infarct dementia (MID),[79, 80] and Binswanger's disease.[47] AD was diagnosed based on the criteria of the National Institute of Neurological and Communicative Disorders and Stroke, and the Alzheimer's disease and Related Disorders Association (NINCDS/ADRDA) for probable AD. Vascular dementia diagnosis varied: CT/MRI evidence, DSM-III-R criteria,[47, 79, 80] Hachinski ischaemia scores,[79] and the criteria of the State of California Alzheimer's Disease Diagnostic and Treatment Centres.[78] In the 18/24 studies of non-demented subjects, 11 compared CBF between subjects having WMHs and normal controls with no or mild WMHs,[81-91] one study performed the comparison between patients with depression (DSM-IV criteria) plus WMHs vs no WMHs,[92] and the other four papers examined the differences in CBF across grades of WMH severity.[48, 93-95] Of these four studies, two used Fazekas WMH rating scores,[48, 95] the other two used self-designed rating systems similar to Fazekas's method.[93, 94] Two studies recruited patients with acute ischaemic symptoms: in Nezu et al.,[81] patients presented with minor ischaemic stroke and brain scans were performed at least three weeks after onset; Huynh et al. only included TIA patients and brain scans were done acutely.[81]

In the other 10/34 studies which only reported association analysis, two were population-based studies,[74, 96] the other nine hospital-based studies included patients

with cerebrovascular risk factors,[73, 97, 98] heart failure,[99] dementia,[100] and manifest arterial diseases.[71]

Longitudinal studies

Four longitudinal prospective studies, including 1079 participants, were included.***(Table 2)*** Three were hospital-based[70, 72, 101] and one from a population-based aging study.[102] Among these four studies, Bernbaum et al. recruited participants who presented acute minor stroke symptoms or transient ischaemic attack (TIA) and had baseline MRI within 48hrs after the onset.[101] The other three studies did not include acute patients. The follow-up durations ranged from 1.5 to 7.7 years. Kraut et al. compared the patterns of long-term CBF change in patients with progressive WMHs to those with stable WMHs,[102] whereas the other three studies performed regression analyses between CBF and WMH data without subdividing patient groups.[70, 72, 101]

Table 2 Characteristics of all included studies

Study	Sample size	Participants	(Baseline) Age (years, mean ± SD)	Methods of measuring CBF	CBF units
Longitudinal studies (4)					
Bernbaum 2015[101]	40	High risk TIA or minor ischaemic stroke	61.0±11.0	DCS PWI	ml/100 g/min
van der Veen 2015[70]	575	Manifest arterial diseases*	57.0±10.0	Phase-contrast MRI	ml/100 ml/min
Kraut 2008[102]	74	Progressive WMH Stable WMH	70.0±6.9 67.1±7.0	PET	Not shown
Ten Dam 2007[72]	390	history of vascular disease or were at increased vascular risk	75.0±3.2	Phase-contrast MRI	ml/min
Cross-sectional studies (34)					
Cognitive impairment/Dementia (6)					
Kimura, N. 2012[76]	98	late-onset AD with WMH AD without WMH	78.6±5.1 77.4±5.0	SPECT	ml/100 g/min
Schuff 2009[78]	26	subcortical vascular dementia cognitively normal	77.0±8.0 73.0±8.0	ASL	ml/100 g/min
Ibayashi 2000[47]	15	dementia of BD age-matched hypertensive controls	60.0±2.0 59.0±2.0	PET	ml/100 ml/min
Yamaji 1997[77]	32	AD with WMH	71.6±3.1	PET	ml/100 ml/min

		AD without WMH	71.0±4.3		
Kawamura 1993[79]	40	MID	64.4±10.2	Xenon CT	ml/100 g/min
		no WMH	67.2±10.5		
Kobari 1990[80]	20	MID	68.1±12.0	Xenon CT	ml/100 g/min
		neurologically normal controls	52.3±5.7		
No cognitive impairment (18)					
Wagner 2015[103]	36	Extensive WMH	71.0	ASL	ml/100 g/min
		No or mild WMH	67.0		
Fu 2014[93]	56	WMH Grade 3[ł]	68.1±8.1	Xenon CT	ml/100 g/min
		WMH Grade 2	68.9±7.7		
		WMH Grade 1	64.5±5.8		
		WMH Grade 0	65.3±6.3		
Nezu 2012[81]	18	lacunar stroke with severe WMHs	76.0	PET	ml/100 g/min
		lacunar stroke with mild WMH	74.0		
Huynh 2008[104]	35	TIA with moderate to severe WMH	77.1±6.0	CT perfusion	ml/100 g/min
		TIA with mild WMH	62.6±16.3		
De Bastos-Leite 2008[94]	21	WMH Grade 3[ł]	77.7±5.7	ASL	ml/100 ml/min
		WMH Grade 2	74.4±4.6		
		WMH Grade 1	74.0±5.0		
Zheng 2006[82]	35	asymptomatic WMH	69.7±8.9	SPECT	ml/g/min
		no WMH	67.1±6.9		
Ramli 2006[83]	42	leukoraiosis on CT	70.19	CT perfusion	ml/100 g/min
		no leukoaraiosis on CT	69.86		

Kimura, M. 2003[92]	20	depression (remission) with WMH	78.5±5.1	SPECT	ml/100 g/min
		depression (remission) without WMH	77.4±5.0		
Cui 2003[84]	98	WMH	70.0	TCD, SPECT	cm/s
		no WMH	66.0		
O'Sullivan 2002[85]	36	WMH	68.9±9.2	PET	ml/100 g/min
		no WMH	72.7±7.7		
Yao 2000[86]	10	extensive WMH	75.0±5.0	Xenon CT	ml/100 g/min
		no WMH	72.0±5.0		
Markus 2000[87]	17	Leukoraiosis	63.3±12.3	MRI Contrast	ml/100 g/min
		no leukoraiosis	68.3±7.3		
Oishi 1999[88]	45	WMH	66.8±8.4	Xenon CT	ml/100 g/min
		no WMH	65.1±8.5		
Hatazawa 1997[89]	33	asymptomatic WMH	71.3±8.6	PET	ml/100 ml/min
		no WMH	68.5±10.2		
Miyazawa 1997[95]	135	WMH Grade IV[‡]	71.90±8.17	Xenon CT	ml/100 g/min
		WMH Grade III	69.00±8.08		
		WMH Grade II	67.30±9.87		
		WMH Grade I	64.20±5.55		
		WMH Grade 0	57.3±12.0		
Kuwabara 1996[48]	24	hypertensive with moderate to severe leukoraiosis[‡]	67.0±9.0	PET	ml/100 ml/min
		Hypertensive with negative to mild leukoraiosis	54.0±7.0		

		normotensive control	60.0±12.0		
Kobayashi 1991[90]	246	apparent PVWMH	67.0±6.1	Xenon CT	ml/100 g/min
		no or mild PVWMH	60.0±8.2		
Fazekas 1988[91]	23	WMH	58.8±5.3	Xenon CT	ml/100 g/min
		no WMH	58.2±2.8		
Studies only showing correlation/regression coefficients (10)					
Crane 2015[105]	26	Mild to severe WMH	73.3±8.8	ASL	ml/100 g/min
Alosco 2013[99]	69	Heart failure with WMH	68.55±8.07	Doppler ultrasound	cm/s
Heliopoulos 2012[97]	52	Hypertension with WMH	71.4±4.5	Doppler ultrasound	cm/s
van Es 2010[73]	447	Cerebrovascular risk factors without major neurological deficits	75.0±3.0	Phase-contrast MRI	ml/min, ml/100 ml/min
Vernooij 2008[74]	892	Population-based	67.5±5.5	Phase-contrast MRI	ml/100 g/min
Bisschops 2004[71]	228	Manifest arterial diseases*	59.0	Phase-contrast MRI	ml/min
Tzourio 2001[96]	628	Population-based	68.9±2.9	Doppler ultrasound	m/s
Ott 1997[100]	40	Mixed dementia	72.8±8.7	SPECT	%rCBF relative to cerebellum
Claus 1996[75]	60	Non-demented WMH	65.0-85.0§	SPECT	%rCBF relative to cerebellum
Isaka 1994[98]	28	Cerebrovascular risk factors	67.8	Xenon CT	ml/100 ml/min

without neurological deficits

SD: standard deviation; CBF: cerebral blood flow; TIA: transient ischaemic attack; DCS-PWI: dynamic susceptibility contrast perfusion-weighted imaging; MRI: magnetic resonance imaging; AD: Alzheimer's disease; MID: multi-infarct dementia; BD: Binswanger's disease; WMH: white matter hyperintensities; SPECT: Single-photon emission computed tomography; ASL: Arterial spin labelling MRI; PET: positron emission tomography; TCD: Transcranial Doppler; CT: computed tomography; PVWMH: periventricular white matter hyperintensities; rCBF: regional cerebral blood flow.

* Include manifest coronary artery disease, cerebrovascular disease, peripheral arterial disease or an abdominal aortic aneurysm.

ł Fazekas WMH score;

‡ Self-designed scoring system for WMH;

§ Age range

Quality assessment

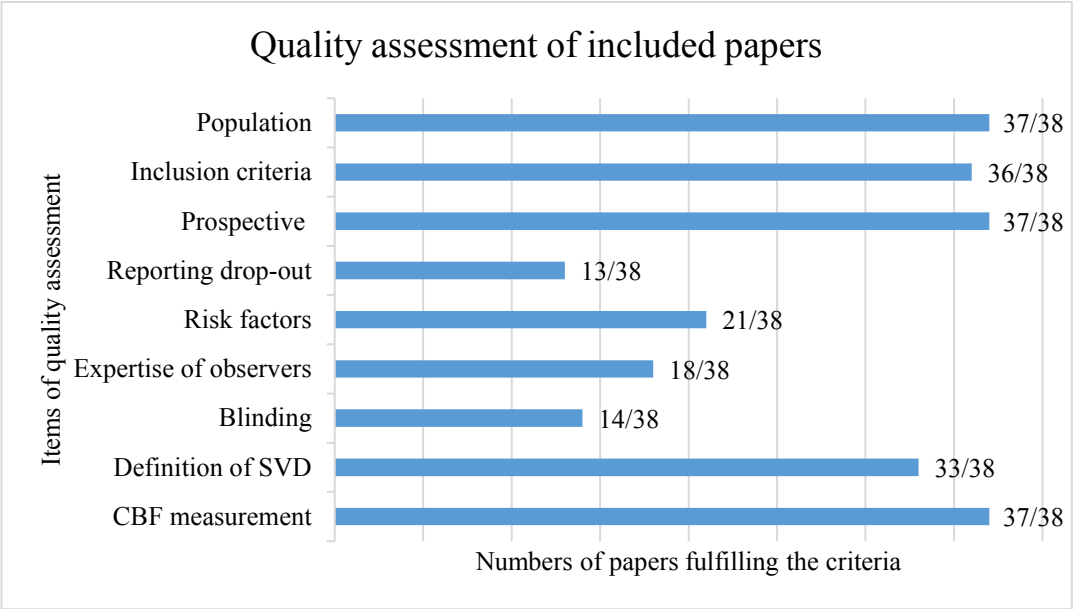

Figure 5 Quality assessment of included papers

The average study quality score was 6/9. Scores were mainly lost for not reporting the drop-outs (25/38), no adjustment or matching for risk factors (including age) (17/38), not reporting expertise of image observers (20/38) and not using blinding (25/38). ***(Figure 5)***

Assessment of CBF measurement methods

Three studies used phase-contrast MRI,[70-74] seven used positron emission tomography (PET),[47, 48, 77, 81, 85, 89, 102] six used single-photon emission computerized tomography (SPECT),[75, 76, 82, 84, 92, 100] two used MRI contrast,[87, 101] two used arterial spin labelling (ASL)-MRI,[78, 103] nine used Xenon-CT,[79, 80, 86, 88, 90, 91, 93, 95] and two

used CT perfusion[83, 104] to assess CBF. Four studies measured CBFv in the MCA using transcranial Doppler ultrasound (TCD).[84, 96, 97]

Meta-analysis of differences in CBF by WMH burden

Meta-analysis using SMD in CBF was only possible for 24 cross-sectional studies. 22 brain regions were extracted, but sufficient data were available from only 11 regions which were used by at least three studies and were selected for the primary meta-analysis. These included: global brain mean CBF, basal ganglia, cortical grey matter (total, frontal, temporal, parietal and occipital gray matter) and white matter (total, frontal and occipital white matter, centrum semiovale). Most data were available for frontal grey matter; few studies provided white matter data.

Figure 6 shows the results of and meta-analyses of global and cortical CBF, and Figure 7 shows the results of white matter CBF. Patients with more severe WMH had lower CBF than patients with mild WMH, globally and in most grey and white matter regions (e.g. mean global CBF: SMD -0.71, 95% CI -1.12, -0.30; total grey matter: SMD -0.50, 95% CI -0.97, -0.03; total white matter: SMD -1.16, 95% CI -1.08, -0.53), except in the basal ganglia (SMD -1.25, 95% CI -2.53, 0.30) and occipital white matter (SMD -0.45, 95% CI -0.96, 0.05) where the difference in CBF did not reach significance.***(Figure 6*** and ***Figure 7)*** No studies in the meta-analysis separated normal appearing white matter (NAWM) and WMH. However, there were heterogeneities between studies for most of these comparisons that were not due to publication bias.***(Figure 8)*** One study found that CBF in patients with lacunar lesions was lower than in those without, however, the result was not adjusted for WMH volume and could not be meta-analysed.[90]

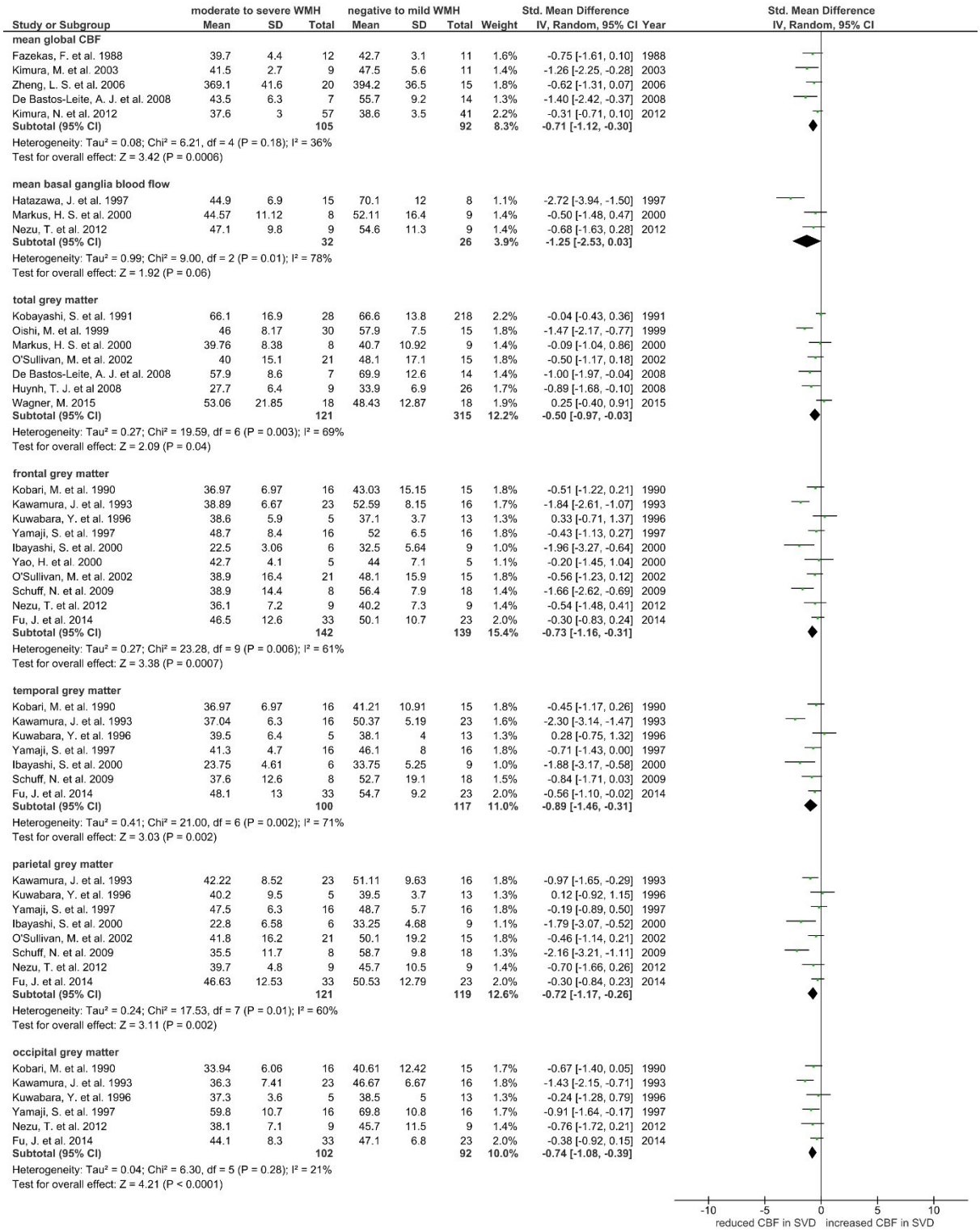

Figure 6 Forest plot showing standard mean differences in global and grey matter CBF in patients with WMH in dementia & non-dementia studies. CBF in different brain regions was analysed in subgroups. CBF: cerebral blood flow.

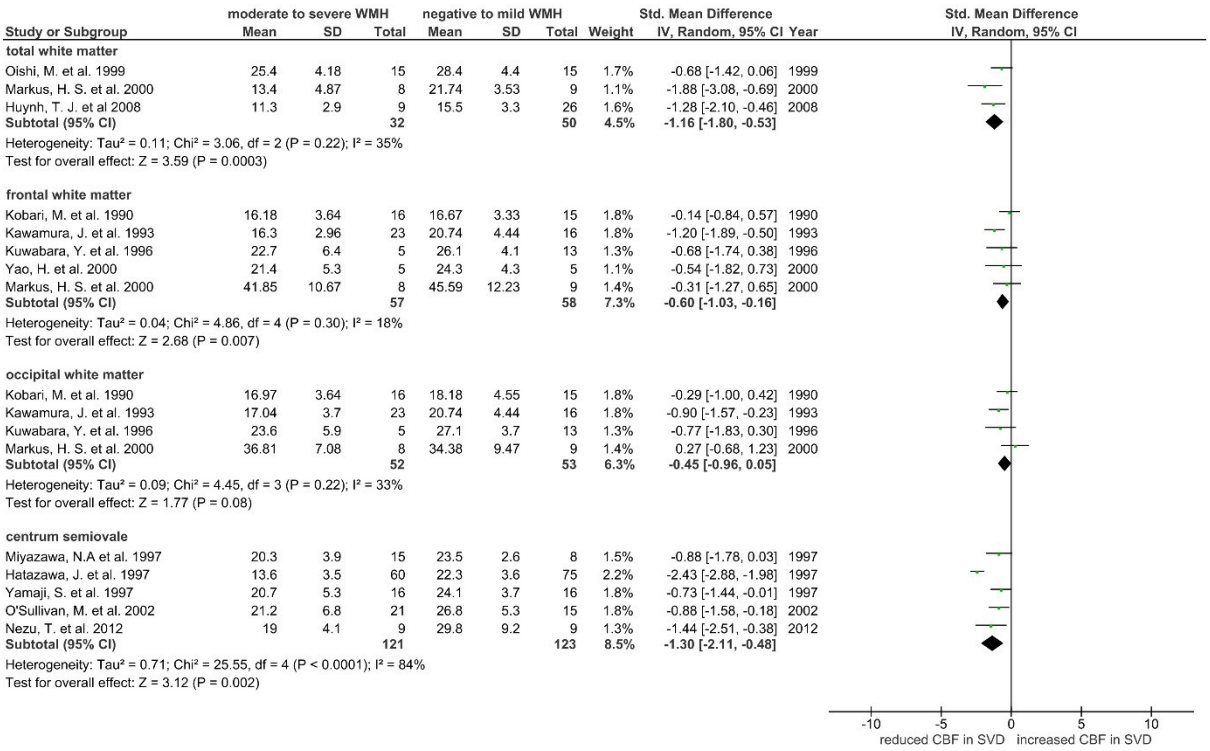

Figure 7 Forest plot showing standard mean differences in white matter CBF in patients with WMH in dementia & non-dementia studies. CBF in different brain regions was analysed in subgroups. CBF: cerebral blood flow; WMH: white matter hyperintensities.

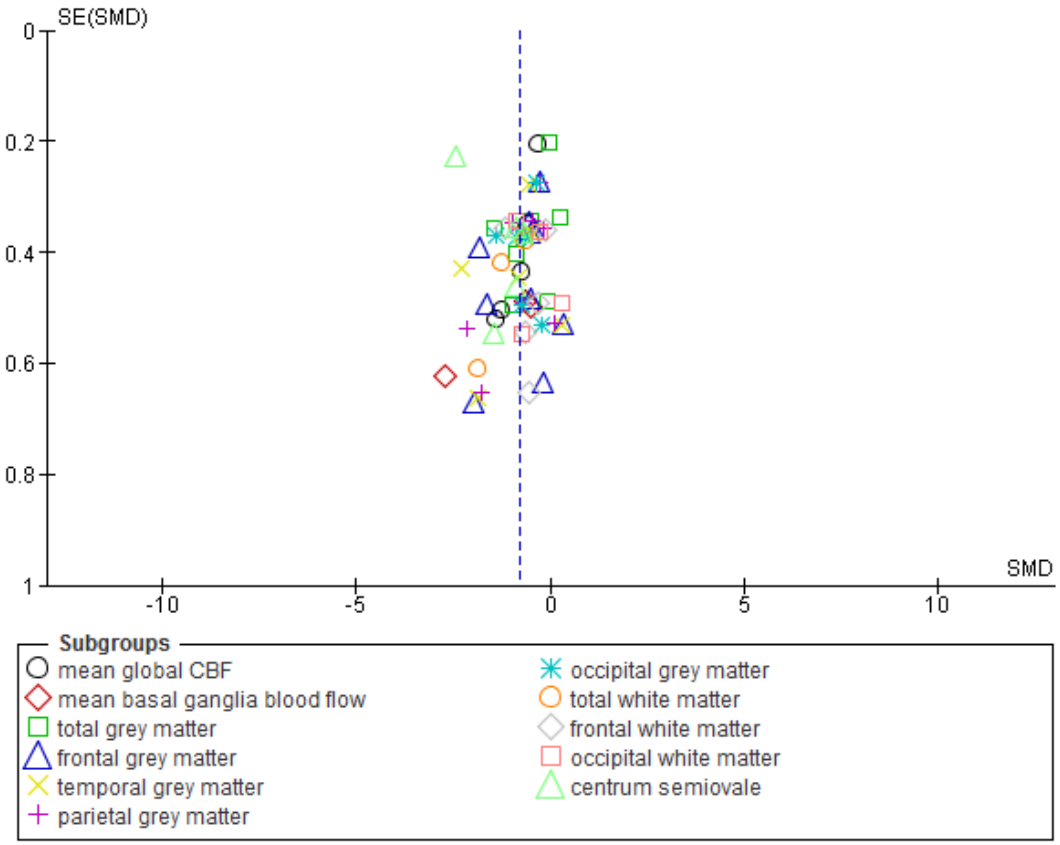

Figure 8 Funnel plot of all include data in meta-analysis. The symmetrical distribution of the plots indicate small publication biases.

Sensitivity analysis of dementia and age

We repeated the meta-analyses after excluding studies that included patients with dementia and then further excluded studies without age-matching. In most grey and white matter regions, the differences in CBF between subjects with high and low WMH burdens attenuated and were no longer significant, except for mean global brain CBF and the centrum semiovale. Most of the trends in the comparisons were still the same, apart from temporal grey matter.***(Figure 9)***

We were not able to do a sensitivity analysis for vascular risk factors. Only one study, Ibayashi et al., used hypertensive but neurologically normal patients as the control group, and found lower CBF in patients with Binswanger's dementia compared to the control group;[47] none of the other studies matched or adjusted for vascular risk factors. Hypertension is significantly more prevalent in patients with more severe WMH.

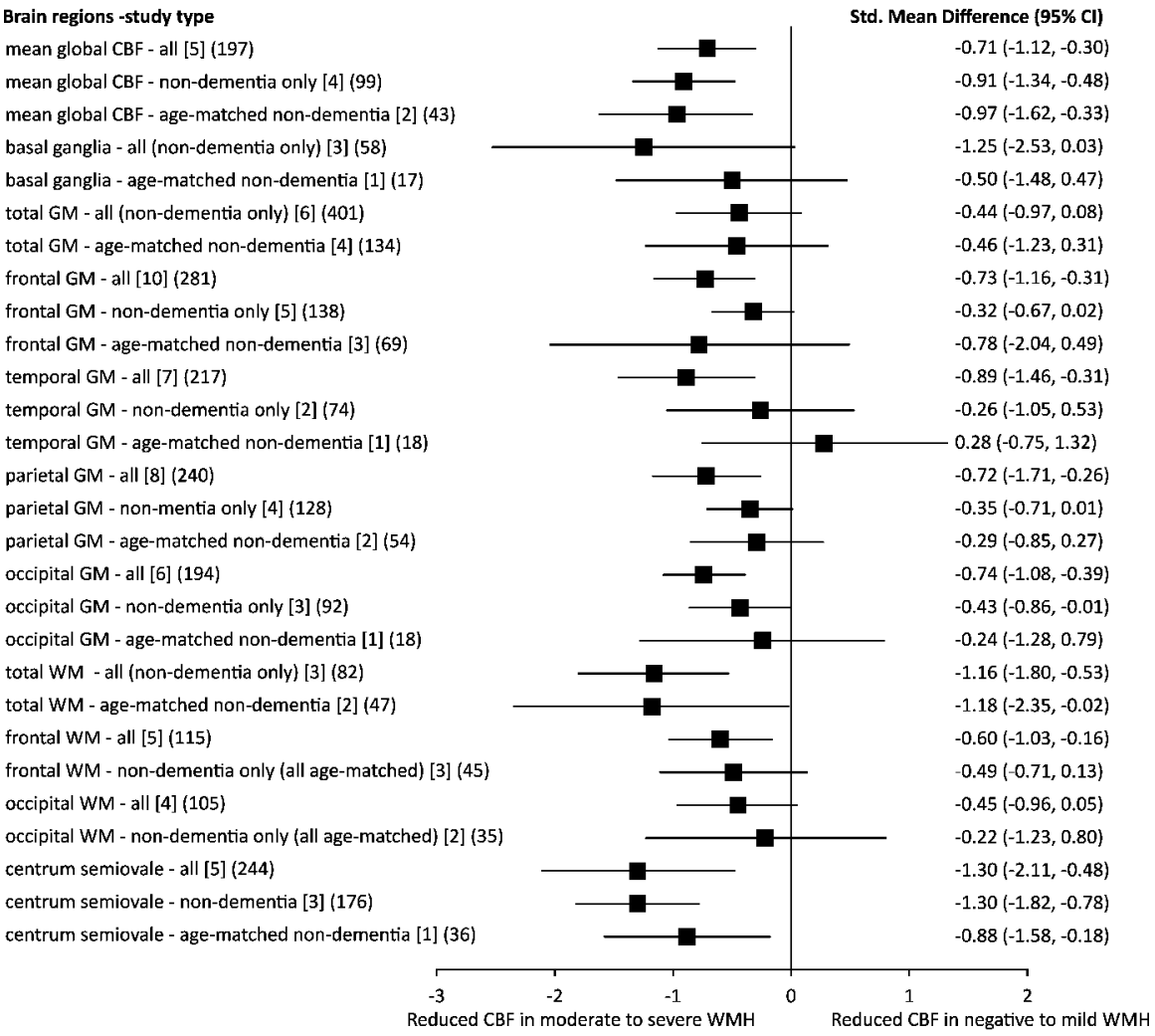

Figure 9 Sensitivity analysis: SMD of CBF in different brain areas in patients with moderate to severe WMH against those with negative to mild WMH. In each brain area, we showed the SMD of CBF in all studies, after excluding dementia studies and furthermore excluding studies without age-matching [number of studies] (number of participants). SMD: standard mean difference; CBF: cerebral blood flow; GM: grey matter; WM: white matter; WMH: white matter hyperintensities; CI: confidence interval.

Cross-sectional studies that provided data on associations between CBF and SVD features

Among the 10 cross-sectional papers which only performed association analysis, three studies did not find an association between CBF and WMH burden.[75, 98, 100] Four studies reported that CBF was negatively related to WMH severity.[71, 73, 74, 105] Negative correlation between WMH features and CBFv were found in three studies, of which one assessed CBFv in ICA,[97] and the other two in MCA.[96, 99] Amongst all 10 studies, six adjusted for covariates such as age, gender, and other vascular risk factors.[71, 74, 75, 96, 99, 105]***(Table 3)***

Table 3 Results of association-only cross-sectional studies

Study	Sample size	Statistical method	Results		P Values	Adjusted for other variables
			Variables	Coefficients		
Crane 2015[105]	26	Partial correlation (post-hoc test)	Mean CBF in cluster (LAP, SC, accumbens, AC and OF) and Fazekas score	Rho=-0.55	0.006	Age, gender
			Mean CBF in cluster (LAI and OF) and Fazekas score	Rho=-0.49	0.015	
			Mean CBF in cluster (LOF and FP) and Fazekas score	Rho=-0.56	0.005	
Alosco 2013[99]	69	Multivariable hierarchical regression	CBFv and WMH volume	β=-0.34	0.02	Age, gender, premorbid intelligence, depressive symptoms, BMI, hypertension, diabetes, thyroid abnormalities, intracranial volume
Heliopoulos 2012[97]	52	Spearman rank-order correlation	CCA-PSV and WMH score	r=-0.256	0.067	No
			CCA-EDV and WMH score	r=-0.205	0.144	
			CCA-MFV and WMH score	r=-0.134	0.342	
			ICA-PSV and WMH	r=-0.135	0.341	

			score			
			ICA-EDV and WMH score	r=-0.324	0.019	
			ICA-MFV and WMH score	r=-0.363	0.008	
van Es 2010[73]	447	Linear regression model	tCBF and WMH volume	r=-0.069	0.148	No
			TCBF and WMH volume	r=-0.106	0.044	
Vernooij 2008[74]	892	Linear regression model	WMH volume and tCBF	0.03*	NS	Age, gender
			WMH volume and TCBF	0.07†	Significant	
Bisschops 2004[71]	282	Linear regression model	WMH score and tCBF	–1.0‡	0.041	Age, gender, IMT, hypertension
Tzourio 2001[96]	628	Multiple logistic regression	Quartiles of mean CBFv and WMH	OR=1.4 (1st quartile)	0.22	age, gender, BMI, hypertension, diabetes, hematocrit, IMT
				OR=1.6 (2nd quartile)	0.11	
				OR=2.3 (3rd quartile)	0.006	
Ott 1997[100]	40	Spearman rank-order correlation	Perfusion score and PVWMH score	r=-0.17	0.3	No
			Perfusion score and SCWMH score	r=-0.13	0.42	
Claus 1996[75]	60	Multiple linear regression	CBF and grades of severity of WMH	-1.7§ (Frontal lobe)	NS	age, gender, type of SPET camera and
				0.4§ (Parietal lobe)	NS	

				1.2[§] (Temporo-parietal area)	NS	ventricle-to-brain ratio
				-0.4[§] (Temporal lobe)	NS	
Isaka 1994[98]	28	Spearman rank-order correlation	PVWMH score and baseline CBF	r=-0.364	NS	No

LAP: left anterior putamen; SC: subcallosal; AC: anterior caudate; OF: orbital frontal; LAI: left anterior insula; LOF: left orbital; FP: frontal pole; CBFv: cerebral blood flow velocity (measured by Doppler ultrasound); WMH: white matter hyperintensities; BMI: Body mass index; CCA: common carotid artery; ICA: internal carotid artery; PSV: peak systolic velocity; EDV: end-diastolic velocity; MFV: mean-flow velocity; tCBF: total cerebral blow flow in ml/min; TCBF: cerebral blood flow per 100 ml brain volume; total brain perfusion: tCBF divided by brain volume; S.D.: standard deviation; lnWMH: natural log transformed white matter hyperintensities volume; IMT: intima media thickness; OR: odds ratio; PVWMH: periventricular white matter hyperintensities; SCWMH: subcortical white matter hyperintensities; NS: not significant; SPET: single-positron emission tomography.

[*] Difference in lnWMH volume per S.D. increase of tCBF;

[ł] Difference in lnWMH volume per S.D. decrease in TCBF;

[‡] Difference in WMH per 100 ml/min increase in tCBF;

[§] Difference in % CBF between persons with no/slight WMH and persons with moderate/severe WMH.

Longitudinal studies

Table 4 summarises the results of four longitudinal studies. The largest study (575 subjects), Van der Veen et al. found that high WMH volume at baseline was significantly associated with falling CBF over 3.9 years follow-up.[70] Ten dam et al. demonstrated in 390 subjects that a decline in global CBF over 2.75 years was associated with a progression in periventricular WMH (PVWMH) but not in deep WMH (DWMH).[70] A small study (n=40) found low CBF in regions that developed WMH over 1.5 years follow-up (baseline WMH volume 9.21±11.87 ml).[101] In contrast to the other findings of falling CBF over time, Kraut et al. demonstrated in 74 subjects that CBF increased in some brain areas (right inferior temporal gyrus, right anterior cingulate, and the left superior temporal gyrus) over 7.7 years in patients with progressive WMH.[102] Falling CBF was observed more in the posterior regions including right inferior parietal lobule and right occipital pole but was not specifically associated with WMH change.

Table 4 Results of longitudinal studies

		Bernbaum 2015[101]	Van der veen 2015[70]	Kraut 2008*[102]	Ten Dam 2007[72]
Sample size		40	575	74	390
Follow-up time (years)		1.5	3.9	7.7	2.75
CBF	at baseline	16.0±0.2 [1] (ml/100 g/min)	52.3±9.8 (ml/100 ml/min)	NA	520.0±88.0 (ml/min)
	at follow-up	NA	NA		504.0±92.0 (ml/min)
WMH (ml)	at baseline	9.21±11.87	2.86±5.44		5.27±9.60
	at follow-up	11.96±13.16	3.74±7.66		7.48±11.70
Association analysis					
bCBF and bWMH volume	Coefficient	NA	NA	NA	TWMH: OR=1.02 [95%CI: 0.86, 1.21]; PVWMH: OR=1.03 [95%CI: 0.87, 1.21] TWMH: OR=0.88 [95%CI: 0.74, 1.06]
	P value				NS
bCBF and ΔWMH volume	Coefficient	OR=0.61 [95%CI: 0.57, 0.65]	PVWMH: B[‡]=0.00 [95%CI: -0.06, 0.05] DWMH: B[‡]=0.04 [95%CI: -0.04, 0.12]		NA
	P value	<0.001	NS		
bWMH volume and ΔCBF	Coefficient	NA	PVWMH: B[§]=-0.61 [95%CI: -1.32, 0.10] DWMH: B[§]=-0.92 [95%CI: -1.56, -0.28]		NA
	P value		PVWMH: NS DWMH: <0.05		
ΔWMH volume and ΔCBF	Coefficient	NA	r=-0.37		TWMH: OR=1.17 [95%CI: 0.84, 1.46];

P value		NS	PVWMH: OR=1.32 [95%CI: 1.06, 1.66]; DWMH: OR=1.00 [95%CI: 0.79, 1.25] TWMH: NS PVWMH: 0.015 DWMH: NS
Adjusted for other variables	Age, sex, diabetes, hypertension	Age, sex, follow-up periods, baseline WMHs, cardiovascular risk factors, IMT, carotid stenosis >50%, non lacunes	Age, sex, baseline atrophy, treatment allocation, baseline CBF

CBF: cerebral blood flow; WMH: white matter hyperintensities; PVWMH: periventricular white matter hyperintensities; DWMH: deep white matter hyperintensities; TWMH: total white matter hyperintensities; bCBF: baseline CBF; bWMH: baseline white matter hyperintensities; ΔWMH: change of white matter hyperintensities; ΔCBF: change of cerebral blood flow; OR: odds ratio; CI: confidence interval; NA: not available; NS: not significant; IMT: intima media thickness.

No numeric data were available from this paper, as statistical parametric mapping methods were used as the image analysis tool;

ł CBF of tissues which were normal appearing white matter at baseline but became WMH at follow-up;

ǂ % change in PVWMH or DWHMs-natural log transformed (% intracranial volume, ICV) per decrease in baseline CBF;

§ Absolute change in CBF per % ICV PVWMH or DWMH (natural log transformed) at baseline

Discussion

WMHs are often considered to be a consequence of chronic hypoperfusion. However, while this review of all available published and some unpublished data show that high WMH load is associated with lower CBF, they do not strongly support causation. In cross-sectional studies, low CBF was observed in most of the patients with more WMHs. However, the association was dampened after removing non-age matched subjects and those with dementia, which suggests that the underlying association is between reduced CBF and age or dementia rather than just WMH. One longitudinal study (n=575) also showed a correlation between high baseline WMH volume and decrease in CBF over time, questioning whether a CBF decline causes the tissue loss or vice versa.[70]

The strengths of this systematic review include the use of well-established guidelines for meta-analysis, cautious exclusion of duplicate data, thorough analysis of different study types and sensitivity analysis of clinically-important subgroups. Some studies provided more than one comparison but we avoided double-counting the total number of participants. We used every piece of data we could obtain. Studies that recruited subjects with AD, heart failure, and depression but compared CBF between patients with and without SVD were also included. Moreover, we included papers in non-English languages, including three papers in Chinese. As most studies measured regional CBF in different brain areas, we carefully chose regions that were mentioned by at least three studies to obtain robust SMDs in meta-analyses.

There are some limitations of the review which in most part reflect the limitation of the literature. Firstly, there are differences between studies in terms of study design and imaging methods which we tried to harmonise to enable comparisons. Longitudinal studies were rare. Data for white matter regions such as centrum semiovale or immediate periventricular white matter were limited or lacking. CBF was obtained by different techniques and varied by technique. However, it is important to note that meta-analysis compares the magnitude of association within one study with that within the others, rather than making direct comparisons of CBF between studies. There are also differences in patient populations: most studies chose patients without neurological symptoms or from community-based populations, whereas three studies recruited patients with acute onset of TIA or minor stroke. Two studies used acute brain MRI as baseline imaging.[101, 104] Image analysis methods differed and few if any studies differentiated normal tissue from WMH in the ROIs, thus including more tissue affected by lesions in subjects with high WMH burdens than with few WMH – an obvious confound if measuring CBF. Secondly, as some studies divided subjects into different severity groups, we converted them into pair-wise comparisons in the form of low WMHs versus high WMHs. Therefore it is possible that disease groups in the original pair-wise studies might include some patients with mild lesions. Thirdly, the sample sizes of the studies included in meta-analyses were small – the whole analysis of 24 studies included 1161 patients (mean 48/study or 24/group). Only a few studies used age-matched controls. Patients with more severe WMHs were in general significantly older than those who had mild or no WMH, introducing an obvious confound; we addressed this in sensitivity analyses but these were underpowered for meta-regression. In addition, only one study

matched for important confounders like vascular risk factors so that sensitivity analysis for risk factors was not possible, and of course hypertension was generally more prevalent in severe WMH groups. Moreover, data for other imaging changes like lacunes or lacunar lesions are lacking.[90]

The meta-analysis demonstrated that CBF measured concurrently was significantly lower in patients with more severe WMH. Cross-sectional studies which only did regression/correlation analyses also showed an association between high WMH burden and low CBF. However, the differences between groups in most brain regions were largely attenuated by excluding dementia and non-age-matched studies, except global mean CBF and CBF in centrum semiovale which remained significant and the point estimate did not move. These results suggest that disease severity and age confound the relationship between WMH and CBF, which was again supported by results from longitudinal studies showing that high burden of WMH predated falling CBF.[70] Additionally, in regression/correlation-only cross-sectional studies where a negative association between WMH and CBF was found, the correlation tends to be significant in more severe patients.[96]

These results indicate that the reduced CBF in patients with WMH might reflect a reduction in the blood supply required by the tissue, due to reduced neuronal activity, or atrophy with fewer cells. As most included studies recorded CBF in cortical grey matter, these associations between reduced CBF and cortical atrophy should not be overlooked. Cortical atrophy is known to occur with the aging process. Results from a large cohort study demonstrated that baseline brain atrophy predicted a decline in

total CBF over time.[106] There are many imaging studies reporting an association between cortical atrophy and WMH severity.[107] However there is little information about cortical volume from included studies. Although data for white matter are limited, CBF in frontal and occipital white matter regions changed in a similar way as in grey matter. Results in DWMH and in PVWM differed: a longitudinal study showed that decreasing CBF over time was related to the progression of PVWMH rather than to that of DWMH,[72] which is in agreement with a cross-sectional study showing depressed CBF only in NAWM in periventricular regions.[85] The contradictory results from white matter indicate that there might be differential vulnerabilities for DWMH and PVWMH as these two brain areas are in different sections of the arteriolar tree.[85] However, such a suggestion is not supported by available data - studies indicate that PVWMH and DWMH are on a continuum in terms of location.[108]

The limitation of resting CBF is that it only provides information of a cut-off time point at which CBF might still be relatively preserved or compensated especially in the early stage of the disease.[109] One of the included studies showed a reduced CBF response to hypercapnia in non-demented hypertensive patients with leukoaraiosis while resting CBF was shown to be unaffected.[48] Many other mechanisms have been suggested, such as the reduced cerebral vascular reactivity which represents the dilatory ability of brain vessels, or increased vascular pulsatility.[53, 110] Risk factors such as hypertension alter the structure of penetrating arterioles by promoting lipohyalinosis and vessel wall thickening, which has led to the suggestion that cerebral arterioles might stiffen and thus cause a decrease in vasodilatory capacity or

become less able to buffer the pulsatile arterial pressure. Further studies are required to investigate how blood flow responsiveness (not just resting CBF) varies across different vessels and tissues (NAWM, WMHs and grey matter), and how it changes over the course of the disease.

Conclusion

In conclusion, despite large heterogeneities across included studies and the cross-sectional nature of most studies, this systematic review showed that CBF was negatively related to WMH severity. The results of this systematic review suggest that hypoperfusion in the whole brain and low cortical blood flow is more likely a consequence of WMH than the cause. However, whether WMH are due to focal ischaemia in particular white matter tissues and whether the development of PVWMH and DWMH differ in mechanisms still remain unanswered. This systematic review emphasizes that more data are needed for white matter, especially separate data for NAWM and WMH. Future studies should obtain longitudinal data from white matter as well as grey matter, have larger sample sizes, include appropriate control groups, stratify by and adjust for important covariates such as age, important risk factors like hypertension, clinical diagnosis, (including the type of dementia if relevant) by different features and severities of SVD, and by cognitive status. In addition, if studying patients with acute stroke, it would be better to avoid the acute phase after stroke for imaging assessments to avoid effects of the acute stroke interfering with the study of WMH. Moreover, investigation of alternative mechanisms such as impaired CVR, increased cerebrovascular pulsatility, and effects

of blood-brain barrier changes should be pursued in parallel with CBF measurement to provide new perspectives on treatment for SVD.

Updates of search after being published

Since the original search for this systematic review was undertaken before December 2015, I updated the search from December 2015 to September 2017 when writing up this thesis. Six studies were identified, including four cross-sectional studies[111-114] (n=269, median=31, range 22-185) and two longitudinal studies (n=290)[115, 116]. As most studies are not suitable for a meta-analysis and had very small sample sizes, I summarised the results in Table 5. Most of the cross-sectional studies found an association between WMH and low CBF in the white matter rather than in the cortical grey matter or global CBF, after the adjustment for age. In one longitudinal study with AD patients (n=38), those who had a higher burden of WMH at baseline showed a more severe CBF decline during a two-year follow-up.[115] In the other longitudinal study (n=252), white matter CBF at baseline was neither associated with baseline WMH burden or WMH progression over five years. [116] These results, especially those of the longitudinal studies, are not only consistent with the original conclusion that low global or cortical blood flow is unlikely the cause of WMH, but in addition further question the cause and effect between WMH and low blood flow in the white matter.

Table 5 Summary of studies on CBF and SVD since December 2015

	sample size	Patient populations/groups	Age at recruitment (years)	Follow-up duration (years)	CBF technique	Summary of results	Adjusted or matched for age
Longitudinal studies							
Nylander R, 2017[116]	252	community-dwelling elderly population	75	5	DSC	Baseline CBF not associated with baseline WMH volume or WMH change over time	yes
Hanaoka T, 2016[115]	38	Alzheimer's disease with WMH at baseline (n=24)	77.2± 7.9	2	SPECT	more severe CBF decline in the cingulate gyrus, parahippocampal gyrus and frontal gyrus	no
		Alzheimer's disease without WMH at baseline (n=14)	74.9 ± 6.8	2			
Cross-sectional studies							
Bahrani A, 2017[111]	26		77.8 ± 6.8	-	ASL	parietal periventricular WMH volume associated with lower CBF frontal, occipital, parietal and temporal lobe	no
Liu J, 2016[113]	36	SVD (n=23)	not known	-	ASL	lower CBF in the right centrum semiovale	not known
		No SVD (n=13)	not known	-			
Hashimoto T, 2016[112]	22	lacunar stroke with ≥ 5 CMBs)	69±7	-	PET	lower CBF in the centrum semiovale, but not in the cortex or basal ganglia	yes
		lacunar stroke with < 5 CMBs)	68±8	-			
van Dalen J.W. 2016[114]	185	community-dwelling elderly population	77±2	-	ASL	WMH volume associated with reduced WMH CBF but not grey matter or NAWM CBF	yes

CBF: cerebral blood flow; SVD: small vessel disease; WMH: white matter hyperintensities; DSC: dynamic susceptibility contrast; SPECT: single photon emission computed tomography; ASL: arterial spin-labelling MRI; PET: positron emission tomography; CMB: cerebral microbleeds; NAWM: normal appearing white matter

Chapter 2B: Intracranial pulsatility in patients with cerebral small vessel disease: a systematic review

Introduction

Increasing evidence suggests that increased vascular pulsatility might be an alternative mechanism of SVD. Autopsy studies showed lipohyalinosis or arteriolosclerosis in the small arteries in the vicinity of "lacunes",[13] WMH[117] or microbleeds.[118] Aging and hypertension are important risk factors for SVD,[119] both of which are associated with loss of elasticity in the vessel walls. It is possible that the stiffened vessel walls would be less able to dampen the arterial pressure pulse via the *Windkessel* effect, leading to high pulsatility being transmitted into the brain and causing or exacerbating vessel and brain tissue damage.[120]

Some large cohort studies have shown a relationship between increased aortic pulsatility and lacunar infarcts or WMH volume [60, 61] However, fewer studies assessed pulsatility in the intracranial vessels. Doppler ultrasound and MRI are two main techniques that have been used to measure intracranial pulsatility. Doppler ultrasound measures the real-time blood flow velocity in the large arteries, mainly ICA and MCA if using TCD. Pulsatility was generally calculated using Gosling's equation (pulsatility index, PI = (peak systolic velocity – peak diastolic velocity)/mean velocity)).[121] There have been cross-sectional studies showing that high ICA[57] (n=700) or MCA[122] (n=159) PI was associated with larger WMH volume. However, the limitation of ultrasound is that it only assesses pulsatility in one particular artery at a time and does not provide information on smaller arterioles, CSF or venous pulsatility.

Phase-contrast MRI can quantify fluid velocity and flow in the intracranial arteries, veins, and CSF. It has mostly been used in disorders such as hydrocephalus that present with abnormal CSF dynamics[123] with few studies in SVD. Vascular PI was also used in MRI studies, calculated using similar equations to ultrasound (flow was used instead of velocity), but indices reported for pulsatility in CSF vary.[124, 125] It is unclear which measures are most relevant and reliable for quantifying intracranial pulsatility in SVD patients.

Furthermore, it is uncertain if high pulsatility and SVD were both simply the result of exposure to vascular risk factors, since some studies also did not adjust for age or important risk factors when assessing the relationship between intracranial pulsatility and SVD.[124] Also, WMH are commonly used by studies to represent SVD burden,[57, 124, 125] and it is not known whether high pulsatility was also related to other features of SVD, such as lacunar stroke or enlarged PVS.

In order to provide a complete summary of all knowledge to date on intracranial pulsatility in patients with SVD, in this chapter, wewill systematically review papers that used either ultrasound or MRI to measure cerebral pulsatility in SVD with a view to performing a meta-analysis. We aimed to determine if there was an association between pulsatility and SVD, the magnitude of any association, whether it was cross-sectional or measured pulsatility and SVD progression longitudinally, and if any individual SVD features were more strongly associated with pulsatility than others.

Several colleagues have contributed to the work mentioned in this chapter. I conceived the idea of this systematic review and designed the search and data

analysis plan. Dr Michael J Thrippleton (M.J.T.) helped revise the searching strategy. I undertook the search, data extraction, data analysis and then drafted the paper. M.J.T., Prof Ian Marshall and Prof Joanna M Wardlaw double checked the result of data extraction, revised the drafts and helped with the table/figure design. "We" in this chapter, wherever mentioned, indicates the above-mentioned people including myself.

Methods

We performed this review according to the MOOSE guidelines for meta-analysis of observational studies.[68] We conducted a literature search of Ovid MEDLINE and Embase from 1946 up to April 2017 using the Ovid Web Gateway. We searched terms related to pulsatility and SVD in all contents of the papers using the strategy: "Pulsatility" or "Resistance" or "Velocity" or "cerebrospinal fluid pulsatility" or "Phase-contrast MRI" and "Cerebral small vessel disease" or "White matter hyperintensities" or "Leukoaraiosis" English and non-English literature were sought. Additional records were identified by hand from relevant reviews, primary papers and from the authors' publication lists. The search and screening was done by myself and cross-checked with a second person if there was any uncertainty. We defined SVD features according to the STRIVE Guideline.[7]

Eligibility Criteria

We included papers that reported primary results of studies that: 1. recruited participants with SVD features; 2. assessed resting-state intracranial pulsatility (including ICA) using any imaging technique; 3. assessed the relationship between

intracranial pulsatility and SVD. We only included studies that focused on sporadic SVD in this review as the mechanisms for hereditary SVDs might differ. We excluded review papers, abstracts, and papers that used pharmacological, CO_2 or other stimuli without providing pre-stimulus data.

Data extraction

We extracted data on participant characteristics, study design, MRI or Doppler technicalities, location and type of pulsatility indices assessed. For studies that compared pulsatility between groups and reported means and SDs, we extracted the results of the comparisons from text or tables where available, or from graphs where necessary; for those that performed association analysis such as correlation or regression models, we extracted the statistical methods, coefficients, P values and confounding factors or covariates (if any) that were adjusted for. For studies that performed both non-adjusted and adjusted analysis, we only included the adjusted results. We assessed the study quality using a checklist devised on the basis of the STROBE statement (www.equator-network.org) and the one I showed in Chapter 2A.[126]***(Table 6)***

Table 6 Checklist for quality assessment

Prospective study?	yes/no (1/0)
Clearly reported study population (stroke, aging cohort, etc.)?	yes/no (1/0)
Clearly defined inclusion criteria?	yes/no (1/0)
Clearly defined SVD?	yes/no (1/0)
Clearly reported MRI acquisition and image processing?	yes/no (1/0)
Observers blinded to clinical data?	reported/not reported (1/0)
Reported number of & expertise of observers of SVD images?	reported/not reported (1/0)
Adjusted/matched for risk factors (including age)?	yes/no (1/0)
Reported drop-out (how the final sample was reached)?	yes/no (1/0)
Reported participants' demographics and vascular risk factors/medical conditions	yes/no (1/0)
Overall score (/10)	

The 10 point study quality checklist applied to all included studies. It was devised using influences from the STROBE statement (https://www.strobe-statement.org/) and Shi. Y et al. 2016.[126]

Statistical analysis

We displayed the results of comparisons between groups using forest plots in the Cochrane Collaboration's Review Manager (Revman Version 5.3) and used SMD to represent the difference between groups. We did not include data from studies that did not provide standard deviations, because the SMD is inestimable without standard deviations. In this review, we were not able to perform robust meta-analyses because of the limited data and the large heterogeneity in study populations and pulsatility measures. Therefore, in the forest plot we did not calculate overall effect sizes. For studies that divided patients into more than two grades of WMH severity, we combined the means and SD of groups to create a single pair-wise comparison using formulae from the Cochrane handbook which I described in chapter 2A. We condensed data into new groups "mild WMHs" indicating none to punctuate WMHs (e.g. Fazekas deep WMH score 0 to 1), and "severe WMHs" as confluent WMHs (e.g. Fazekas deep WMH score 2 to 3).(***Equation 1*** in Chapter 2A**)**

Results

The search strategy identified 518 papers, of which 48 were potentially eligible and 27 were ultimately selected for further review.***(Figure 10)*** We excluded reviews (3), drug trials without providing baseline information on pulsatility and SVD (2), non-SVD (sporadic) study (8), studies that used stimulus only (2) or did not assess intracranial pulsatility (6). One MRI study compared CSF pulsatility between patients with late-life depression and age-matched healthy volunteers but we

included the results in the forest plot because patients had higher WMH burden than the healthy volunteers.[65]

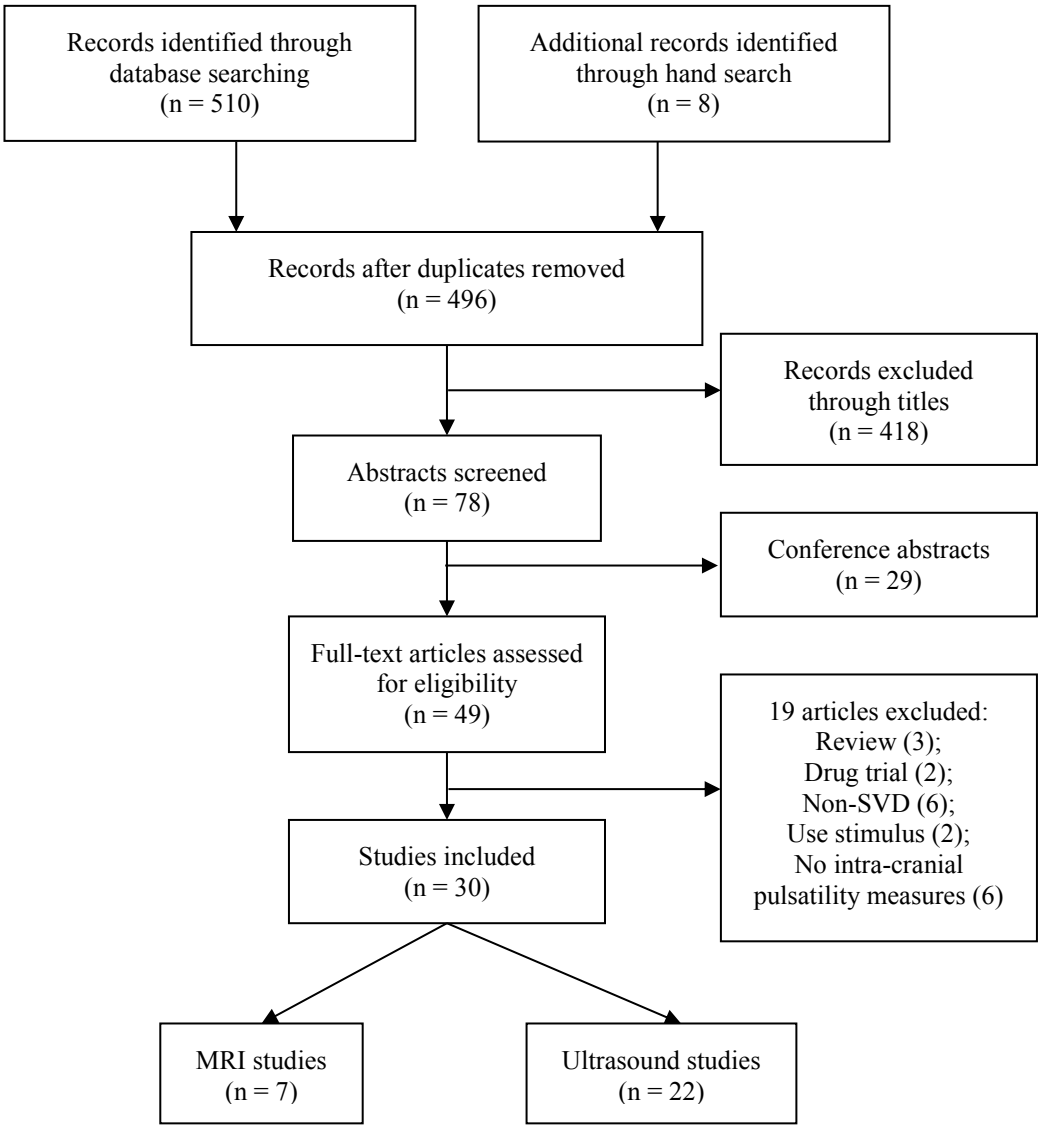

Figure 10 PRISMA flow diagram of literature search and its results

Characteristics of included studies

Twenty-seven (n=3356) were included, of which 20 used ultrasound[57, 59, 97, 122, 124, 127-142] and seven used MRI to measure pulsatility,[58, 64, 65, 125, 143, 144] 26/27 were cross-sectional and one was a clinical trial of cilostazol[141] from which we only extracted the data obtained at baseline.

Doppler ultrasound studies

Table 7 summarises patient characteristics from 20 ultrasound studies (n=2935) with sample sizes ranging from 9 to 700 (median=107). Fourteen used WMH (if MRI used for structural brain imaging) or white matter hypoattenuation (if CT used) to represent SVD burden. Two studies included patients with stroke: one compared pulsatility between lacunar and non-lacunar ischaemic stroke,[133] and one compared pulsatility between patients with lacunar stroke (according to TOAST classification) and age- and sex-matched healthy controls.[138] One study included patients with multi-infarct dementia[130] and one recruited patients with cerebral amyloid angiopathy (CAA).[137] ***(Table 7)***

Three studies assessed pulsatility in the ICA (cervical), seventeen in the MCA, one in the basilar artery, one in the posterior cerebral artery (PCA) and one in the central retinal artery. Most studies calculated PI using Gosling's equation. One study one measured brain tissue pulsatile movement.[128]

Table 7 Patient characteristics of Ultrasound studies

First Author	Subjects/disease	Sample size	Group	Age (years)	Vessels of interest
Sanahuja 2016[136]	Type 2 Diabetes	202	Higher SVD score (n=21) Lower SVD score (n=181)		MCA
Del Brutto 2015[139]	Community	70	Mild WMH (n=42)	72.2±5.5 77.4±7.34	MCA ,Vertebral artery
Ghorbani 2015[140]	Patients who had SVD on imaging	104	Patients who had WMH or lacunar infarct on MRI Patients who had no lesion on MRI	68.4 62.6	MCA
Turk 2015[129]	Leukoraiosis	96	Leukoaraiosis (n=52) Age and sex-matched healthy volunteers (n=44)	54.9±8.3 52.39±7.34	ICA
Aribisala 2014[57]	Lothian birth cohort 1936	700	-	70	ICA
Ternifi 2014[128]	Healthy volunteers	9	-	70.56±5.46	Brain tissue displacement
Sargento-Freitas 2014[135]	Patients who visited neurosonology lab	439	-	63.47±14.94	MCA
Purkayastha 2014[134]	Patients with vascular risk factors	48	-	75±7	MCA
Han 2014[141]	Lacunar stroke	130	-	64.7	MCA

Webb 2012[59]	TIA or minor stroke	110	Fazekas 3 (n=25) Fazekas 2 (n=24) Fazekas 1 (n=21) Fazekas 0 (n=30)	74.9±7.9 68.5±11 66.5±12 53±15	MCA
Mok 2012[122]	Community	205	With severe WMH without severe WMH	74±6 69±6	MCA
Heliopoulos 2012[97]	Hypertensive patients	52	-	71.4±4.5	MCA
Bettermann 2012[142]	Patients with WMH	26	Patients with WMH Control without WMH	63.5±11.25 55.07±7.91	MCA
Rodriguez 2010[133]	Ischaemic stroke	186	Lacunar (n=35) Non-lacunar (n=151)	69.7±10.8 71.6±8.1	MCA
Tanaka 2009[127]	Diabetic patients	122	Hypertensive (n=43) Non hypertensive (n=79)	66.9±9.8 62.0±11.0	ICA
Smith 2008[137]	CAA	20	CAA (n=11) Healthy volunteers (n=9)	73.5±7.4 70.9±7.9	Basilar artery
Kidwell 2001[131]	Retrospective review in patients who had both TCD and MRI	55	-	62(range 28-98)	MCA
Sánchez-Pérez 2003[132]	Patients (>60 years) who visited neurological department for minor symptoms	116	-	74.44±6.35	MCA
Hiroki 2002[138]	Stroke	167	Small vessel disease (TOAST)	70.9±9.0	Central retinal

			(n=103) age and sex-matched controls (n=64)	69.7±8.8	artery
Biedert 1995[130]	Dementia	78	Multi-infarct dementia (n=19) AD (n=23) age-matched healthy volunteers (n=36)	Age range 60-69 for all	MCA, basilar artery

MCA: middle cerebral artery; SVD: small vessel disease; WMH: white matter hyperintensities; MRI: magnetic resonance imaging; ICA: internal carotid artery; TIA: transient ischaemic attack; CAA: cerebral amyloid angiopathy; TCD: transcranial Doppler; AD: Alzheimer's disease.

MRI studies

Patient characteristics and scanner information of seven MRI studies (n=421, range 35-101, median=51) are shown in Table 8. Three studies recruited patients with dementia or cognitive impairment, including idiopathic dementia,[124] AD,[64] vascular dementia[64] and mild cognitive impairment.[143] Only one reported the diagnosis criteria for Alzheimer's disease and vascular dementia.[64] One study recruited patients with the late onset major depressive disorder.[65] Three studies recruited healthy volunteers (age range: 43-82; 18-75; 62-82 years).[58, 125, 144] ***(Table 8)***

All seven studies used phase-contrast MRI. Four studies used 1.5 Tesla and three used 3 Tesla scanners. All studies used retrospective gated phase-contrast MRI: four used peripheral pulse- and two used electrocardiogram (ECG)- gating; four studies reported the numbers of time points measured per cardiac cycle, among which three used 32 whereas one used 16 time points.***(Table 8)***

Table 8 Patient characteristics and scanner information of MRI studies

First author	Subjects/disease	sample size	Groups	Age (years)	Scanner and sequences	TE/TR (ms)	Venc	Time points per cc
Beggs 2016[125]	Healthy volunteers	101	-	44.7±17.8 (range 18-75)	GE 3 Tesla; Retrospectively peripheral pulse-gated 2-D phase contrast cine sequences	7.9/40	20 cm/s aqueduct	32
Wåhlin 2014[144]	Healthy volunteers	37	-	71±6	Philips 3 Tesla; Retrospectively peripheral pulse or ECG-gated 2-D phase contrast cine sequences	6-11/10-16	70 cm/s for arteries and 7 cm/s for CSF	32
Jolly 2013[58]	Healthy volunteers	35	-	65.67±9.31 (range 43-82)	Siemens 3 Tesla; Retrospectively ECG-gated 2-D phase contrast cine sequences	6.9/26.5	Arteries 75 cm/s, veins 40 cm/s, CSF 22 cm/s	Not mentioned
Henry-Feugeas 2009[143]	Mild cognitive impairment	71	significant WHM (n=42) no significant WHM (n=29)	74±5 69±5	GE 1.5 Tesla; Retrospectively ECG-gated 2-D phase contrast cine sequences	7.6-9.9/20-23	Not mentioned	16
Bateman 2008[64]	Senile dementia	48	AD (n=12) Vascular dementia (n=12) Normal aging (n=12)	76±4 70±11 70±5	Siemens 1.5 Tesla; Retrospectively ECG-gated 2-D phase contrast cine sequences	7/29	Arteries 75 cm/s, veins 40 cm/s, CSF 10 cm/s	Not mentioned

			Normal young (n=12)	25±12				
Naish 2006[65]	Late onset major depressive disorder	51	Responders to antidepressant monotherapy (n=21)	71.0±6.54	Philips 1.5 Tesla; Retrospectively peripheral pulse-gated 2-D phase contrast cine sequences	7-8.2/14-15 ms	Not mentioned	16
			Non responders (n=8)	75.2±6.18				
			Age-matched control (n=22)	72.9±5.38				
			Young (n=19)	27.5±4.4				
Bateman 2002[124]	Idiopathic dementia	78	Fazekas 0 (n=10)	71±8	1.5 Tesla; Retrospectively ECG-gated 2-D phase contrast cine sequences	7/29 ms	Not mentioned	Not mentioned
			Fazekas 1(n=18)	75±8				
			Fazekas 2 (n=24)	76±7				
			Fazekas 3 (n=8)	77±8				
			Healthy controls (n=18)	42±17				

cc: cardiac cycle; TE: Echo time; TR: repetition time; Venc: velocity encoding parameter; ECG: electrocardiogram; WMH: white matter hyperintensities; AD: Alzheimer's disease; CSF: cerebrospinal fluid.

There were large differences between studies as to where flow was measured. Figure 11 shows the ROIs used in these studies. Six included the ICA(s);[58, 64, 124, 125, 143, 144] in posterior circulation five chose the basilar artery[58, 64, 124, 125, 143] and one selected the vertebral arteries[144]; four studied pulsatility in the venous sinuses;[58, 64, 124, 143] six measured CSF flow, among which one selected the cervical subarachnoid spaces,[144] one selected tentorial incisura,[64] and four measured the cerebral aqueduct.[58, 65, 125, 143] In total, three studies measured flow or pulsatility across the cerebral arteries, veins and the CSF system.[64, 65, 143] ***(Figure 11)***

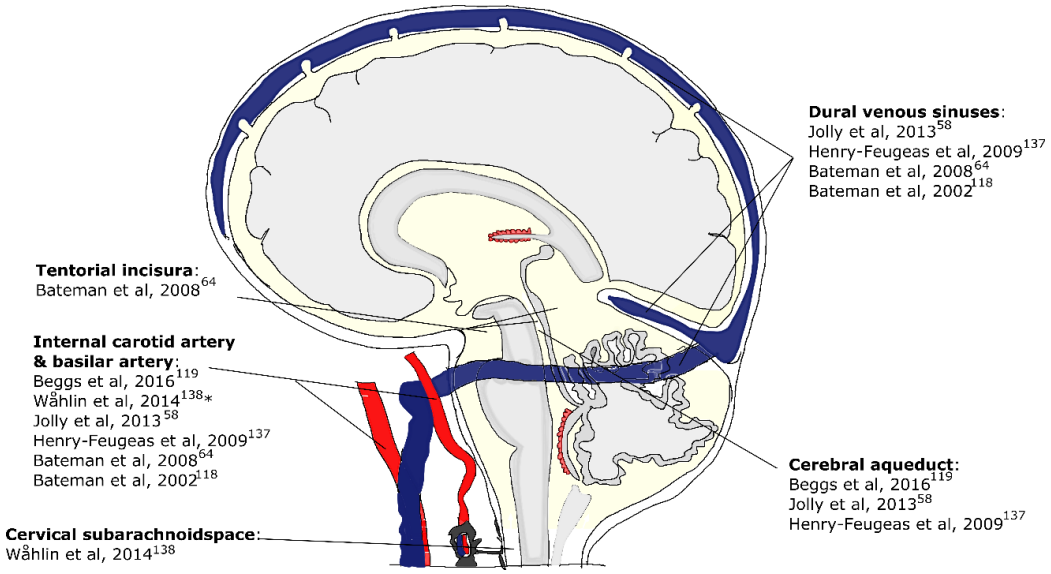

Figure 11 Regions of interest for flow measurement used in phase-contrast MRI studies included in this review. *Anders Wahlin et al. selected the vertebral arteries instead of the basilar artery.[138]

Quality assessment

The average quality score of 27 studies was 6.85/10. 26/27 studies were prospective. However, seven studies did not report participants' demographic information or general health condition. Only about half of the studies adjusted or matched for risk factors (15/27) or reported the expertise of observers of structural MRI (15/27). Less than half of the studies reported dropout (12/27) or use of blinding in structural image analysis (11/27). ***(Figure 12)***

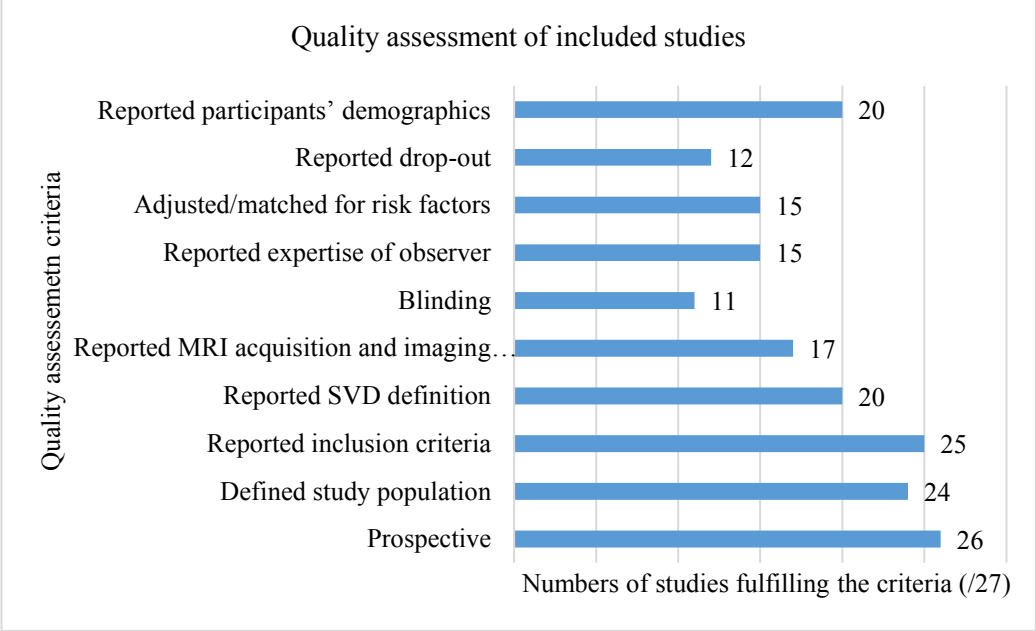

Figure 12 Quality assessment of included studies

Result of comparisons of pulsatility measures

Doppler ultrasound studies

Three studies (n=356, median=96) compared arterial PI between patients with different WMH severities. One study examined the ICA, one chose MCA, and one chose both MCA and basilar artery. PI was generally higher in patients with more severe WMH in the ICA,[129] MCA[122, 130] and the basilar artery[130] (e.g. in MCA: SMD= 3.24, 95% CI [2.4, 4.07]), although the result for ICA did not reach statistical significance (SMD= 0.38, 95% CI[-0.02, 0.79]).[130] 2/3 of the studies were age-matched[129, 130] and one of them also matched for gender.[129] ***(Figure 13A)***

Two studies looked at other SVD features. One study (n=167) showed that patients with lacunar stroke (TOAST) had higher PI in the central retinal artery compared to age- and sex-matched healthy controls (SMD=0.35, 95% CI[0.03, 0.66]).[129] ***(Figure 13B)*** One study of CAA (n=20) found that patients with CAA had a significantly higher PI in PCA than non-age-matched healthy elderly controls (SMD=1.07, 95% CI[0.12, 2.03]).[129] ***(Figure 13C)***

MRI studies

Three phase-contrast MRI studies (n=124, median=50) performed comparisons of cerebrovascular or CSF pulsatility between patients with different WMH severities. None of them corrected for age. The indices for pulsatility included PI, stroke volume, and the delay between waveform peaks. The trend in all the comparisons is that higher arterial or venous PI (e.g. arterial PI: SMD=0.93, 95% CI[0.40, 1.47]),[124] larger arterial or venous or CSF stroke volume (e.g. CSF stroke volume: SMD=1.58, 95% CI[0.64, 2.52])[64] was associated with more WMH, although some results did

not reach a statistical significance (e.g. venous PI: SMD=0.18, 95% CI[-0.33, 0.69]).[124] ***(Figure 13D)***

Two studies (n=110) calculated the delay between waveform systolic peaks. There was no significant difference in arterial-venous (n=60, SMD= 0.95% CI[-0.51, 0.51])[64] or arterial-aqueduct peak delays (n=51, SMD=0.49, 95% CI[-0.07, 1.06])[65] between different severities of WMH. ***(Figure 13E)***

A. Doppler ultrasound: Pulsatility (ICA, MCA or basilar artery) vs WMH

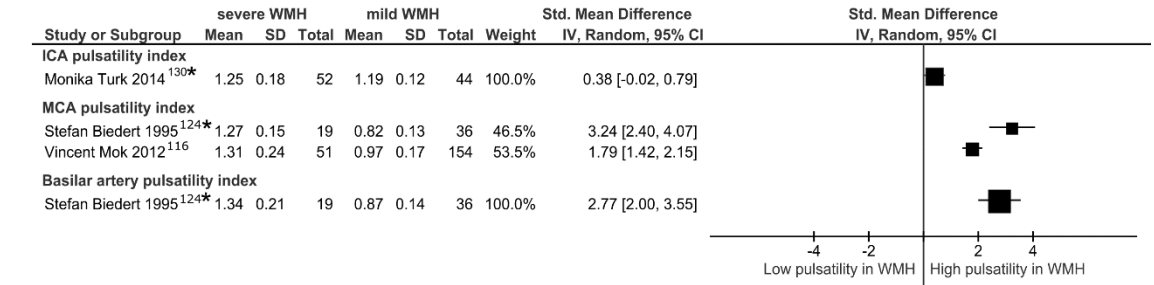

B. Doppler ultrasound: Pulsatility (central retinal artery) vs SVD (in TOAST)

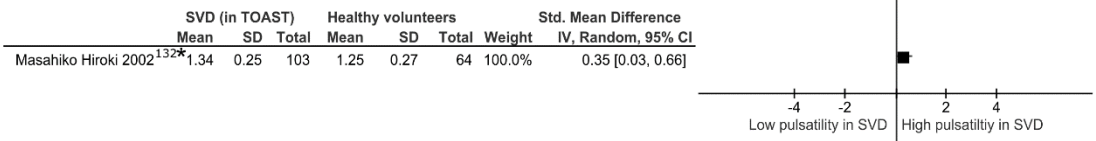

C. Doppler ultrasound: Pulsatility (posterior cerebral artery) vs CAA

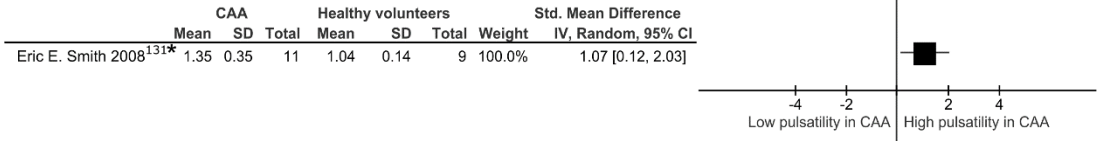

D. MRI: Intracranial pulsatility (arteries, veins or CSF) vs WMH

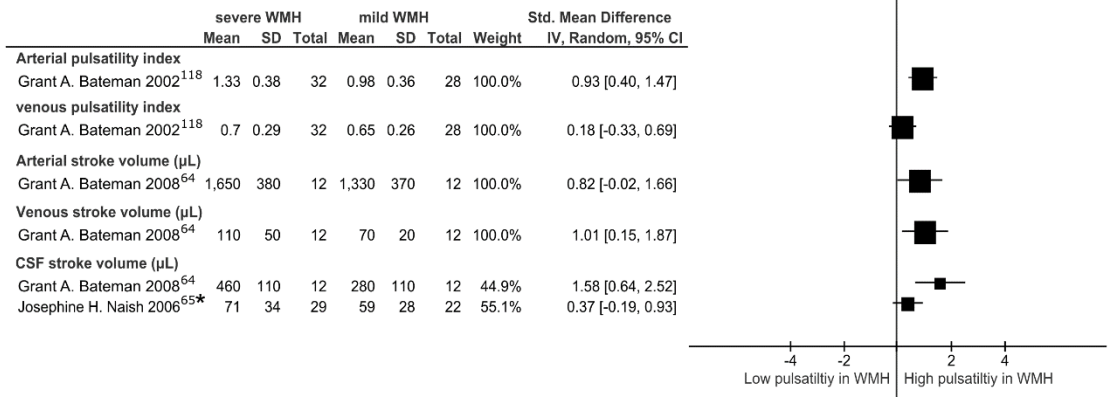

E. MRI: Flow waveform peak delays vs WMH

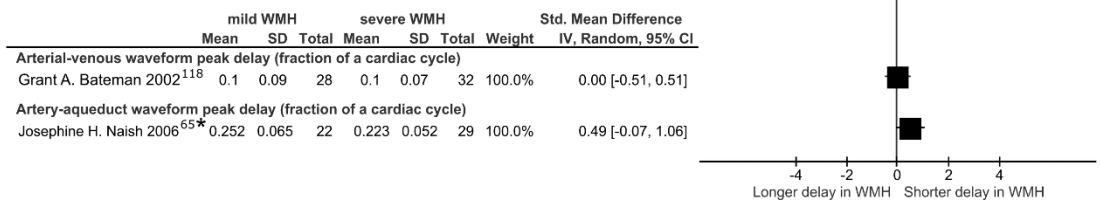

Figure 13 Forest plots of studies that compared pulsatility (using Doppler ultrasound or MRI) between SVD and control groups. *indicates studies that matched for age. A-C: Pulsatility was measured by Doppler ultrasound. A. Comparison of vascular pulsatility between patients with severe and mild white matter hyperintensities (WMH); B. Comparison of central retinal artery pulsatility between patients with SVD-stroke (TOAST classification) and healthy volunteers; C. Comparison of posterior cerebral artery pulsatility between patients with cerebral amyloid angiopathy (CAA) and healthy volunteers;

D and E: pulsatility was measured by phase-contrast MRI. D. Comparison of vascular or CSF pulsatility between patients with severe and mild WMH; E. Comparison of flow waveform peak delays between patients with severe and mild WMH. It is worth noting that, in forest plot E, shorter peak delay is suggested by the authors to represent higher intracranial stiffness.

Results of studies that performed regression or correlation analysis

Table 9 summarises studies that performed regression or correlation analysis, including 13 Doppler ultrasound (n=9-700, median=116) and three MRI studies (n=35-100, median=37). 14/16 studies adjusted for covariates, of which twelve included age. No studies adjusted for blood pressure although five considered the history of hypertension.

Doppler ultrasound studies

Two studies measured ICA and eleven measured MCA. Most studies (apart from two[127, 132]) reported a significant association between increased ICA or MCA PI and more WMH after adjustment for age. One (n=186) found that higher MCA PI was predictive of having a lacunar infarct (vs other types of infarct).[133] One paper (n=159) mentioned that they did not find a significant association between MCA PI and microbleeds or lacunes, although no detailed information was provided.[122]

One study (n=9) found that higher brain tissue displacement, which was used for representing brain tissue pulsatility, was significantly correlated with larger WMH volume, however it did not adjust for any co-variates.[128] ***(Table 9)***

MRI studies

All three MRI studies adjusted for age. Two assessed WMH volume: increased WMH volume was found to be significantly associated with higher CSF systolic peak velocity in one study (n=101, β= -124.903, P=0.041),[125] but not with arterial or venous pulsatility (pulse amplitude, pulse width or PI) in the other (n=35).[58]

One study (n=37) found that increased arterial PI and cervical CSF pulsatility were associated with smaller brain volume in healthy volunteers.[144] ***(Table 9)***

Table 9 Results of correlation analyses in MRI and Ultrasound studies

First author	Sample size	Correlation or regression models	Variables (y~x)	Coefficient	P value	Adjustment for confounding factors
Ultrasound studies						
ICA						
Aribisala 2014[57]	700	Multiple variable regression	WMH volume ~ ICA PI	β=0.09	0.016	Age, sex, ICV, HBp history
Tanaka 2009[127]	122	Multivariate regression analysis	WMH volume ~ ICA PI	not shown	>0.05	Age
MCA						
Brutto 2015[139]	70	Generalised linear model	WMH severity ~ MCA PI	β=0.065, 95% CI[-0.474 0.084, 0.177]		Age, sex, the cardiovascular health status
			WMH severity ~ vertebral artery	β=0.066, 95% CI [-0.024, 0.156]	0.146	
Sargento-Freitas 2014[135]	439	Multiple ordinal regression	DWMH score~ MCA PI	OR 17.994, 95% CI [6.875, 47.11]	<0.001	Age, sex, HBp history, DM, smoking, dyslipidemia, coronariopathy, heart failure, obesity, peripheral artery disease, alcoholism, IMT
			PVH score ~ MCA PI	OR 5.739, 95% CI [2.288, 14.397]	<0.001	
			Basal ganglia score ~ MCA PI	OR 11.844, 95% CI [4.486, 31.268]	<0.001	

Han 2014[145]	130	Pearson correlation	WMH volume ~ MCA PI	R=0.195	0.026	No
Purkayastha 2014[134]	48	Multivariable linear regression	WMH/ICV~ MCA PI	OR 1.25, 95% CI [0.14, 2.09]	<0.01	Age, sex, race, DM, HBp
Webb 2012[59]	110	Ordinal regression	WMH score ~ MCA PI	Beta = 4.33	P=0.037	Age, sex, physiology
Mok 2012[122]	159*	Multiple logistic regression	Severe WMH (vs without severe WMH) ~ MCA PI	OR=1.33, 95% CI [1.04,1.70] per 0.1 increase in PI	<0.01	Age
Heliopoulos 2012[97]	52	Multivariable regression	WMH score ~ MCA PI	beta=0.262	P=0.025	Age, sex, BMI, HBp, DM, hyperlipidemia, smoking
Rodriguez 2010[133]	186	Multivariate logistic analysis	Lacunar infarct (vs non-lacunar) ~ MCA PI	OR=8.13, 95% CI [1.17, 56.27]	0.034	Previous ranking score, WMH, retinal microangiopathy
Sánchez-Pérez 2003[132]	116	Multiple linear regression	Leukoaraiosis severity score ~MCA PI	β=-0.108	0.353	Age, sex, vascular risk factors, cognitive performance, blood flow velocity in MCA
Kidwell 2001[131]	55	Multivariate regression	WMH score ~ MCA PI	0.71	P<0.05	Age, sex, HBp, coronary artery disease
Brain tissue pulsatility						
Ternifi 2014[128]	9	Non-parametric spearman correlation	WMH volume ~ Max BTD	ρ=-0.86	<0.001	No
			WMH volume ~ Mean BTD	ρ=-0.72	<0.001	No
MRI studies						
Beggs 2016[125]	101	Multiple linear regression	total WMH volume ~ CSF peak negative velocity	β =-124.903	P=0.041	Age
Wåhlin 2014[144]	37	Ordinary linear regression	Total brain volume ~ arterial PI	β = -0.42	P<0.01	Age, ICV, arterial net flow

			Total brain volume ~ CSF flow volume pulsatility	β = -0.44	P<0.01	Age, ICV, arterial net flow
Jolly 2013[58]	35	Partial correlation	WMH volume ~ pulse wave amplitude in arteries or venous sinuses	not shown	P>0.05	Age
			WMH volume ~ pulse width in arteries or sinuses	not shown	P>0.05	Age
			WMH volume ~ PI in arteries or venous sinuses	not shown	P>0.05	Age

WMH: white matter hyperintensities; CSF: cerebrospinal fluid; PI: pulsatility index; ICA: internal carotid artery; ICV: intracranial volume; BTD: brain tissue displacement; MCA: middle cerebral artery; DWI: diffusion-weighted imaging; SD: standard deviation; CI: confidence interval; DWMH: deep white matter hyperintensities; PVH: periventricular white matter hyperintensities; OR: odds ratio; DM: diabetes mellitus; IMT: intima-media thickness; HBp: hypertension. BMI: body mass index.

*The original sample size of this study was 205 but only 159 participants were included in the analysis.

Discussion

We identified 27 studies that assessed intracranial pulsatility in relation to SVD including 3356 SVD subjects. Most studies found a significant association between increased intracranial pulsatility and SVD. However, these studies showed considerable heterogeneity with regard to participants' characteristics, adjustment for covariates, image acquisitions, vessels of interest, and pulsatility measures. About half of the studies gave little detail on control of bias, such as the use of blinding, or on the expertise in SVD image assessment. We were not able to perform meta-analyses due to the substantial heterogeneities and limited data.

The limitations of the literature include that SVD features differed or were assessed differently across studies. Most studies used WMH volume or semi-quantitative score to represent SVD burden. Only half of the papers reported the expertise of the observers doing the SVD rating. Three studies used symptomatic lacunar ischaemic stroke as the SVD feature: two referred to subcortical infarct on imaging whereas one used the definition of "small vessel disease" in the TOAST classification. Although there might be some overlap between the two definitions, "small vessel disease" in TOAST involves clinical features and consideration of vascular risk factors and does not necessarily need imaging evidence.[146] Studies that assessed pulsatility in relation to other SVD features including lacunes,[122] microbleeds[122] or atrophy[144] were rather scant and some lacked details of the analysis. Although some have hypothesised that perivascular spaces become enlarged and more visible in the presence of high pulsatile flow,[39, 40] so far no studies have reported the relationship between cerebrovascular pulsatility and perivascular spaces visibility.

A third of papers provided little detail on patients' demographic or health characteristics. Age and blood pressure are thought to influence intracranial pulsatility[147, 148] and are also important risk factors of SVD,[11] therefor they should be adjusted for in relevant studies. Most studies that performed correlation or regression analysis have adjusted for age, but in studies that performed comparisons of WMH, patients with more severe WMH were significantly older than those with mild WMH.[59, 124, 142, 143] Very few studies accounted for blood pressure in their analyses although some included history of hypertension as a covariate.

Indices used to represent pulsatility also varied. Most studies focused on ICA or MCA. When calculating vascular PI, both MRI and ultrasound studies applied Gosling's equation. However, some MRI scanners only collected flow value at 16 time points in the cardiac cycle,[65, 143] and low temporal resolution might affect the accuracy of the PI value as the peak flow might have been missed. Although the reliability of Gosling's PI in representing vascular resistance has been questioned,[149] there is evidence that ICA and MCA PI are well correlated with cerebrovascular reactivity measured using CO2 stimulus or invasive monitoring.[150, 151] The agreement between PI derived from MRI and from ultrasound was generally moderate.[152, 153] Two studies measured brain tissue pulsatility using ultrasound or BOLD MRI, but both had a very small sample sizes thus the validity needs to be tested in larger samples.[128, 154]

Apart from including large arteries, four MRI studies also considered pulsatility in veins and CSF. According to *Windkessel* theory, the venous system and CSF are also important components in compensating for arterial pressure.[62] Two studies calculated venous PI[58, 124] and one measured venous stroke volume.[64] CSF pulsatility

assessment varied in terms of both locations and indices. There is so far no accepted definition of pulsatility in CSF, although stroke volume seemed to be the most used. Futures studies need to test the reliability of different measures and also select ones that provide more relevant measurements of pulsatility. In addition, one MRI study measured the delay between arterial peak and venous sinus peak whereas another looked at the delay between arterial blood and aqueduct CSF pulsations. These two measures also might be non-comparable, as it has been suggested CSF pulse through the aqueduct is associated with capillary expansion whereas the venous pulse at neck level relates more directly to arterial expansion.[62] So far no studies have measured pulsatility in smaller vessels than MCA. Techniques such as 4D phase-contrast MRI or 7-T MRI which enables the assessment in multiple vessels including perforating arteries,[155, 156] or ultra-fast magnetic resonance encephalography which might be able to measure pulsatility in glymphatic system,[157] could be considered by future SVD studies.

Despite these heterogeneities, generally most cross-sectional studies have found that arterial or venous pulsatility was associated with worse SVD, although the relationship could be confounded by risk factors, particularly age and blood pressure. For ICA, one community based-study (n=700) with all participants aged 70 years that adjusted for age and other medical covariates found increased ICA PI to be independently associated with larger WMH volume,[57] whereas in another study of diabetic patients the significance of the association disappeared after adjustment for age.[127] The relationship between increased MCA PI and WMH or lacunar infarct was found in most studies after adjustment for confounding factors. We are unable to draw conclusions on the relationship between CSF pulsatility and WMH because of

different indices and locations used in each study, but the trend seems to be that larger CSF stroke volume is related to more WMH. It was also impossible to conclude if any specific SVD features are more associated with pulsatility due to the very limited data on any features other than WMH.

This is the first study to comprehensively summarise studies that have measured intracranial pulsatility in relation to SVD. The strengths included a systematic search including papers in non-English languages and a careful assessment of all included studies. However, we were not able to perform a meta-analysis due to many sources of heterogeneity, or to pool the results of association analyses as regression analyses were performed differently in each study.

In conclusion, most of the data support a cross-sectional association between SVD and higher pulsatility in large intracranial arteries such as MCA and ICA, although whether a specific SVD feature is more related to high intracranial pulsatility remains unknown, and it is not known if high pulsatility leads to more WMH or more WMH leads to higher pulsatility. Therefore, methodologically robust longitudinal studies are required to establish the cause and effect. Future studies should clearly define participants' clinical features, use blinding, improve expertise in SVD assessment, and adjust for relevant covariates. Agreement on reliable measures of intracranial pulsatility is also needed to allow for better comparison between studies, especially for CSF pulsatility. Although Doppler ultrasound might be affordable and more widely used, MRI techniques enable assessment of pulsatility in multiple and smaller vessels and in different types of brain tissues, which therefore should be encouraged in future studies.

Chapter 3: Method: a reproducibility analysis of phase-contrast MRI in healthy volunteers and an observational study on cerebral blood flow and intracranial pulsatility in patients with SVD

Introduction

As I mentioned in Chapters one and two, some studies have investigated the relationship between cerebrovascular/CSF pulsatility and WMH in patients with dementia (such as G.A. Bateman et al. 2008, n=48)[64] or healthy volunteers (Clive B Beggs et al. 2016, n=101)[125]. However, so far, there are no studies that have assessed the intracranial pulsatility in stroke patients who had SVD. Thus we recruited a group of patients with minor non-disabling ischaemic stroke in whom SVD features are common. In the following chapters, I will first assess the reproducibility of cerebral blood flow (CBF) and intracranial pulsatility measured by MRI using data from healthy volunteers, and then investigate the association between CBF and intracranial pulsatility measures and SVD features in stroke patients.

This chapter is a method-chapter. I will introduce the methods that we used in the data collection and data analysis, including recruitment of subjects and imaging techniques, which apply to the results presented in chapter 4 and 5. When assessing the relationship between cerebral haemodynamics and SVD features, I will mainly focus on WMH and PVS, as they are thought to be the most relevant SVD presentations to increased pulsatility and the most commonly seen features in the patient group in our study.

It is worth noting that the work related to chapter 3 to chapter 5 involves collaboration from various people. The contributions are listed below. Dr Michael J

Thrippleton (MJT) and myself (YS) recruited the healthy volunteers for the reproducibility study. The main study involving SVD patients was originally designed by Prof Joanna M Wardlaw (JMW). Dr Gordon Blair (GB), Dr Fergus Doubal (FD) and JMW recruited patients with SVD for the main study. GB and a group of radiographers helped scanned the patients. GB (a neurologist trainee) did the Doppler ultrasound scans. GB, Iona Hamilton and myself did the radial pulse tonometry. Dr David Alexander Dickie (DAD) helped with structural image processing and generated the automatic masks for brain tissues. MJT processed the primary phase-contrast images from the MRI scanner. I manually corrected the brain tissue masks, drew regions of interest (ROI) on processed flow images and carried out further flow data processing and statistical analyses. I also did all the visual rating for WMH and PVS and then cross-checked with JMW. "We" in this chapter and the following chapter 4 to chapter 6 indicates the relevant people in the above-mentioned list or the whole team.

Methods

Subject recruitment

We recruited healthy volunteers and patients with a past history of minor stroke following Research Ethics Committee approvals (ref. 14/HV/0001 and 14/EM/1126) and according to the principles expressed in the Declaration of Helsinki. Written informed consent was obtained from all participants.

In order to assess the reproducibility of flow and pulsatility measured by phase-contrast MRI, we recruited healthy volunteers from the surrounding area who had no cardiovascular disease, stroke, hypertension, migraine, anxiety disorders or panic

attacks. We also excluded those who had a known family history of intracranial aneurysms, subarachnoid haemorrhage, arteriovenous malformation, or who had contraindications to MRI. Healthy volunteers were asked to attend two phase-contrast scanning sessions in the same scanner and using the same sequences within one week. As the two scan sessions were not on the same day, I used the term "reproducibility" to describe the analysis of agreement between measures derived from the two scans.

We recruited patients prospectively with a symptomatic minor (i.e. non-disabling) ischaemic stroke presenting to the NHS Lothian stroke service between October 2014 and April 2016. NHS Lothian covers three major hospitals and is managed by one centralised team of stroke physicians. Diagnosis and classification of stroke were based on the combination of clinical presentation and appearance on MR brain imaging with DWI and other relevant diagnostic sequences, and was carefully crossed-checked by a panel of experts in stroke (FD and JMW). 'Non-disabling' was defined as not requiring assistance in activities of daily living. We excluded patients with disabling stroke, poorly-controlled diabetes mellitus, poorly-controlled hypertension, and any psychiatric illness that would limit compliance with study procedures. We also excluded patients with a known family history of intracranial aneurysms, subarachnoid haemorrhage, arteriovenous malformation, and those with contraindications to MRI.

Imaging protocols

All participants were imaged on the same 1.5 tesla MRI scanner (Signa HDxt, General Electric, Milwaukee, WI, USA) using an 8-channel phased-array head coil.

We acquired velocity images using a 2-D cine phase-contrast pulse sequence with retrospective peripheral pulse gating, as described previously.[147, 158] Figure 14 illustrates the slices and regions we selected for flow measurements in phase-contrast MRI. Vascular flow (TR/TE=9/5 ms, 25° flip angle, 256 x 128 matrix, 2 signal averages) was determined in the distal cervical ICA, vertebral arteries, and internal jugular veins axially, superior to the carotid bifurcation where the ICA walls are parallel. We measured venous sinus flow (TR/TE=9/5 ms (approx.), 25° flip angle, 256 x 128 matrix, 2 signal averages) in the superior sagittal sinus, straight sinus, and transverse sinuses. A coronal-oblique slice that intersected the superior sagittal sinus at about 2cm above the torcular and through the midpoint of straight sinus was selected. We also measured CSF flow through slices perpendicular to the cerebral aqueduct (TR/TE=11/6.5 ms (approx.), 20° flip angle, 256 x 256 matrix, 2 signal averages) and axially at C2-C3 level (TR/TE=11/7 ms (approx.), 20° flip angle, 256 x 128 matrix, 3 signal averages).***(Figure 14)***

All velocities were measured at 32 time points during the cardiac cycle, with velocity encoding value set to 70 cm/s for neck arteries, 50 cm/s for dural venous sinuses, 10 cm/s for the aqueduct CSF, and 6 cm/s for the cervical CSF. Views per segment were set to 2 in all phase-contrast MRI scans.

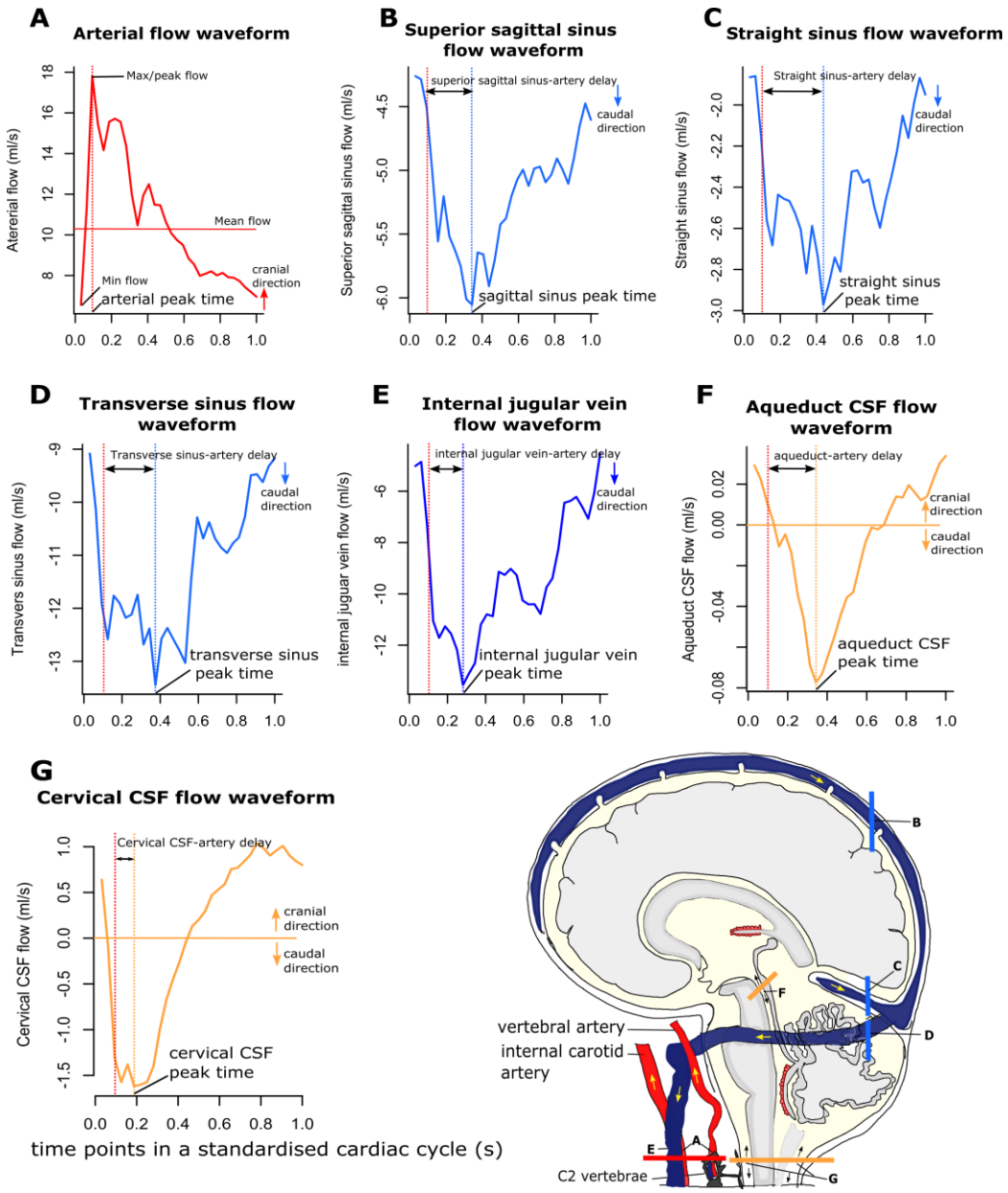

Figure 14 Locations sampled with phase-contrast MRI, and example flow waveforms of selected vessels and cerebrospinal fluid (CSF) spaces in one standardised cardiac cycle. Thick color lines on the sagittal image indicate the locations of slices for phase-contrast MRI scans. Arrows indicate the directions of flow. In each waveform, dashed lines in the same colour as the flow curve point to the time of peak flow, while red dashed lines in all waveforms show the time of arterial peak flow. For the arterial flow waveform, we combined the flow from both internal carotid arteries (ICA) and both vertebral arteries in this example, but we calculated PI for the ICAs and vertebral arteries separately in the analyses. A: arteries including both ICA and vertebral arteries; B: superior sagittal sinus; C: straight sinus; D: transverse sinus; E: internal jugular vein; F: cerebral aqueduct; G: cervical subarachnoid space.

We acquired structural images using the following sequences: 3D T1W imaging (inversion recovery-prepared spoiled gradient echo (SPGR), sagittal acquisition, TR/TE/TI=9.6/4.0/500 ms, 8° flip angle, 25.6 x 25.6 cm FoV, 192 × 192 acquisition matrix, 160 x 1.3 mm slices), axial T2W (TR/TE=7000/90 ms, 24 x 24 cm FoV, PROPELLER acquisition with matrix size 384, 1.5 signal averages, 36 x 4 mm contiguous slices), axial FLAIR (TR/TE/TI=8000/100/2000, 24 x 24 cm FoV, 320 × 256 acquisition matrix, 36 x 4 mm contiguous slices), axial GRE (TR/TE=900/15 ms, 20° flip angle, 24 x 24 cm FoV, 384 × 256 acquisition matrix, 36 x 4 mm contiguous slices).

We performed ICA Doppler ultrasound on patients on a portable SonoSite MicroMaxx ultrasound machine (Sonasite, USA).The blood flow velocity readings were obtained in the supine position at rest and 10 minutes after patients finished the MRI scan. We measured peak systolic and end diastolic blood flow velocities from the ICA and averaged the right and left velocities. We calculated the ICA PI, and the resistance index (RI) using the following equations: Gosling's equation: PI= ($Velocity_{max}$ – $Velocity_{min}$) / $Velocity_{mean}$;[121] Pourcelot's equation: RI= ($Velocity_{max}$-$Velocity_{min}$) / $Velocity_{max}$).[159]

We also measured the aortic augmentation index (AIx) to represent aortic stiffness in patients. In order to estimate the aortic AIx, we performed the radial artery pulse wave analysis using a tonometry device (SphygmoCor, Sydney, Australia). We obtained the radial artery pressure waveform via a transducer with a small sensor that could non-invasively detect the pulse of the radial artery. The aortic pressure waveform was then estimated from the radial artery pressure waveform using a mathematical formula that was reported in a previous study and is now generally

accepted.[160] The aortic AIx was calculated as the aortic augmentation pressure divided by the aortic pulse pressure and was then normalised to a heart rate of 75 bpm, because it is sensitive to heart rate.[161] ***(Figure 15)*** Indeed, the aortic AIx is a measure of aortic wave reflection. In young and healthy vessels, the reflected wave arrives back at the route of the aorta during systole. When vessels stiffen with aging or vascular risk factors, the speed of travel of the reflected wave becomes faster thus the reflected wave arrives back to the aorta during systolic ejection, which generates a higher pressure peak (augmentation pressure) after the first systolic peak.[162] Therefore, in many studies, aortic AIx was used to estimate aortic stiffness.[161, 162]

There are other measures for estimating aortic stiffness, such as the carotid-femoral pulse wave velocity which is suggested by some researchers as the gold standard. However, we chose the radial artery tonometry because it is more comfortable for our patients and easier to carry out in the setting of our study. This study was primarily designed for measuring cerebrovascular function using MRI, thus patients needed to be scanned for about 75 minutes in the MRI scanner including 25 minutes for phase-contrast imaging, 20 minutes for CVR acquisition (not discussed in this thesis) and 30 minutes for structural image acquisitions. In addition to the MRI scan, we also performed other exams such as the retinal photography, carotid ultrasound, and pulse wave analysis. Thus the radial artery tonometry which does not require undressing, as opposed to the carotid-femoral artery evaluation, was more acceptable to our patients.

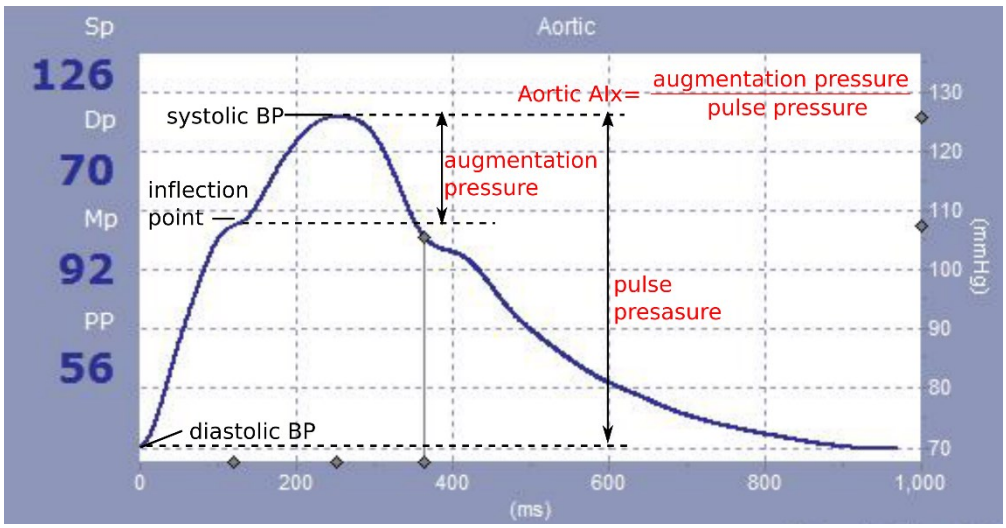

Figure 15 Example of aortic pressure waveform with aortic systolic pressure, aortic diastolic pressure, inflection point where the forward aortic wave merges with the reflected wave. The aortic pressure waveform is estimated from a radial pressure waveform in the radial artery tonometry using a mathematical formulas.[154] The augmentation pressure is the difference between the systolic pressure and the pressure at the inflection point. The aortic augmentation index is calculated as the ratio between the augmentation pressure and pulse pressure. As the augmentation index is sensitive to the heart rate, it is then normalised to a heart rate of 75 bpm.[155]

Imaging processing

Structural imaging analysis

All imaging analysts (DAD, MJT, YS, JMW) were blinded to patients' clinical data and haemodynamic measures generated from the phase-contrast MRI. Structural image acquisitions were co-registered within each subject.[163] WMH were automatically calculated by a validated software which first diffeomorphically registering a white matter probability map to each subject using T1W image data. The probability map was previously created from 313 volunteers aged 18-96 years.[164] The diffeomorphic registration was performed using the symmetric image normalisation algorithm within Advanced Normalisation Tools version 2.1.0 on a Linux Red Hat Server.[165] This provided a "clean" estimate of the white matter for

each subject, e.g., a white matter surface without gaps/ holes created by WMH. Hyperintense outliers were identified on FLAIR by transforming each voxel to a standard (z) score.[166] Voxels with z≥1.5 and within the estimated white matter surface were initially defined as WMH. Final WMH estimates were defined by 3D Gaussian smoothing to reduce noise and account for partial volumes around WMH edges. WMH masks were then manually corrected for each participant and stroke lesions were excluded manually according to STRIVE guidelines[7] and supervision from an experienced neuroradiologist (JMW). A stroke lesion on FLAIR was defined as a hyperintense area with a corresponding increased signal on patient's previous DWI scan and/or compatible with relevant stroke symptoms. Normal appearing tissues including cortical grey matter, subcortical grey matter, white matter, and cerebellum were segmented using within subject T1 intensity data and population specific probability maps, which gives the brain volume.[167] Intracranial volume (ICV) was calculated in two stages: firstly by running FSL's Brain Extraction Tool on the GRE image from each patient; secondly, hypointense outliers (generally skull and bone in GRE) were automatically removed via Z scores. Any hypointensities within the cranial vault (e.g., microbleeds) were refilled using the MATLAB fill holes function. Finally, ICVs were checked and edited by trained image analysts (YS) overseen by a consultant neuroradiologist (JMW).

As well as quantitative volumetrics, periventricular and deep WMH were assessed using clinical scoring with the Fazekas scale from 0-3 (Deep WMH: 0 =absent,1 = punctuate foci, 2 =beginning of confluence, 3= large confluent areas; periventricular WMH: 0= absent, 1= "caps" or pencil-thin lining, 2= smooth "halo", 3= irregular periventricular signal extending into the deep white matter).[168]***(Figure 16)*** Total

Fazekas score was generated from the sum of the two. We also rated the PVS[7] in both basal ganglia and centrum semiovale according to a validated semiquantitative scale from 0-4 (0=no visible PVS; 1= <10 PVS; 2= 11-20 PVS; 3= 21-40 PVS; 4= > 40 PVS).[33, 36]***(Figure 17)***

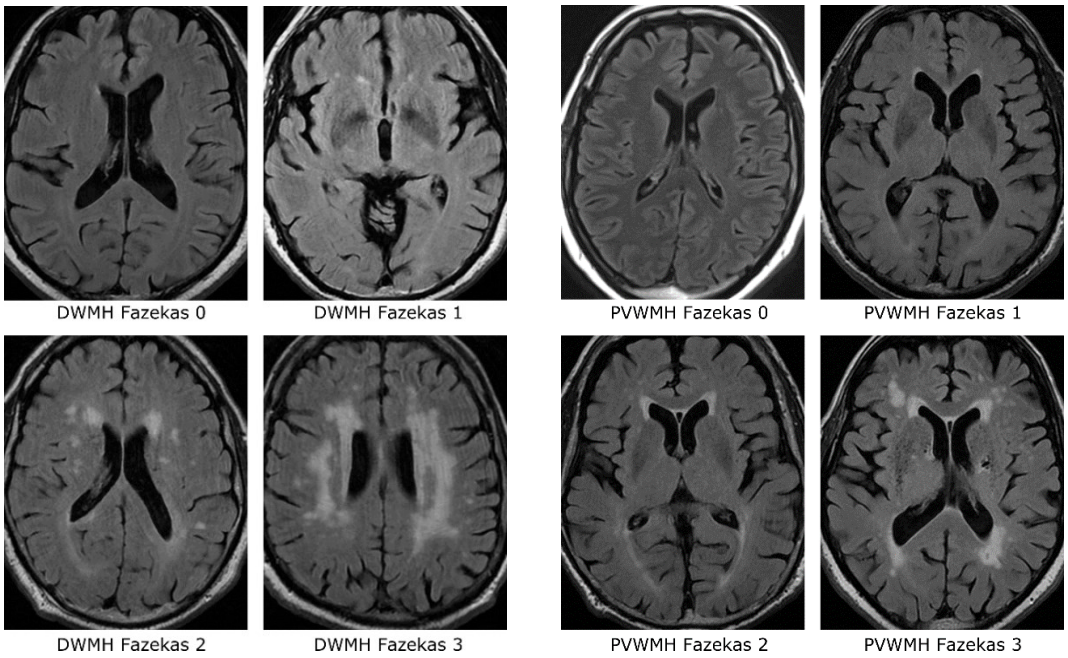

Figure 16 Fazekas score for deep white matter hyperintensities (DWMH) and periventricular white matter hyperintensities (PVWMH). DWMH: 0 =absent,1 = punctuate foci, 2 =beginning of confluence, 3= large confluent areas; PVWMH: 0= absent, 1= "caps" or pencil-thin lining, 2= smooth "halo", 3= irregular periventricular signal extending into the deep white matter. Images were from patients from our study.

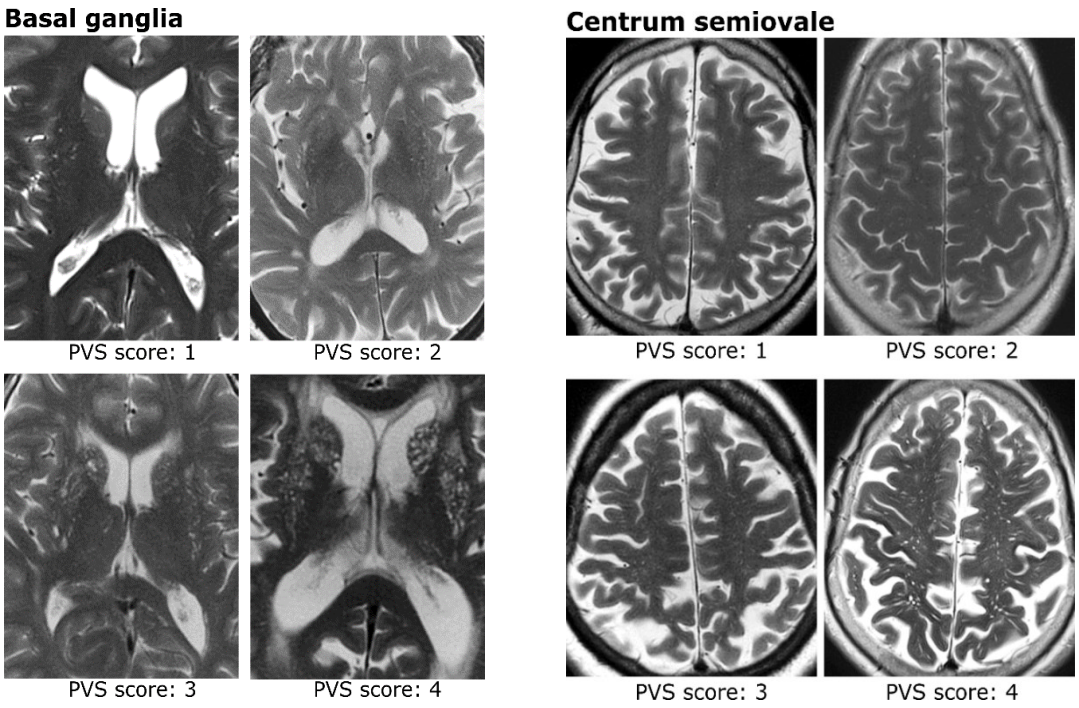

Figure 17 Visual rating score for perivascular spaces (PVS) in basal ganglia and centrum semiovale. 0=no visible PVS; 1= <10 PVS; 2= 11-20 PVS; 3= 21-40 PVS; 4= > 40 PVS. Images were from patients from our study.

Flow and pulsatility measurements

4-D velocity and magnitude images from each selected slices showing the flow in a cardiac cycle were generated from the scanner. To determine the flow values, I manually drew ROIs around the ICAs, vertebral arteries, internal jugular veins, venous sinuses, aqueduct, and cervical subarachnoid spaces on an averaged magnitude image of the correspondent slice of each patient. Then the background phase error was corrected by carefully placing background ROIs close to but not including the studied ROIs and then subtracted the mean velocity of the background ROIs.[169] (***Figure 18-Figure 21***) The sums of the flow in ICAs and vertebral arteries on both sides gave the value of total arterial flow. The sum of the flow in transverse

sinuses and internal jugular veins on both sides represented total transverse sinus and internal jugular vein flow respectively. For each vessel, the PI was calculated from an adapted Gosling's equation ($(Flow_{maximum} - Flow_{minimum})/Flow_{mean}$). We also calculated the RI for the vessels ($(Flow_{maximum} - Flow_{minimum})/Flow_{maximum}$).

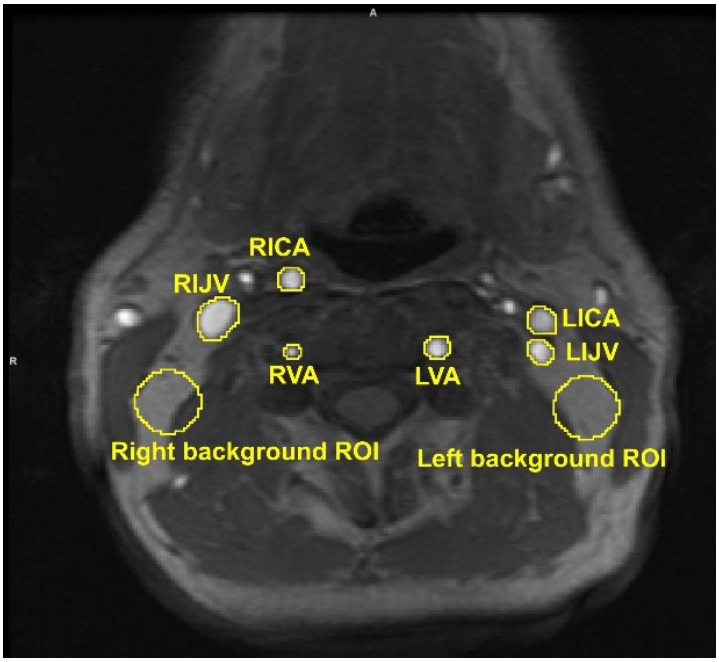

Figure 18 Example of regions of interests for vessels at the cervical level on magnitude image. RICA: right internal carotid artery; LICA: left internal carotid artery; RIJV: right internal jugular vein; LIJV: left internal jugular vein; RVA: right vertebral artery; LVA: left vertebral artery; ROI: region of interest.

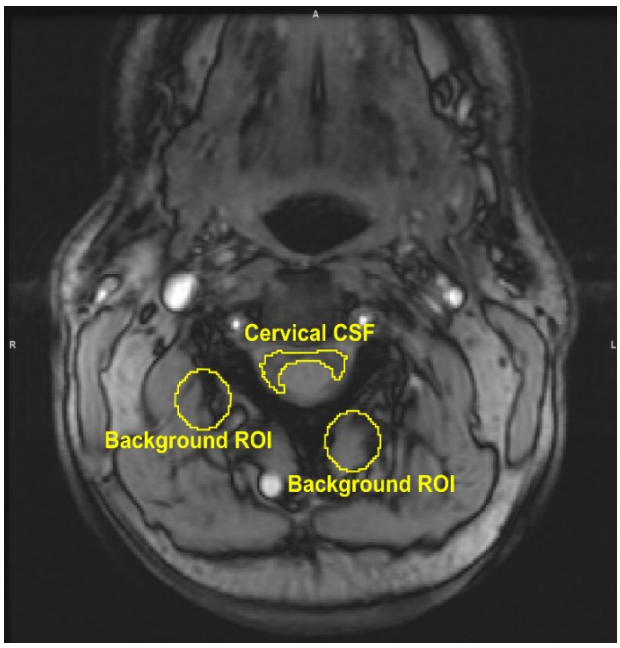

Figure 19 Example of regions of interest for cervical CSF on magnitude image. CSF: cerebrospinal fluid; ROI: regions of interest.

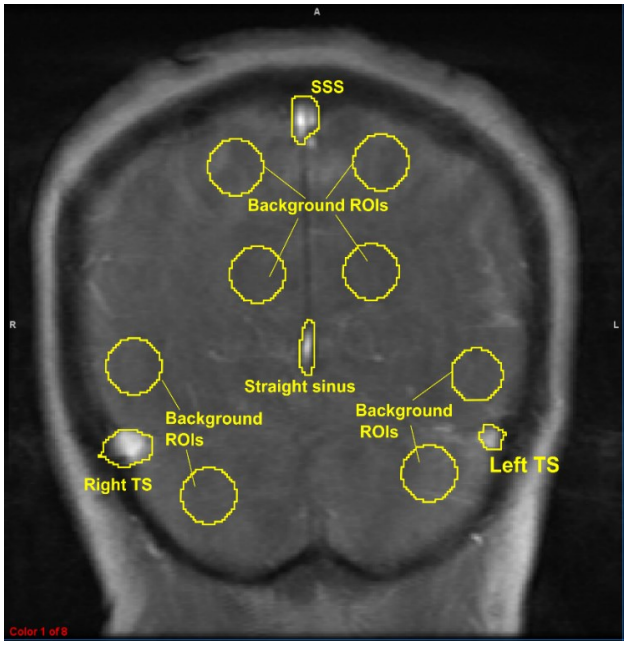

Figure 20 Example of regions of interest for dural venous sinuses on magnitude image. SSS: superior sagittal sinus; ROI: region of interest; TS: transverse sinus. We drew background ROIs separately for each venous sinus.

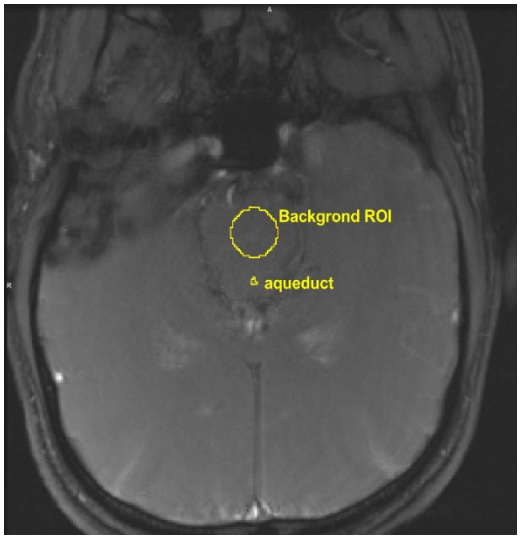

Figure 21 Example of regions of interest for the aqueduct on magnitude image. ROI: region of interest.

We calculated the total net CSF flow in the aqueduct and cervical subarachnoid space, by integrating positive and negative flow values in caudal and cranial directions, the stroke volume by averaging the absolute flow volume in both directions. We defined the systolic phase in the CSF space as the caudal phase, as during the systolic phase the CSF is expected to leave the cranial space and returns to the cranial space in diastole;[62] hence the diastolic phase represented the cranial phase. We calculated the duration of the systolic phase in CSF spaces. These methods for CSF data processing were similar to those reported in a previous study.[124]

We normalised flow waveforms in all vessels and CSF spaces to one standardised cardiac cycle. We measured the time delay between systolic pulse wave peaks in arteries and veins or CSF spaces to estimate the timing of pulse wave at each point through the whole brain.(***Figure 14***)

Statistical analysis

The sample size was determined to detect an effect in a similar vascular function measure called cerebrovascular reactivity (CVR), since very little data were available for PI or RI in veins or CSF. We estimated from the literature that it would be possible to detect a relative difference in CVR of 25%, standard deviation 40%, between those with high SVD scores and low SVD scores with 80% power and alpha level 0.05. This estimated a sample size of 40 participants, however, we aimed to include 60 patients to allow for technical failures or patient withdrawal from the procedure, for multivariate analysis and to increase the possibility of detecting effects on the other vascular function measures.

I performed all statistical analyses using Rstudio version 1.0.136 (RStudio Inc, Boston, MA) and SPSS version 21 (SPSS Inc, Chicago, IL). All the detailed statistical methods and models will be described in each individual chapter.

Chapter 4: Reproducibility analysis of CBF and intracranial pulsatility and comparability of internal carotid artery pulsatility indices between MRI and Doppler ultrasound

Introduction

Reduced CBF and increased intracranial pulsatility have been suggested as the underlying mechanisms of SVD. Recently, a few studies have used phase-contrast MRI to measure CBF, CSF flow and pulsatility in patients who had SVD features such as WMH or vascular dementia.[64, 65, 143] As I showed in the systematic reviews in Chapter 2, higher intracranial pulsatility and low CBF was found to be associated with higher SVD burden in cross-sectional studies, which indicates that they might be used as potential secondary endpoints in future clinical trials of SVD, or be followed-up in the long term as the longitudinal relationship between these measures and SVD remains largely unknown. However, the indices of intracranial pulsatility used by these studies, such as the stroke volume, net flow, duration of systole and peak velocities of CSF, varied substantially. It is unclear how reproducible these measures are or which of these measures are more reliable.

Different from the heterogeneities in CSF measures, the cerebrovascular PI and RI calculated from blood flow waveforms were more consistently used by previous studies.[124, 144] These two measures were adapted from the Gosling's PI and Pourcelot's RI equations in the Doppler ultrasound, although in Doppler ultrasound they were calculated from the velocity waveforms. As Doppler ultrasound has already been a well-established method in detecting blood velocity, the PI and RI is widely used in research[59, 122, 128, 129] and the clinical routine. However, it is yet

unknown whether the flow-based MRI pulsatility indices are comparable to their counterparts in Doppler ultrasound.

Thus, in this chapter, I aim to assess the reproducibility of CBF, CSF flow, and pulsatility measures in a group of healthy volunteers who had repeated phase-contrast MRI scans; and to assess the comparability of ICA pulsatility indices in MRI and Doppler ultrasound in our patients who had SVD.

Methods

The recruitment of participants and image processing have been described in Chapter 3. All the measures were normally distributed. Thus for statistical analyses, descriptive statistics will be presented as mean ± SD. I used paired-samples t-test to test the differences within participants. A statistical significance is defined as $p < 0.05$. No multi-test corrections were applied in these t-tests, as these data were mainly for descriptive purposes. The within-subject coefficient of variation (within-subject CV = $\sqrt{Mean(SD_i/mean_i)^2}$, i indicates each participant) and Bland-Altman plots were used to estimate the reproducibility. The between-subject CV was obtained from the variance of the means of the duplicate observations (between-subject CV=$SD\ (mean_i)/(\frac{\sum mean_i}{n})$, i indicates each participants, n represents the total number of participants). I calculated the CVs for all the measures apart from the total net CSF flow. As theoretically, the value of the net CSF flow in a cardiac cycle is zero, the CV calculation is non-applicable, but the reproducibility of the net CSF flow will be demonstrated in the Bland-Altman plots. The comparability between

MRI and Doppler ultrasound pulsatility indices was tested by Bland-Altman plots and Pearson's correlation analysis.

Results

Ten healthy volunteers (6 males, mean age=35.2±9.8 years, range 22-50 years) were included and finished two visits of phase- contrast MRI scans (median duration between scan = 6 days). Nine completed scans for arteries, dural venous sinuses, cerebral aqueduct and cervical subarachnoid spaces, whereas one did not have complete data for venous sinuses due to technical issues.

60 patients who had minor non-disabling ischaemic stroke and SVD were recruited, of which 56 (67.80±8.27 years, 40 males) had both MRI and Doppler ultrasound data. Four patients did not have complete MRI data: one due to claustrophobia, one due to an incidental finding of a subdural hematoma, and two had pulse gating issues during the scan. The other details of the patients will be discussed in the next chapter.

Summary of flow and pulsatility measures at two visits in healthy volunteers

Means and SDs of CBF and intracranial pulsatility measures for each visit are shown in Table 9. Total arterial flow (ICA + vertebral arteries; 776.90 ±125.33 ml/min) was similar to but higher than flow in the internal jugular veins (597.47±195.05 ml/min) or transverse sinuses (638.62±113.78 ml/min). PI and RI were highest in the arteries (e.g. ICA PI = 1.00±0.15), followed by internal jugular veins (PI = 0.32±0.08), and lowest in dural venous sinuses (e.g. superior sagittal sinus PI = 0.57±0.30). The net

CSF flow was larger in the cervical subarachnoid space (-1.02±4.74 ml/min) than in the aqueduct (0.04±0.01 ml/min), as was the stroke volume (0.58±0.20 ml in cervical CSF vs 0.04±0.01 ml in the aqueduct). Here and throughout the thesis, for the net CSF flow, the positive value indicates flow in the caudal direction and the negative value indicates the cranial direction. The waveform peak delay with reference to the arterial peak was relatively short in the cervical subarachnoid (0.04±0.05 s), followed by the internal jugular vein (0.11±0.10 s) and straight sinus (0.12±0.13 s), and longest in the transverse sinus (0.20±0.15 s), superior sagittal sinus (0.20±0.15 s), and aqueduct (0.21±0.05 s). There were no statistically significant differences between two visits in any of these measures. (***Table 10***)

Table 10 Summary of flow and pulsatility measures at two visits in healthy volunteers

	Visit 1 (n=10)	Visit 2 (n=10)	Average of two visits	P value
Cerebral blood flow (ml/min)				
Total arterial flow	772.65 ± 121.55	781.15 ± 128.85	776.90 ±125.33	0.89
Total internal jugular vein flow	615.02 ± 190.48	579.91 ± 197.97	597.47±195.05	0.71
Total transverse sinus flow	664.60 ± 118.58	612.64 ± 102.39	638.62±113.78	0.36
Pulsatility/resistance index				
ICA PI	1.03 ± 0.16	0.98 ± 0.14	1.00±0.15	0.47
ICA RI	0.62 ± 0.06	0.69 ± 0.05	0.61±0.06	0.36
Vertebral PI	1.43 ± 0.25	1.33 ± 0.21	1.38±0.23	0.36
Vertebral RI	0.72 ± 0.05	0.69 ± 0.04	0.70±0.04	0.35
Superior sagittal sinus PI*	0.33 ± 0.09	0.32 ± 0.10	0.57±0.30	0.83
Superior sagittal sinus RI*	0.28 ± 0.06	0.28 ± 0.07	0.42±0.16	0.80
Straight sinus PI*	0.32 ± 0.08	0.32 ± 0.07	0.29±0.09	0.94
Straight sinus RI*	0.28 ± 0.06	0.27 ± 0.05	0.26±0.07	0.92
Transverse sinus PI*	0.29 ± 0.07	0.29 ± 0.11	0.33±0.09	0.98
Transverse sinus RI*	0.26 ± 0.06	0.26 ± 0.08	0.28±0.07	1.00
Internal jugular vein PI	0.60 ± 0.32	0.54 ± 0.29	0.32±0.08	0.65

Internal jugular vein RI	0.44 ± 0.16	0.40 ± 0.15	0.27±0.06	0.59
CSF flow and pulsatility				
Total net aqueduct CSF flow (ml/min)[#]	0.42 ± 0.41	0.60 ± 0.34	0.51±0.39	0.30
Aqueduct CSF stroke volume (ml)	0.04 ± 0.01	0.04 ± 0.01	0.04±0.01	0.51
Aqueduct CSF systolic duration (s)	0.51 ± 0.07	0.51 ± 0.07	0.51±0.07	0.96
Total net cervical CSF flow (ml/min)[#]	-1.06 ± 4.79	-0.98 ± 4.46	-1.02±4.74	0.97
Cervical CSF stroke volume (ml)	0.61 ± 0.20	0.56 ± 0.19	0.58±0.20	0.59
Cervical CSF systolic duration (s)	0.41 ± 0.10	0.41 ± 0.09	0.41±0.10	0.88
Waveform peak delay (s) (with reference to arterial peak)				
Superior sagittal sinus*	0.24 ± 0.15	0.16 ± 0.14	0.20±0.15	0.25
Straight sinus*	0.14 ± 0.13	0.10 ± 0.12	0.12±0.13	0.50
Transverse sinus*	0.23 ± 0.15	0.17 ± 0.15	0.20±0.15	0.46
Internal jugular vein	0.10 ± 0.09	0.11 ± 0.11	0.11±0.10	0.74
Aqueduct CSF	0.22 ± 0.05	0.20 ± 0.05	0.21±0.05	0.37
Cervical CSF	0.05 ± 0.04	0.03 ± 0.06	0.04±0.05	0.46

ICA: internal carotid arteries; PI: pulsatility index; RI: resistance index; CSF: cerebrospinal fluid.
* n=9. One subject did not have complete data of venous sinus during one visit.
[#] For net CSF flow in either the aqueduct or the cervical subarachnoid space, positive values indicate flow in the caudal direction and negative values indicate the cranial direction.

Reproducibility of flow and pulsatility measures in healthy volunteers

The within-subject and between-subject CVs were shown in Table 10. The within-subject CVs were generally lower than 10% in blood flow measures and pulsatility indices in the vessels, apart from PI in the internal jugular veins (CV=10.04%) and the straight sinus (CV=11.01%). In CSF measures, the duration of the systole in both cervical CSF and aqueduct CSF had a CV of less than 10%. Stroke volumes in both aqueduct (CV%=18.02%) and cervical CSF (CV%=11.62%) had a reasonably good

reproducibility. CV% of peak delay were generally larger than 30% (ranging from 34.52-62.96%), apart from 14.38% in the aqueduct-artery delay. (***Table 10***)

The between-subject CVs of flow and pulsatility measures were mostly larger than 20% (21.96-165.10%). In the ICA and vertebral arteries, the variations of arterial flow and pulsatility indices (7.12-21.96%) were smaller than in veins or CSF spaces. All the between-subject CVs were not adjusted for age. (***Table 11***)

Table 11 Within-subject and between-subject coefficients of variance of flow and pulsatility measures in healthy volunteers

	Within-subject CV (%)	Between-subject CV (%)
Cerebral blood flow (ml/min)		
Total arterial flow	4.49	21.96
Total internal jugular vein flow	7.65	45.12
Total transverse sinus flow	6.29	23.33
Pulsatility/resistance index		
ICA PI	6.47	19.41
ICA RI	3.96	12.39
Vertebral PI	8.23	21.07
Vertebral RI	3.78	7.12
Internal jugular vein PI	10.04	74.20
Internal jugular vein RI	8.69	52.04
Transverse sinus PI	9.89	41.68
Transverse sinus RI	8.82	35.93
Superior sagittal sinus PI	9.98	38.97
Superior sagittal sinus RI	9.05	32.81
Straight sinus PI	11.01	30.72
Straight sinus RI	9.85	27.97
CSF flow and pulsatility		
Total net aqueduct CSF flow (ml/min)*	-	-
Aqueduct CSF stroke volume (ml)	18.02	45.08
Aqueduct CSF systolic duration (s)	6.47	17.66
Total net cervical CSF flow	-	-

(ml/min)*		
Cervical CSF stroke volume (ml)	11.62	45.20
Cervical CSF systolic duration (s)	9.86	30.89
Waveform peak delay (s) (with reference to arterial peak)		
Superior sagittal sinus	40.08	81.33
Straight sinus	62.96	83.75
Transverse sinus	34.52	89.74
Internal jugular vein	45.47	117.35
Aqueduct CSF	14.38	28.64
Cervical CSF	47.63	165.10

CV: coefficient of variation; ICA: internal carotid arteries; PI: pulsatility index; RI: resistance index; CSF: cerebrospinal fluid. All the CVs were not adjusted for age.

*Theoretically, the mean values of net CSF flow in the aqueduct and cervical subarachnoid spaces are zero, thus the calculation of CV is non-applicable. The reproducibility of net CSF flow will be demonstrated in the Bland-Altman plots below.

Bland-Altman plots of the above-mentioned flow and pulsatility measures are shown in Figure 22 to Figure 25. In Figure 22 and Figure 23, the limits of agreement were generally small for CBF and pulsatility/resistance indices for arteries and veins. In Figure 24, the limits of agreements for total net CSF flow and stroke volume in both cerebral aqueduct and cervical subarachnoid space were large although the mean differences were about zero, which represents a poor reproducibility. For the systolic duration in both cervical and aqueduct CSF, the limits of agreement and mean differences were relatively small. Figure 25 shows that the reproducibility of waveform peak delays was generally poor with large limits of agreements apart from in the aqueduct, which is consistent with the results in Table 10. No particular trend was observed between the means of two measures (X-axis) and the mean differences (Y-axis) in any of the plots.

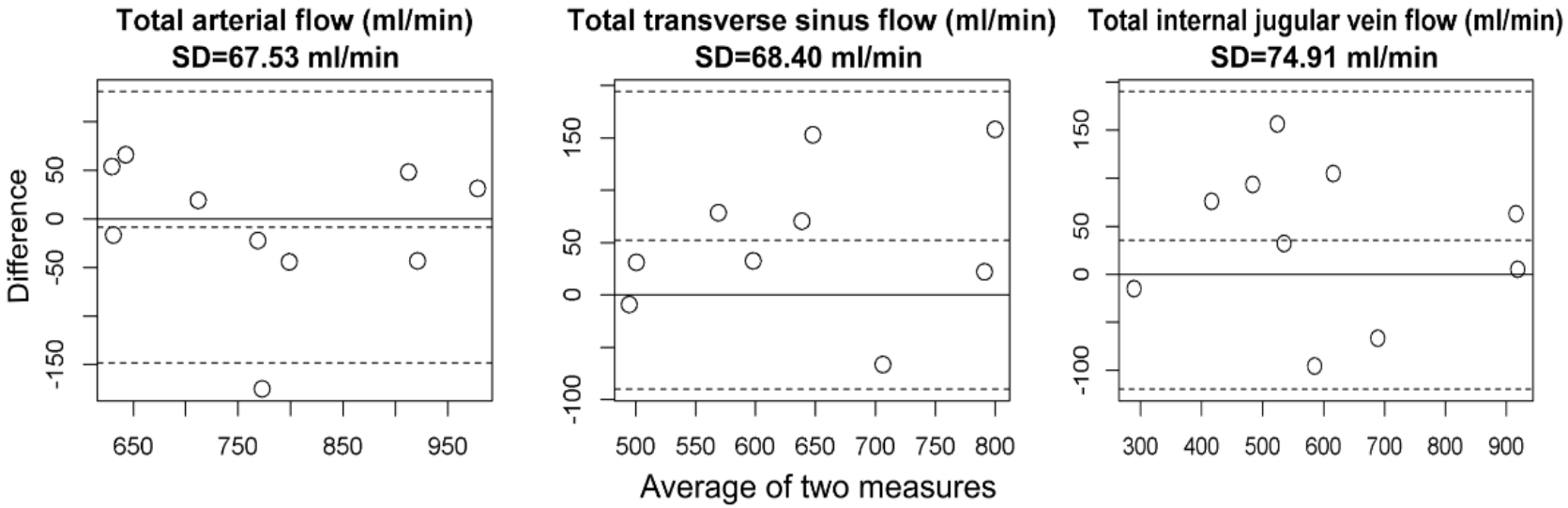

Figure 22 Bland-Altman plots showing the reproducibility of cerebral blood flow in the arteries, transverse sinuses and internal jugular veins. Data points represent the mean value of two visits (X-axis) and the difference between two visits (value at visit one minus value at visit two, Y-axis); dashed lines show the mean difference between the two measurements and the mean difference ± 1.96 × standard deviation (SD); the solid lines indicate the zero lines of the mean differences. The SDs of the differences are shown under the titles of each plot.

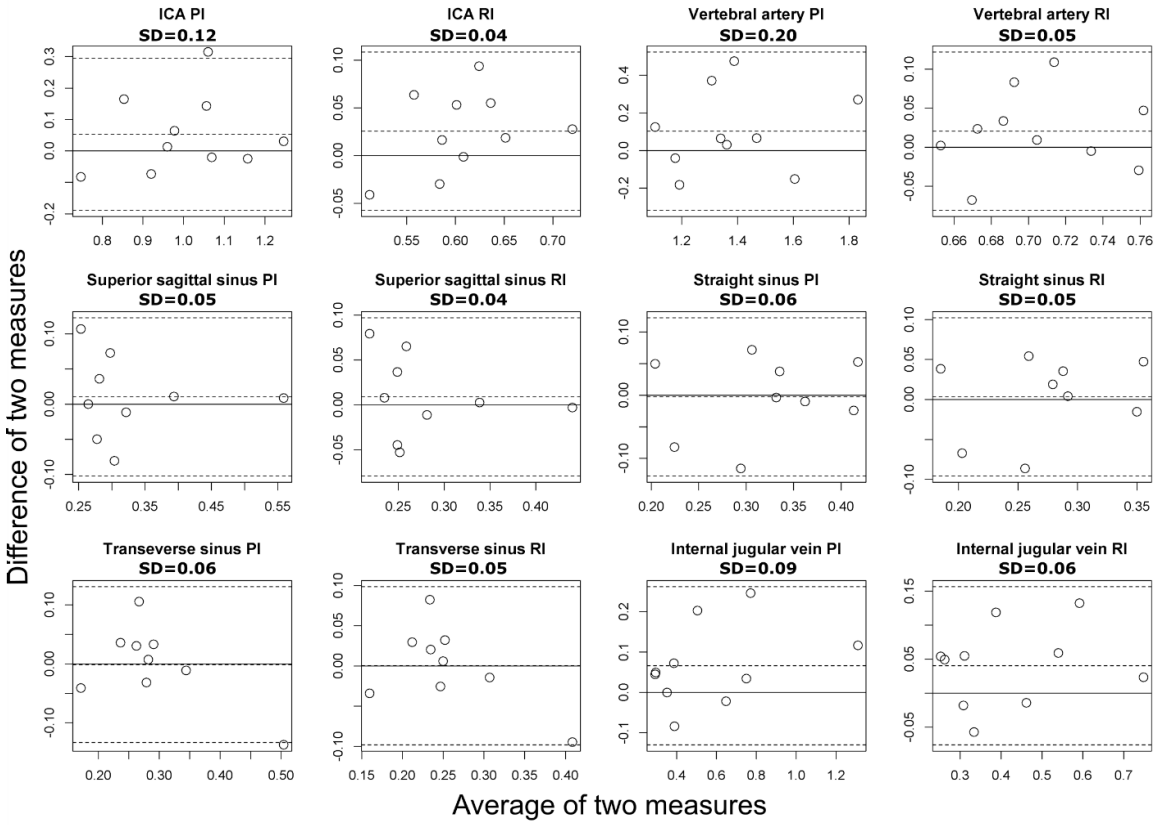

Figure 23 Bland-Altman plots showing the reproducibility of pulsatility index (PI) and resistance index (RI) in the vessels including: internal carotid arteries (ICA), vertebral arteries, superior sagittal sinus, straight sinus, transverse sinuses, and internal jugular veins. Data points represent the mean value of two visits (X-axis) and the difference between two visits (value at visit one minus value at visit two, Y-axis); dashed lines show the mean difference between two measurements and the mean difference ± 1.96 × standard deviation (SD); the solid lines indicate the zero lines of the mean differences. The SDs of the differences are shown under the titles of each plot.

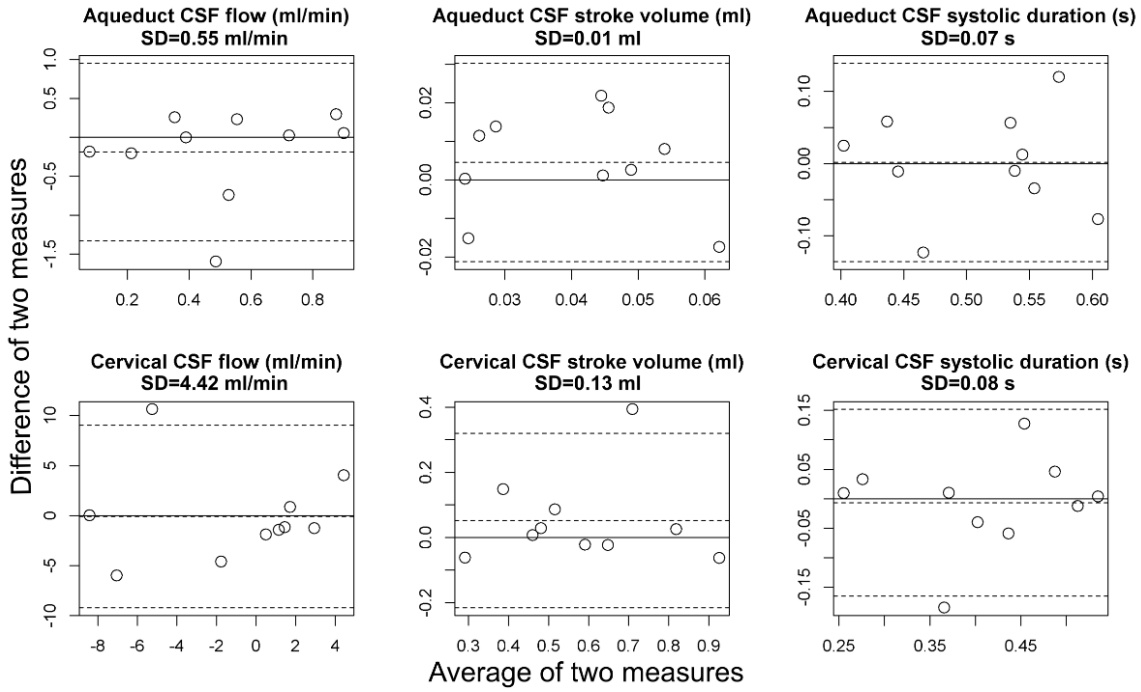

Figure 24 Bland-Altman plots showing the reproducibility of CSF flow and pulsatility measures in the cerebral aqueduct and cervical subarachnoid space. Data points represent the mean value of two visits (X-axis) and the difference between two visits (value at visit one minus value at visit two, Y-axis); dashed lines show the mean difference between two measurements and the mean difference ± 1.96 × standard deviation (SD); the solid lines indicate the zero lines of the mean differences. The SDs of the differences are shown under the titles of each plot.

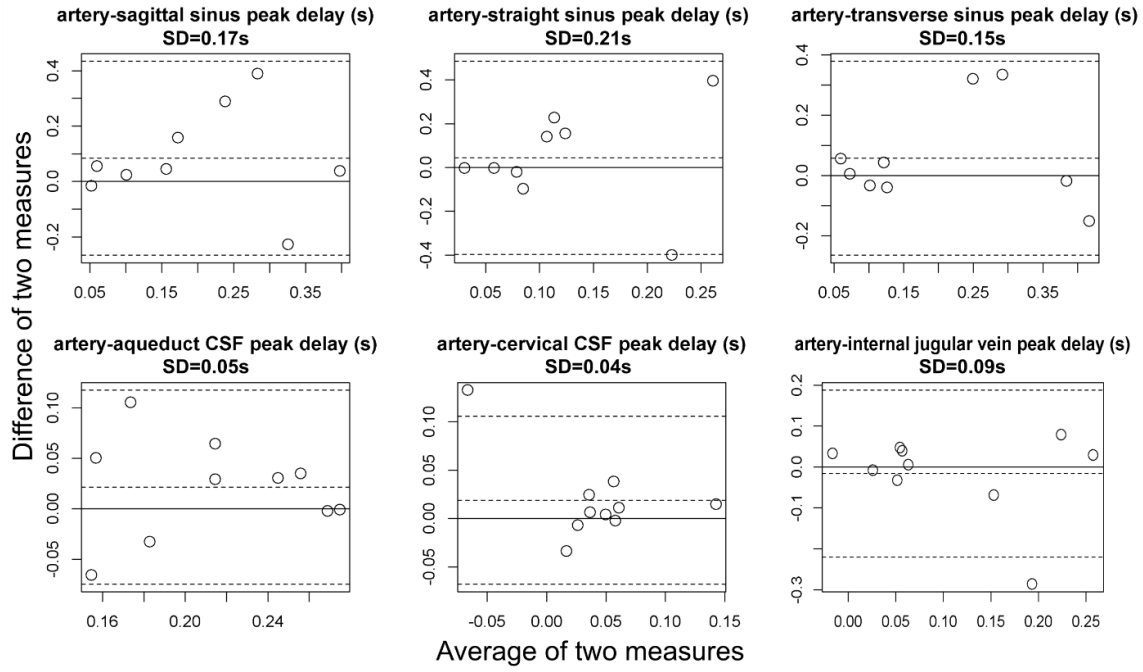

Figure 25 Bland-Altman plots showing the reproducibility of peak delays from arteries to veins and CSF spaces. Data points represent the mean value of two visits (X-axis) and the difference between two visits (value at visit one minus value at visit two, Y-axis); dashed lines show the mean difference between two measurements and the mean difference ± 1.96 × standard deviation (SD); the solid lines indicate the zero lines of the mean differences. The SDs of the differences are shown under the titles of each plot.

Comparability between Doppler ultrasound and MRI measurements in ICA pulsatility indices

In Figure 26, a direct comparison of waveforms shows that the ICA flow waveform reconstructed from phase contrast MRI and blood velocity waveform in Doppler ultrasound shared a similar shape. Both images were from the same patient.

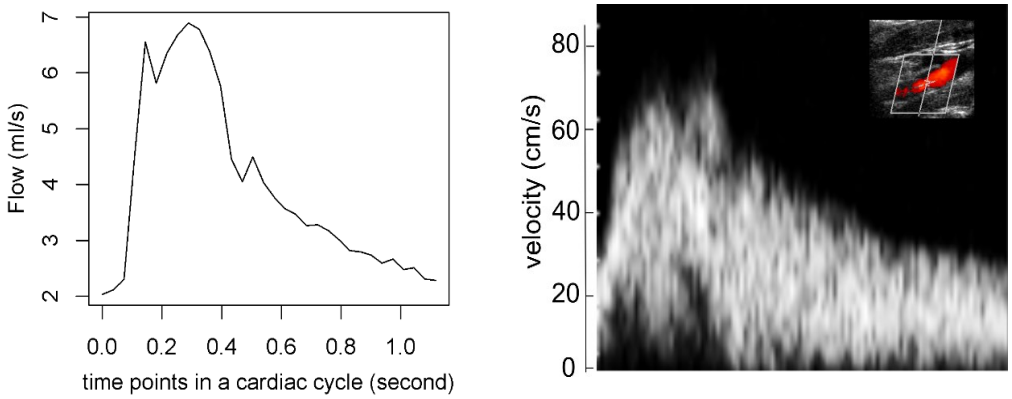

Figure 26 Blood flow waveform derived from MRI (left) and velocity waveform from Doppler ultrasound (right) of an internal carotid artery in the same patient.

Table 12 shows the mean PI and RI from both MRI (PI 1.27±0.31; RI 0.69±0.07) and Doppler ultrasound (PI 1.53±0.38; RI 0.72±0.07). Paired-sample t-tests showed that MRI measures were smaller than those in Doppler ultrasound (PI: P<0.001; RI: P=0.002).

Table 12 ICA PI and RI in phase contrast MRI and Doppler ultrasound

	Phase-contrast MRI	Doppler ultrasound	P value
ICA PI	1.27±0.31	1.53±0.38	<0.001
ICA RI	0.69±0.07	0.72±0.07	0.002

ICA: internal carotid arteries; PI: pulsatility index; RI: resistance index. P values from paired-samples t-tests.

In the correlation analysis, there was a reasonably good correlation between PI (r = 0.45) and RI (r = 0.47) measured by MRI and Doppler ultrasound considering the differences in the two techniques. ***(Figure 27)***

In Figure 28, the Bland-Altman plots demonstrate that the limits of agreement for both PI and RI were relatively small, especially for RI, representing a good comparison between the two. The PI and RI in MRI were lower than that measured by Doppler ultrasound as there are more points below the zero line than above.

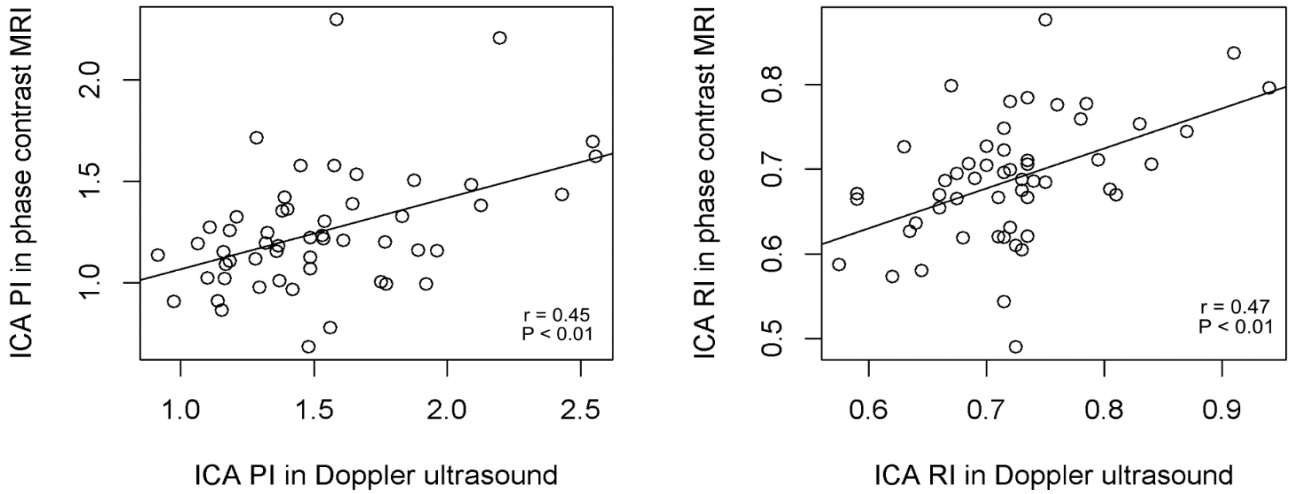

Figure 27 Correlation between phase contrast MRI and Doppler ultrasound measurements in pulsatility index (PI; left) and resistance index (RI; right) of internal carotid arteries (ICA). In both techniques, values of ICA PI and RI were averaged from both sides. r coefficients and P values were from Pearson's correlation analysis.

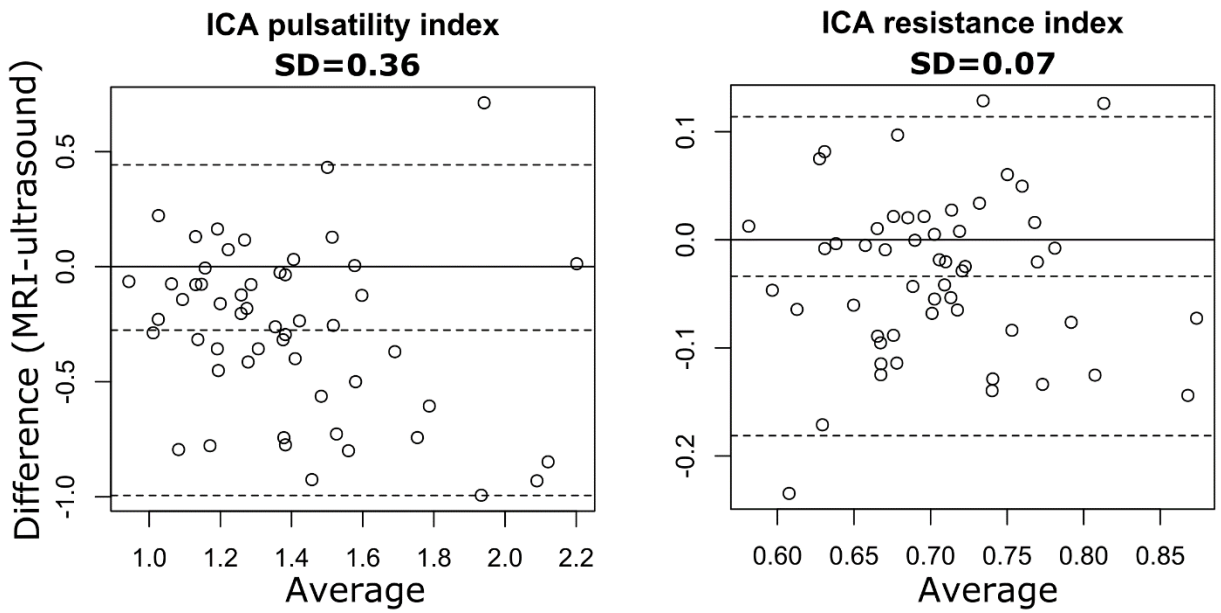

Figure 28 Bland-Altman plots showing the comparability between Doppler ultrasound and MRI measurements of pulsatility index (left) and resistance index (right) in the internal carotid arteries (ICA). Data points represent the mean value of two measurements (X-axis) and the difference between the two measurements (MRI- Doppler ultrasound, Y-axis); dashed lines show the mean difference between the two measurements and the mean difference ± 1.96 × standard deviation (SD); the solid lines indicate the zero lines of the mean differences. The SDs of the differences are shown under the titles of each plot.

Discussion

The results of this chapter show that in ten healthy volunteers (35.2±9.78 years), the blood flow and pulsatility measures in large intracranial arteries and veins were highly reproducible with within-subject CV of 3.78%-11.10%. In CSF flow and pulsatility measures, stroke volume and systolic duration of both cervical and aqueduct CSF were more reproducible (within-subject CV% = 6.47-18.02%) than the total net CSF flow (within-subject CV% >70%). Waveform peak delays in veins and CSF had poor reproducibility with large within-subject CV (34.52%-62.96%) apart from the artery-aqueduct delay (CV%=14.38%). Between-subject variations of all flow and pulsatility measures were generally large. When comparing ICA pulsatility indices measured by MRI to that measured by Doppler ultrasound in 56 patients (67.80±8.27 years) with minor stroke and SVD, the shape of flow waveform in MRI was similar to velocity waveform in Doppler ultrasound, and the pulsatility indices calculated from these waveforms were reasonably correlated (PI: r=0.45; RI: r=0.47; both $P<0.01$). PI and RI in MRI were slightly lower than those in Doppler ultrasound.

There are some limitations of this study. First, the within-subject variability might come from various sources, such as the variability of the participants' physical conditions as they were not scanned on the same day and were repositioned. Indeed, rather than measuring the repeatability of the scan acquisition and imaging processing, the aim of this study is to estimate whether the whole scan and imaging processing procedure could be reproduced in longitudinal studies such as clinical trials or in multicentre studies, and the results showed good reproducibility of the flow and pulsatility measures in such scenarios. Second, the sample size (n=10) of

healthy volunteers was small which limits the power of statistical analysis, although in previous literature the sample sizes for repeatability analysis were generally around 10. Third, as I focus on blood flow and pulsatility measures in this thesis, the comparison between velocity in both MRI and Doppler ultrasound was not included in this chapter. However, several previous studies have discussed this topic and generally showed good correlations between the two methods in blood velocity.[170-172] Fourth, due to the limitations of our Doppler ultrasound, we were not able to measure cerebral vessels other than ICAs in our patient group, thus the comparisons of pulsatility indices were only available for ICAs.

The value of total arterial flow (776.90 ±125.33 ml/min) in this study was in agreement with other studies in young healthy volunteers (700±100 ml/min, n=8, mean age=21 years;[173] 776±150 ml/min, n=20, mean age=31 years;[174] 715 ml/min, n=12, mean age=32±10 years[175]). Total internal jugular vein flow (597.47±195.05 ml/min in our study) was also generally smaller than total arterial flow in these studies (550±138 ml/min;[174] 298 ml/min[175]). The net flow rate and stroke volume of CSF was also similar to the values reported by other studies in healthy volunteers using either manual or automatic ROIs (aqueduct flow: 0.6 ml/min;[175] 0.305±0.145 ml/min, n=23, 21-39 years;[176] aqueduct stroke volume: 0.04±0.02 ml, n=21, mean age=40.8±18.7 years;[175] cervical CSF flow: -2.7 ml/min[175]) (positive value indicates flow in the caudal direction and negative indicates flow in the cranial direction). We found large between-subject variations in all these flow and pulsatility measures, which might be due to the relatively wide range of age.[147, 177]

Our results of high reproducibility in arterial and internal jugular flow in healthy volunteers are also consistent with previous studies.[173-175] In one study, the repeated scans were conducted on the same day consecutively without repositioning,[173] while in the other study the gap between both scans ranged from 7 to 110 days,[174] which suggests that the total arterial and internal jugular flow measured by MRI are highly reproducible even in a long-term follow-up. One 4D flow MRI showed a high reproducibility of dural venous sinus flow (ml/cardiac cycle) in healthy volunteers (n=10, mean age=36±14 years),[178] but otherwise 2-D phase contrast MRI studies on venous sinuses were scant. We showed small variability between scans in venous flow metrics, despite the fact that large veins may collapse and be too small to generate reliable ROIs when subjects lie in a supine position, which could limit the accuracy and also increase the variability of flow values.[179, 180]

Studies that have assessed the reproducibility of CSF flow are limited, but in general CSF had higher within-subject (between-scan) variability than arterial or venous flow regardless of the time gap between scans and the location of CSF (Foramen Magnum or aqueduct).[174, 175] Among various CSF measures, stroke volumes showed a higher reproducibility than other measures such as peak systolic velocity or total net flow.[181, 182] We also showed that durations of systole (duration of caudal flow) in the CSF flow waveform had a reasonably good reproducibility which had not yet been studied previously. Thus the stroke volume and the temporal characteristics of the CSF flow waveform might be more adequate than net flow for reproducibility and long-term follow-up purposes. There are substantial variabilities in waveform peak delay measures, which might be because these waveforms were collected from

different cardiac cycles with variable heart rates and the temporal resolution of MRI scanner is low. So far there is no consensus on how to calculate the waveform peak form delay. In this thesis, the waveform peak delays were calculated from a normalised cardiac cycle. I also attempted averaging the heart rates of two scan sessions (e.g. aqueduct and arteries) to estimate the peak delay between the two waveforms, which gives very similar results to what was currently shown in this thesis. The implication of the waveform delays remains unclear. It was interpreted as an indicator of pulse wave transmission velocity in some studies.[65] However, our results suggest that caution should be taken when interpreting a single measure of waveform peak delays.

The difference between the reproducibility of blood flow and CSF measures might be due to several reasons. The small size of the aqueduct makes the velocity or flow measurements susceptible to the partial volume effect. A previous study of 2D phase-contrast MRI showed that a measurement accuracy of within 10% required at least 16 voxels in the cross section of ROI when measuring vessels.[183] In our study the ROIs of aqueduct generally had less than 10 voxels due to the low resolution. Although ROIs of cervical CSF have larger areas, the low velocity in cervical CSF and the difficulty in distinguishing CSF from neighbouring tissues might have contributed to the variability of CSF flow measures. Background correction could be another source of the variability in CSF measures, which we used for reducing the impact of background noises on flow measures. Although background correction brought the mean CSF flow significantly closer to physiological expected values, it

substantially increased the intra-subject CV% of mean CSF flow from 17% to158%.[175]

So far there are no studies that have assessed the reproducibility of cerebrovascular pulsatility and resistance index calculated from MRI flow waveforms. Objectively, the MRI flow waveform had a similar shape to the velocity waveform from the Doppler ultrasound in the same patient, both of which had similar peaks and slopes at the similar timing in a cardiac cycle. Quantitatively, this study also showed a good reproducibility and a small inter-visit variation of both vascular pulsatility indices. The two indices are generally calculated in Doppler ultrasound using blood velocity waveform. We compared the ICA pulsatility indices in the MRI with those in Doppler ultrasound (performed immediately after MRI) in patients who had stroke and SVD, and showed a reasonable correlation between them (r=0.45-0.47). Usually an r coefficient of around 0.5 would be seen as a "moderate" correlation, in our case, we classified the correlation as "reasonably good" considering the difference between the two techniques and that we used a portable Doppler ultrasound machine which is not the optimal type of the technology. The Bland-Altman plots also showed similar results, as the difference between the two values (e.g. for PI mostly within ±0.5) were small compared to the averaged value (PI mostly within 1.0-1.8). Both MRI and ultrasound pulsatility indices gave similar relative value, although the MRI waveform represents the average of multiple waveforms and takes the whole vessel as an example, whereas the Doppler ultrasound only samples the centre of a vessel. MRI-generated ICA PI and RI were slightly lower than in Doppler ultrasound, which was consistent with a previous study (n=14, healthy volunteers, mean

age=33±3.8 years).[172] The same previous study found a moderate correlation in PI (r=0.36) and RI (r=0.39) between MRI and Doppler ultrasound.[172] Some other studies performed the similar comparisons in different vessels such as small cerebral arteries near an aneurysm[152] or MCA,[153] and showed heterogeneous results (r=0.14-0.35, n=4, animal study;[152] r=0.69-0.81, n=11, healthy volunteers, mean age=31 years[153]). In general, these data suggest that measurements of pulsatility indices in MRI are comparable to Doppler ultrasound given the differences between two technologies.

There are limitations and strengths in both techniques. Doppler ultrasound is more accessible and has high temporal resolution, but it does not provide information about the whole cross section of the vessels, which could cause potential measurement bias, has limited access to more intracranial vessels, is strongly user-dependent, and the position of where measures were performed may vary during the follow-up; whereas although phase-contrast MRI is more expensive and non-portable and has relatively low time-resolution, it enables measurements in more vessels at a time such as venous sinuses and ever smaller vessels if using high-field techniques, is less user-dependent and more consistent with the slices selected for flow detection.

In conclusion, flow and pulsatility measures in the arteries and veins, CSF stroke volume and systolic duration in phase-contrast MRI had generally good reproducibility in consideration of future follow-up. In patients with mild stroke and SVD, ICA PI and RI by phase-contrast MRI (calculated from flow waveform) and by Doppler ultrasound (calculated from velocity waveform) have reasonable

comparability. Higher spatial and temporal resolution of phase-contrast MRI may increase the specificity and accuracy, and thus the reproducibility of the vascular pulsatility and CSF flow measures.

Chapter 5: An observational study of CBF and intracranial pulsatility in patients with SVD– Results

Introduction

SVD increases with age and increases the risk of stroke.[24] A quarter of ischaemic strokes are lacunar.[22, 184] WMH are commonly seen in stroke patients, regardless of the stroke aetiology.[185, 186] Some studies have assessed the CBF, or intracranial pulsatility in patients with some SVD features, such as in vascular dementia,[124] or "healthy" volunteers.[58] However, vascular risk factors were generally not well controlled for in the literature as I showed in Chapter 2; and few studies have addressed vascular and CSF pulsatility contemporaneously with CBF in stroke patients in whom SVD is common. Also, there is lack of studies that have investigated the relationship between extracranial vascular haemodynamic measures and intracranial pulsatility. Furthermore, in most previous studies, SVD burden was represented by WMH whereas PVS was rarely mentioned, despite the hypothesis that PVS visibility increases when cerebral interstitial fluid dynamic is impaired and is related to arterial pulsation.[40] Thus we carried out a cross-sectional study in patients with minor ischaemic stroke and SVD features, assessed the CBF and intracranial pulsatility using phase-contrast MRI, in an attempt to address the above-mentioned questions in this pilot study.

This chapter will be divided into 5 sections. In Chapter 5A, I will summarise the characteristics of the patients and the haemodynamic measures, then investigate how these haemodynamic measures are related to age and stroke subtype (lacunar vs cortical), and examine whether there is any relationship between intracranial and

extracranial measures including systemic (brachial) BP and aortic stiffness. In Chapter 5B, I will investigate the association between CBF and the main SVD features (WMH and PVS). Chapter 5C will be focusing on pulsatility in brain vessels as well as aortic stiffness and WMH or PVS. Then in Chapter 5D, I will investigate how the CSF pulsatility and waveform peak delays relate to WMH and PVS. Lastly, in Chapter 5E, I will explore how cerebrovascular pulsatility relates to CBF; and as ICAs are responsible for transmitting most of the pulse into the intracranial space, I will also look at how PI in the veins is related to ICA PI.

Methods

The details of patient recruitment and image processing methods have been described in Chapter 3. For statistical analysis, categorical variables were presented as numbers and percentage, such as the history of vascular risk factors, numbers of patients under each Fazekas score or PVS score; continuous variables that are normally distributed were presented as mean ± SD, including BP and all flow and pulsatility measures; continuous variables that were non-normally distributed were presented as medians and ranges, including the WMH volume and WMH/ICV ratio. Differences in continuous variables between Fazekas groups or PVS score groups were assessed by the analysis of variance (ANOVA) and illustrated using boxplots. Figure 29 shows an example of components in a boxplot.

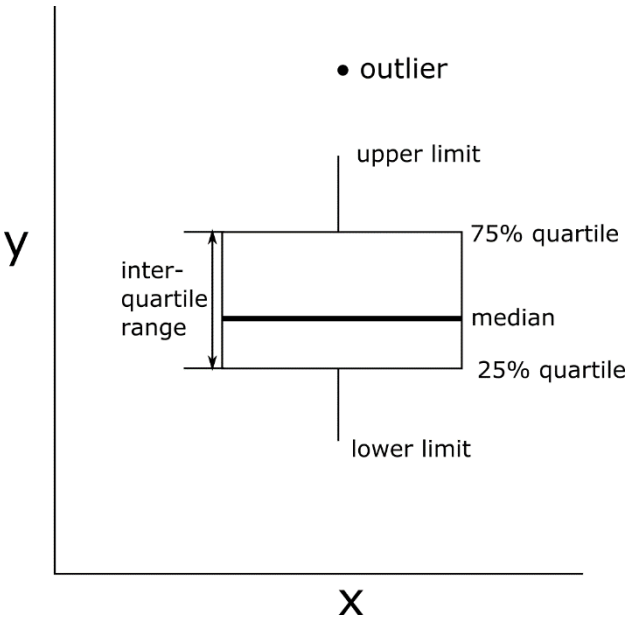

Figure 29 Example of a typical boxplot, which includes the median, values at the 25% and 75% quartile (Q1, Q3), inter-quartile range (IQR), upper and lower limit, and outliers. The upper limit is defined as Q3 + 1.5 × IQR, and the lower limits is defined as Q1 – 1.5 × IQR. An outlier is a data point that is located outside the range within the lower and upper limit.

When assessing the relationships between variables, I will use linear regression models if the outcome variable is continuous, such as haemodynamic measures and the WMH/ICV ratio; ordinal regression models if the outcome is categorical and ordinal, such as PVS scores. In the regression models where the WMH/ICV is used as the outcome variable, I will natural log transform the WMH/ICV in order to obtain normally distributed residuals in the models. Histogram review and Q-Q plots were used to check the normality of distributions of residuals for each model. Also to note that, although the WMH volume and Fazekas scores are both validated measures for representing WMH burden, only WMH volume will be used in regression models as it is a quantitative measure whereas Fazekas scores are based on visual rating, but I will also investigate whether haemodynamic measures differ when stratifying by Fazekas scores. In Chapter 5E where I am going to assess the association between

ICA pulsatility and other haemodynamic measures, I will use only PI to represent vascular pulsatility rather than repeating the analyses using RI again, as PI and RI are calculated similarly.

As the final sample size for data analyses is 56, the number of covariates that are allowed in each multiple regression model is limited to three. Age, gender and mean arterial pressure (MAP) will be adjusted for in most models but there are also exceptions. When BP is used as the main predictor variable, history of hypertension will be used instead of MAP to avoid collinearities. In Chapter 5E, when assessing the relationship between intracranial haemodynamic measures, I will adjust for WMH volume (instead of gender) as it might be a strong confounding factor. Non-standardised β coefficients will be presented as the results of linear regression models, whereas odds ratios (OR) will be used in ordinal regression models.

Chapter 5A: Summary of patient characteristics and intracranial haemodynamic measures

Patient characteristics

Table 13 summarises the basic demographics, past medical history and SVD features of the patients. We recruited 60 patients, of whom 56 (40% male; mean age 67.8±8.27 years old) had analysable MRI data. One patient did not complete the MRI scan due to claustrophobia and another due to a finding of a subdural hematoma. I excluded data from another two patients because of the poor finger pulse signal during the phase-contrast MRI scan.

The stroke subtype was lacunar in 36/56 and cortical in 20/56 patients. Overall, 6/56 patients had a past history of stroke and 42/56 were hypertensive, 31/56 patients were taking antihypertensive treatment before the stroke, 51/56 used statins and 51/56 used antiplatelet agents. The supine BP immediately after the MRI scan was 138.62±21.6/81.02±12.04 mmHg. 35/56 patients had lacunes and 8/56 had CMBs. Median WMH volume was 10.74 ml (range 1.40-74.97 ml), representing median 0.77% (range 0.11-5.17%) of ICV. According to the Fazekas scale, most patients (43/56) had mild to moderate WMH (total Fazekas 1-4). Most patients also had mild to moderate PVS: 51/56 scored 0-3 in PVS (i.e. the number of PVS <40) in the basal ganglia, and 48/56 scored 0-3 in PVS in the centrum semiovale.

Vascular risk factors and most SVD features including CMBs, WMH burden, and PVS did not differ between lacunar and cortical stroke, apart from that lacunes are more frequently seen in those with lacunar stroke than cortical stroke (27/36 vs 8/20, p=0.02).

Table 13 Summary of patient characteristics

	Overall (n=56)	Lacunar (n=36)	Cortical (n=20)
Demographic and health condition			
Age (years)	67.80±8.27	67.36±8.32	68.60±8.32
Sex = male (%)	40 (71.4)	29 (80.6)	11 (55.0)
History of stroke (%)	6 (10.7)	5 (13.9)	1 (5.0)
Diabetes (%)	7 (12.5)	4 (11.1)	3 (15.0)
AF (%)	5 (8.9)	2 (5.6)	3 (15.0)
Hyperlipidaemia (%)	37 (66.1)	23 (63.9)	14 (70.0)
Hypertension (%)	42 (75.0)	28 (77.8)	14 (70.0)
BP (mmHg)			
Systolic	138.62±21.60	138.33±22.86	138.50±19.27
Diastolic	81.02±12.04	82.08±12.00	79.90±12.52
Smoking (%)			
Never	22 (39.3)	16 (44.4)	6 (30.0)
Current smoker	10 (17.9)	6 (16.7)	4 (20.0)
Quit less than 1 year	3 (5.4)	2 (5.6)	1 (5.0)
Quit more than 1 year	21 (37.5)	12 (33.3)	9 (45.0)
SVD related measures			
Presence of lacune (%)	35 (62.5)	**27 (75.0)**	**8 (40.0)**
Presence of CMB (%)	8 (14.3)	6 (16.7)	2 (10.0)
WMH volume (ml) (median [range])	10.73 [1.40, 74.97]	12.38 [1.40, 72.17]	8.12 [3.31, 74.97]
ICV volume (ml)	1478.77±134.48	1484.33±126.38	1468.76±150.89
WMH/ICV (%) (median [range])	0.77 [0.11, 1.21]	0.92 [0.11, 4.53]	0.60 [0.21, 5.17]
PVWMH Fazekas score (%)			
0	0 (0)	0	0
1	27 (48.2)	15 (41.7)	12 (60.0)
2	17 (30.4)	12 (33.3)	5 (25.0)
3	12 (21.4)	9 (25.0)	3 (15.0)
DWMH Fazekas score (%)			
0	4 (7.1)	3 (8.3)	1 (5.0)
1	26 (46.4)	14 (38.9)	12 (60.0)
2	16 (28.6)	12 (33.3)	4 (20.0)
3	10 (17.9)	7 (19.4)	3 (15.0)
Total Fazekas score (%)			
1	4 (7.1)	3 (8.3)	1 (5.0)
2	20 (35.7)	10 (27.8)	10 (50.0)
3	9 (16.1)	6 (16.7)	3 (15.0)
4	10 (17.9)	7 (19.4)	3 (15.0)
5	4 (7.1)	4 (11.1)	0 (0)

6	9 (16.1)	6 (16.7)	3 (15.0)
Basal ganglia PVS score (%)			
0	0 (0)	0	0
1	19 (33.9)	9 (25.0)	10 (50.0)
2	21 (37.5)	16 (44.4)	5 (25.0)
3	12 (21.4)	8 (22.2)	4 (20.0)
4	4 (7.1)	3 (8.3)	1 (5.0)
Centrum semiovale PVS score (%)			
0	0 (0)	0	0
1	11 (19.6)	5 (13.9)	6 (30.0)
2	17 (30.4)	10 (27.8)	7 (25.0)
3	20 (35.7)	14 (38.9)	6 (30.0)
4	8 (14.3)	7 (19.4)	1 (5.0)

AF: atrial fibrillation; SVD: small vessel disease; CMB: cerebral microbleeds; WMH: white matter hyperintensities; ICV: intracranial volume; PVWMH: periventricular white matter hyperintensities; DWMH: deep white matter hyperintensities; PVS: perivascular spaces.

*Results in bold represent $p<0.05$. P values were from paired-samples t-tests. No multi-test corrections were used in this table since it is mainly for descriptive purposes.

Summary of CBF and pulsatility measures

As shown in Table 14, mean total cerebral arterial flow was 645.32±113.00 ml/min or 60.17±9.52 ml/min per 100 ml brain volume. Mean total transverse sinus flow was 562.67±117.00 ml/min or 51.98±11.34 per 100 ml brain volume, and mean total internal jugular vein flow was 521.98±163.56 ml/min or 48.12±14.82 per 100 ml brain volume.

PI was highest in the arteries (e.g. 1.27±0.31 in ICA), followed by internal jugular veins (0.94±0.52) and lowest in venous sinuses (e.g. 0.58±0.24 in superior sagittal sinus). RI followed the same pattern as PI and was generally smaller than PI in the same vessel.

Total net CSF flow was 0.20±0.78 ml/min (positive value indicates flow towards the caudal direction) in the aqueduct and -1.73±4.46 ml/min (a negative value indicates flow towards the cranial direction) in the cervical subarachnoid space. Flow waveform peak delays (with reference to arterial peak) were significantly different across veins and CSF spaces, being shortest in the cervical subarachnoid space (0.0451±0.0797 s), followed by the internal jugular vein (0.1127±0.1045 s), transverse sinus (0.1173±0.0931 s), straight sinus (0.1253±0.1061 s), superior sagittal sinus (0.1615±0.1020 s), and longest in the aqueduct (0.1831±0.0708 s).

Table 14 Summary of extra- and intra- cranial haemodynamic measures

	Mean ± SD
Aortic measures	
Aortic augmentation index	24.81±9.69
CBF	
Total arterial flow (ml/min)	654.32±113.00
Total transverse sinuses flow (ml/min)	562.67±117.00
Total internal jugular flow (ml/min)	521.98±163.56
Total arterial flow (ml/min/100 ml brain volume)	60.17±9.52
Total transverse sinus flow (ml/min/100 ml brain volume)	51.98±11.34
Total internal jugular flow (ml/min/100 ml brain volume)	48.12±14.82
Pulsatility indices in brain vessels	
ICA PI	1.27±0.31
ICA RI	0.69±0.07
Vertebral artery PI	1.48±0.38
Vertebral artery RI	0.74±0.09
Superior sagittal sinus PI	0.58±0.24
Superior sagittal sinus RI	0.43±0.13
Straight sinus PI	0.52±0.19
Straight sinus RI	0.41±0.11
Transverse sinus PI	0.53±0.21
Transverse sinus RI	0.41±0.12
Internal jugular vein PI	0.94±0.52
Internal jugular vein RI	0.61±0.21
CSF flow and pulsatility measures	
Total aqueduct CSF flow (ml/min)*	0.20±0.78
Aqueduct stroke volume (ml)	0.06±0.04
Duration of systolic phase in aqueduct (s)	0.46±0.07
Total cervical CSF flow (ml/min)*	-1.73±4.46
Cervical CSF stroke volume (ml)	0.48±0.21
Duration of systolic phase in Cervical CSF (s)	0.36±0.07
Waveform peak delays (with reference to arterial peak)	
Superior sagittal sinus (s)	0.16±0.10
Straight sinus (s)	0.13±0.10
Transverse sinus (s)	0.12±0.09
Internal jugular vein (s)	0.11±0.10
Aqueduct (s)	0.18±0.07
Cervical CSF (s)	0.05±0.08

SD: standard deviation; CBF: cerebral blood flow; ICA: internal carotid artery; PI: pulsatility index; RI: resistance index; CSF: cerebrospinal fluid.
* For the CSF flow, a positive value indicates flow towards the caudal direction, whereas a negative value indicates flow towards the cranial direction.

The association between CBF, pulsatility measures, and age and stroke subtype

Table 15 shows the results of univariate linear regression between CBF or pulsatility measures, and age and stroke subtypes. To note that, for CBF, in order to adjust for the potential confounding effect of brain atrophy, only the values normalised to the brain volume (ml/min/100 ml brain volume) will be used in further analyses; for CSF pulsatility and waveform peak delays, only the ones that were well reproducible (defined as within-subject CV < 20%, see Table 10 in Chapter 4) will be used, including the stroke volumes, systolic durations, aqueduct-to-artery peak delay and internal jugular vein-to-artery peak delay.

Aortic AIx significantly increased with age (0.407 increase per year, p=0.01). There was no significant association between age and CBF in either arteries or veins. In general, pulsatility indices in most vessels increased with age, although it only reached statistical significance in the straight sinus (both PI and RI. e.g. PI: 0.008 increase per year, p=0.014) and ICA (RI: 0.003 increase per year, p=0.015).

There were no significant associations between the aqueduct and cervical CSF pulsatility measures and age. None of the CBF or pulsatility measures was associated with stroke subtypes.

Table 15 Univariate regression between haemodynamic measures and age, stroke classification

	Predictors					
	Age (years)			Lacunar stroke (vs cortical)		
Outcomes	β	95% CI	P value	β	95% CI	P
Aortic stiffness						
Aortic augmentation index	**0.407**	**[0.107, 0.707]**	**0.010**	-3.247	[-8.646, 2.151]	0.233
CBF (ml/min/100 ml brain volume)						
Total arterial flow	-0.262	[-0.568, 0.044]	0.091	2.459	[-2.871, 7.789]	0.359
Total transverse sinus flow	-0.012	[-0.386, 0.362]	0.949	-3.799	[-10.113, 2.514]	0.233
Total internal jugular vein flow	-0.391	[-0.868, 0.086]	0.106	-0.048	[-8.410, 8.313]	0.991
Pulsatility indices in brain vessels						
ICA PI	0.009	[-0.001, 0.019]	0.078	0.002	[-0.170, 0.175]	0.978
Superior sagittal sinus PI	0.007	[-0.001, 0.015]	0.074	0.020	[-0.115, 0.155]	0.772
Straight sinus PI	**0.008**	**[0.002, 0.014]**	**0.014**	0.059	[-0.049, 0.168]	0.277
Transverse sinus PI	0.005	[-0.002, 0.012]	0.141	0.048	[-0.070, 0.166]	0.421
Internal jugular vein PI	-0.001	[-0.018, 0.017]	0.940	0.137	[-0.157, 0.431]	0.354
ICA RI	**0.003**	**[0.001, 0.005]**	**0.015**	0.005	[-0.037, 0.046]	0.829
Superior sagittal sinus RI	0.004	[0.000, 0.008]	0.074	0.020	[-0.051, 0.091]	0.572
Straight sinus RI	**0.004**	**[0.001, 0.008]**	**0.020**	0.040	[-0.022, 0.102]	0.201
Transverse sinus RI	0.003	[-0.001, 0.007]	0.153	0.033	[-0.035, 0.102]	0.333
Internal jugular vein RI	-0.001	[-0.008, 0.005]	0.687	0.049	[-0.067, 0.164]	0.401
CSF pulsatility measures						
Aqueduct stroke volume	0	[-0.0004, 0.002]	0.160	-0.011	[-0.032, 0.010]	0.288
Aqueduct systolic duration	-0.001	[-0.004, 0.001]	0.269	-0.015	[-0.055, 0.025]	0.45
Cervical CSF stroke volume	0	[-0.007, 0.007]	0.932	-0.017	[-0.134, 0.101]	0.777
Cervical CSF systolic duration	-0.001	[-0.003, 0.001]	0.308	0	[-0.04, 0.04]	0.961
Waveform peak delays						
Aqueduct-artery peak delay	0	[-0.003,0.002]	0.708	-0.011	[-0.051,0.029]	0.577
Internal jugular vein-artery peak	-0.002	[-0.005,0.002]	0.332	0.006	[-0.053,0.065]	0.837

Results in bold represent P value <0.05. CBF: cerebral blood flow; ICA: internal carotid artery; PI: pulsatility index; RI: resistance index; CSF: cerebrospinal fluid.

The association between intracranial haemodynamic measures and BP

Table 16 shows the relationship between intracranial haemodynamic measures and systemic BP measures. Pulsatility indices in some veins significantly increased with lower diastolic BP (e.g. straight sinus PI: β=-0.005, p=0.028) and lower MAP (e.g. Internal jugular vein PI: β=-0.012, p=0.019) but not with systolic BP. There were no significant associations between pulsatility indices and systolic BP or pulse pressure.

There were no significant associations between CSF stroke volumes or systolic durations and any BP measurements. Also, the waveform peak delay (with reference to the arterial peak) in either aqueduct CSF or internal jugular vein was not associated with BP measurements.

Table 16 The associations between intracranial haemodynamic measures and BP

	Predictor variables (in separate models adjusted for age, gender and history of hypertension)											
	Systolic BP			Diastolic BP			Pulse pressure			Mean arterial pressure		
	β	95% CI	P	β	95% CI	P	β	95% CI	P	β	95% CI	P value
Outcome variables (in separate models)												
CBF (ml/min/100 ml brain volume)												
Arterial flow	0.097	[-0.021,0.215]	0.11	**0.222**	**[0.021,0.424]**	**0.03**	0.041	[-0.116,0.198]	0.60	**0.192**	**[0.014,0.37]**	**0.04**
Transverse sinus flow	-0.032	[-0.159,0.095]	0.61	0.111	[-0.109,0.331]	0.32	-0.117	[-0.28,0.046]	0.16	0.032	[-0.163,0.228]	0.74
Internal jugular vein flow	0.006	[-0.182,0.194]	0.95	0.051	[-0.278,0.379]	0.76	-0.018	[-0.264,0.227]	0.88	0.031	[-0.259,0.32]	0.83
Pulsatility indices in brain vessels												
ICA PI	0.002	[-0.002,0.006]	0.26	0.002	[-0.005,0.009]	0.57	0.003	[-0.002,0.008]	0.29	0.003	[-0.003,0.009]	0.36
Superior sagittal sinus PI	0.001	[-0.002,0.004]	0.70	-0.002	[-0.008,0.003]	0.37	0.002	[-0.002,0.006]	0.24	-0.001	[-0.005,0.004]	0.74
Straight sinus PI	-0.001	[-0.004,0.001]	0.23	**-0.005**	**[-0.009,-0.001]**	**0.03**	0	[-0.003,0.003]	0.97	-0.004	[-0.007,0]	0.06
Transverse sinus PI	0	[-0.002,0.003]	0.84	-0.003	[-0.008,0.001]	0.16	0.002	[-0.001,0.006]	0.19	-0.001	[-0.006,0.003]	0.48
Internal jugular vein PI	-0.006	[-0.012,0.001]	0.10	**-0.015**	**[-0.026,-0.003]**	**0.01**	0.001	[-0.01,0.008]	0.76	**-0.012**	**[-0.022,-0.002]**	**0.02**
ICA RI	0.001	[0,0.001]	0.25	0	[-0.001,0.002]	0.75	0.001	[0,0.002]	0.20	0.001	[-0.001,0.002]	0.44
Superior sagittal sinus RI	0	[-0.001,0.002]	0.76	-0.002	[-0.004,0.001]	0.26	0.001	[-0.001,0.003]	0.21	-0.001	[-0.003,0.002]	0.62
Straight sinus RI	-0.001	[-0.002,0.001]	0.40	-0.002	[-0.005,0]	0.05	0	[-0.002,0.002]	0.74	-0.002	[-0.004,0]	0.11
Transverse sinus RI	0	[-0.001,0.002]	0.83	-0.002	[-0.005,0.001]	0.17	0.001	[-0.001,0.003]	0.18	-0.001	[-0.003,0.002]	0.49

Internal jugular vein RI	-0.002	[-0.005,0.001]	0.12	**-0.007**	**[-0.010,-0.002]**	**0.01**	0	[-0.004,0.003]	0.96	**-0.005**	**[-0.009,-0.001]**	**0.02**
CSF pulsatility												
Aqueduct CSF stroke volume	0	[0,0.001]	0.483	0	[-0.001,0.001]	0.618	0	[0,0.001]	0.16	0	[-0.001,0.001]	0.95
Aqueduct CSF systolic duration	-0.001	[-0.002,0]	0.096	-0.001	[-0.003,0.001]	0.188	-0.001	[-0.002,0]	0.24	-0.001	[-0.002,0]	0.10
Cervical CSF stroke volume	0	[-0.003,0.003]	0.985	0	[-0.005,0.005]	0.926	0	[-0.004,0.004]	0.98	0	[-0.004,0.004]	0.99
Cervical CSF systolic duration	0	[-0.001,0.001]	0.925	0.001	[-0.001,0.002]	0.292	0	[-0.001,0.001]	051	0	[-0.001,0.002]	0.51
Waveform peak delays												
Aqueduct-artery peak delay	0	[-0.001,0]	0.271	-0.001	[-0.002,0.001]	0.200	0	[-0.001,0.001]	0.63	-0.001	[-0.002,0]	0.19
Internal jugular vein-artery peak delay	0.001	[-0.001,0.002]	0.267	0.002	[-0.001,0.004]	0.142	0	[-0.001,0.002]	0.72	0.001	[-0.001,0.004]	0.15

Results in bold represent P value <0.05. CBF: cerebral blood flow; ICA: internal carotid artery; PI: pulsatility index; RI: resistance index; CSF: cerebrospinal fluid.

The association between cerebrovascular pulsatility measures and aortic stiffness

Table 17 shows the associations between CBF or intracranial pulsatility and aortic AIx. There were no significant associations between aortic AIx and CBF (e.g. arterial flow: β=0.136, p=0.36). Higher aortic AIx was significantly associated with lower ICA PI (β=-0.011, p=0.04). There was no significant association between aortic AIx and venous pulsatility indices.

None of the CSF pulsatility measures or waveform peak delays were associated with aortic AIx.

Table 17 The associations between CBF, cerebrovascular pulsatility, and aortic AIx

	Aortic AIx (predictor variable)		
	β	95% CI	P value
Outcome variables (in separate models*)			
CBF (ml/min/100 ml brain volume)			
Arterial flow	0.215	[-0.115,0.546]	0.197
Transverse sinus flow	0.102	[-0.262, 0.466]	0.576
Internal jugular vein flow	0.419	[-0.109, 0.948]	0.117
Pulsatility indices in brain vessels			
ICA PI	**-0.011**	**[-0.022, -0.001]**	**0.040**
Superior sagittal sinus PI	0.004	[-0.005, 0.012]	0.396
Straight sinus PI	0.002	[-0.005, 0.009]	0.533
Transverse sinus PI	0.004	[-0.003, 0.012]	0.255
Internal jugular vein PI	-0.007	[-0.026,0.012]	0.456
ICA RI	-0.002	[-0.005, 0.001]	0.117
Superior sagittal sinus RI	0.002	[-0.003, 0.007]	0.382
Straight sinus RI	0.001	[-0.003, 0.005]	0.552
Transverse sinus RI	0.002	[-0.002, 0.007]	0.292
Internal jugular vein RI	-0.004	[-0.011, 0.004]	0.299
CSF pulsatility			
Aqueduct CSF stroke volume	0	[-0.002,0.001]	0.740
Aqueduct CSF systolic duration	0.001	[-0.002,0.003]	0.644
Cervical CSF stroke volume	0.001	[-0.007,0.009]	0.886
Cervical CSF systolic duration	-0.002	[-0.004,0.001]	0.197
Waveform peak delays			
Aqueduct-artery peak delay	-0.001	[-0.004,0.001]	0.349
Internal jugular vein-artery peak delay	-0.001	[-0.005,0.003]	0.633

*All models were adjusted for age, gender and mean arterial pressure. Results in bold represent P value <0.05. CBF: cerebral blood flow; ICA: internal carotid artery; PI: pulsatility index; RI: resistance index; CSF: cerebrospinal fluid.

Chapter 5B: The associations between CBF and SVD features

The association between CBF and WMH

Univariate comparisons of CBF according to Fazekas scores

Figure 30 and

Table 18 shows the univariate comparisons of arterial and venous flow according to the total Fazekas score. There were no significant differences in any CBF value across Fazekas groups. (e.g. total arterial flow total Fazekas 1-2 vs 3-4 vs 5-6 was 62.62±10.65 vs 58.27±8.31 vs 58.43±8.57 ml/min/100 ml brain volume, p=0.25).

CBF also did not differ across either periventricular ***(Table 18)*** or deep WMH Fazekas scores ***(Table 19).***

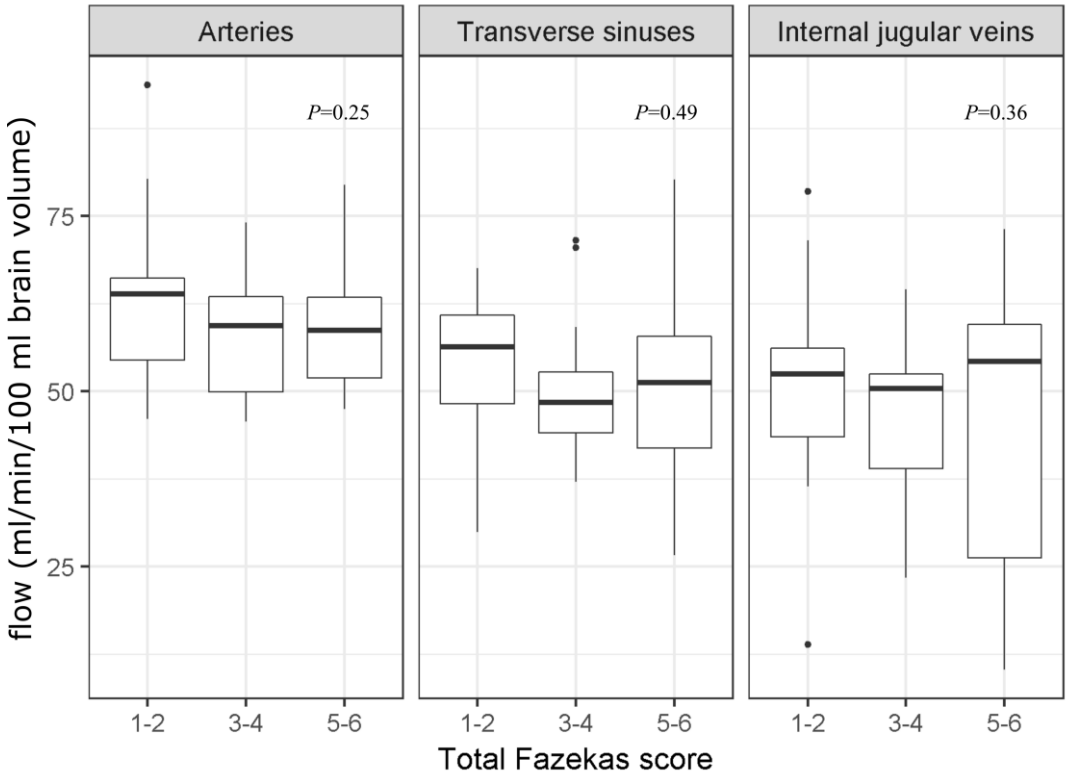

Figure 30 Boxplots showing the comparisons of CBF (ml/min/100 ml brain volume) in arteries and veins according to total Fazekas score. P values were from ANOVA. Sample sizes in each group: Fazekas score 1-2 (n=24); 3-4 (n=19); 5-6 (n=13). Arterial CBF included blood flow in the internal carotid arteries and vertebral arteries.

Table 18 CBF according to total Fazekas scores

	Total Fazekas score			
CBF (ml/min/100 ml brain volume)	1-2 (n=24)	3-4 (n=19)	5-6 (n=13)	P value
Total arterial flow	62.62±10.65	58.27±8.31	58.43±8.57	0.25
Total transverse sinus flow	53.98±10.31	49.80±9.65	51.46±15.17	0.49
Total internal jugular flow	51.28±13.32	46.14±11.72	45.20±20.62	0.39

P values were from ANOVA.

Table 19 CBF according to periventricular WMH Fazekas scores

	Fazekas score for periventricular WMH			
CBF (ml/min/100 ml brain volume)	1 (n=27)	2 (n=17)	3 (n=12)	P value
Total arterial flow	62.24±10.62	57.47±8.11	59.34±8.27	0.26
Total transverse sinus flow	53.51±10.28	49.36±9.60	52.24±15.57	0.50
Total internal jugular flow	51.39±12.96	43.89±12.21	46.78±20.70	0.25

P values were from ANOVA.

Table 20 CBF according to deep WMH Fazekas scores

	Fazekas score for deep WMH				
CBF (ml/min/100 ml brain volume)	0 (n=4)	1 (n=26)	2 (n=16)	3 (n=10)	P value
Total arterial flow	65.26±19.88	60.67± 8.47	59.57± 8.12	57.80± 9.69	0.61
Total transverse sinus flow	48.63± 11.35	54.32± 9.97	48.89± 8.94	52.16± 17.19	0.46
Total internal jugular flow	45.82± 27.40	51.85± 8.47	43.82± 15.85	46.25± 19.86	0.36

P values were from ANOVA.

Linear regression analyses of CBF on WMH volume

Table 21 demonstrates the results of linear regression analysis between CBF and WMH volume (normalised to ICV). There were no significant associations between CBF and WMH, especially after the adjustment for age, gender and MAP (e.g. arterial flow: β=-0.018, p=0.153). Older age was significantly associated with larger WMH volume in all models ($\beta \approx 0.06$, $P<0.001$).

Table 21 The associations between CBF and WMH

ln WMH/ICV ratio as the outcome (linear regression)							
Non-adjusted linear regression				Multiple linear regression			
Predictors	β	95% CI	P value	Predictors	β	95% CI	P value
Total arterial flow (ml/min/100 ml brain volume)	-0.024	[-0.050, 0.002]	0.065	Total arterial flow	-0.018	[-0.042, 0.007]	0.153
				Age	**0.056**	**[0.028, 0.084]**	**<0.001**
				MAP	0.012	[-0.005, 0.028]	0.157
				gender	0.029	[-0.463, 0.522]	0.153
Total transverse sinus flow (ml/min/100 ml brain volume)	-0.009	[-0.031, 0.013]	0.403	Total transverse sinus flow	-0.011	[-0.033, 0.012]	0.34
				Age	**0.059**	[0.032, 0.087]	**<0.001**
				MAP	0.009	[-0.007, 0.024]	0.277
				gender	-0.061	[-0.644, 0.522]	0.834
Total internal jugular vein flow (ml/min/100 ml brain volume)	-0.011	[-0.028, 0.005]	0.173	Total internal jugular vein flow	-0.004	[-0.020, 0.011]	0.573
				Age	**0.059**	**[0.031, 0.088]**	**<0.001**
				MAP	0.008	[-0.007, 0.024]	0.291
				gender	0.059	[-0.447, 0.565]	0.816

Results in bold represent P value <0.05.

The association between CBF and PVS

Univariate comparisons of CBF according to PVS scores

Figure 31 and Figure 32 demonstrate the results of CBF stratified by PVS score in the basal ganglia and centrum semiovale. There were no significant differences in any CBF measures across basal ganglia ***(Figure 31)*** or centrum semiovale (***Figure 32***) PVS scores.

The details of the comparisons are shown in Table 22 and Table 23 below the relevant figures.

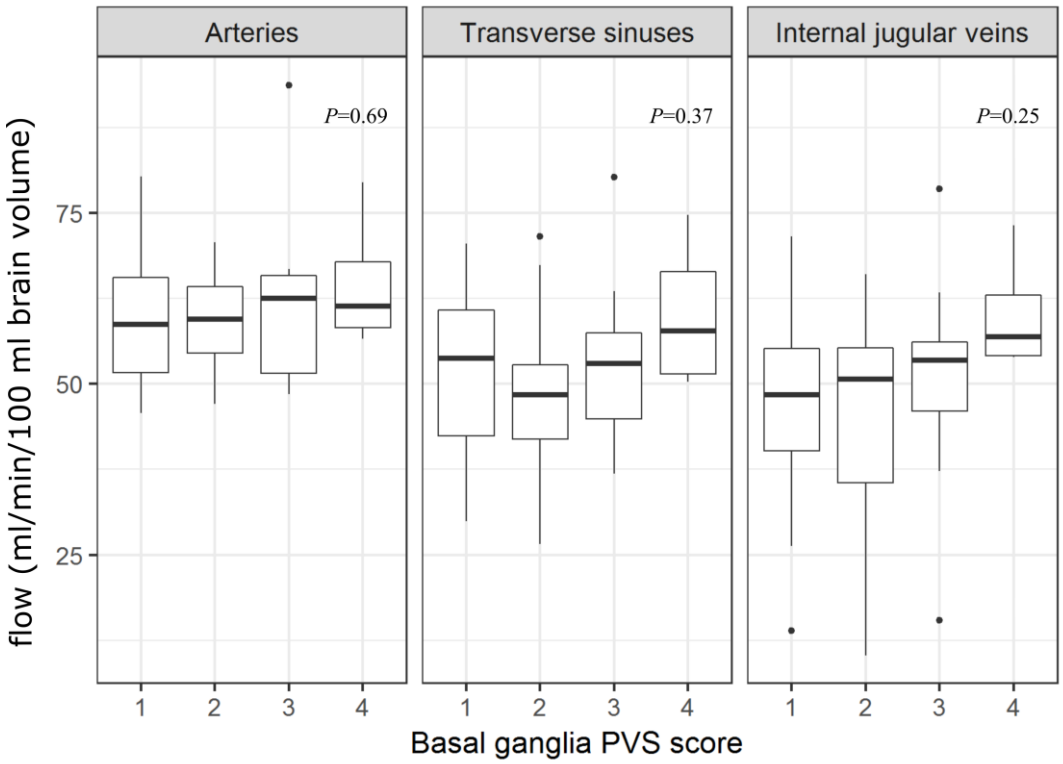

Figure 31 Boxplots showing the comparisons of blood flow (ml/min/100 ml brain volume) in arteries and veins according to basal ganglia perivascular space (PVS) score. P values were from ANOVA. Sample sizes in each group: PVS score 1 (n=19); 2 (n=21); 3 (n=12); 4 (n=4). Arterial CBF included blood flow in the internal carotid arteries and vertebral arteries.

Table 22 CBF according to basal ganglia PVS score

CBF (ml/min/100 ml brain volume	Basal ganglia PVS score				
	1 (n=19)	2 (n=21)	3 (n=12)	4 (n=4)	P
Total arterial flow	59.28±9.86	59.30±7.45	61.60±12.31	64.70±10.34	0.69
Total transverse sinus flow	52.42±11.31	49.45±10.93	52.97±11.95	60.13±11.42	0.37
Total internal jugular flow	47.31±13.90	44.88±15.69	51.05±15.11	60.21±9.00	0.25

P values were from ANOVA.

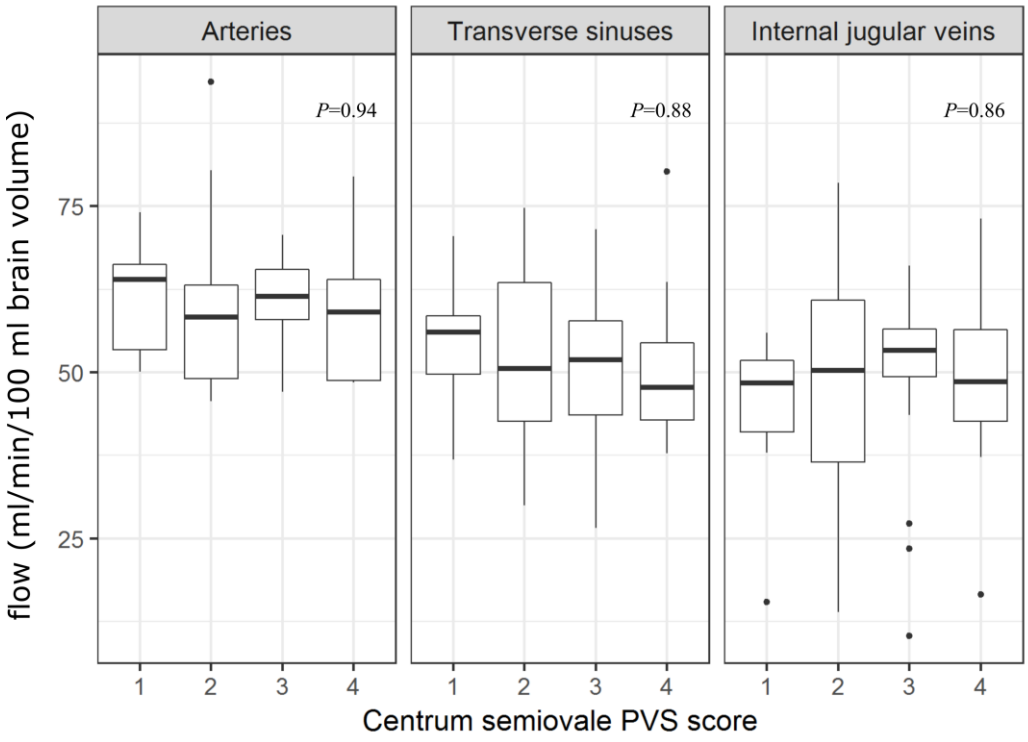

Figure 32 Boxplots showing the comparisons of blood flow (ml/min/100 ml brain volume) in arteries and veins according to centrum semiovale perivascular space (PVS) score. P values were from ANOVA. Sample sizes in each group: PVS score 1 (n=11); 2 (n=16); 3 (n=20); 4 (n=8). Arterial CBF included blood flow in the internal carotid arteries and vertebral arteries.

Table 23 CBF according to centrum semiovale PVS score

CBF (ml/min/100 ml brain volume)	Centrum semiovale PVS score				
	1 (n=11)	2 (n=17)	3 (n=20)	4 (n=8)	P value
Total arterial flow	61.40±7.88	59.47±12.61	60.51±7.18	59.11±10.71	0.94
Total transverse sinus flow	53.78±9.26	52.78±13.00	50.52±10.25	51.42±14.24	0.88
Total internal jugular flow	44.72±11.44	48.75±17.61	49.54±13.93	47.93±16.67	0.86

P values were from ANOVA.

Ordinal regression analyses of CBF on PVS

Table 24 and Table 25 show the results of logistic ordinal regression models between CBF and PVS in the basal ganglia and centrum semiovale. No significant associations between CBF and PVS in either location were observed, apart from the almost negligible association between higher internal jugular vein flow and higher PVS score in the basal ganglia (OR=1.047, 95% CI [1.005, 1.09]). PVS in both basal ganglia and centrum semiovale significantly increased with older age (OR≈1.1 per year increase).

Table 24 Association between CBF and PVS in the basal ganglia

PVS score in basal ganglia as outcome					
Non-adjusted ordinal regression			Multiple ordinal regression		
Predictors	OR	95% CI	Predictors	OR	95% CI
Total arterial flow (per ml/min/100 ml brain volume)	1.027	[0.973, 1.084]	Total arterial flow	1.067	[0.999, 1.138]
			Age (per year)	**1.137**	**[1.055, 1.227]**
			MAP (per mmHg)	1.015	[0.978, 1.054]
			Gender (male)	1.171	[0.357, 3.836]
Total Transverse sinus flow (per ml/min/100 ml brain volume)	1.011	[0.969, 1.056]	Total Transverse sinus flow	1.03	[0.975, 1.089]
			Age	**1.117**	**[1.041, 1.199]**
			MAP	1.025	[0.986, 1.064]
			Gender (male)	1.46	[0.378, 5.646]
Total Internal jugular vein flow (per ml/min/100 ml brain volume)	1.018	[0.985, 1.053]	**Total Internal jugular vein flow**	**1.047**	**[1.005, 1.09]**
			Age	**1.143**	**[1.060, 1.234]**
			MAP	1.024	[0.987, 1.062]
			Gender	1.435	[0.426, 4.832]

Results in bold represent results that do not overlap with the null value (OR=1).

Table 25 Association between CBF and PVS in the centrum semiovale

Centrum semiovale PVS score as outcome					
Non-adjusted ordinal regression			Multiple ordinal regression		
Predictors	OR	95% CI	Predictors	OR	95% CI
Total arterial flow (per ml/min/100 ml brain volume)	0.993	[0.945, 1.042]	Total arterial flow	1.013	[0.958, 1.072]
			Age (per year)	**1.087**	**[1.013, 1.166]**
			MAP (per mmHg)	1.008	[0.970, 1.047]
			Gender (Male)	3.01	[0.835, 10.847]
Total transverse sinus flow (per ml/min/100 ml brain volume)	0.984	[0.944, 1.027]	Total transverse sinus flow	1.01	[0.959, 1.065]
			Age	**1.084**	**[1.013, 1.161]**
			MAP	1.01	[0.975, 1.047]
			Gender (Male)	3.327	[0.716, 15.451]
Total internal jugular vein flow (per ml/min/100 ml brain volume)	1.009	[0.978, 1.042]	Total internal jugular vein flow	1.024	[0.990, 1.060]
			Age	**1.094**	**[1.022, 1.172]**
			MAP	1.009	[0.973, 1.045]
			Gender (Male)	3.438	[0.961, 12.302]

Results in bold represent results that do not overlap with the null value (OR=1)

Chapter 5C: The associations between aortic AIx, cerebrovascular pulsatility and SVD features

The association between cerebrovascular pulsatility and WMH

Univariate comparisons of cerebrovascular pulsatility according to Fazekas scores

Figure 33 and Table 26 show the results of cerebrovascular PI and RI stratified by total Fazekas scores. PI and RI in all venous sinuses was significantly higher, incrementally, in patients with higher total Fazekas score (e.g. in the superior sagittal sinus, the PI in Fazekas 1-2 vs 3-4 vs 5-6 was 0.48±0.12 vs 0.60±0.24 vs 0.73±0.32, P=0.007).

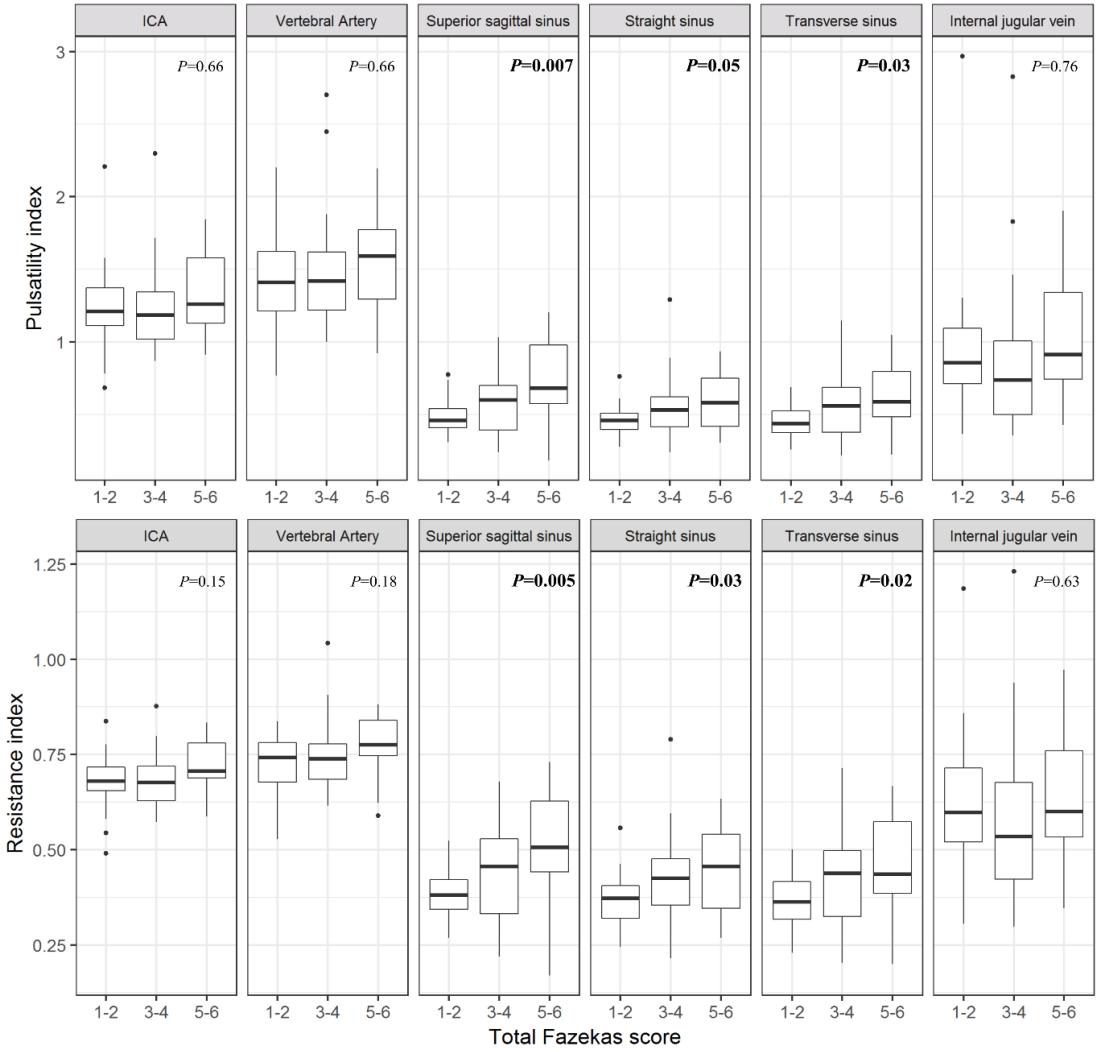

Figure 33 Boxplot showing the univariate comparisons of pulsatility and resistance index in the arteries to veins according to total Fazekas score. P values were from ANOVA and were marked bold when less than 0.05. Sample sizes in each group: Fazekas 1-2 (n=24); 3-4 (n=19); 5-6 (n=13). ICA: internal carotid artery.

Table 26 Aortic augmentation index and cerebrovascular pulsatility according to total Fazekas score

	Total Fazekas score			
	1-2 (n=24)	3-4 (n=19)	5-6 (n=13)	P value
Aortic augmentation index	22.04±11.43	26.50±7.28	27.46±8.57	0.174
ICA PI	1.24±0.30	1.25±0.33	1.34±0.29	0.66
Vertebral artery PI	1.43±0.34	1.51±0.44	1.54±0.38	0.66
Superior sagittal sinus PI	**0.48±0.12**	**0.60±0.24**	**0.73±0.32**	**0.007**
Straight sinus PI	**0.45±0.11**	**0.57±0.24**	**0.59±0.20**	**0.05**
Transverse sinus PI	**0.45±0.12**	**0.57±0.24**	**0.63±0.24**	**0.03**
Internal jugular vein PI	0.94±0.50	0.88±0.62	1.03±0.44	0.76
ICA RI	0.68±0.07	0.69±0.07	0.72±0.08	0.15
Vertebral artery RI	0.72±0.08	0.75±0.10	0.77±0.09	0.18
Superior sagittal sinus RI	**0.38±0.07**	**0.45±0.13**	**0.50±0.16**	**0.005**
Straight sinus RI	**0.37±0.07**	**0.43±0.13**	**0.45±0.12**	**0.03**
Transverse sinus RI	**0.37±0.08**	**0.43±0.14**	**0.46±0.14**	**0.02**
Internal jugular vein RI	0.62±0.18	0.58±0.24	0.65±0.19	0.63

P values were from ANOVA. Results in bold represent p value <0.05.

Table 27 and Table 28 show the results of cerebrovascular PI and RI stratified by periventricular and deep WMH Fazekas scores. PI and RI were significantly higher in patients with higher periventricular Fazekas score (e.g. in the superior sagittal sinus, the PI in Fazekas 1 vs 2 vs 3 was 0.48±0.14 vs 0.62±0.23 vs 0.75±0.33, P=0.003).***(Table 27)*** However, patients who had different deep WMH Fazekas scores did not differ in PI or RI in any vessels. (***Table 28***)

Table 27 Cerebrovascular pulsatility according to periventricular Fazekas scores

	Fazekas score for periventricular WMH			
	1 (n=27)	2 (n=17)	3 (n=12)	P value
ICA PI	1.23±0.29	1.26±0.34	1.36±0.29	0.44
Vertebral artery PI	1.42±0.34	1.52±0.45	1.56±0.39	0.505
Superior sagittal sinus PI	**0.48±0.14**	**0.62±0.23**	**0.75±0.33**	**0.003**
Straight sinus PI	**0.45±0.11**	**0.57±0.26**	**0.61±0.19**	**0.024**
Transverse sinus PI	**0.45±0.14**	**0.58±0.24**	**0.65±0.24**	**0.013**
Internal jugular vein PI	0.93±0.49	0.89±0.63	1.05±0.45	0.724
ICA RI	0.67±0.07	0.69±0.07	0.72±0.07	0.148
Vertebral artery RI	0.72±0.08	0.76±0.10	0.78±0.09	0.178
Superior sagittal sinus RI	**0.38±0.08**	**0.46±0.12**	**0.51±0.17**	**0.005**
Straight sinus RI	**0.37±0.07**	**0.43±0.14**	**0.46±0.11**	**0.026**
Transverse sinus RI	**0.36±0.09**	**0.44±0.13**	**0.47±0.14**	**0.018**
Internal jugular vein RI	0.61±0.18	0.58±0.25	0.66±0.20	0.629

P values were from ANOVA. Results in bold represent P value <0.05.

Table 28 Cerebrovascular pulsatility according to deep WMH Fazekas scores

	Fazekas score for deep WMH				
	0 (n=4)	1 (n=26)	2 (n=16)	3 (n=10)	P
ICA PI	1.04±0.24	1.25±0.28	1.33±0.37	1.30±0.27	0.41
Vertebral artery PI	1.28±0.40	1.48±0.40	1.54±0.40	1.48±0.31	0.71
Superior sagittal sinus PI	0.49±0.10	0.53±0.19	0.60±0.29	0.71±0.27	0.18
Straight sinus PI	0.42±0.11	0.50±0.21	0.54±0.18	0.58±0.20	0.50
Transverse sinus PI	0.47±0.17	0.49±0.16	0.56±0.27	0.63±0.22	0.28
Internal jugular vein PI	0.77±0.31	0.99±0.52	0.92±0.65	0.92±0.43	0.88
ICA RI	0.62±0.07	0.68±0.07	0.70±0.08	0.71±0.07	0.19
Vertebral artery RI	0.70±0.13	0.74±0.10	0.76±0.09	0.77±0.08	0.53
Superior sagittal sinus RI	0.39±0.06	0.41±0.10	0.44±0.16	0.50±0.13	0.25
Straight sinus RI	0.35±0.08	0.39±0.12	0.42±0.11	0.44±0.11	0.42
Transverse sinus RI	0.37±0.11	0.39±0.10	0.42±0.15	0.46±0.12	0.39
Internal jugular vein RI	0.54±0.18	0.64±0.19	0.59±0.26	0.59±0.17	0.78

P values were from ANOVA.

Linear regression analyses of aortic AIx and cerebrovascular pulsatility on WMH volume

In univariate regression models, higher aortic AIx (β=0.026, P=0.040), pulsatility indices in the ICA (e.g. PI: β=0.841, P=0.038), superior sagittal sinus (e.g. PI: β=1.594, P=0.002), straight sinus (e.g. PI: β=1.399, P=0.028), and transverse sinuses (e.g. PI: β=1.654, P=0.004) were all significantly associated with large WMH volume.

After the adjustment for age, gender and MAP, the associations remained significant only in the superior sagittal sinus (e.g. PI: β=1.287, P=0.005) and transverse sinuses (e.g. PI: β=1.364, P=0.008) remained significant, but not in the ICA or with aortic AIx. There was no significant association between pulsatility in the internal jugular veins and WMH. ***(Table 29)***

Table 29 Association between aortic augmentation index, cerebrovascular pulsatility, and WMH

ln WMH/ICV ratio as the outcome (linear regression)							
Univariate linear regression models				Multiple linear regression models			
Predictors	β	95% CI	P value	Predictors	β	95% CI	P value
Aortic augmentation index	**0.026**	**[0.001,0.051]**	**0.040**	Aortic augmentation index	0.011	[-0.019,0.040]	0.462
				Age	**0.059**	**[0.030, 0.087]**	**<0.001**
				MAP	0.006	[-0.012,0.023]	0.512
				Gender	0.193	[-0.373, 0.760]	0.496
ICA PI	**0.841**	**[0.050, 1.633]**	**0.038**	ICA PI	0.435	[-0.293, 1.163]	0.236
				Age	**0.057**	**[0.030, 0.085]**	**<0.001**
				MAP	0.007	[-0.009, 0.023]	0.374
				Gender	0.062	[-0.428, 0.553]	0.799
Vertebral artery PI	0.332	[-0.323, 0.986]	0.314	Vertebral artery PI	0.090	[-0.492, 0.673]	0.757
				Age	**0.061**	**[0.033, 0.089]**	**<0.001**
				MAP	0.292	[-0.007, 0.024]	0.292
				Gender	0.082	[-0.415, 0.580]	0.741
Superior sagittal sinus PI	**1.594**	**[0.636, 2.552]**	**0.002**	**Superior sagittal sinus PI**	**1.287**	**[0.402, 2.172]**	**0.005**
				Age	**0.055**	**[0.029, 0.081]**	**<0.001**
				MAP	0.009	[-0.005, 0.024]	0.210
				Gender	0.244	[-0.226, 0.715]	0.302
Straight sinus PI	**1.399**	**[0.159, 2.640]**	**0.028**	Straight sinus PI	0.900	[-0.311, 2.111]	0.142
				Age	**0.056**	**[0.028, 0.084]**	**<0.001**
				MAP	0.011	[-0.005, 0.027]	0.160

				Gender	0.150	[-0.342, 0.641]	0.544
Transverse sinus PI	**1.654**	**[0.545, 2.762]**	**0.004**	**Transverse sinus PI**	**1.364**	**[0.366, 2.362]**	**0.008**
				Age	**0.056**	**[0.031, 0.082]**	**<0.001**
				MAP	0.010	[-0.005, 0.025]	0.173
				Gender	0.199	[-0.270, 0.668]	0.398
Internal jugular vein PI	0.104	[-0.376, 0.583]	0.667	Internal jugular vein PI	0.204	[-0.227, 0.635]	0.347
				Age	**0.062**	**[0.035, 0.089]**	**<0.001**
				MAP	0.011	[-0.006, 0.027]	0.200
				Gender	0.106	[-0.386, 0.598]	0.667
ICA RI	**4.326**	**[1.132, 7.520]**	**0.038**	ICA RI	2.267	[-0.778, 5.312]	0.141
				Age	**0.055**	**[0.027, 0.083]**	**<0.001**
				MAP	0.007	[-0.009, 0.023]	0.375
				Gender	0.091	[-0.393, 0.576]	0.707
Vertebral artery RI	2.437	[-0.240, 5.114]	0.074	Vertebral artery RI	0.094	[-1.519, 3.401]	0.446
				Age	**0.059**	**[0.031, 0.087]**	**<0.001**
				MAP	0.008	[-0.008, 0.024]	0.312
				Gender	0.096	[-0.397, 0.588]	0.698
Superior sagittal sinus RI	**2.878**	**[1.044, 4.713]**	**0.003**	**Superior sagittal sinus RI**	**2.281**	**[0.589, 3.973]**	**0.009**
				Age	**0.055**	**[0.029, 0.081]**	**<0.001**
				MAP	0.010	[-0.005, 0.024]	0.196
				Gender	0.223	[-0.250, 0.696]	0.349
Straight sinus RI	**2.437**	**[0.279, 4.595]**	**0.028**	Straight sinus RI	1.537	[-0.524, 3.597]	0.141

				Age	**0.056**	**[0.028, 0.084]**	**<0.001**
				MAP	0.011	[-0.005, 0.027]	0.176
				Gender	0.136	[-0.353, 0.624]	0.579
Transverse sinus RI	**2.664**	**[0.745, 4.583]**	**0.007**	**Transverse sinus RI**	**2.154**	**[0.431, 3.876]**	**0.015**
				Age	**0.057**	**[0.031, 0.083]**	**<0.001**
				MAP	0.010	[-0.005, 0.025]	0.186
				Gender	0.181	[-0.291, 0.654]	0.444
Internal jugular vein RI	0.226	[-0.996, 1.448]	0.712	Internal jugular vein RI	0.600	[-0.497, 1.698]	0.277
				Age	**0.063**	**[0.036, 0.090]**	**<0.001**
				MAP	0.011	[-0.005, 0.028]	0.183
				Gender	0.107	[-0.383, 0.597]	0.664

Results in bold represent P value <0.05.

The association between cerebrovascular pulsatility and PVS

Univariate comparisons of cerebrovascular pulsatility according to PVS scores

Figure 34 and Table 30 show that aortic AIx, and PI and RI in most vessels were significantly and incrementally higher in patients with higher basal ganglia PVS score (e.g. in the superior sagittal sinus, the PI in PVS score 1 vs 2 vs 3 vs 4 was 0.50±0.22 vs 0.53±0.19 vs 0.69±0.26 vs 0.87±0.25, P=0.006).

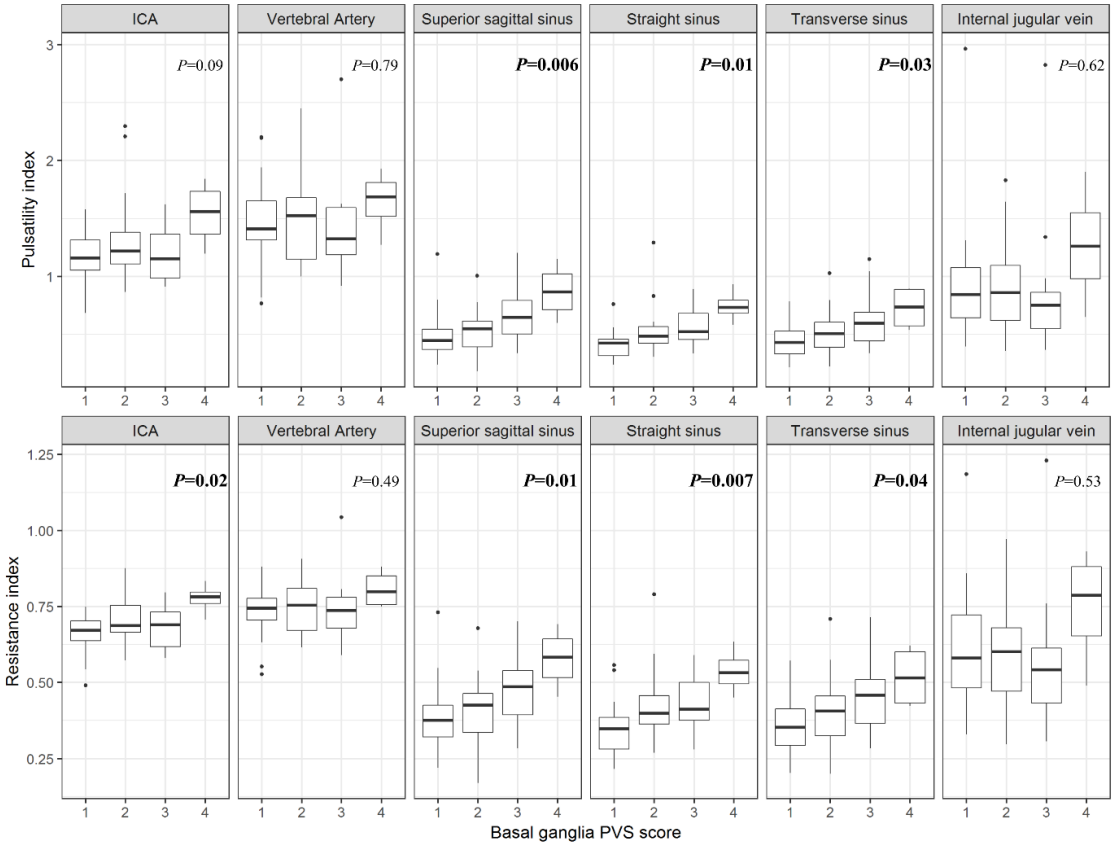

Figure 34 Boxplot showing univariate comparisons of pulsatility and resistance index in the arteries to veins according to the basal ganglia PVS score. P values were from ANOVA and were marked bold when less than 0.05. Sample sizes in each group: PVS score 1 (n=19); 2 (n=21); 3 (n=12); 4 (n=4). ICA: internal carotid artery.

Table 30 Aortic augmentation index and cerebrovascular pulsatility according to basal ganglia PVS score

	Basal ganglia PVS score				
	1 (n=19)	2 (n=21)	3 (n=12)	4 (n=4)	P value
Aortic augmentation index	**19.42±11.50**	**26.50±6.86**	**28.25±8.48**	**31.25±6.80**	**0.016**
ICA PI	1.18±0.23	1.33±0.37	1.19±0.23	1.54±0.29	0.09
Vertebral artery PI	1.46±0.39	1.50±0.36	1.42±0.46	1.64±0.28	0.79
Superior sagittal sinus PI	**0.50±0.22**	**0.53±0.19**	**0.69±0.26**	**0.87±0.25**	**0.006**
Straight sinus PI	**0.43±0.15**	**0.54±0.21**	**0.57±0.18**	**0.74±0.14**	**0.011**
Transverse sinus PI	**0.45±0.17**	**0.51±0.19**	**0.63±0.25**	**0.73±0.19**	**0.025**
Internal jugular vein PI	0.95±0.56	0.90±0.41	0.89±0.67	1.27±0.53	0.62
ICA RI	**0.66±0.06**	**0.71±0.08**	**0.68±0.07**	**0.78±0.05**	**0.02**
Vertebral artery RI	0.73±0.09	0.75±0.08	0.74±0.12	0.81±0.06	0.49
Superior sagittal sinus RI	**0.39±0.12**	**0.41±0.11**	**0.49±0.13**	**0.58±0.10**	**0.01**
Straight sinus RI	**0.35±0.09**	**0.42±0.11**	**0.44±0.10**	**0.54±0.08**	**0.007**
Transverse sinus RI	**0.36±0.10**	**0.40±0.12**	**0.46±0.13**	**0.52±0.10**	**0.04**
Internal jugular vein RI	0.62±0.20	0.60±0.19	0.57±0.25	0.75±0.20	0.53

P values were from ANOVA. Results in bold represent $P<0.05$.

Figure 35 and Table 31 show that there were no significant associations between PI or RI and centrum semiovale PVS score (e.g. in the superior sagittal sinus, the PI in PVS score 1 vs 2 vs 3 vs 4 was 0.53±0.25 vs 0.60±0.29 vs 0.57±0.25 vs 0.62±0.12, P=0.86).

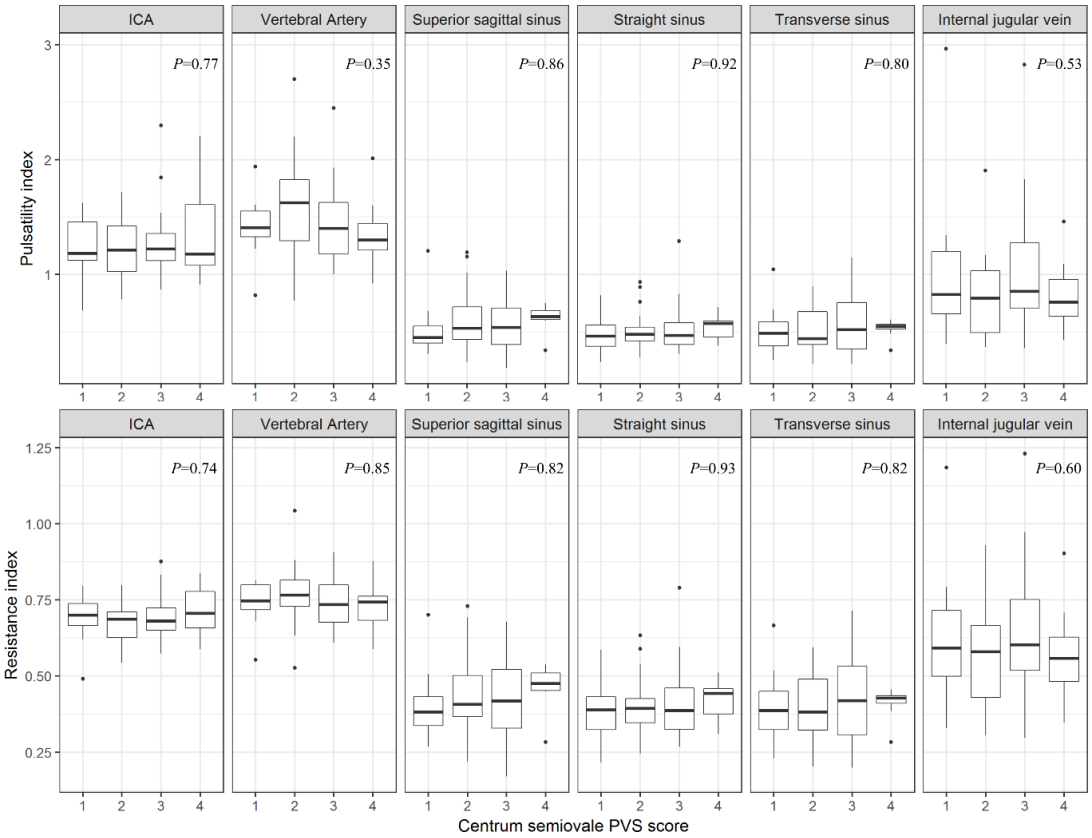

Figure 35 Boxplot showing univariate comparisons of pulsatility and resistance index in the arteries to veins according to the centrum semiovale PVS score. P values were from ANOVA. Sample sizes in each group: PVS score 1 (n=11); 2 (n=17); 3 (n=20); 4 (n=8). ICA: internal carotid artery.

Table 31 Aortic augmentation index and cerebrovascular pulsatility according to centrum semiovale PVS score

	Centrum semiovale PVS score				
	1 (n=11)	2 (n=17)	3 (n=20)	4 (n=8)	P value
Aortic augmentation index	24.00±11.53	21.47±12.12	25.73±5.84	30.75±7.01	0.15
ICA PI	1.24±0.28	1.22±0.25	1.28±0.32	1.36±0.44	0.77
Vertebral artery PI	1.42±0.28	1.61±0.48	1.45±0.35	1.36±0.33	0.35
Superior sagittal sinus PI	0.53±0.25	0.60±0.28	0.57±0.25	0.62±0.12	0.86
Straight sinus PI	0.49±0.18	0.52±0.19	0.54±0.23	0.54±0.11	0.92
Transverse sinus PI	0.51±0.22	0.51±0.19	0.57±0.26	0.53±0.28	0.80
Internal jugular vein PI	1.04±0.71	0.82±0.39	1.04±0.58	0.83±0.33	0.53
ICA RI	0.69±0.08	0.68±0.07	0.69±0.07	0.71±0.08	0.74
Vertebral artery RI	0.74±0.08	0.76±0.11	0.74±0.09	0.73±0.08	0.85
Superior sagittal sinus RI	0.41±0.12	0.44±0.14	0.43±0.14	0.46±0.08	0.82
Straight sinus RI	0.39±0.12	0.40±0.11	0.41±0.13	0.42±0.07	0.93
Transverse sinus RI	0.40±0.12	0.39±0.11	0.43±0.15	0.41±0.05	0.82
Internal jugular vein RI	0.63±0.23	0.56±0.19	0.65±0.23	0.58±0.17	0.60

P values were from ANOVA.

Ordinal regression analyses of aortic AIx, cerebrovascular pulsatility on PVS

PVS in the basal ganglia

Higher aortic AIx and higher pulsatility in all venous sinuses were significantly associated with higher PVS score in the basal ganglia, in both non-adjusted (e.g. OR=1.532, 95%CI [1.120, 2.095] per 0.1 increase in straight sinus PI) and models adjusted for age, gender and MAP (OR=1.502, 95%CI [1.085, 2.079] per 0.1 increase in straight sinus PI). However, PI in the arteries or internal jugular veins were not associated with basal ganglia PVS. Older age was significantly associated with more PVS in all models (OR≈1.1 per year older)***.(Table 32)***

Table 32 The associations between aortic AIx, cerebrovascular pulsatility and PVS in basal ganglia

PVS score in the basal ganglia as outcome variable					
Univariate ordinal regression			Multiple ordinal regression		
Predictors	OR	95% CI	Predictors	OR	95% CI
Aortic AIx (per unit)	**1.032**	**[1.032, 1.171]**	**Aortic AIx**	**1.028**	**[1.028, 1.221]**
			Age (per year)	1.096	[1.021, 1.176]
			MAP (per mmHg)	1.003	[0.964, 1.045]
			Gender (male)	3.017	[0.716, 12.718]
ICA PI (per 0.1)	1.079	[0.926, 1.257]	ICA PI	1.001	[0.847, 1.182]
			Age	**1.107**	**[1.032, 1.186]**
			MAP	1.021	[0.983, 1.061]
			Gender	0.99	[0.316, 3.105]
Vertebral artery PI (per 0.1)	1.008	[0.885, 1.148]	Vertebral artery PI	0.956	[0.832, 1.098]
			Age	**1.113**	**[1.037, 1.193]**
			MAP	1.021	[0.985, 1.060]
			Gender	1.025	[0.322, 3.257]
Superior sagittal sinus PI (per 0.1)	**1.42**	**[1.113, 1.812]**	**Superior sagittal sinus PI**	**1.379**	**[1.061, 1.792]**
			Age	**1.092**	**[1.018, 1.172]**
			MAP	1.026	[0.988, 1.066]
			Gender	1.552	[0.455, 5.296]
Straight sinus PI (per 0.1)	**1.532**	**[1.120, 2.095]**	**Straight sinus PI**	**1.502**	**[1.085, 2.079]**
			Age	**1.084**	**[1.009, 1.164]**

			MAP	1.038	[0.997, 1.082]
			Gender	1.48	[0.440, 4.974]
Transverse sinus PI (per 0.1)	**1.444**	**[1.112, 1.877]**	**Transverse sinus PI**	**1.426**	**[1.086, 1.873]**
			Age	**1.099**	**[1.025, 1.179]**
			MAP	1.028	[0.989, 1.069]
			Gender	1.386	[0.416, 4.618]
Internal jugular vein PI (per 0.1)	1.008	[0.913, 1.112]	Internal jugular vein PI	1.034	[0.924, 1.156]
			Age	**1.108**	**[1.035, 1.186]**
			MAP	1.025	[0.986, 1.064]
			Gender	1.039	[0.327, 3.296]
ICA RI (per 0.1)	1.853	[0.942, 3.645]	ICA RI	1.335	[0.641, 2.783]
			Age	**1.099**	**[1.025, 1.179]**
			MAP	1.018	[0.981, 1.057]
			Gender	1.028	[0.328, 3.224]
Vertebral artery RI (per 0.1)	1.305	[0.757, 2.249]	Vertebral artery RI	0.993	[0.553, 1.784]
			Age	**1.107**	**[1.032, 1.187]**
			MAP	1.022	[0.985, 1.060]
			Gender	0.989	[0.315, 3.108]
Superior sagittal sinus RI (per 0.1)	**1.835**	**[1.182, 2.848]**	**Superior sagittal sinus RI**	**1.73**	**[1.078, 2.774]**
			Age	**1.093**	**[1.019, 1.172]**
			MAP	1.027	[0.988, 1.066]
			Gender	1.472	[0.437, 4.957]

Straight sinus RI (per 0.1)	**2.14**	**[1.266, 3.619]**	**Straight sinus RI**	**2.061**	**[1.183, 3.593]**
			Age	**1.085**	**[1.011, 1.165]**
			MAP	1.036	[0.995, 1.079]
			Gender	1.422	[0.425, 4.759]
Transverse sinus RI (per 0.1)	**1.804**	**[1.168, 2.787]**	**Transverse sinus RI**	**1.768**	**[1.121, 2.789]**
			Age	**1.1**	**[1.026, 1.18]**
			MAP	1.027	[0.988, 1.068]
			Gender	1.344	[0.407, 4.442]
Internal jugular vein RI (per 0.1)	0.996	[0.782, 1.268]	Internal jugular vein RI	1.075	[0.823, 1.405]
			Age	**1.109**	**[1.036, 1.188]**
			MAP	1.024	[0.986, 1.064]
			Gender	1.03	[0.326, 3.261]

Results in bold represent results that do not overlap with the null value (OR=1).

PVS in the centrum semiovale

Higher aortic AIx was significantly associated with higher centrum semiovale PVS score in the adjusted model (OR=1.080, 95% CI [1.008, 1.156] per unit change in aortic AIx) but not in the non-adjusted model. There were no associations between pulsatility indices in any brain vessels and centrum semiovale PVS score. Older age was significantly associated with higher PVS in the centrum semiovale (OR≈1.1 per year older).***(Table 33)***

Table 33 Associations between aortic AIx, cerebrovascular pulsatility and PVS in centrum semiovale

PVS score in the centrum semiovale as outcome variable					
Univariate ordinal regression			Multiple ordinal regression		
Predictors	OR	95% CI	Predictors	OR	95% CI
Aortic AIx	1.047	[0.996, 1.101]	**Aortic AIx**	**1.080**	**[1.008, 1.156]**
			Age (per year)	1.062	[0.992, 1.136]
			MAP (per mmHg)	0.001	[0.952, 1.030]
			Gender (male)	**6.869**	**[1.536, 30.721]**
ICA PI (per 0.1)	1.025	[0.881, 1.193]	ICA PI	0.968	[0.824, 1.138]
			Age (per year)	**1.084**	**[1.013, 1.161]**
			MAP (per mmHg)	1.012	[0.977, 1.049]
			Gender (male)	2.834	[0.826, 9.723]
Vertebral artery PI (per 0.1)	0.957	[0.850,1.079]	Vertebral artery PI	0.928	[0.820,1.050]
			Age	1.091	[1.019,1.169]
			MAP	1.010	[0.975,1.046]
			Gender (male)	2.834	[0.829,9.693]
Superior sagittal sinus PI (per 0.1)	1.048	[0.864, 1.273]	Superior sagittal sinus PI	1.061	[0.859, 1.311]
			Age	**1.077**	**[1.007, 1.152]**
			MAP	1.011	[0.976, 1.047]
			Gender (male)	3.081	[0.856, 11.089]
Straight sinus PI (per 0.1)	1.129	[0.901, 1.415]	Straight sinus PI	1.129	[0.875, 1.456]
			Age	1.069	[0.997, 1.147]
			MAP	1.015	[0.979, 1.052]

			Gender	3.119	[0.896, 10.866]
Transverse sinus PI (per 0.1)	1.038	[0.844, 1.278]	Transverse sinus PI	1.053	[0.843, 1.315]
			Age	**1.078**	**[1.009, 1.153]**
			MAP	1.011	[0.976, 1.047]
			Gender (male)	2.986	[0.842, 10.589]
Internal jugular vein PI (per 0.1)	1.025	[0.881, 1.193]	Internal jugular vein PI	0.968	[0.824, 1.138]
			Age	**1.084**	**[1.013, 1.161]**
			MAP	1.012	[0.977, 1.049]
			Gender (male)	2.834	[0.826, 9.723]
ICA RI (per 0.1)	1.047	[0.586, 1.872]	ICA RI	0.898	[0.494, 1.633]
			Age	**1.083**	**[1.013, 1.159]**
			MAP	1.012	[0.977, 1.048]
			Gender (male)	2.733	[0.799, 9.340]
Vertebral artery RI (per 0.1)	0.876	[0.530, 1.449]	Vertebral artery RI	0.761	[0.447, 1.297]
			Age	1.091	[1.018, 1.170]
			MAP	1.012	[0.977, 1.048]
			Gender (male)	2.603	[0.756, 8.959]
Superior sagittal sinus RI (per 0.1)	1.121	[0.777, 1.619]	Superior sagittal sinus RI	1.151	[0.773, 1.715]
			Age	**1.076**	**[1.006, 1.151]**
			MAP	1.011	[0.976, 1.047]
			Gender	3.139	[0.879, 11.212]
Straight sinus RI (per 0.1)	1.236	[0.828, 1.844]	Straight sinus RI	1.209	[0.778, 1.878]
			Age	1.071	[0.999, 1.148]
			MAP	1.014	[0.978, 1.051]

			Gender (male)	3.034	[0.879, 10.476]
Transverse sinus RI (per 0.1)	1.084	[0.761, 1.543]	Transverse sinus RI	1.108	[0.760, 1.615]
			Age	**1.078**	**[1.009, 1.153]**
			MAP	1.011	[0.976, 1.048]
			Gender	3.009	[0.852, 10.627]
Internal jugular vein RI (per 0.1)	0.976	[0.783, 1.216]	Internal jugular vein RI	1.045	[0.828, 1.318]
			Age	**1.083**	**[1.013, 1.157]**
			MAP	1.013	[0.977, 1.050]
			Gender (male)	2.858	[0.831, 9.825]

Results in bold represent results that do not overlap with the null value (OR=1).

Chapter 5D: The associations between CSF pulsatility, waveform peak delays, and SVD features

CSF pulsatility, waveform peak delays, and WMH

Univariate comparisons of CSF pulsatility and waveform delays according to Fazekas scores

Figure 36 and Table 34 show the univariate comparisons of CSF pulsatility and waveform peak delays across total Fazekas scores. Aqueduct-to-artery and internal jugular vein-to-artery peak delay significantly shortened with higher total Fazekas score (e.g. the aqueduct-to-artery peak delay in total Fazekas 1-2 vs 3-4 vs 5-6 was 0.21±0.07 vs 0.17±0.06 vs 0.16±0.08 s, p=0.047). Otherwise, there were no significant differences in CSF stroke volumes or systolic durations across total Fazekas groups.

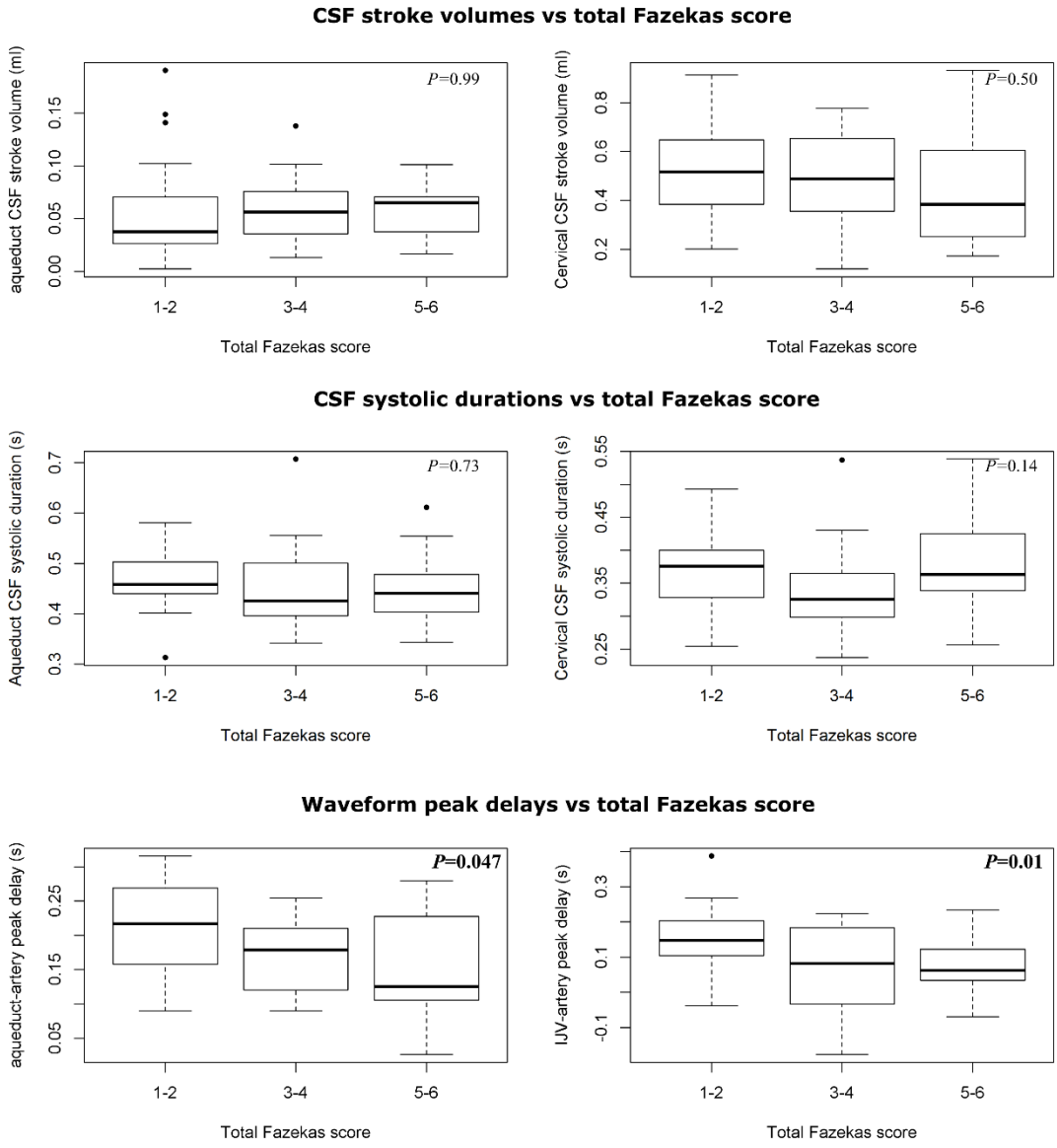

Figure 36 Boxplots showing comparisons of the CSF pulsatility and waveform peak delays according to total Fazekas scores. P values were from ANOVA and were marked bold when less than 0.05. Sample sizes in each group: Fazekas 1-2 (n=24); 3-4 (n=19); 5-6 (n=13). CSF: cerebrospinal fluid; IJV: internal jugular vein.

Table 34 CSF pulsatility and waveform peak delays according to total Fazekas score

	Total Fazekas score			
	1-2 (n=24)	3-4 (n=19)	5-6 (n=13)	P value
Aqueduct CSF stroke volume (ml)	0.06±0.05	0.06±0.03	0.06±0.03	0.987
Aqueduct CSF systolic duration (s)	0.47±0.06	0.46±0.09	0.45±0.07	0.788
Cervical CSF stroke volume (ml)	0.51±0.21	0.48±0.20	0.43±0.22	0.503
Cervical CSF systolic duration (s)	0.37±0.06	0.34±0.07	0.38±0.08	0.143
Internal jugular vein to artery waveform peak delay (s)	**0.16±0.09**	**0.07±0.12**	**0.09±0.08**	**0.011**
Aqueduct CSF to artery waveform peak delay (s)	**0.21±0.07**	**0.17±0.06**	**0.16±0.08**	**0.047**

P values were from ANOVA. Results in bold represent $p<0.05$.

Table 35 and Table 36 demonstrate the CSF pulsatility and waveforms peak delays stratified by periventricular and deep Fazekas score. There were no significant differences in CSF pulsatility and waveform peak delays across Fazekas groups, either in periventricular or deep WMH, apart from the cervical CSF systolic duration (0.38±0.07 vs 0.32±0.05 vs 0.38±0.08 s in periventricular Fazekas score of 1 vs 2 vs 3, P=0.025).

Table 35 CSF pulsatility and waveform peak delays according to periventricular WMH Fazekas scores

	Fazekas score for periventricular WMH			
	1 (n=27)	2 (n=17)	3 (n=12)	P value
Aqueduct stroke volume (ml)	0.06± 0.05	0.06±0.03	0.06±0.03	0.927
Aqueduct systolic duration (s)	0.47±0.06	0.45±0.09	0.45±0.08	0.754
Cervical CSF stroke volume (ml)	0.50±0.20	0.47±0.22	0.44±0.22	0.695
Cervical CSF systolic duration (s)	**0.38±0.07**	**0.32±0.05**	**0.38±0.08**	**0.025**
Internal jugular vein to artery waveform peak delay (s)	0.13±0.12	0.09±0.10	0.10±0.07	0.427
Aqueduct CSF to artery waveform peak delay (s)	0.20±0.07	0.17±0.06	0.16±0.08	0.093

P values were from ANOVA. Results in bold represent $p<0.05$.

Table 36 CSF pulsatility and waveform peak delays according to deep WMH Fazekas scores

	Fazekas score for deep WMH				
	0 (n=4)	1 (n=26)	2 (n=16)	3 (n=10)	P value
Aqueduct stroke volume (ml)	0.07± 0.06	0.05±0.04	0.06±0.03	0.06±0.03	0.735
Aqueduct systolic duration (s)	0.45±0.01	0.46±0.06	0.48±0.09	0.44±0.06	0.536
Cervical CSF stroke volume (ml)	0.33±0.17	0.53±0.22	0.45±0.18	0.48±0.23	0.298
Cervical CSF systolic duration (s)	0.38±0.10	0.36±0.05	0.34±0.09	0.39±0.06	0.370
Internal jugular vein to artery waveform peak delay (s)	0.16±0.03	0.13±0.11	0.09±0.11	0.07±0.08	0.220
Aqueduct CSF to artery waveform peak delay (s)	0.19±0.06	0.20±0.08	0.18±0.06	0.15±0.08	0.297

P values were from ANOVA.

Linear regression analyses of CSF pulsatility or waveform peak delays on WMH volume

Table 37 demonstrates that there were no significant associations between CSF pulsatility or waveform peak delays and WMH volume (normalised to ICV) in either univariate or multiple regression models. Age was significantly associated with larger WMH volume in all models.

Table 37 The associations between CSF pulsatility and waveform peak delays and WMH volume

WMH/ICV ratio as outcome (linear regression)							
Non-adjusted models				Models adjusted for age, MAP, and gender			
Predictors	β	95% CI	P value	Predictors	β	95% CI	P value
Aqueduct CSF stroke volume	2.697	[-3.943, 9.337]	0.419	Aqueduct CSF stroke volume	-0.038	[-6.038, 5.961]	0.990
				Age	**0.062**	**[0.034, 0.090]**	**<0.001**
				MAP	0.008	[-0.008, 0.024]	0.300
				Gender	0.091	[-0.417, 0.599]	0.721
Aqueduct CSF systolic duration	-0.974	[-4.503, 2.556]	0.582	Aqueduct CSF systolic	0.321	[-2.982, 3.624]	0.884
				Age	**0.062**	**[0.034, 0.089]**	**<0.001**
				MAP	0.009	[-0.008, 0.025]	0.298
				Gender	0.076	[-0.442, 0.593]	0.760
Cervical CSF stroke volume	-0.57	[-1.77,0.631]	0.345	Cervical CSF stroke volume	-0.549	[-1.579, 0.48]	0.289
				Age	**0.062**	**[0.035, 0.089]**	**<0.001**
				MAP	0.0080	[-0.007, 0.024]	0.295
				Gender	.101	[-0.389, 0.591]	0.680
Cervical CSF systolic duration	-1.899	[-5.554, 1.756]	0.302	Cervical CSF systolic duration	-1.021	[-4.228, 2.186]	0.526
				Age	**0.06**	**[0.033, 0.088]**	**<0.001**
				MAP	0.009	[-0.007, 0.024]	0.277
				Gender	0.081	[-0.413, 0.575]	0.745
Aqueduct-Artery peak delay	-2.517	[-6.009,0.976]	0.154	Aqueduct-Artery peak delay	-2.509	[-5.794, 0.776]	0.131

				Age	**0.063**	**[0.036, 0.090]**	**<0.001**
				MAP	0.057	[-0.443, 0.556]	0.304
				Gender	0.008	[-0.008, 0.024]	0.821
Internal jugular vein-Artery peak delay	-1.252	[-3.638, 1.134]	0.297	Internal jugular vein-Artery peak delay	-0.965	[-3.107, 1.177]	0.370
				Age	**0.061**	**[0.034, 0.088]**	**<0.001**
				MAP	0.129	[-0.370, 0.628]	0.231
				Gender	0.01	[-0.006, 0.026]	0.606

Results in bold represent $p<0.05$.

CSF pulsatility, waveform peak delays, and PVS

Univariate comparisons of CSF pulsatility and waveform peak delays according to PVS scores

Figure 37 and Figure 38 shows that CSF pulsatility and waveform peak delays did not differ across PVS scores in either basal ganglia (***Figure 37***) or centrum semiovale (***Figure 38***). The detailed comparisons were shown in Table 38 and Table 39.

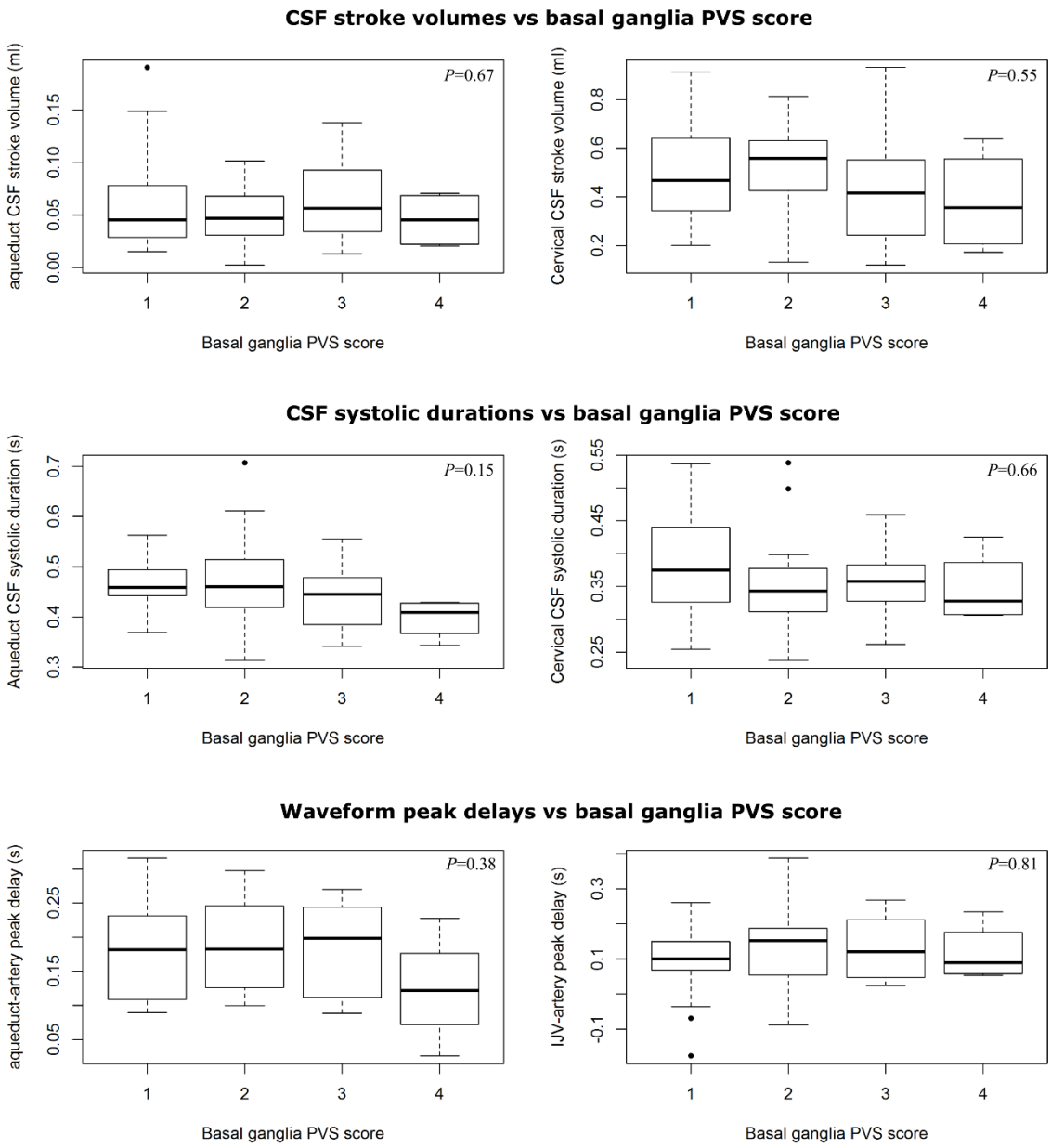

Figure 37 Boxplot showing the univariate comparisons of CSF pulsatility and waveform peak delays according to basal ganglia PVS score. P values were from ANOVA. Sample sizes in each group: PVS score 1 (n=19); 2 (n=21); 3 (n=12); 4 (n=4). CSF: cerebrospinal fluid; IJV: internal jugular vein.

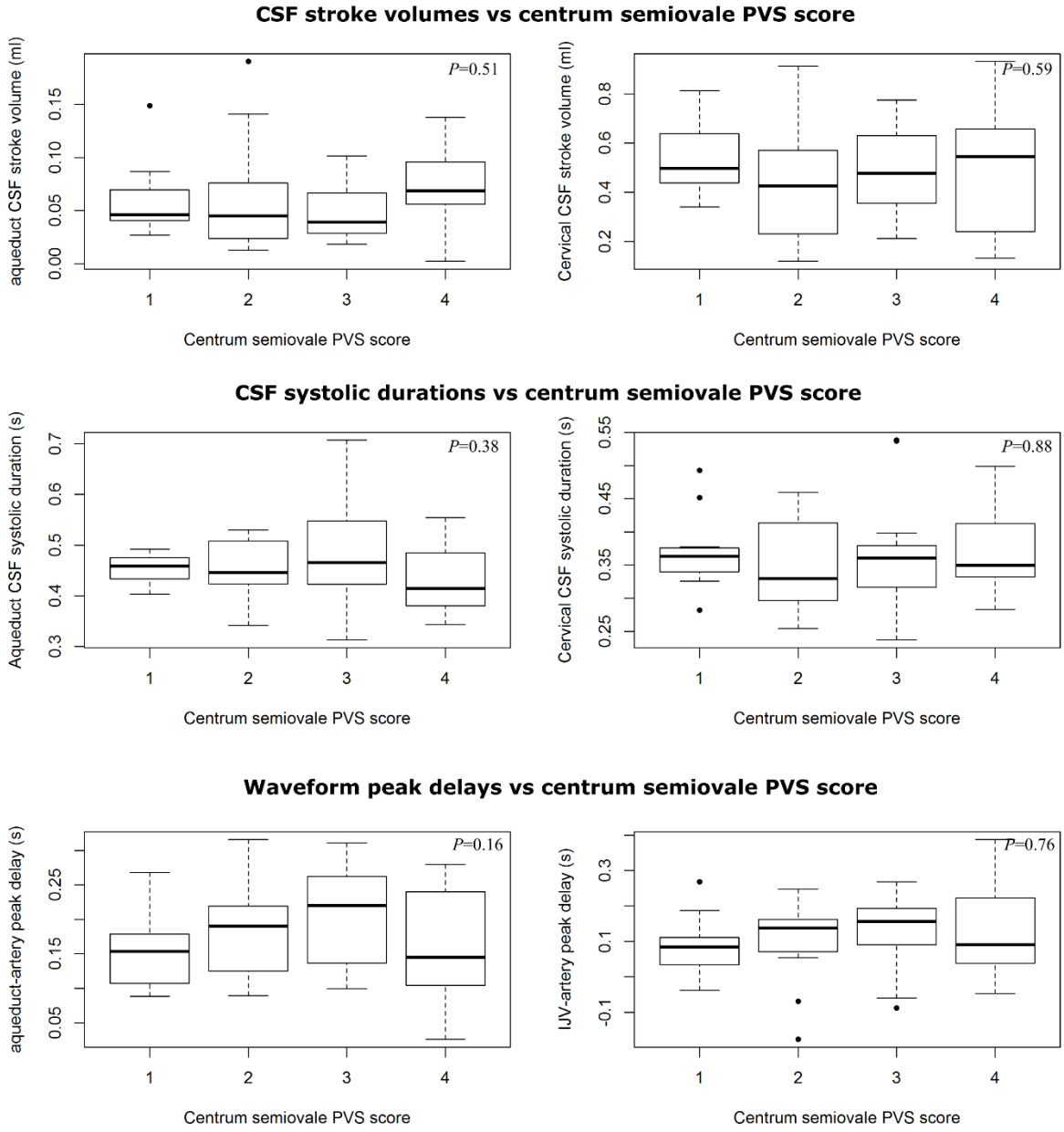

Figure 38 Boxplot showing the univariate comparisons of CSF pulsatility and waveform peak delays according to centrum semiovale PVS score. P values were from ANOVA. Sample sizes in each group: PVS score 1 (n=11); 2 (n=20); 3 (n=20); 4 (n=8). CSF: cerebrospinal fluid; IJV: internal jugular vein.

Table 38 CSF pulsatility and waveform peak delays according to basal ganglia PVS score

	Basal ganglia PVS score				
	1 (n=19)	2 (n=21)	3 (n=12)	4 (n=4)	P value
Aqueduct stroke volume (ml)	0.12±0.10	0.10±0.06	0.12±0.08	0.09±0.05	0.67
Aqueduct systolic duration (s)	0.47±0.05	0.47±0.09	0.44±0.06	0.40±0.04	0.15
Cervical CSF stroke volume (ml)	0.49±0.22	0.51±0.19	0.43±0.23	0.38±0.21	0.56
Cervical CSF systolic duration (s)	0.38±0.08	0.35±0.07	0.36±0.05	0.35±0.06	0.66
Internal jugular vein to artery waveform peak delay (s)	0.09±0.10	0.12±0.12	0.14±0.09	0.12±0.09	0.70
Aqueduct CSF to artery waveform peak delay (s)	0.18±0.08	0.19±0.06	0.20±0.08	0.13±0.09	0.49

P values were from ANOVA. Results in bold represent $p<0.05$.

Table 39 CSF pulsatility and waveform peak delays according to centrum semiovale PVS score

	Centrum semiovale PVS score				
	1 (n=11)	2 (n=17)	3 (n=20)	4 (n=8)	P value
Aqueduct stroke volume (ml)	0.12±0.07	0.12±0.10	0.10±0.05	0.14±0.08	0.51
Aqueduct systolic duration (s)	0.45±0.03	0.45±0.06	0.48±0.09	0.43±0.07	0.36
Cervical CSF stroke volume (ml)	0.54±0.16	0.43±0.24	0.48±0.17	0.49±0.27	0.59
Cervical CSF systolic duration (s)	0.37±0.06	0.35±0.07	0.36±0.07	0.37±0.07	0.88
Internal jugular vein to artery waveform peak delay (s)	0.09±0.09	0.11±0.10	0.13±0.10	0.13±0.15	0.81
Aqueduct CSF to artery waveform peak delay (s)	0.15±0.06	0.19±0.07	0.21±0.08	0.16±0.07	0.20

P values were from ANOVA.

Ordinal regression analyses of CSF pulsatility or waveform peak delays on PVS

Table 40 and Table 41 show the results of ordinal regression models between CSF pulsatility measures, waveform peak delays, and PVS scores in the basal ganglia (***Table 40***) or centrum semiovale (***Table 41***).

CSF pulsatility (stroke volume, systolic duration) or waveform peak delays (in the aqueduct or internal jugular veins) were not significantly associated with PVS scores in either location.

Table 40 The associations between CSF pulsatility and waveform peak delays and PVS in the basal ganglia

Basal ganglia PVS score as outcome					
Non-adjusted models			Models adjusted for age, MAP, and gender		
Predictors	OR	95% CI	Predictors	OR	95% CI
Aqueduct CSF stroke volume (per 0.01 ml)	0.984	[0.919, 1.054]	Aqueduct CSF stroke volume	0.944	[0.869, 1.026]
			Age (per year)	**1.127**	**[1.047, 1.214]**
			MAP (per mmHg)	1.021	[0.983, 1.060]
			Gender (Male)	1.287	[0.392, 4.223]
Aqueduct CSF systolic duration (per 0.1 s)	0.615	[0.316, 1.197]	Aqueduct CSF systolic duration	0.672	[0.326, 1.386]
			Age	**1.107**	**[1.034, 1.185]**
			MAP	1.017	[0.980, 1.056]
			Gender (Male)	1.243	[0.367, 4.205]
Cervical CSF stroke volume (per 0.01 ml)	0.278	[0.025, 3.124]	Cervical CSF stroke volume	0.313	[0.026, 3.793]
			Age	**1.107**	**[1.034, 1.185]**
			MAP	1.021	[0.984, 1.059]
			Gender (Male)	1.015	[0.322, 3.202]
Cervical CSF systolic duration (per 0.1 s)	0.664	[0.323, 1.366]	Cervical CSF systolic duration	0.71	[0.335, 1.503]
			Age	**1.105**	**[1.032, 1.183]**
			MAP	1.022	[0.985, 1.061]
			Gender (Male)	0.983	[0.315, 3.071]

Aqueduct - Artery peak delay (per 0.01 s)	0.977	[0.910, 1.049]	Aqueduct - Artery peak delay	0.983	[0.907, 1.064]
			Age	**1.107**	**[1.035, 1.185]**
			MAP	1.021	[0.984, 1.059]
			Gender (Male)	1.098	[0.317, 3.801]
Internal jugular vein - Artery peak delay (per 0.01 s)	1.021	[0.976, 1.068]	Internal jugular vein - Artery peak delay	1.035	[0.984, 1.088]
			Age	**1.115**	**[1.041, 1.196]**
			MAP	1.014	[0.976, 1.054]
			Gender (Male)	0.865	[0.268, 2.790]

Results in bold represent results that do not overlap with the null value (OR=1).

Table 41 The associations between CSF pulsatility and waveform peak delays and PVS in the centrum semiovale

Centrum semiovale PVS score as outcome					
Non-adjusted models			Models adjusted for age, MAP, and gender		
Predictors	OR	95% CI	Predictors	OR	95% CI
Aqueduct CSF stroke volume (per 0.01 ml)	1.005	[0.943, 1.070]	Aqueduct CSF stroke volume	0.986	[0.925, 1.052]
			Age (per year)	**1.083**	**[1.013, 1.159]**
			MAP (per mmHg)	1.011	[0.976, 1.047]
			Gender (Male)	2.932	[0.840, 10.235]
Aqueduct CSF systolic duration (per 0.1 s)	1.056	[0.557, 2.004]	Aqueduct CSF systolic duration	1.064	[0.529, 2.136]
			Age	**1.081**	**[1.012, 1.155]**
			MAP	1.012	[0.976, 1.049]
			Gender (Male)	2.693	[0.758, 9.571]
Cervical CSF stroke volume (per 0.01 ml)	0.799	[0.080, 7.991]	Cervical CSF stroke volume	0.98	[0.095, 10.120]
			Age	**1.081**	**[1.011, 1.155]**
			MAP	1.011	[0.976, 1.047]
			Gender (Male)	2.773	[0.814, 9.446]
Cervical CSF systolic duration (per 0.1 s)	1.009	[0.539, 2.099]	Cervical CSF systolic duration	1.024	[0.631, 2.615]
			Age	**1.094**	**[1.015, 1.161]**
			MAP	1.009	[0.974, 1.046]
			Gender (Male)	3.438	[0.855, 10.043]

Aqueduct - Artery peak delay (per 0.01 s)	1.035	[0.965, 1.110]	Aqueduct - Artery peak delay	1.028	[0.952, 1.111]
			Age	**1.08**	**[1.011, 1.153]**
			MAP	1.014	[0.978, 1.052]
			Gender (Male)	2.316	[0.616, 8.702]
Internal jugular vein - Artery peak delay (per 0.01s)	1.026	[0.980, 1.075]	Internal jugular vein - Artery peak delay	1.028	[0.978, 1.081]
			Age	**1.084**	**[1.015, 1.158]**
			MAP	1.009	[0.974, 1.046]
			Gender (Male)	2.448	[0.701, 8.544]

Results in bold represent results that do not overlap with the null value (OR=1).

Chapter 5E: The associations between intracranial haemodynamic measures

Cerebrovascular pulsatility and CBF

Table 42 shows the association between pulsatility and CBF in the same vessels. Arterial PI was averaged from PI in the ICAs and vertebral arteries, as the arterial flow was the sum of blood flow in the four arteries. Higher arterial PI was significantly associated with lower arterial flow (β＝-8.59, p=0.047), although the p value was not corrected for multiple testing.(***Table 42***) I also illustrated this association in Figure 39, although the coefficient in the figure was from non-adjusted models (β＝-9.784, p=0.029).

However, CBF in the transverse sinuses and internal jugular veins were not associated with pulsatility indices in the correspondent vessels (e.g. transverse sinus: β=1.50, p=0.851). (***Table 42***)

Table 42 The associations between vascular pulsatility and flow

Outcome variables (in separate models)	Predictor variables (in separate models adjusted for age, MAP, WMH volume)		
	Arterial PI	Transverse sinus PI	Internal jugular vein PI
Arterial flow	**β＝-8.59 [-17.09, -0.099]*, p=0.047**	-	-
Transverse sinus flow	-	β＝1.50 [-14.44, 17.44]*, p=0.851	-
Internal jugular vein flow	-	-	β＝-0.31 [-8.50, 7.88]*, p=0.94

*Numbers in the brackets [ ] represent 95% CI; results in bold represent p<0.05. P values were not corrected for multiple testing.

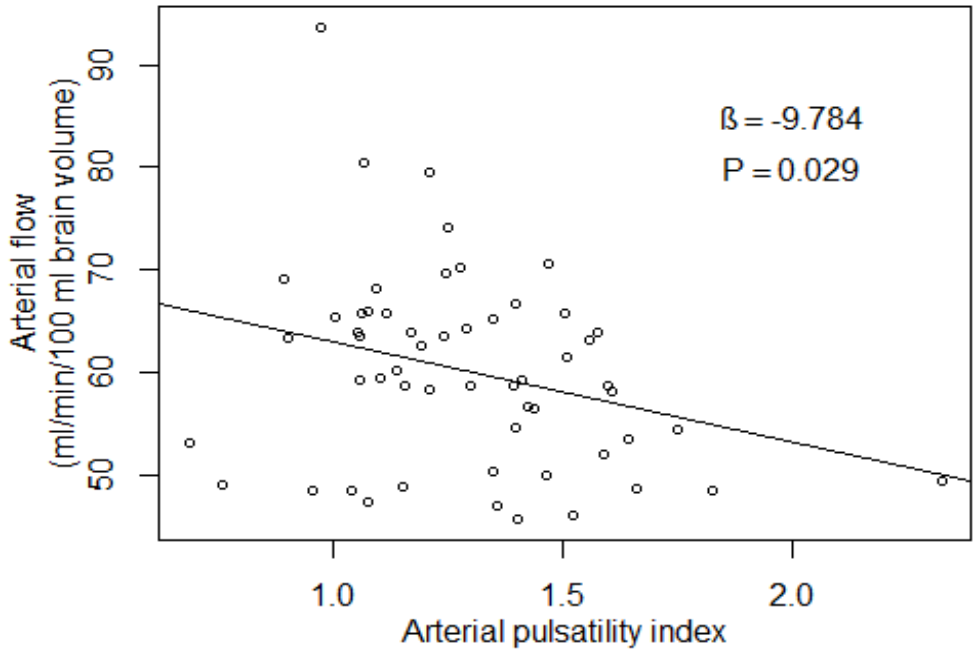

Figure 39 The association between arterial flow and arterial pulsatility (univariate)

ICA and venous pulsatility

Results in Table 43 show that pulsatility in all the venous sinuses and the internal jugular veins were significantly associated with ICA pulsatility (e.g. superior sagittal sinus: β=0.247, p=0.019; internal jugular veins: β=0.622, p=0.007), after the adjustment for age, MAP and WMH volume.**(*Table 43*)** I also illustrated these associations in the scatterplots in Figure 40 where all results were from univariate regression models (e.g. superior sagittal sinus: β=0.287, p=0.005; internal jugular vein: β=0.52, p=0.023).

Table 43 The associations between ICA pulsatility and pulsatility in veins and CSF

	ICA PI as predictor variable (in separate models*)		
	β	95% CI	P value
Superior sagittal sinus PI	**0.247**	**[0.043,0.451]**	**0.019**
Straight sinus PI	**0.298**	**[0.152,0.444]**	**<0.001**
Transverse sinus PI	**0.264**	**[0.088,0.441]**	**0.004**
Internal jugular vein PI	**0.622**	**[0.179,1.064]**	**0.007**

*All models were adjusted for age, MAP and WMH volume. Results in bold represent p<0.05.

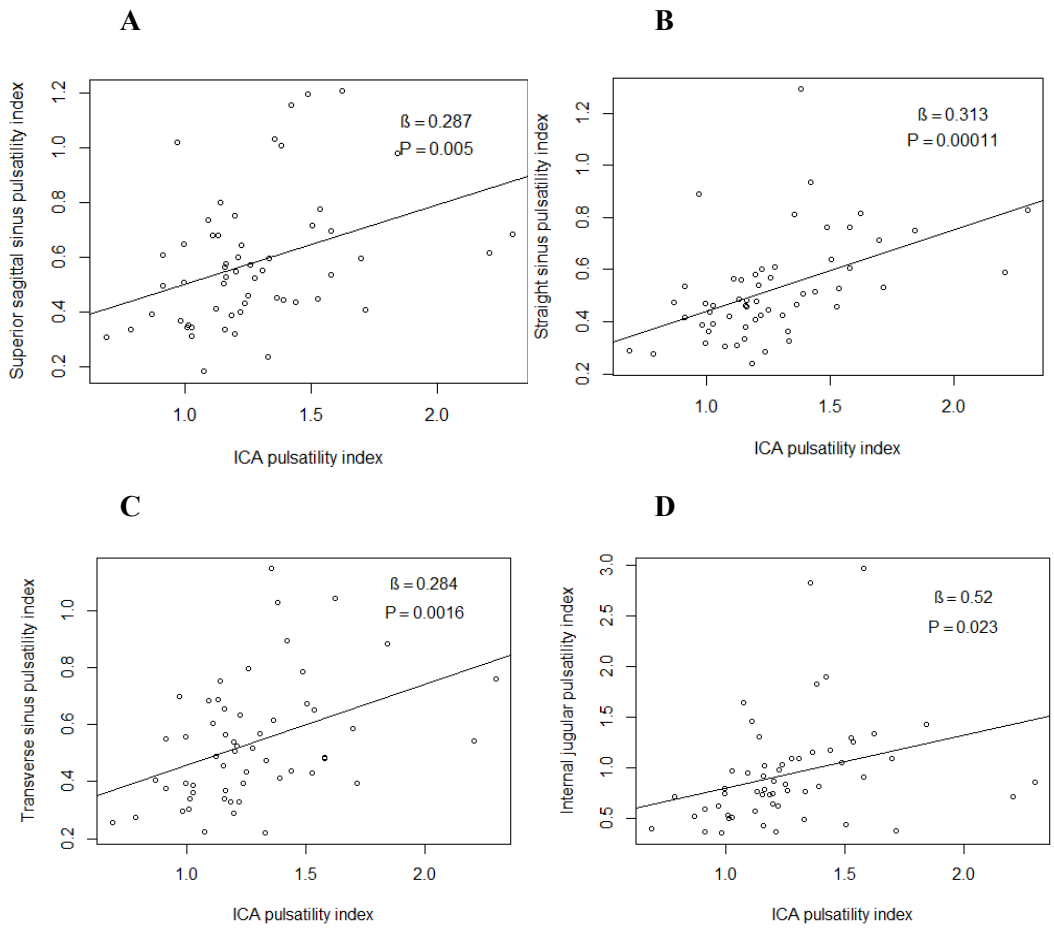

Figure 40 The associations between ICA pulsatility and venous pulsatility (univariate). A: superior sagittal sinus pulsatility index (PI) vs ICA PI; B: straight sinus PI vs ICA PI; C: transverse sinus PI vs ICA PI; D: internal jugular vein PI vs ICA PI.

Chapter 6: Cross-sectional study of CBF and intracranial pulsatility in SVD patients - Discussion

Summary of results

This chapter is the discussion of the results presented in chapter 5. The main findings of this study were summarised in Figure 41. In Chapter 5A, I aimed to summarise the haemodynamic measures we obtained from patients and investigate how these measures related to age, stroke subtype, SVD features as well as to systemic measures. I included data from 56 patients (age 67.8 ± 8.3 years) with minor stroke and SVD features on brain imaging. 36 patients had a lacunar and 20 had a cortical stroke. Most patients were hypertensive and had mild to moderate SVD burden according to Fazekas score and PVS score. Age, vascular risk factors, and most SVD features did not differ between lacunar and cortical stroke. Older age was associated with higher aortic AIx and higher pulsatility indices in most brain vessels, but not with CBF (ml/min/100 brain volume) or CSF pulsatility. Stroke subtype was not associated with any intracranial or extracranial haemodynamic measures. Higher diastolic BP and MAP was associated with higher arterial blood flow but not with the venous flow. Lower diastolic BP and MAP were significantly associated with higher pulsatility indices in venous sinuses. Higher aortic AIx was associated with lower ICA pulsatility indices, but not with pulsatility in the veins or CSF.

Then, in Chapter 5B-5D, I investigated the role of intracranial measures and aortic stiffness in WMH and PVS. Higher aortic AIx was associated with larger WMH volume, but the association disappeared after the adjustment for age and other covariates. Higher aortic AIx was also associated with higher PVS score in the basal

ganglia but not centrum semiovale. Neither arterial nor venous flow was associated with WMH or PVS. High PI and RI in the venous sinuses were significantly associated with higher WMH burden and basal ganglia PVS score (not centrum semiovale), which was independent of age, gender, and blood pressure. Shorter aqueduct-to-artery and artery-to-internal jugular vein delays were observed in patients with higher Fazekas score but not associated with WMH volume or PVS scores. We did not observe significant associations between CSF pulsatility and WMH or PVS. ***(Figure 41)***

In order to better understand the implications of cerebrovascular pulsatility, in Chapter 5E, I assessed the association between PI and blood flow in the same vessels, and between venous and arterial PI. It was only in arteries but not veins that higher pulsatility was associated with lower CBF. PI in all the venous sinuses and internal jugular veins were significantly associated with arterial pulsatility. ***(Figure 41)***

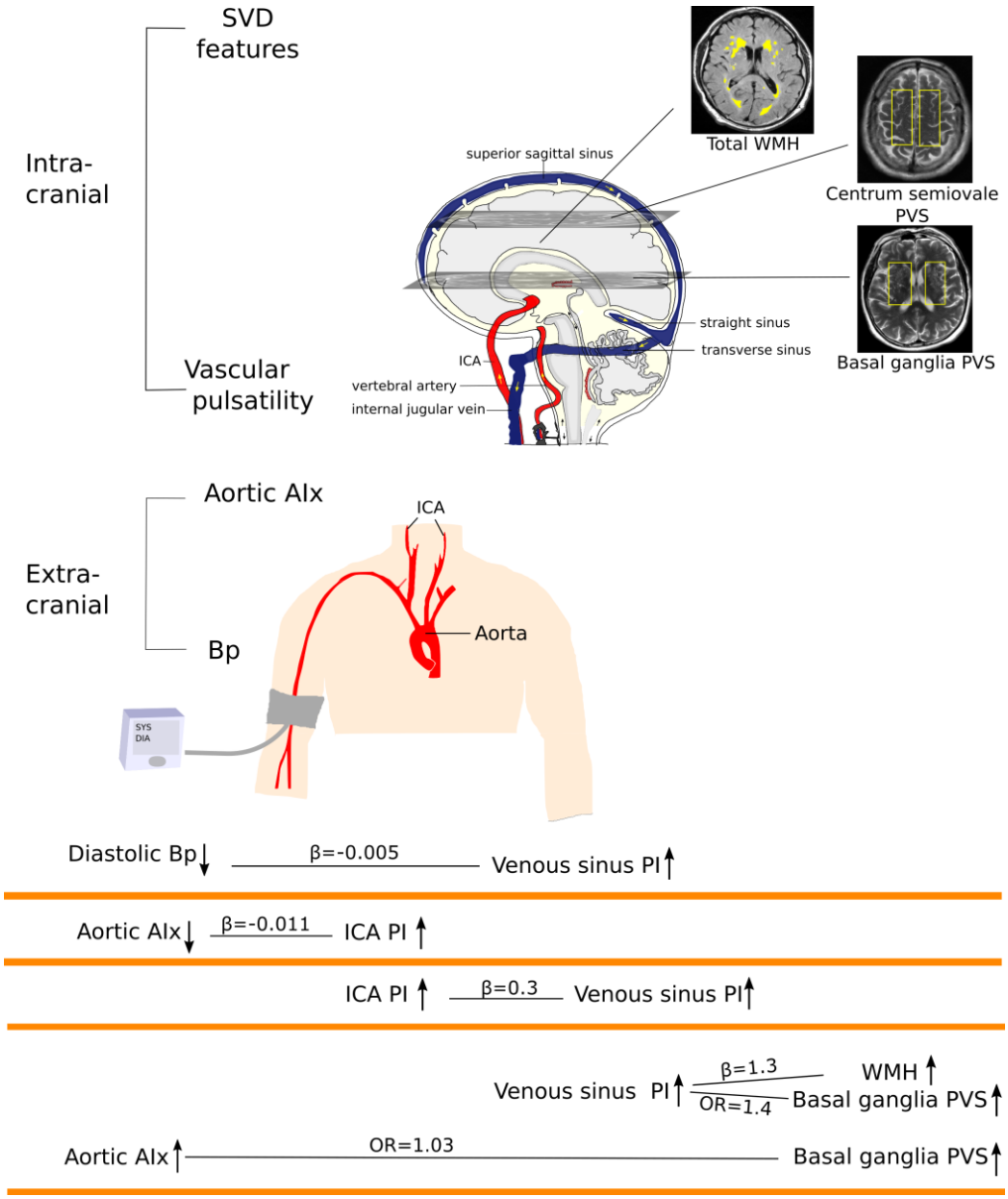

Figure 41 Summary of associations between extracranial and intracranial haemodynamic measures, and SVD features. All models were adjusted for age, gender and MAP. WMH burden was calculated as WMH volume, and semi-quantitative scores (0-4) were used for PVS. Results of RI were similar to PI (see Chapter 5). For simplicity, only results of PI were shown here. SVD: small vessel disease; PVS: perivascular spaces; WMH: white matter hyperintensities; ICA: internal carotid artery; Bp: blood pressure; AIx: augmentation index; PI: pulsatility index; RI: resistance index; OR: odds ratio.

Strengths

In this study, we recruited a group of representative patients with minor stroke in whom SVD is very common. All these patients underwent a careful assessment of stroke classification by a panel of stroke specialists. We took various approaches to reduce the biases in every step of the analysis. For image processing, we used a well-established and validated method for brain tissue segmentation, including masks for total brain volume, ICV, and WMH volume. All these masks were automatically generated, and then corrected manually by a neurologist and cross-checked by an experienced neuroradiologist, who also cross-checked all the visual rating scores of SVD features. All the image analysts were blinded to any clinical or flow/pulsatility data. Although both visual rating and volumetric measurements of WMH were included in the analysis, most of the conclusions were based on the results using WMH volumes, because there is an inherent ceiling effect in the visual rating methods such as Fazekas scores which limits the differentiation for severe WMH. We also adjusted for necessary covariates in the statistical analysis. The other strengths include a thorough assessment of the flow and pulsatility in cerebral arteries, veins and CSF in a single session, and for the first time assessed the relationship between PVS and pulsatility in humans.

Weaknesses

Weaknesses include the sample size (n=56) that limited the power for very comprehensive multivariate analysis. However, as we mentioned previously, this is a pilot study that mainly aimed to set up a reliable methodology for future studies,

such as sample size estimation for larger studies or long-term follow-ups. The second weakness is that we included both lacunar stroke and cortical stroke, although both groups had WMH and PVS. The reason was that patients who had minor stroke, regardless of the aetiologies, are a typical group that could be affected by SVD pathologies. However, it is possible that including both stroke subtypes could lead to a potential selection bias. The third limitation is that some patients were under anti-hypertensive treatments such as angiotensin converting enzyme inhibitors (ACEIs) that have vasoactive effects, which may reduce the vessel stiffness and PI. However, our sample size is not powerful enough for a sensitivity analysis that could address the impact of these medications on our final results, which could be considered in future larger studies. There are also some other weaknesses in the methodology. We had limited assessment for aortic stiffness. We obtained the aortic pressure waveform via the estimation from the radial artery tonometry, which is a widely accepted and most common method, and calculated the aortic AIx to represent the aortic stiffness. However, aortic AIx is a measure of aortic wave reflection and is related to aortic pulse wave velocity (another indicator of aortic stiffness) which we did not have in this study. We were also not able to measure smaller cerebral vessels (e.g. penetrating arteries) due to limited MRI resolution or to acquire independent CBF measures for different tissues. All the associations that we assessed were cross-sectional, thus we were not able to address any causal relationships between variables in this study. Lastly, all the p values that were provided in this thesis were not corrected for multiple testing such as Bonferroni adjustment. It is possible that some p values that were just close to 0.05 might not survive multi-testing corrections.

However, an important aim of this study is to generate new hypotheses for future research, of which the validity could be tested in suitable powered larger studies.

Haemodynamic measures and their relation to age and stroke subtype

The value of total arterial flow was 645.32±113.00 ml/min (60.17±9.52 ml/min per 100 ml brain volume), which is consistent with values reported in other studies with elderly populations (n=36, age≈70 years, mean arterial flow=580-710 ml/min;[64] n=60, age 65.67±9.31 year, 709±135 ml/min[58]). Venous flow in the transverse sinuses and internal jugular veins were in general smaller than in the arteries, consisting of 75-80% of total blood flow, as reported in the literature.[187] The difference between arterial inflow and internal jugular outflow might be due to a small amount of blood draining through extra-jugular venous systems such as vertebral, cavernous region or deep neck veins, which was not recorded in our study.[158, 188]

Some previous cross-sectional studies showed a yearly CBF decrease of 4.8-6.3 ml/min (n=250-447, age 19-88 years).[73, 189] However, the decreasing CBF (ml/min) might be largely confounded by the brain volume which also decreased with age.[73, 74] In the PROSPER study (n=447, age=75±3 years) the relationship between CBF and age disappeared after using ml/min/100 ml brain volume instead of ml/min, which is consistent with our finding. These results suggest that some studies may have overestimated the decline in CBF with age, and that future studies which aim to

investigate the role of CBF in any pathology related to ageing should normalise the CBF to the brain volume.

We found that aortic AIx and pulsatility indices in some brain vessels were significantly associated with older age. Aortic AIx is a measure of pulse wave reflection and an indirect indicator of aortic stiffness. Although increasing evidence has shown that the aorta stiffens with ageing,[120] the relationship between aortic AIx and age varied in the literature. Aortic AIx increased with age in some studies with small population or patients with coronary artery diseases (n=41-67, age≈30-50 years);[190, 191] whereas in some large-scale studies with healthy populations (n=4001-4561, age 18-90 years), the relationship seemed nonlinear: it increased before 60 years old but plateaued afterwards.[192, 193] However, these studies were all cross-sectional and therefore were possibly confounded by including healthier older and less healthy young subjects. In our study, all patients had had a stroke, and hypertension was very common, which was more complicated than normal ageing. The vascular risk factors might co-associate with age, which we were not able to untangle fully with a small sample size.

Previous studies on age and cerebrovascular pulsatility were scarce. One study (n=78, age 20-85 years) showed that both ICA PI and RI increased with age.[194] One study found that healthy elderly (n=12, age 71±9 years) had smaller CSF stroke volume in the aqueduct and cervical subarachnoid spaces compared with healthy young volunteers (n=12, age 27.5±4.4 years) but no differences in waveform peak delay between groups.[147] However we did not find any linear association between CSF flow or pulsatility and age.

None of the extra- and intra-cranial haemodynamic measures were associated with stroke subtype (lacunar vs cortical). As I showed previously, patients with lacunar and cortical stroke did not differ between most SVD features (except lacunes) or any vascular risk factors, suggesting a similar cerebrovascular disease burden.

The association between extracranial and intracranial measures

The relationship between CBF and blood pressure is complex and nonlinear. In a brain with an intact autoregulation system, CBF remains relatively constant across a wide range of cerebral perfusion pressure (60-150 mmHg) and systemic arterial pressure.[195] However in this study, we found a positive relationship between CBF and diastolic and mean arterial pressure. As the CBF autoregulation is thought to be achieved primarily by small arteries and arterioles, it is likely that pathologies in the small vessels might result in a failed or compromised CBF autoregulation, such as in patients with SVD. A previous study showed that in patients with chronic hypertension (n=13, age 44-64 years), the lower end of the plateau of CBF autoregulation shifted to a higher blood pressure,[196] suggesting an impaired autoregulation and that a lowered blood pressure might possibly cause an insufficient blood supply to brain tissues.

This is the first study that has addressed the relations between pulsatility in various cerebral vessels concurrently with CSF and haemodynamic measures in the systemic circulation. Some studies have measured one single type of brain artery, such as ICAs or MCAs. In the Lothian Birth cohort study (n=694, age 72.6±0.7 years), higher ICA PI (averaged from both sides) was associated with higher systolic BP,

lower diastolic BP, and higher pulse pressure. It is worth noting that a longitudinal rise in pulse pressure between 69 and 72 years was due to falling diastolic BP, since systolic BP did not change.[57] In another two studies (n=165-334, age 19-86 years) that assessed MCA, higher MCA PI was associated with higher pulse pressure but no results for other brachial BP measures were shown.[197, 198] Although in our study, the association between lower diastolic BP and higher pulsatility indices was only significant in the straight sinus and the internal jugular vein but not in the ICA, the overall trend between diastolic BP and cerebrovascular pulsatility was consistent across all brain vessels and with the literature.

Apart from systemic BP measures, I also investigated how intracranial pulsatility indices were related to aortic AIx. There is a hypothesis that in normal ageing, as the aorta stiffens more than peripheral arteries with age, excessive pulsatile power would be more easily transmitted forward and dissipated into the peripheral circulation.[120] Interestingly, we found a contrasting result in the ICA: higher aortic AIx was associated with lower ICA pulsatility, despite that both measures showed a similar trend with age. Likewise, another study (n=159, age 61±1.1 years) observed that decreasing aortic AIx was associated with increasing impedance in the carotid artery but decreasing impedance in distal peripheral circulation.[199] Aortic AIx is an indicator of aortic wave reflection, which is theoretically determined by the impedance mismatch between central and peripheral arteries. According to an analysis on the physical principle of wave reflection, the reflection ratio in a central artery is expressed as $(Z_{dist}-Z_{prox})/ (Z_{dist}+Z_{prox})$ where Z_{dist} indicates distal impedance and Z_{prox} means impedance in the proximal.[200] According to this equation, the magnitude of the reflected wave back to the aorta is dependent on the ratio between

the impedance at proximal and distal arteries. Thus the increased impedance in the proximal artery, such as in the ICA, might result in a smaller reflected wave that returns to the aorta. These results also raise a concern that aortic AIx is a complex measure which might not be sensitive in detecting aortic stiffness in the elderly, which has been discussed in other studies.[120, 201]

Very few studies have assessed aortic stiffness and pulsatility in vessels more downstream than ICA. One study (n=100, age≈50-80 years) showed that high MCA PI is associated with high aortic pulse wave velocity,[59] but we did not find a significant association between venous pulsatility and aortic AIx. The association between higher aortic AIx and PVS in the basal ganglia might suggest a relationship between aortic stiffness and pulsatility in distal cerebral vessels, as enlarged PVS are hypothesised to be the result of a fluid blockage in the perivascular spaces due to abnormal pulsatility in deep arterioles.[59] Furthermore, we also showed that higher aortic AIx was associated with shorter artery-to-aqueduct systolic peak delay which was also suggested as an indicator of microvascular pathologies.[65] However, the cause and effect between aortic stiffness and high pulsatility in distal cerebral vessels is unclear: whether it is high distal impedance that causes a high reflected wave in the aorta or it is the less dampened pulse from stiffened aorta that was transmitted into the distal vessels is not known. We were unable to address the question in this study.

We showed that the higher aortic AIx was not associated with WMH volume after the adjustment for age and other covariates. In the literature, the relationship between aortic AIx and WMH was found in some[202, 203] but not in other studies,[60] despite the

varying sample sizes and participants population across the studies. These results might suggest that aortic stiffness is part of, but not necessarily the cause of WMH.

The associations between intracranial measures and SVD features

Age was prominently associated with both WMH and PVS in all analyses, which is not surprising and emphasizes the importance of the adjustment for age in any SVD-related analysis. The barely existing association between total CBF and WMH in our patients is detected only in arteries and disappeared when corrected for age, which is consistent with previous evidence from both large-scale cross-sectional and longitudinal studies.[126] However, it is noteworthy that we were unable to measure CBF in white matter and grey matter separately. The effect on regional CBF in white matter and grey matter might differ. A cross-sectional analysis from the Third International Stroke Trial (IST-3) (n=115) showed that higher total SVD score was associated with lower CBF in the white matter.[204] Thus techniques that enable the detection of CBF in different tissues especially in the white matter should be encouraged and would better clarify the role of CBF in SVD.

The relationship between ICA pulsatility and WMH partly reflects a co-association with age, which is consistent with a previous study (n=122, age 63.73±10.85 years).[127] In other studies such as the Lothian Birth Cohort (n=694, age 72.6±0.7 years), high ICA PI remained associated with WMH after the adjustment for age.[57] Similarly, we also did not find associations between ICA pulsatility and PVS, despite the suggestion in animal studies and mathematical models that arterial pulsatility is the key driver of fluid dynamics in perivascular spaces.[40, 205] The wide age range and

the small size of our study may have made it difficult for us to untangle the confounding effect of age on ICA PI-SVD, a relationship which appears to be inherently weaker than venous PI-SVD. We did not find any significant association between vertebral artery pulsatility and WMH or PVS, perhaps reflecting the low flow volume in the vertebral arteries.

Unlike in the arteries, we found that the PI and RI in the superior sagittal and transverse sinuses remained associated with WMH, which is independent of age and MAP. The relationship between high venous sinus pulsatility and white matter damage was supported in some studies in other diseases. In patients with idiopathic dementia (n=60, age 75±8 years), those with more severe WMH had higher superior sagittal sinus PI;[124] in a healthy population (n=70, 43-82 years) where most participants had mild or negligible WMH, high venous PI was associated with white matter microstructural damage although not with total WMH volume.[58]

This study is the first to observe the relationship between increased cerebrovascular pulsatility and basal ganglia PVS in humans. Other indirect clinical evidence comes from a population-based study (n=1009, age 68±8 years) which showed that higher systemic (brachial) pulse pressure was associated with PVS.[206] We also found that high PI and RI was only associated with basal ganglia but not centrum semiovale PVS, which might reflect known differences in the arterioles in the two regions. This result is consistent with apparent differences in associations of PVS in the two locations. Some studies suggest that basal ganglia PVS may be more associated with inflammation,[56] hypertension[207] or lacunar stroke,[33] and centrum semiovale PVS more with cerebral amyloid angiography.[207] A theoretical mathematical model also

shows that in hypertension, the arteriolar pressure in the basal ganglia was higher than in cortical vessels.[208]

However, despite the hypothetical differences in PVS in these two locations, they are co-associated with each other.[33] A previous study showed that the visual rating score for PVS in the centrum semiovale had a higher intra- and inter-observer variability than PVS in the basal ganglia, which might partly be due to more WMH in the centrum semiovale that makes it difficult to rate PVS and more slices that contain PVS in the centrum semiovale. Thus before more data and detailed studies are available, it might be too early to conclude on the differences in the mechanisms of PVS in the two areas. We suggest that future studies should collect information on both sites. There is a suggestion that different SVD features share a common pathology and should be regarded as a "whole-brain" disease.[119] Total PVS (basal ganglia and centrum semiovale combined) are associated with WMH.[33] PVS and WMH are both associated with an impaired BBB.[209] Increased cerebrovascular pulsatility may be affecting cerebral interstitial fluid drainage accounting for the increased visibility of PVS and worse WMH, providing further support for a shared aetiology between PVS and WMH, although it is uncertain whether PVS precede, follow, or appear concurrently with WMH.

We did not find associations between CSF stroke volumes or systolic durations and SVD features. The association between CSF pulsatility and WMH was conflicting in previous studies: present in some[125, 143] but not others[58]. Theoretically, PVS might be related to perivascular CSF pulsatility driven by arterial pulse, but the indices we used here were not designed to detect this pulse at the microscopic level. Some researchers hypothesise that the CSF flow in the aqueduct represents flow in the

capillary bed and shorter artery-to-aqueduct peak delay might indicate capillary dysfunction.[65] However, we did not find associations between any peak delays with WMH volume nor with PVS score. 2D phase-contrast MRI has limited temporal resolution and the reliability of the pulse wave peak delays requires more research. Improved imaging techniques with high temporal and spatial resolution that enable detection of small vessels in more detail, or that identifies intracranial pulsation with higher sensitivity would benefit further research.

The implication of cerebrovascular pulsatility

Although no studies have directly compared cerebral vascular pulsatility and CBF, one study showed a higher ICA pulsatility and lower arterial flow in patients with WMH compared to healthy controls.[129] These findings are in agreement with the trend for both measures in our study and the inverse association between arterial pulsatility and arterial flow. These results also led to the suggestion that increased vascular stiffness might locally affect the blood flow, which maybe eventually result in a reduced CBF at the end stage of the disease.

The implication of venous pulsatility remains unclear. It is still not known how the changes in the pulsatility in the large vessels relates to pathologies in small vessels. On one hand, it is possible that the increased pulsatility detected in the large vessels, especially in the large veins, was a result of high cardiac pulse that could not be sufficiently buffered in the stiffened small vessels. On the other hand, the increased pulsatility in large vessels, regardless of the source, could in turn lead to high

pulsatile energy being transmitted into small vessels, exacerbate endothelial damages and impair the perivascular clearance pathway.

Although the association between PI (and RI) and SVD features was only significant in the venous sinuses but not arteries, it might not necessarily suggest a particular significance of the venous pathology. The non-significant PI-SVD relationship after the adjustment of age might be due to our small sample size. The pulsatility in the arteries and veins were significantly correlated. Pulsatility in the venous sinuses might indicate inefficient dampening of the arterial pulse, and perhaps is a more sensitive measure in reflecting the compliance of the whole brain.[210] However, the details of the passage of pulse transmission through the older brain are largely under-researched. One hypothesis suggests that the systolic arterial expansion produces a pressure wave within the CSF spaces, which is then partly transmitted into the major dural sinuses via arachnoid granulations.[62, 211] We found that the systolic peak delay time from arteries was shortest to cervical CSF, followed by the transverse and straight sinuses, then the superior sagittal sinus, similar to the pattern of cardiac pulse transmission (from skull base to the cortex) observed in another study using ultra-fast magnetic resonance encephalography.[157]

Venous pulsatility could also be partly from capillaries. Increased capillary pulsatility from the less dampened arterial pulse could be transmitted to veins through blood flow or inward expansion.[62] However, the relationship between capillary and venous pulsatility is uncertain. As a sufficient venous backpressure is also important for maintaining a constant capillary flow,[62] venous pathologies could in turn result in increased capillary pulsatility. Indeed, there are autopsy studies (n=13, age>60 years) showing a collagenous thickening in periventricular venules

which was related to PVWMH severity,[212] but it is unknown whether the venule damage was caused by excessive pressure filtered from the arteries or was an intrinsic pathology. It is likely that pathologies in the arterioles and venules coexist. Future SVD studies including pathology, clinical or any models, should consider both arteries and veins.

Conclusion

This is the first study to investigate the flow and pulsatility in the main cerebral arteries, veins, and CSF concurrently, and compared them to both WMH and PVS in patients with minor ischaemic stroke. It is also the first comprehensive study to look at the relationship between intracranial and systemic haemodynamic measures. Our results suggest that aortic AIx is related to lower ICA pulsatility, but might not necessarily be the cause of WMH. The finding of no significant association between low CBF and WMH challenges the traditional hypothesis that low CBF is the cause of WMH, but is consistent with the overall message from longitudinal data which indicates that high WMH burden precedes low CBF. WMH and basal ganglia PVS are closely associated with cerebrovascular pulsatility. Although the implication of venous sinus pulsatility requires further research, this study confirms the role for increased intracranial pulsatility in SVD, as well as suggesting that venous PI specifically is important in SVD, thus advancing knowledge in the field and identifying potential targets for future studies of mechanism, treatment, and prevention of SVD.

Chapter 7: General discussion

Summary of the results

In this thesis, I summarised the current evidence of clinical studies on CBF and intracranial pulsatility in SVD, developed a method to measure CBF and pulsatility using phase-contrast MRI, and then applied this method in 60 patients with minor ischaemic stroke and SVD imaging features. The results of the systematic reviews question the cause and effect between reduced global CBF and SVD, and suggest increased intracranial pulsatility as an alternative mechanism of SVD. The systematic reviews also highlighted the importance on the adjustment of important covariates such as age and blood pressure in SVD studies, and called for more studies of high quality and longitudinal data.

Then in the cross-sectional study, I showed that the MRI CBF and pulsatility measures were well reproducible and comparable to that in the Doppler ultrasound. The results again did not support an association between low global CBF and SVD, but suggest that increased cerebrovascular pulsatility plays an important role in the pathophysiology of WMH and PVS, thus advancing the current understanding of SVD mechanisms and providing potential targets for SVD prevention and treatment. More importantly, this thesis sets up a reliable methodology for futures SVD studies to measure CBF and intracranial pulsatility using phase contrast MRI, and to use these measures as a secondary outcome in clinical trials.

Strengths

The thesis has several strengths. First, I carried out two comprehensive systematic reviews of clinical studies, which not only summarised the results of previous studies, but also addressed the potential limitations of the current evidence. Second, we showed that phase-contrast MRI had high reproducibility and good comparability with Doppler ultrasound in measuring cerebrovascular pulsatility, which provides strong evidence for cerebrovascular pulsatility to be used as a secondary outcome for monitoring cerebrovascular function in future longitudinal studies and clinical trials. The results of the associations between the flow and pulsatility and SVD features also allow us to estimate sample sizes for further studies. Third, in the cross-sectional study, I used various approaches to control the potential biases, including the use of blinding (to clinical and flow data) and validated methods in the structural image processing, cross-checking of the visual rating scores with an experienced neuroradiologist. Fourth, all statistical analyses were carefully performed. Age was adjusted wherever possible in the statistical analyses, including in the systematic reviews and the cross-sectional study. We also adjusted for gender and blood pressure in all the multiple variable analyses. In all the statistical models, the numbers of covariates were carefully selected according to the sample size, with avoidance of any collinearity between covariates.

Weaknesses

The first limitation is the relatively small sample sizes in both systematic reviews and our own study, which limited more comprehensive statistical analyses. However,

the sample sizes of the systematic reviews actually reflect the limitation of previous studies. Second, all associations assessed in this thesis were cross-sectional. We were not able to address the cause and effect between predictor and outcome variables, which requires longitudinal studies. However, one of the aims of this pilot study was to set up a reliable measure of CBF and intracranial pulsatility and use it in future clinical trials or for long-term follow ups. Indeed, after this study, we have already applied this method in 27 patients in the ongoing Lacunar Intervention Trial 1 (LACI-1) funded by the Alzheimer's Society.[213](protocol has been published, see **Appendix**) This technique will also be used in several larger multicentre studies (e.g. Investigate and Treat SVDs with centres from Edinburgh, Oxford, Munich, Maastricht, and Utrecht; Leduc study of sleep and sporadic SVDs with centres from Edinburgh and Toronto). Thus the longitudinal relationship between CBF, pulsatility, and SVD could be addressed in these future studies with larger populations.

Implications for future research

Most of the previous studies and our study only measured the global CBF. However, the relationship between the local CBF or blood flow in the penetrating arteries, or at an even more microscopic level and SVD changes remained unknown. We showed that increased arterial pulsatility was associated with lower arterial blood flow, indicating that stiffened vessels might potentially limit local CBF. Thus, it is likely that, at the end stage of the disease if the brain small vessels stiffen diffusely, the CBF in patients with SVD would eventually drop, as shown in some studies that recruited patients with very severe SVD or vascular dementia. But at earlier stages of

the disease, such as in our study, where most patients had mild to moderate WMH or PVS burden, the global CBF might be compensated by the not-yet-exhausted cerebrovascular autoregulation. Nevertheless, it is still not impossible that, at the microscopic level, limited local blood supply due to impaired arteriole autoregulation could be one of the factors that lead to brain tissue damage. Animal studies have showed that white matter and glial cells were vulnerable to low blood flow. Imaging methods such as arterial-spin labelling MRI and dynamic contrast-enhanced MRI that have higher spatial resolution and can localise CBF measurement to specific tissues might benefit future studies. On the other hand, the oxygen metabolism of brain tissues is not simply related to blood flow, but also (maybe more importantly) to the flow-metabolism coupling.[214] In a capillary with a disturbed flow, high CBF might even show a low oxygen availability and cause reperfusion injury to brain tissues.[214] Thus only measuring CBF is not enough for understanding the pathophysiology of SVD.

Increasing evidence has revealed that early cerebral endothelial dysfunction might be a precipitator of SVD. Various mechanisms have been suggested to be related to the endothelial failure, of which increased intracranial pulsatility is supported by growing data. This study for the first time showed the association between increased venous sinus pulsatility and PVS, which is considered as a possible marker of the impaired BBB.[15] PVS might also play an important role in the metabolite clearance in the central nervous system via the glymphatic system.[215] However PVS was still relatively under-researched. Also, whether PVS in different locations have separate physiology is unclear. Therefore, more animal and human studies on PVS are needed.

The implication of high pulsatility in the venous sinuses also requires more research: whether it is due to the venous pathologies, or whether because it is a more sensitive indicator of intracranial pulsatility or pulsatility in small penetrating arteries is unclear. We suggest that future pathology and pathophysiology studies, or mathematical models, of SVD, should include both arteries and veins whenever possible. Brain imaging techniques with higher resolution, such as 7T MRI scanners might also be helpful. In addition, the reproducibility of CSF measures in our study was mostly poor, which might be due to the difficulty in measuring CSF with low flow. Future studies that use techniques with higher temporal and spatial resolution might facilitate better CSF measurements and generate more reliable data. Apart from clinical studies, animal studies might have its advantages in elucidating the relationship between intracranial pulsatility, and endothelial dysfunction and perivascular spaces at the microscopic level.

We found a complicated relationship between aortic stiffness and intracranial haemodynamics. We did not find aortic AIx to be associated with venous sinus pulsatility, but instead an inverse relationship with ICA pulsatility. In addition, aortic AIx was associated with basal ganglia PVS but not with WMH. AIx is a complex measure that is an indicator of aortic wave reflection, which is associated with aortic stiffness but also related to other factors such as impedance mismatch between proximal and distal arteries. After all, these results might suggest that aortic stiffness has contributed to the increased intracranial pulsatility and cerebral small vessel damage, but might not be the single reason. The reduced diastolic pressure was also associated with increased ICA and venous pulsatility. For patients who had SVD, the stiffened small vessels could be the main source of the high intracranial pulsatility.

However, restricted by the limited assessment of aortic stiffness and spatial resolution of phase contrast MRI, we were not able to assess other indices of aortic stiffness such as aortic pulse wave velocity and pulsatility in smaller penetrating cerebral vessels, which could be considered in future studies.

In addition, future studies should examine the long-term effect of high intracranial pulsatility on patients' cognition, recurrent stroke, disabilities, and the progression of different SVD lesions, in order to better understand the cause and effect between pulsatility and SVD, and to seek potential treatment and prevention of SVD.

Implications for treatment and prevention of SVD

Currently, the management of traditional modifiable risk factors is still the main approach for treating or preventing SVD, despite the fact that most of these treatments have not yet shown desired effects on long-term outcomes. Antihypertensive treatment produced contradicting results: it reduced WMH progression in some observational studies[216] but showed little or no effect in randomized controlled trials.[217, 218] There is a suggestion that ACEIs and angiotensin receptor blocker (ARBs) are superior to other antihypertensive drugs in reducing arterial stiffness,[219] but clinical trials on either Perindopril or Telmisartan (on top of other antihypertensive drugs) did not show significant effects on long-term SVD progression. Although hypertension has been reported to be highly associated with SVD, other factors may be involved, or be influenced by genetic factors,[220] but more evidence is required. Nevertheless, lowering blood pressure too much could be potentially harmful. With an impaired cerebral autoregulation, reducing blood

pressure might also reduce the CBF, thus caution needs to be taken when lowering blood pressure in patients who had severe SVD, prior strokes and in older patients.[221, 222] Most lipid-lowering treatment had also neutral results in preventing WMH, like pravastatin,[223] but statins might have other therapeutic effects including anti-inflammatory and pro-endothelial activities.[224] Some small studies showed that physical exercise might be able to prevent age-related arterial stiffness in healthy individuals,[225, 226] and aerobic exercise could improve cardiovascular function related to arterial stiffness after stroke.[227] However, the required intensity, frequency and duration of physical exercise remains unknown, and it might not be suitable for all age groups.[219] Smoking is another well-known modifiable risk factor for SVD and dementia and increases arterial stiffness.[228, 229] Although so far there is no evidence on smoking cessation for preventing SVD progression, quitting smoking greatly reduces the risk of stroke.[230]

Prevention and treatment of SVD in the future should consider targeting the BBB, brain endothelium and microvascular function. There are multiple potential endothelial targets, such as the nitric oxide/cyclic guanosine monophosphate (cGMP) systems and prostacyclin/cyclic adenosine monophosphate (cAMP) system which might also improve the BBB integrity.[224] Therefore interventions that could induce cAMP or cGMP or reduce their degradation appear promising. There are several licensed drugs that have these properties such as some nitric oxide donors and phosphodiesterase (PDE)-5 inhibitors.[224] Dipyridamole has been licensed in the secondary prevention of stroke in addition to the mono-antiplatelet therapy.[224, 231] Other PDE-5 inhibitors, such as sildenafil, is used to reduce the vascular resistance in the pulmonary circulation in pulmonary hypertension. In animal models of stroke,

sildenafil improved the vascular density and endothelial cell proliferation, although clinical data are lacking.[232] Many other drugs are still in development. More laboratory studies are required. But meantime, management of traditional risk factors according to guidelines should still be encouraged.

References

1. World Alzheimer Report 2015. The Global Impact of Dementia.
2. Mackay J and Mensah GA. The atlas of heart disease and stroke. World health organization and Center for disease control and prevention. [Last accessed on 2013 Feb 14].
3. Gorelick PB, Scuteri A, Black SE, et al. Vascular contributions to cognitive impairment and dementia: a statement for healthcare professionals from the american heart association/american stroke association. *Stroke*. 2011; 42: 2672-713.
4. Pantoni L. Cerebral small vessel disease: from pathogenesis and clinical characteristics to therapeutic challenges. *Lancet Neurol*. 2010; 9: 689-701.
5. Herrmann LL, Le Masurier M and Ebmeier KP. White matter hyperintensities in late life depression: a systematic review. *J Neurol Neurosurg Psychiatry*. 2008; 79: 619-24.
6. de Laat KF, Tuladhar AM, van Norden AG, Norris DG, Zwiers MP and de Leeuw FE. Loss of white matter integrity is associated with gait disorders in cerebral small vessel disease. *Brain*. 2011; 134: 73-83.
7. Wardlaw JM, Smith EE, Biessels GJ, et al. Neuroimaging standards for research into small vessel disease and its contribution to ageing and neurodegeneration. *Lancet Neurol*. 2013; 12: 822-38.
8. Hachinski VC, Iliff LD, Zilhka E, et al. Cerebral blood flow in dementia. *Arch Neurol*. 1975; 32: 632-7.
9. Snyder HM, Corriveau RA, Craft S, et al. Vascular contributions to cognitive impairment and dementia including Alzheimer's disease. *Alzheimer's and Dementia*. 2015; 11: 710-7.
10. Investigators SPS, Benavente OR, Hart RG, et al. Effects of clopidogrel added to aspirin in patients with recent lacunar stroke. *N Engl J Med*. 2012; 367: 817-25.
11. Wardlaw JM, Smith C and Dichgans M. Mechanisms of sporadic cerebral small vessel disease: insights from neuroimaging. *Lancet Neurol*. 2013; 12: 483-97.
12. Mori E, Tabuchi M and Yamadori A. Lacunar syndrome due to intracerebral hemorrhage. *Stroke*. 1985; 16: 454-9.
13. Fisher CM. Lacunes: Small, Deep Cerebral Infarcts. *Neurology*. 1965; 15: 774-84.
14. Wardlaw JM, Dennis MS, Warlow CP and Sandercock PA. Imaging appearance of the symptomatic perforating artery in patients with lacunar infarction: occlusion or other vascular pathology? *Ann Neurol*. 2001; 50: 208-15.
15. Wardlaw JM, Doubal F, Armitage P, et al. Lacunar stroke is associated with diffuse blood-brain barrier dysfunction. *Ann Neurol*. 2009; 65: 194-202.
16. Durand-Fardel M. *Traité du Ramolissment du Cerveau.* . Baillière. Paris, 1843.
17. Potter GM, Marlborough FJ and Wardlaw JM. Wide variation in definition, detection, and description of lacunar lesions on imaging. *Stroke*. 2011; 42: 359-66.
18. Franke CL, van Swieten JC and van Gijn J. Residual lesions on computed tomography after intracerebral hemorrhage. *Stroke*. 1991; 22: 1530-3.
19. Hernandez Mdel C, Piper RJ, Wang X, Deary IJ and Wardlaw JM. Towards the automatic computational assessment of enlarged perivascular spaces on brain magnetic resonance images: a systematic review. *J Magn Reson Imaging*. 2013; 38: 774-85.
20. Potter GM, Doubal FN, Jackson CA, et al. Enlarged perivascular spaces and cerebral small vessel disease. *Int J Stroke*. 2015; 10: 376-81.
21. Snowdon DA, Greiner LH, Mortimer JA, Riley KP, Greiner PA and Markesbery WR. Brain infarction and the clinical expression of Alzheimer disease. The Nun Study. *JAMA*. 1997; 277: 813-7.
22. Vermeer SE, Longstreth WT, Jr. and Koudstaal PJ. Silent brain infarcts: a systematic review. *Lancet Neurol*. 2007; 6: 611-9.

23. Vermeer SE, Prins ND, den Heijer T, Hofman A, Koudstaal PJ and Breteler MM. Silent brain infarcts and the risk of dementia and cognitive decline. *N Engl J Med*. 2003; 348: 1215-22.
24. Debette S and Markus HS. The clinical importance of white matter hyperintensities on brain magnetic resonance imaging: systematic review and meta-analysis. *BMJ*. 2010; 341: c3666.
25. Wardlaw JM, Valdes Hernandez MC and Munoz-Maniega S. What are white matter hyperintensities made of? Relevance to vascular cognitive impairment. *J Am Heart Assoc*. 2015; 4: 001140.
26. Madden DJ, Bennett IJ, Burzynska A, Potter GG, Chen NK and Song AW. Diffusion tensor imaging of cerebral white matter integrity in cognitive aging. *Biochim Biophys Acta*. 2012; 1822: 386-400.
27. Munoz DG, Hastak SM, Harper B, Lee D and Hachinski VC. Pathologic correlates of increased signals of the centrum ovale on magnetic resonance imaging. *Arch Neurol*. 1993; 50: 492-7.
28. Black S, Gao F and Bilbao J. Understanding white matter disease: imaging-pathological correlations in vascular cognitive impairment. *Stroke*. 2009; 40: S48-52.
29. Feigin I and Popoff N. Neuropathological Changes Late in Cerebral Edema: The Relationship to Trauma, Hypertensive Disease and Binswanger's Encephalopathy. *J Neuropathol Exp Neurol*. 1963; 22: 500-11.
30. Braffman BH, Zimmerman RA, Trojanowski JQ, Gonatas NK, Hickey WF and Schlaepfer WW. Brain MR: pathologic correlation with gross and histopathology. 1. Lacunar infarction and Virchow-Robin spaces. *AJR Am J Roentgenol*. 1988; 151: 551-8.
31. Potter GM, Chappell FM, Morris Z and Wardlaw JM. Cerebral perivascular spaces visible on magnetic resonance imaging: development of a qualitative rating scale and its observer reliability. *Cerebrovasc Dis*. 2015; 39: 224-31.
32. Groeschel S, Chong WK, Surtees R and Hanefeld F. Virchow-Robin spaces on magnetic resonance images: normative data, their dilatation, and a review of the literature. *Neuroradiology*. 2006; 48: 745-54.
33. Doubal FN, MacLullich AM, Ferguson KJ, Dennis MS and Wardlaw JM. Enlarged perivascular spaces on MRI are a feature of cerebral small vessel disease. *Stroke*. 2010; 41: 450-4.
34. Heier LA, Bauer CJ, Schwartz L, Zimmerman RD, Morgello S and Deck MD. Large Virchow-Robin spaces: MR-clinical correlation. *AJNR Am J Neuroradiol*. 1989; 10: 929-36.
35. Zhu YC, Tzourio C, Soumare A, Mazoyer B, Dufouil C and Chabriat H. Severity of dilated Virchow-Robin spaces is associated with age, blood pressure, and MRI markers of small vessel disease: a population-based study. *Stroke*. 2010; 41: 2483-90.
36. Maclullich AM, Wardlaw JM, Ferguson KJ, Starr JM, Seckl JR and Deary IJ. Enlarged perivascular spaces are associated with cognitive function in healthy elderly men. *J Neurol Neurosurg Psychiatry*. 2004; 75: 1519-23.
37. Zhu YC, Dufouil C, Soumare A, Mazoyer B, Chabriat H and Tzourio C. High degree of dilated Virchow-Robin spaces on MRI is associated with increased risk of dementia. *J Alzheimers Dis*. 2010; 22: 663-72.
38. Wuerfel J, Haertle M, Waiczies H, et al. Perivascular spaces--MRI marker of inflammatory activity in the brain? *Brain*. 2008; 131: 2332-40.
39. Weller RO, Djuanda E, Yow HY and Carare RO. Lymphatic drainage of the brain and the pathophysiology of neurological disease. *Acta Neuropathol*. 2009; 117: 1-14.
40. Iliff JJ, Wang M, Zeppenfeld DM, et al. Cerebral arterial pulsation drives paravascular CSF-interstitial fluid exchange in the murine brain. *J Neurosci*. 2013; 33: 18190-9.
41. van Dijk EJ, Breteler MM, Schmidt R, et al. The association between blood pressure, hypertension, and cerebral white matter lesions: cardiovascular determinants of dementia study. *Hypertension*. 2004; 44: 625-30.

42. Wardlaw JM, Allerhand M, Doubal FN, et al. Vascular risk factors, large-artery atheroma, and brain white matter hyperintensities. *Neurology*. 2014; 82: 1331-8.
43. Pantoni L, Garcia JH and Gutierrez JA. Cerebral white matter is highly vulnerable to ischemia. *Stroke*. 1996; 27: 1641-6; discussion 7.
44. Petito CK, Olarte JP, Roberts B, Nowak TS, Jr. and Pulsinelli WA. Selective glial vulnerability following transient global ischemia in rat brain. *J Neuropathol Exp Neurol*. 1998; 57: 231-8.
45. Potter GM, Doubal FN, Jackson CA, Sudlow CL, Dennis MS and Wardlaw JM. Lack of association of white matter lesions with ipsilateral carotid artery stenosis. *Cerebrovasc Dis*. 2012; 33: 378-84.
46. Kwon HM, Lynn MJ, Turan TN, et al. Frequency, Risk Factors, and Outcome of Coexistent Small Vessel Disease and Intracranial Arterial Stenosis: Results From the Stenting and Aggressive Medical Management for Preventing Recurrent Stroke in Intracranial Stenosis (SAMMPRIS) Trial. *JAMA Neurol*. 2016; 73: 36-42.
47. Ibayashi S, Nagao T, Kuwabara Y, Sasaki M and Fujishima M. Mechanism for decreased cortical oxygen metabolism in patients with leukoaraiosis: Is disconnection the answer? *Journal of Stroke and Cerebrovascular Diseases*. 2000; 9: 22-6.
48. Kuwabara Y, Ichiya Y, Sasaki M, et al. Cerebral blood flow and vascular response to hypercapnia in hypertensive patients with leukoaraiosis. *Ann Nucl Med*. 1996; 10: 293-8.
49. Farrall AJ and Wardlaw JM. Blood-brain barrier: ageing and microvascular disease--systematic review and meta-analysis. *Neurobiol Aging*. 2009; 30: 337-52.
50. Abbott NJ. Inflammatory mediators and modulation of blood-brain barrier permeability. *Cell Mol Neurobiol*. 2000; 20: 131-47.
51. Fornage M, Chiang YA, O'Meara ES, et al. Biomarkers of Inflammation and MRI-Defined Small Vessel Disease of the Brain: The Cardiovascular Health Study. *Stroke*. 2008; 39: 1952-9.
52. Al-Solaiman Y, Jesri A, Zhao Y, Morrow JD and Egan BM. Low-Sodium DASH reduces oxidative stress and improves vascular function in salt-sensitive humans. *J Hum Hypertens*. 2009; 23: 826-35.
53. de Roos A, van der Grond J, Mitchell G and Westenberg J. Magnetic Resonance Imaging of Cardiovascular Function and the Brain: Is Dementia a Cardiovascular-Driven Disease? *Circulation*. 2017; 135: 2178-95.
54. Garcia-Polite F, Martorell J, Del Rey-Puech P, et al. Pulsatility and high shear stress deteriorate barrier phenotype in brain microvascular endothelium. *J Cereb Blood Flow Metab*. 2017; 37: 2614-25.
55. Tan Y, Tseng PO, Wang D, et al. Stiffening-induced high pulsatility flow activates endothelial inflammation via a TLR2/NF-kappaB pathway. *PLoS One*. 2014; 9: e102195.
56. Aribisala BS, Wiseman S, Morris Z, et al. Circulating inflammatory markers are associated with magnetic resonance imaging-visible perivascular spaces but not directly with white matter hyperintensities. *Stroke*. 2014; 45: 605-7.
57. Aribisala BS, Morris Z, Eadie E, et al. Blood pressure, internal carotid artery flow parameters, and age-related white matter hyperintensities. *Hypertension*. 2014; 63: 1011-8.
58. Jolly TA, Bateman GA, Levi CR, Parsons MW, Michie PT and Karayanidis F. Early detection of microstructural white matter changes associated with arterial pulsatility. *Front Hum Neurosci*. 2013; 7: 782.
59. Webb AJ, Simoni M, Mazzucco S, Kuker W, Schulz U and Rothwell PM. Increased cerebral arterial pulsatility in patients with leukoaraiosis: arterial stiffness enhances transmission of aortic pulsatility. *Stroke*. 2012; 43: 2631-6.
60. Mitchell GF, van Buchem MA, Sigurdsson S, et al. Arterial stiffness, pressure and flow pulsatility and brain structure and function: the Age, Gene/Environment Susceptibility--Reykjavik study. *Brain*. 2011; 134: 3398-407.
61. Poels MM, Zaccai K, Verwoert GC, et al. Arterial stiffness and cerebral small vessel disease: the Rotterdam Scan Study. *Stroke*. 2012; 43: 2637-42.

62. Stivaros SM and Jackson A. Changing concepts of cerebrospinal fluid hydrodynamics: role of phase-contrast magnetic resonance imaging and implications for cerebral microvascular disease. *Neurotherapeutics*. 2007; 4: 511-22.
63. Kellie G. An account of the appearances observed in the dissection of two of three individuals presumed to have perished in the storm of the 3d, and whose bodies were discovered in the vicinity of Leith on the morning of the 4th, November 1821 : with some reflections on the pathology of the brain. *Transactions of the Medico-Chirurgical Society of Edinburgh*. 1824; 1: 84-196.
64. Bateman GA, Levi CR, Schofield P, Wang Y and Lovett EC. The venous manifestations of pulse wave encephalopathy: windkessel dysfunction in normal aging and senile dementia. *Neuroradiology*. 2008; 50: 491-7.
65. Naish JH, Baldwin RC, Patankar T, et al. Abnormalities of CSF flow patterns in the cerebral aqueduct in treatment-resistant late-life depression: a potential biomarker of microvascular angiopathy. *Magn Reson Med*. 2006; 56: 509-16.
66. Jeerakathil T, Wolf PA, Beiser A, et al. Stroke risk profile predicts white matter hyperintensity volume: the Framingham Study. *Stroke*. 2004; 35: 1857-61.
67. Yata K and Tomimoto H. Chronic cerebral hypoperfusion and dementia. *Neurol Clin Neurosci*. 2014; 2: 129-34.
68. Stroup DF, Berlin JA, Morton SC, et al. Meta-analysis of observational studies in epidemiology: a proposal for reporting. Meta-analysis Of Observational Studies in Epidemiology (MOOSE) group. *JAMA*. 2000; 283: 2008-12.
69. Bailey EL, Smith C, Sudlow CL and Wardlaw JM. Pathology of lacunar ischemic stroke in humans--a systematic review. *Brain Pathol*. 2012; 22: 583-91.
70. van der Veen PH, Muller M, Vincken KL, et al. Longitudinal relationship between cerebral small-vessel disease and cerebral blood flow: the second manifestations of arterial disease-magnetic resonance study. *Stroke*. 2015; 46: 1233-8.
71. Bisschops RHC, Van Der Graaf Y, Mali WPTM and Van Der Grond J. High total cerebral blood flow is associated with a decrease of white matter lesions. *J Neurol*. 2004; 251: 1481-5.
72. Ten Dam VH, Van Den Heuvel DMJ, De Craen AJM, et al. Decline in total cerebral blood flow is linked with increase in periventricular but not deep white matter hyperintensities. *Radiology*. 2007; 243: 198-203.
73. van Es AC, van der Grond J, ten Dam VH, et al. Associations between total cerebral blood flow and age related changes of the brain. *PLoS One*. 2010; 5: e9825.
74. Vernooij MW, van der Lugt A, Ikram MA, et al. Total cerebral blood flow and total brain perfusion in the general population: the Rotterdam Scan Study. *J Cereb Blood Flow Metab*. 2008; 28: 412-9.
75. Claus JJ, Breteler MMB, Hasan D, et al. Vascular risk factors, atherosclerosis, cerebral white matter lesions and cerebral perfusion in a population-based study. *Eur J Nucl Med*. 1996; 23: 675-82.
76. Kimura N, Nakama H, Nakamura K, Aso Y and Kumamoto T. Effect of white matter lesions on brain perfusion in alzheimer's disease. *Dement Geriatr Cogn Disord*. 2012; 34: 256-61.
77. Yamaji S, Ishii K, Sasaki M, et al. Changes in cerebral blood flow and oxygen metabolism related to magnetic resonance imaging white matter hyperintensities in Alzheimer's disease. *J Nucl Med*. 1997; 38: 1471-4.
78. Schuff N, Matsumoto S, Kmiecik J, et al. Cerebral blood flow in ischemic vascular dementia and Alzheimer's disease, measured by arterial spin-labeling magnetic resonance imaging. *Alzheimer's and Dementia*. 2009; 5: 454-62.
79. Kawamura J, Meyer JS, Ichijo M, Kobari M, Terayama Y and Weathers S. Correlations of leuko-araiosis with cerebral atrophy and perfusion in elderly normal subjects and demented patients. *J Neurol Neurosurg Psychiatry*. 1993; 56: 182-7.

80. Kobari M, Meyer JS, Ichijo M and Oravez WT. Leukoaraiosis: Correlation of MR and CT findings with blood flow, atrophy, and cognition. *AJNR Am J Neuroradiol*. 1990; 11: 273-81.
81. Nezu T, Yokota C, Uehara T, et al. Preserved acetazolamide reactivity in lacunar patients with severe white-matter lesions: 15 O-labeled gas and H 2 O positron emission tomography studies. *J Cereb Blood Flow Metab*. 2012; 32: 844-50.
82. Zheng LS, Xu J and Wang JP. Quantitative evaluation of regional cerebral blood flow in patients with silent Leukoaraiosis. [Chinese]. *Chinese Journal of Clinical Rehabilitation*. 2006; 10: 80-2.
83. Ramli N, Ho KL, Nawawi O, Chong HT and Tan CT. CT perfusion as a useful tool in the evaluation of leuko-araiosis. *Biomed Imaging Interv J*. 2006; 2.
84. Cui BW, Qi X and Guo HZ. Comparative study on the cerebral hemodynamics changes between Leukoaraiosis and Binswanger disease. [Chinese]. *Chinese Journal of Clinical Rehabilitation*. 2003; 7: 3460-1.
85. O'Sullivan M, Lythgoe DJ, Pereira AC, et al. Patterns of cerebral blood flow reduction in patients with ischemic leukoaraiosis. *Neurology*. 2002; 59: 321-6.
86. Yao H, Yuzuriha T, Fukuda K, et al. Cerebral blood flow in nondemented elderly subjects with extensive deep white matter lesions on magnetic resonance imaging. *J Stroke Cerebrovasc Dis*. 2000; 9: 172-5.
87. Markus HS, Lythgoe DJ, Ostegaard L, O'Sullivan M and Williams SCR. Reduced cerebral blood flow in white matter in ischaemic leukoaraiosis demonstrated using quantitative exogenous contrast based perfusion MRI. *J Neurol Neurosurg Psychiatry*. 2000; 69: 48-53.
88. Oishi M and Mochizuki Y. Differences in regional cerebral blood flow in two types of leuko- araiosis. *J Neurol Sci*. 1999; 164: 129-33.
89. Hatazawa J, Shimosegawa E, Satoh T, Toyoshima H and Okudera T. Subcortical hypoperfusion associated with asymptomatic white matter lesions on magnetic resonance imaging. *Stroke*. 1997; 28: 1944-7.
90. Kobayashi S, Okada K and Yamashita K. Incidence of silent lacunar lesion in normal adults and its relation to cerebral blood flow and risk factors. *Stroke*. 1991; 22: 1379-83.
91. Fazekas F, Niederkorn K, Schmidt R, et al. White matter signal aities in normal individuals: Correlation with carotid ultrasonography, cerebral blood flow measurements, and cerebrovascular risk factorsbnormal. *Stroke*. 1988; 19: 1285-8.
92. Kimura M, Shimoda K, Mizumura S, et al. Regional cerebral blood flow in vascular depression assessed by 123I-IMP SPECT. *J Nippon Med Sch*. 2003; 70: 321-6.
93. Fu J, Tang J, Han J and Hong Z. The reduction of regional cerebral blood flow in normal-appearing white matter is associated with the severity of white matter lesions in elderly: A xeon-ct study. *PLoS ONE*. 2014; 9.
94. De Bastos-Leite AJ, Kuijer JPA, Rombouts SARB, et al. Cerebral blood flow by using pulsed arterial spin-labeling in elderly subjects with white matter hyperintensities. *American Journal of Neuroradiology*. 2008; 29: 1296-301.
95. Miyazawa N, Satoh T, Hashizume K and Fukamachi A. Xenon contrast CT-CBF measurements in high-intensity foci on T2-weighted MR images in centrum semiovale of asymptomatic individuals. *Stroke*. 1997; 28: 984-7.
96. Tzourio C, Levy C, Dufouil C, Touboul PJ, Ducimetiere P and Alperovitch A. Low cerebral blood flow velocity and risk of white matter hyperintensities. *Ann Neurol*. 2001; 49: 411-4.
97. Heliopoulos I, Artemis D, Vadikolias K, Tripsianis G, Piperidou C and Tsivgoulis G. Association of ultrasonographic parameters with subclinical white-matter hyperintensities in hypertensive patients. *Cardiovasc Psychiatry Neurol*. 2012.

98. Isaka Y, Okamoto M, Ashida K and Imaizumi M. Decreased cerebrovascular dilatory capacity in subjects with asymptomatic periventricular hyperintensities. *Stroke*. 1994; 25: 375-81.
99. Alosco ML, Brickman AM, Spitznagel MB, et al. Cerebral perfusion is associated with white matter hyperintensities in older adults with heart failure. *Congest Heart Fail*. 2013; 19: E29-E34.
100. Ott BR, Faberman RS, Noto RB, et al. A SPECT imaging study of MRI white matter hyperintensity in patients with degenerative dementia. *Dement Geriatr Cogn Disord*. 1997; 8: 348-54.
101. Bernbaum M, Menon BK, Fick G, et al. Reduced blood flow in normal white matter predicts development of leukoaraiosis. *J Cereb Blood Flow Metab*. 2015; 35: 1610-5.
102. Kraut MA, Beason-Held LL, Elkins WD and Resnick SM. The impact of magnetic resonance imaging-detected white matter hyperintensities on longitudinal changes in regional cerebral blood flow. *J Cereb Blood Flow Metab*. 2008; 28: 190-7.
103. Wagner M, Helfrich M, Volz S, et al. Quantitative T2, T2*, and T2' MR imaging in patients with ischemic leukoaraiosis might detect microstructural changes and cortical hypoxia. *Neuroradiology*. 2015; 57: 1023-30.
104. Huynh TJ, Murphy B, Pettersen JA, et al. CT perfusion quantification of small-vessel ischemic severity. *AJNR Am J Neuroradiol*. 2008; 29: 1831-6.
105. Crane DE, Black SE, Ganda A, et al. Grey matter blood flow and volume are reduced in association with white matter hyperintensity lesion burden: A cross-sectional MRI study. *Front Aging Neurosci*. 2015; 7.
106. Zonneveld HI, Loehrer EA, Hofman A, et al. The bidirectional association between reduced cerebral blood flow and brain atrophy in the general population. *J Cereb Blood Flow Metab*. 2015; 35: 1882-7.
107. Schmidt R, Ropele S, Enzinger C, et al. White matter lesion progression, brain atrophy, and cognitive decline: The Austrian Stroke Prevention Study. *Ann Neurol*. 2005; 58: 610-6.
108. Ryu WS, Woo SH, Schellingerhout D, et al. Grading and interpretation of white matter hyperintensities using statistical maps. *Stroke*. 2014; 45: 3567-75.
109. Ostergaard L, Engedal TS, Moreton F, et al. Cerebral small vessel disease: Capillary pathways to stroke and cognitive decline. *J Cereb Blood Flow Metab*. 2016; 2: 23.
110. Liem MK, Lesnik Oberstein SA, Haan J, et al. Cerebrovascular reactivity is a main determinant of white matter hyperintensity progression in CADASIL. *AJNR Am J Neuroradiol*. 2009; 30: 1244-7.
111. Bahrani AA, Powell DK, Yu G, Johnson ES, Jicha GA and Smith CD. White Matter Hyperintensity Associations with Cerebral Blood Flow in Elderly Subjects Stratified by Cerebrovascular Risk. *Journal of Stroke and Cerebrovascular Diseases*. 2017; 26: 779-86.
112. Hashimoto T, Yokota C, Koshino K, et al. Cerebral blood flow and metabolism associated with cerebral microbleeds in small vessel disease. *Annals of Nuclear Medicine*. 2016; 30: 494-500.
113. Liu J, Zhao H, Gao M, Xie H, Lu R and Liang X. Arterial spin labeling and DTI in evaluation on cerebral perfusion and white matter of cerebral small vessel disease patients. [Chinese]. *Chinese Journal of Medical Imaging Technology*. 2016; 32: 1170-4.
114. Van Dalen JW, Mutsaerts HJMM, Nederveen AJ, et al. White matter hyperintensity volume and cerebral perfusion in older individuals with hypertension using arterial spin-labeling. *American Journal of Neuroradiology*. 2016; 37: 1824-30.
115. Hanaoka T, Kimura N, Aso Y, et al. Relationship between white matter lesions and regional cerebral blood flow changes during longitudinal follow up in Alzheimer's disease. *Geriatrics and Gerontology International*. 2016; 16: 836-42.
116. Nylander R, Fahlstrom M, Rostrup E, et al. Quantitative and qualitative MRI evaluation of cerebral small vessel disease in an elderly population: a longitudinal study. *Acta Radiol*. 2017: 284185117727567.

117. Fazekas F, Kleinert R, Offenbacher H, et al. Pathologic correlates of incidental MRI white matter signal hyperintensities. *Neurology*. 1993; 43: 1683-9.
118. Fazekas F, Kleinert R, Roob G, et al. Histopathologic analysis of foci of signal loss on gradient-echo T2*-weighted MR images in patients with spontaneous intracerebral hemorrhage: evidence of microangiopathy-related microbleeds. *AJNR Am J Neuroradiol*. 1999; 20: 637-42.
119. Shi Y and Wardlaw J. Update on cerebral small vessel disease: a dynamic whole-brain disease. *Stroke and Vascular Neurology*. 2016; 2: 83-92.
120. Mitchell GF. Effects of central arterial aging on the structure and function of the peripheral vasculature: implications for end-organ damage. *J Appl Physiol (1985)*. 2008; 105: 1652-60.
121. Gosling RG and King DH. Arterial assessment by Doppler shift ultrasound. *Proc R Soc Med*. 1974; 67: 447-9.
122. Mok V, Ding D, Fu J, et al. Transcranial doppler ultrasound for screening cerebral small vessel disease: A community study. *Stroke*. 2012; 43: 2791-3.
123. Battal B, Kocaoglu M, Bulakbasi N, Husmen G, Tuba Sanal H and Tayfun C. Cerebrospinal fluid flow imaging by using phase-contrast MR technique. *Br J Radiol*. 2011; 84: 758-65.
124. Bateman GA. Pulse-wave encephalopathy: A comparative study of the hydrodynamics of leukoaraiosis and normal-pressure hydrocephalus. *Neuroradiology*. 2002; 44: 740-8.
125. Beggs CB, Magnano C, Shepherd SJ, et al. Dirty-Appearing White Matter in the Brain is Associated with Altered Cerebrospinal Fluid Pulsatility and Hypertension in Individuals without Neurologic Disease. *Journal of Neuroimaging*. 2016; 26: 136-43.
126. Shi Y, Thrippleton MJ, Makin SD, et al. Cerebral blood flow in small vessel disease: A systematic review and meta-analysis. *J Cereb Blood Flow Metab*. 2016; 36: 1653-67.
127. Tanaka T, Shimizu T and Fukuhara T. The relationship between leukoaraiosis volume and parameters of carotid artery duplex ultrasonographic scanning in asymptomatic diabetic patients. *Computerized Medical Imaging and Graphics*. 2009; 33: 489-93.
128. Ternifi R, Cazals X, Desmidt T, et al. Ultrasound measurements of brain tissue pulsatility correlate with the volume of MRI white-matter hyperintensity. *Journal of Cerebral Blood Flow and Metabolism*. 2014; 34: 942-4.
129. Turk M, Zupan M, Zaletel M, Zvan B and Oblak JP. Carotid arterial hemodynamic in ischemic levkoaraiosis suggests hypoperfusion mechanism. *European Neurology*. 2015; 73: 310-5.
130. Biedert S, Forstl H and Hewer W. Multiinfarct dementia vs Alzheimer's disease: Sonographic criteria. *Angiology*. 1995; 46: 129-35.
131. Kidwell CS, El-Saden S, Livshits Z, Martin NA, Glenn TC and Saver JL. Transcranial doppler pulsatility indices as a measure of diffuse small-vessel disease. *Journal of Neuroimaging*. 2001; 11: 229-35.
132. Sanchez-Perez RM, Hernandez-Lorido R, Castano P, Diaz-Marin C, Carneado-Ruiz J and Molto-Jorda J. Evaluation of hemodynamic parameters by transcranial Doppler in patients with leukoaraiosis. [Spanish]. *Revista de Neurologia*. 2003; 37: 301-11.
133. Rodriguez I, Lema I, Blanco M, Rodriguez-Yanez M, Leira R and Castillo J. Vascular retinal, neuroimaging and ultrasonographic markers of lacunar infarcts. *International Journal of Stroke*. 2010; 5: 360-6.
134. Purkayastha S, Fadar O, Mehregan A, et al. Impaired cerebrovascular hemodynamics are associated with cerebral white matter damage. *Journal of Cerebral Blood Flow and Metabolism*. 2014; 34: 228-34.
135. Sargento-Freitas J, Felix-Morais R, Ribeiro J, et al. Different locations but common associations in subcortical hypodensities of presumed vascular origin: Cross-sectional study on clinical and neurosonologic correlates. *BMC Neurology*. 2014; 14 (1) (no pagination).

136. Sanahuja J, Alonso N, Diez J, et al. Increased burden of cerebral small vessel disease in patients with type 2 diabetes and retinopathy. *Diabetes Care*. 2016; 39: 1614-20.
137. Smith EE, Vijayappa M, Lima F, et al. Impaired visual evoked flow velocity response in cerebral amyloid angiopathy. *Neurology*. 2008; 71: 1424-30.
138. Hiroki M, Miyashita K, Yoshida H, Hirai S and Fukuyama H. Central retinal artery Doppler flow parameters reflect the severity of cerebral small-vessel disease. *Stroke; a journal of cerebral circulation*. 2003; 34: e92-4.
139. Del Brutto OH, Mera RM, De La Luz Andrade M, Castillo PR, Zambrano M and Nader JA. Disappointing reliability of pulsatility indices to identify candidates for magnetic resonance imaging screening in population-based studies assessing prevalence of cerebral small vessel disease. *Journal of Neurosciences in Rural Practice*. 2015; 6: 336-8.
140. Ghorbani A, Ahmadi MJ and Shemshaki H. The value of transcranial Doppler derived pulsatility index for diagnosing cerebral small-vessel disease. *Adv Biomed Res*. 2015; 4: 54.
141. Han SW, Song TJ, Bushnell CD, et al. Cilostazol decreases cerebral arterial pulsatility in patients with mild white matter hyperintensities: Subgroup analysis from the effect of cilostazol in acute lacunar infarction based on pulsatility index of transcranial doppler (ECLIPse) study. *Cerebrovascular Diseases*. 2014; 38: 197-203.
142. Bettermann K, Slocomb JE, Shivkumar V and Lott MEJ. Retinal vasoreactivity as a marker for chronic ischemic white matter disease? *Journal of the Neurological Sciences*. 2012; 322: 206-10.
143. Henry-Feugeas MC, Roy C, Baron G and Schouman-Claeys E. Leukoaraiosis and pulse-wave encephalopathy: Observations with phase-contrast MRI in mild cognitive impairment. *Journal of Neuroradiology*. 2009; 36: 212-8.
144. Wahlin A, Ambarki K, Birgander R, Malm J and Eklund A. Intracranial pulsatility is associated with regional brain volume in elderly individuals. *Neurobiol Aging*. 2014; 35: 365-72.
145. Zhang CE, Wong SM, Uiterwijk R, et al. Intravoxel Incoherent Motion Imaging in Small Vessel Disease: Microstructural Integrity and Microvascular Perfusion Related to Cognition. *Stroke*. 2017; 48: 658-63.
146. Adams HP, Jr., Bendixen BH, Kappelle LJ, et al. Classification of subtype of acute ischemic stroke. Definitions for use in a multicenter clinical trial. TOAST. Trial of Org 10172 in Acute Stroke Treatment. *Stroke*. 1993; 24: 35-41.
147. Stoquart-ElSankari S, Baledent O, Gondry-Jouet C, Makki M, Godefroy O and Meyer ME. Aging effects on cerebral blood and cerebrospinal fluid flows. *J Cereb Blood Flow Metab*. 2007; 27: 1563-72.
148. Wagshul ME, Eide PK and Madsen JR. The pulsating brain: A review of experimental and clinical studies of intracranial pulsatility. *Fluids Barriers CNS*. 2011; 8: 5.
149. Michel E and Zernikow B. Gosling's Doppler pulsatility index revisited. *Ultrasound Med Biol*. 1998; 24: 597-9.
150. Czosnyka M, Richards HK, Whitehouse HE and Pickard JD. Relationship between transcranial Doppler-determined pulsatility index and cerebrovascular resistance: an experimental study. *J Neurosurg*. 1996; 84: 79-84.
151. Beasley MG, Blau JN and Gosling RG. Changes in internal carotid artery flow velocities with cerebral vasodilation and constriction. *Stroke*. 1979; 10: 331-5.
152. Jiang J, Strother C, Johnson K, et al. Comparison of blood velocity measurements between ultrasound Doppler and accelerated phase-contrast MR angiography in small arteries with disturbed flow. *Phys Med Biol*. 2011; 56: 1755-73.
153. Seitz J, Strotzer M, Schlaier J, Nitz WR, Volk M and Feuerbach S. Comparison between magnetic resonance phase contrast imaging and transcranial Doppler ultrasound with regard to blood flow velocity in intracranial arteries: work in progress. *J Neuroimaging*. 2001; 11: 121-8.

154. Makedonov I, Black SE and Macintosh BJ. BOLD fMRI in the white matter as a marker of aging and small vessel disease. *PLoS One*. 2013; 8: e67652.
155. Rivera-Rivera LA, Turski P, Johnson KM, et al. 4D flow MRI for intracranial hemodynamics assessment in Alzheimer's disease. *J Cereb Blood Flow Metab*. 2016; 36: 1718-30.
156. Bouvy WH, Geurts LJ, Kuijf HJ, et al. Assessment of blood flow velocity and pulsatility in cerebral perforating arteries with 7-T quantitative flow MRI. *NMR Biomed*. 2016; 29: 1295-304.
157. Kiviniemi V, Wang X, Korhonen V, et al. Ultra-fast magnetic resonance encephalography of physiological brain activity - Glymphatic pulsation mechanisms? *J Cereb Blood Flow Metab*. 2016; 36: 1033-45.
158. Stoquart-Elsankari S, Lehmann P, Villette A, et al. A phase-contrast MRI study of physiologic cerebral venous flow. *J Cereb Blood Flow Metab*. 2009; 29: 1208-15.
159. Pourcelot L. Applicaitions cliniques de l'examen Doppler transcutane. *Coloques de l'Inst Natl Santé Rech Med*. 1974; 34: 213-40.
160. Chen CH, Nevo E, Fetics B, et al. Estimation of central aortic pressure waveform by mathematical transformation of radial tonometry pressure. Validation of generalized transfer function. *Circulation*. 1997; 95: 1827-36.
161. Butlin M and Qasem A. Large Artery Stiffness Assessment Using SphygmoCor Technology. *Pulse (Basel)*. 2017; 4: 180-92.
162. Steppan J, Barodka V, Berkowitz DE and Nyhan D. Vascular stiffness and increased pulse pressure in the aging cardiovascular system. *Cardiol Res Pract*. 2011; 2011: 263585.
163. Jenkinson M and Smith S. A global optimisation method for robust affine registration of brain images. *Med Image Anal*. 2001; 5: 143-56.
164. Tustison NJ, Cook PA, Klein A, et al. Large-scale evaluation of ANTs and FreeSurfer cortical thickness measurements. *Neuroimage*. 2014; 99: 166-79.
165. Avants BB, Epstein CL, Grossman M and Gee JC. Symmetric diffeomorphic image registration with cross-correlation: evaluating automated labeling of elderly and neurodegenerative brain. *Med Image Anal*. 2008; 12: 26-41.
166. Freedman D, Pisani R and Purves R. *Statistics*. New York: W. W. Norton, 2007.
167. Avants BB, Tustison NJ, Wu J, Cook PA and Gee JC. An open source multivariate framework for n-tissue segmentation with evaluation on public data. *Neuroinformatics*. 2011; 9: 381-400.
168. Fazekas F, Chawluk JB, Alavi A, Hurtig HI and Zimmerman RA. MR signal abnormalities at 1.5 T in Alzheimer's dementia and normal aging. *AJR Am J Roentgenol*. 1987; 149: 351-6.
169. Walker PG, Cranney GB, Scheidegger MB, Waseleski G, Pohost GM and Yoganathan AP. Semiautomated method for noise reduction and background phase error correction in MR phase velocity data. *J Magn Reson Imaging*. 1993; 3: 521-30.
170. Ku JP, Elkins CJ and Taylor CA. Comparison of CFD and MRI flow and velocities in an in vitro large artery bypass graft model. *Ann Biomed Eng*. 2005; 33: 257-69.
171. Wendt RE, 3rd, Rokey R, Wong WF and Marks A. Magnetic resonance velocity measurements in small arteries. Comparison with Doppler ultrasonic measurements in the aortas of normal rabbits. *Invest Radiol*. 1992; 27: 499-503.
172. Seitz J, Strotzer M, Wild T, et al. Quantification of blood flow in the carotid arteries: comparison of Doppler ultrasound and three different phase-contrast magnetic resonance imaging sequences. *Invest Radiol*. 2001; 36: 642-7.
173. Spilt A, Box FM, van der Geest RJ, et al. Reproducibility of total cerebral blood flow measurements using phase contrast magnetic resonance imaging. *J Magn Reson Imaging*. 2002; 16: 1-5.
174. Wahlin A, Ambarki K, Hauksson J, Birgander R, Malm J and Eklund A. Phase contrast MRI quantification of pulsatile volumes of brain arteries, veins, and cerebrospinal

fluids compartments: repeatability and physiological interactions. *J Magn Reson Imaging*. 2012; 35: 1055-62.
175. Piechnik SK, Summers PE, Jezzard P and Byrne JV. Magnetic resonance measurement of blood and CSF flow rates with phase contrast--normal values, repeatability and CO2 reactivity. *Acta Neurochir Suppl*. 2008; 102: 263-70.
176. Huang TY, Chung HW, Chen MY, et al. Supratentorial cerebrospinal fluid production rate in healthy adults: quantification with two-dimensional cine phase-contrast MR imaging with high temporal and spatial resolution. *Radiology*. 2004; 233: 603-8.
177. Unal O, Kartum A, Avcu S, Etlik O, Arslan H and Bora A. Cine phase-contrast MRI evaluation of normal aqueductal cerebrospinal fluid flow according to sex and age. *Diagn Interv Radiol*. 2009; 15: 227-31.
178. Schrauben EM, Johnson KM, Huston J, et al. Reproducibility of cerebrospinal venous blood flow and vessel anatomy with the use of phase contrast-vastly undersampled isotropic projection reconstruction and contrast-enhanced MRA. *AJNR Am J Neuroradiol*. 2014; 35: 999-1006.
179. Zivadinov R, Galeotti R, Hojnacki D, et al. Value of MR venography for detection of internal jugular vein anomalies in multiple sclerosis: a pilot longitudinal study. *AJNR Am J Neuroradiol*. 2011; 32: 938-46.
180. Niggemann P, Seifert M, Forg A, Schild HH, Urbach H and Krings T. Positional venous MR angiography: an operator-independent tool to evaluate cerebral venous outflow hemodynamics. *AJNR Am J Neuroradiol*. 2012; 33: 246-51.
181. Wentland AL, Wieben O, Korosec FR and Haughton VM. Accuracy and reproducibility of phase-contrast MR imaging measurements for CSF flow. *AJNR Am J Neuroradiol*. 2010; 31: 1331-6.
182. Tawfik AM, Elsorogy L, Abdelghaffar R, Naby AA and Elmenshawi I. Phase-Contrast MRI CSF Flow Measurements for the Diagnosis of Normal-Pressure Hydrocephalus: Observer Agreement of Velocity Versus Volume Parameters. *AJR Am J Roentgenol*. 2017; 208: 838-43.
183. Tang C, Blatter DD and Parker DL. Accuracy of phase-contrast flow measurements in the presence of partial-volume effects. *J Magn Reson Imaging*. 1993; 3: 377-85.
184. Sudlow CL and Warlow CP. Comparable studies of the incidence of stroke and its pathological types: results from an international collaboration. International Stroke Incidence Collaboration. *Stroke*. 1997; 28: 491-9.
185. Staals J, Makin SD, Doubal FN, Dennis MS and Wardlaw JM. Stroke subtype, vascular risk factors, and total MRI brain small-vessel disease burden. *Neurology*. 2014; 83: 1228-34.
186. Rost NS, Rahman RM, Biffi A, et al. White matter hyperintensity volume is increased in small vessel stroke subtypes. *Neurology*. 2010; 75: 1670-7.
187. Bergsneider M, Alwan AA, Falkson L and Rubinstein EH. The relationship of pulsatile cerebrospinal fluid flow to cerebral blood flow and intracranial pressure: a new theoretical model. *Acta Neurochir Suppl*. 1998; 71: 266-8.
188. Doepp F, Schreiber SJ, von Munster T, Rademacher J, Klingebiel R and Valdueza JM. How does the blood leave the brain? A systematic ultrasound analysis of cerebral venous drainage patterns. *Neuroradiology*. 2004; 46: 565-70.
189. Buijs PC, Krabbe-Hartkamp MJ, Bakker CJ, et al. Effect of age on cerebral blood flow: measurement with ungated two-dimensional phase-contrast MR angiography in 250 adults. *Radiology*. 1998; 209: 667-74.
190. Lemogoum D, Flores G, Van den Abeele W, et al. Validity of pulse pressure and augmentation index as surrogate measures of arterial stiffness during beta-adrenergic stimulation. *J Hypertens*. 2004; 22: 511-7.
191. O'Rourke MF, Staessen JA, Vlachopoulos C, Duprez D and Plante GE. Clinical applications of arterial stiffness; definitions and reference values. *Am J Hypertens*. 2002; 15: 426-44.

192. McEniery CM, Yasmin, Hall IR, et al. Normal vascular aging: differential effects on wave reflection and aortic pulse wave velocity: the Anglo-Cardiff Collaborative Trial (ACCT). *J Am Coll Cardiol*. 2005; 46: 1753-60.
193. Janner JH, Godtfredsen NS, Ladelund S, Vestbo J and Prescott E. Aortic augmentation index: reference values in a large unselected population by means of the SphygmoCor device. *Am J Hypertens*. 2010; 23: 180-5.
194. Scheel P, Ruge C and Schoning M. Flow velocity and flow volume measurements in the extracranial carotid and vertebral arteries in healthy adults: reference data and the effects of age. *Ultrasound Med Biol*. 2000; 26: 1261-6.
195. Lassen NA. Cerebral blood flow and oxygen consumption in man. *Physiol Rev*. 1959; 39: 183-238.
196. Strandgaard S. Cerebral blood flow in the elderly: impact of hypertension and antihypertensive treatment. *Cardiovasc Drugs Ther*. 1991; 4 Suppl 6: 1217-21.
197. Xu TY, Staessen JA, Wei FF, et al. Blood flow pattern in the middle cerebral artery in relation to indices of arterial stiffness in the systemic circulation. *Am J Hypertens*. 2012; 25: 319-24.
198. Kwater A, Gasowski J, Gryglewska B, Wizner B and Grodzicki T. Is blood flow in the middle cerebral artery determined by systemic arterial stiffness? *Blood Press*. 2009; 18: 130-4.
199. Mitchell GF, Lacourciere Y, Arnold JM, Dunlap ME, Conlin PR and Izzo JL, Jr. Changes in aortic stiffness and augmentation index after acute converting enzyme or vasopeptidase inhibition. *Hypertension*. 2005; 46: 1111-7.
200. Nichols WN, O'Rourke MF and Vlachopoulos C. *McDonald's Blood Flow in Arteries Theoretical, experimental and clinical principles* 6th ed. London: Arnold, p. 200.
201. Fantin F, Mattocks A, Bulpitt CJ, Banya W and Rajkumar C. Is augmentation index a good measure of vascular stiffness in the elderly? *Age Ageing*. 2007; 36: 43-8.
202. Nakano T, Munakata A, Shimaura N, Asano K and Ohkuma H. Augmentation index is related to white matter lesions. *Hypertens Res*. 2012; 35: 729-32.
203. Barnes JN, Harvey RE, Zuk SM, et al. Aortic hemodynamics and white matter hyperintensities in normotensive postmenopausal women. *J Neurol*. 2017; 264: 938-45.
204. Arba F, Mair G, Carpenter T, et al. Cerebral White Matter Hypoperfusion Increases with Small-Vessel Disease Burden. Data From the Third International Stroke Trial. *J Stroke Cerebrovasc Dis*. 2017; 26: 1506-13.
205. Bilston LE, Fletcher DF, Brodbelt AR and Stoodley MA. Arterial pulsation-driven cerebrospinal fluid flow in the perivascular space: a computational model. *Comput Methods Biomech Biomed Engin*. 2003; 6: 235-41.
206. Gutierrez J, Elkind MS, Cheung K, Rundek T, Sacco RL and Wright CB. Pulsatile and steady components of blood pressure and subclinical cerebrovascular disease: the Northern Manhattan Study. *J Hypertens*. 2015; 33: 2115-22.
207. Yakushiji Y, Charidimou A, Hara M, et al. Topography and associations of perivascular spaces in healthy adults: the Kashima scan study. *Neurology*. 2014; 83: 2116-23.
208. Blanco PJ, Müller LO and Spence JD. Blood pressure gradients in cerebral arteries: a clue to pathogenesis of cerebral small vessel disease. *stroke and Vascular Neurology*. 2017; 2: e000087.
209. Starr JM, Wardlaw J, Ferguson K, MacLullich A, Deary IJ and Marshall I. Increased blood-brain barrier permeability in type II diabetes demonstrated by gadolinium magnetic resonance imaging. *J Neurol Neurosurg Psychiatry*. 2003; 74: 70-6.
210. Hu X, Alwan AA, Rubinstein EH and Bergsneider M. Reduction of compartment compliance increases venous flow pulsatility and lowers apparent vascular compliance: implications for cerebral blood flow hemodynamics. *Med Eng Phys*. 2006; 28: 304-14.
211. Greitz D, Greitz T and Hindmarsh T. A new view on the CSF-circulation with the potential for pharmacological treatment of childhood hydrocephalus. *Acta Paediatr*. 1997; 86: 125-32.

212. Moody DM, Brown WR, Challa VR and Anderson RL. Periventricular venous collagenosis: association with leukoaraiosis. *Radiology*. 1995; 194: 469-76.
213. Blair G, Appleton JP, Law ZK, et al. Preventing Cognitive Decline and Dementia from Cerebral Small Vessel Disease: The LACI-1 Trial. Protocol and statistical analysis plan of a phase IIa dose escalation trial testing tolerability, safety and effect on intermediary endpoints of isosorbide mononitrate and cilostazol, separately and in combination. *Int J Stroke*. In press.
214. Jespersen SN and Ostergaard L. The roles of cerebral blood flow, capillary transit time heterogeneity, and oxygen tension in brain oxygenation and metabolism. *J Cereb Blood Flow Metab*. 2012; 32: 264-77.
215. Mestre H, Kostrikov S, Mehta RI and Nedergaard M. Perivascular spaces, glymphatic dysfunction, and small vessel disease. *Clin Sci (Lond)*. 2017; 131: 2257-74.
216. Dufouil C, de Kersaint-Gilly A, Besancon V, et al. Longitudinal study of blood pressure and white matter hyperintensities: the EVA MRI Cohort. *Neurology*. 2001; 56: 921-6.
217. Dufouil C, Chalmers J, Coskun O, et al. Effects of blood pressure lowering on cerebral white matter hyperintensities in patients with stroke: the PROGRESS (Perindopril Protection Against Recurrent Stroke Study) Magnetic Resonance Imaging Substudy. *Circulation*. 2005; 112: 1644-50.
218. Weber R, Weimar C, Blatchford J, et al. Telmisartan on top of antihypertensive treatment does not prevent progression of cerebral white matter lesions in the prevention regimen for effectively avoiding second strokes (PRoFESS) MRI substudy. *Stroke*. 2012; 43: 2336-42.
219. Chen Y, Shen F, Liu J and Yang G. Arterial stiffness and stroke: de-stiffening strategy, a therapeutic target for stroke. *Stroke and Vascular Neurology*. 2017; 2: 65-72.
220. Turner ST, Fornage M, Jack CR, Jr., et al. Genomic susceptibility loci for brain atrophy in hypertensive sibships from the GENOA study. *Hypertension*. 2005; 45: 793-8.
221. Ovbiagele B, Diener HC, Yusuf S, et al. Level of systolic blood pressure within the normal range and risk of recurrent stroke. *JAMA*. 2011; 306: 2137-44.
222. Sabayan B, van Vliet P, de Ruijter W, Gussekloo J, de Craen AJ and Westendorp RG. High blood pressure, physical and cognitive function, and risk of stroke in the oldest old: the Leiden 85-plus Study. *Stroke*. 2013; 44: 15-20.
223. ten Dam VH, van den Heuvel DM, van Buchem MA, et al. Effect of pravastatin on cerebral infarcts and white matter lesions. *Neurology*. 2005; 64: 1807-9.
224. Bath PM and Wardlaw JM. Pharmacological treatment and prevention of cerebral small vessel disease: a review of potential interventions. *Int J Stroke*. 2015; 10: 469-78.
225. Tanaka M, Sugawara M, Ogasawara Y, Izumi T, Niki K and Kajiya F. Intermittent, moderate-intensity aerobic exercise for only eight weeks reduces arterial stiffness: evaluation by measurement of stiffness parameter and pressure-strain elastic modulus by use of ultrasonic echo tracking. *J Med Ultrason (2001)*. 2013; 40: 119-24.
226. Tabara Y, Yuasa T, Oshiumi A, et al. Effect of acute and long-term aerobic exercise on arterial stiffness in the elderly. *Hypertens Res*. 2007; 30: 895-902.
227. Tang A, Eng JJ, Krassioukov AV, et al. Exercise-induced changes in cardiovascular function after stroke: a randomized controlled trial. *Int J Stroke*. 2014; 9: 883-9.
228. van Dijk EJ, Prins ND, Vrooman HA, Hofman A, Koudstaal PJ and Breteler MM. Progression of cerebral small vessel disease in relation to risk factors and cognitive consequences: Rotterdam Scan study. *Stroke*. 2008; 39: 2712-9.
229. Rehill N, Beck CR, Yeo KR and Yeo WW. The effect of chronic tobacco smoking on arterial stiffness. *Br J Clin Pharmacol*. 2006; 61: 767-73.
230. Shah RS and Cole JW. Smoking and stroke: the more you smoke the more you stroke. *Expert Rev Cardiovasc Ther*. 2010; 8: 917-32.
231. Verro P, Gorelick PB and Nguyen D. Aspirin plus dipyridamole versus aspirin for prevention of vascular events after stroke or TIA: a meta-analysis. *Stroke*. 2008; 39: 1358-63.

232. Sandner P, Hutter J, Tinel H, Ziegelbauer K and Bischoff E. PDE5 inhibitors beyond erectile dysfunction. *Int J Impot Res*. 2007; 19: 533-43.

Appendix

List of Published papers

1. **Shi Y**, Thrippleton MJ, Makin SD, et al. Cerebral blood flow in small vessel disease: A systematic review and meta-analysis. J Cereb Blood Flow Metab. 2016; 36: 1653-67.

2. **Shi Y** and Wardlaw J. Update on cerebral small vessel disease: a dynamic whole-brain disease. Stroke and Vascular Neurology. 2016; 2: 83-92.

3. **Shi Y**, Thrippleton MJ, Marshall I et al. Intracranial pulsatility in patients with cerebral small vessel disease: a systematic review. Clin Sci (Lond). 2018; 132: 157-171.

4. Thrippleton MJ, **Shi Y**, Blair G, et al. Cerebrovascular reactivity measurement in cerebral small vessel disease: Rationale and reproducibility of a protocol for MRI acquisition and image processing. Int J Stroke. 2017; In press.

5. Blair G, Appleton JP, Law ZK, Doubal F, Flaherty K, Dooley R, Shuler K, Richardson C, Hamilton I, **Shi Y**, Stringer M, Boyd J, Thrippleton MJ, Sprigg N, Bath PM and Wardlaw J. Preventing Cognitive Decline and Dementia from Cerebral Small Vessel Disease: The LACI-1 Trial. Protocol and statistical analysis plan of a phase IIa dose escalation trial testing tolerability, safety and effect on intermediary endpoints of isosorbide mononitrate and cilostazol, separately and in combination. Int J Stroke. doi: 10.1177/1747493017731947

Copies of the above-listed papers will be presented in the following pages. Permissions to use these publications in this thesis which is authored by myself were already obtained from the relevant publishers and other co-authors.

Review Article

JCBFM

Journal of Cerebral Blood Flow & Metabolism
2016, Vol. 36(10) 1653–1667

DOI: 10.1177/0271678X16662891
jcbfm.sagepub.com

SAGE

Cerebral blood flow in small vessel disease: A systematic review and meta-analysis

Yulu Shi[1,2], Michael J Thrippleton[1], Stephen D Makin[1,3], Ian Marshall[1], Mirjam I Geerlings[4], Anton JM de Craen[5,†], Mark A van Buchem[6] and Joanna M Wardlaw[1]

Abstract

White matter hyperintensities are frequent on neuroimaging of older people and are a key feature of cerebral small vessel disease. They are commonly attributed to chronic hypoperfusion, although whether low cerebral blood flow is cause or effect is unclear. We systematically reviewed studies that assessed cerebral blood flow in small vessel disease patients, performed meta-analysis and sensitivity analysis of potential confounders. Thirty-eight studies ($n = 4006$) met the inclusion criteria, including four longitudinal and 34 cross-sectional studies. Most cerebral blood flow data were from grey matter. Twenty-four cross-sectional studies ($n = 1161$) were meta-analysed, showing that cerebral blood flow was lower in subjects with more white matter hyperintensity, globally and in most grey and white matter regions (e.g. mean global cerebral blood flow: standardised mean difference −0.71, 95% CI −1.12, −0.30). These cerebral blood flow differences were attenuated by excluding studies in dementia or that lacked age-matching. Four longitudinal studies ($n = 1079$) gave differing results, e.g., more baseline white matter hyperintensity predated falling cerebral blood flow (3.9 years, $n = 575$); cerebral blood flow was low in regions that developed white matter hyperintensity (1.5 years, $n = 40$). Cerebral blood flow is lower in subjects with more white matter hyperintensity cross-sectionally, but evidence for falling cerebral blood flow predating increasing white matter hyperintensity is conflicting. Future studies should be longitudinal, obtain more white matter data, use better age-correction and stratify by clinical diagnosis.

Keywords

Cerebral blood flow, cerebral small vessel disease, white matter hyperintensities, systematic review, meta-analysis

Received 17 May 2016; Revised 7 July 2016; Accepted 8 July 2016

Introduction

White matter hyperintensities (WMHs) are commonly seen on brain magnetic resonance imaging (MRI) in older people and are considered as one of the core neuroimaging findings of cerebral small vessel disease (SVD). They are defined as patchy or confluent hyperintensities on T2-weighted or FLAIR images, without cavitation, in subcortical white or deep grey matter regions.[1] WMHs are associated with increasing age and vascular risk factors such as hypertension and diabetes.[2] Although the aetiology is not completely understood, chronic hypoperfusion is thought to be a key mechanism,[3] perhaps resulting from narrowing of the arteriolar lumena secondary to lipohyalinosis and arteriolosclerosis. Based on this theory, mechanically induced hypoperfusion models, for example, partial

[1]Centre for Clinical Brain Sciences, University of Edinburgh, Edinburgh, United Kingdom
[2]Department of Neurology, Zhongnan Hospital, Wuhan University, Wuhan, China
[3]Institute of Cardiovascular and Medical Sciences, University of Glasgow, Glasgow, United Kingdom
[4]University Medical Center Utrecht, Julius Center for Health Sciences and Primary Care, Utrecht, The Netherlands
[5]Department of Gerontology and Geriatrics, Leiden University Medical Centre, Leiden, Netherlands
[6]Department of Radiology, Leiden University Medical Centre, Leiden, Netherlands
[†]Deceased.

Corresponding author:
Joanna M Wardlaw, Centre for Clinical Brain Sciences, University of Edinburgh, Edinburgh EH16 4SB, United Kingdom.
Email: Joanna.Wardlaw@ed.ac.uk

or complete carotid artery occlusion, are used to create pathology that appears to mimic human SVD. However, no direct association between carotid artery stenosis and lacunar stroke or WMH has been found in human studies.[4]

Additionally, the relationship between cerebral blood flow (CBF) and WMH is not consistent across human studies. In some cross-sectional studies, low CBF was significantly related to more WMHs, whereas in other studies, no such relationship was found.[5,6] These studies had different study designs, sample sizes and locations where low CBF was detected and most studies were cross-sectional. There are few longitudinal studies. Thus it is unclear whether there is causal relationship between low CBF and WMHs in humans, or whether there is region specificity.

We sought to establish if WMH was related to changes in CBF levels, or whether differences in CBF might be related to potential confounders such as age and tissue loss. We systematically reviewed the available longitudinal and cross-sectional studies in humans, performed a meta-analysis of cross-sectional studies to assess the overall effect size of CBF differences by WMH burden in different brain regions, assessed study quality and performed sensitivity analyses on important confounders.

Methods

We performed this review according to guidelines[7] and a pre-specified protocol. We conducted a literature search of MEDLINE and EMBASE from 1946 up to December 2015, using the Ovid Web Gateway. We used exploded headings related to *Small Vessel Disease* and *Cerebral Blood Flow* with the Boolean operator AND [Supplementary methods]. English and non-English literature were sought. Additional records were identified by hand searching from January 1990 to December 2015 of *Stroke* and *Journal of Cerebral Blood Flow & Metabolism*. We also checked references cited in reviews and primary papers.

Eligibility criteria

We sought longitudinal and cross-sectional primary research studies assessing CBF in subjects with cerebral SVD.[8] Studies measuring cerebral blood flow velocity (CBFv) using Doppler ultrasound techniques were also considered eligible. We excluded studies targeting unilateral or bilateral severe carotid stenosis or occlusion, studies in children, animal studies, duplicate publications, conference abstracts and cross-sectional studies from which we could not extract either absolute values of CBF or correlation/regression coefficients.

Data extraction and analysis

We screened all potentially relevant full papers and extracted data using a standardised form. All data were cross-checked by a second reviewer (JMW). From those that met the inclusion criteria, we extracted data on study population characteristics, study design, SVD and CBF measurement techniques and units. We assessed the study quality using a checklist devised on the basis of the Strengthening the Reporting of Observational Studies in Epidemiology statement (www.equator-network.org) and checklist in a previous paper,[9] including factors such as study population and bias controlling (Supplementary Table S1).

For cross-sectional studies which reported means and standard deviations (S.D.s) of CBF, we extracted data on CBF in disease and control groups or according to SVD burden. Means and S.D.s were extracted from text or tables where available, or from graphs where necessary. For cross-sectional studies where only qualitative data for association between CBF and WMH were available, we included the studies in the review but not in the meta-analysis: we noted the statistical methods, coefficients, P values and other covariates included in regression.

For longitudinal studies, we also listed follow-up durations and primary results extracted from the papers, and contacted the authors to request unpublished data on baseline and follow-up CBF and WMH volume.

Data transformation and analysis

All studies reporting means and S.D.s were included for meta-analysis. For studies that divided patients into more than two grades of WMH severity, we combined the means and S.D.s of groups to create a single pair-wise comparison [Supplementary methods]. As most studies measured CBF in several regions of interest (ROIs), such as different grey matter and white matter regions, we conducted subgroup analysis by brain region. Due to various units of CBF being used in different papers, we calculated the standardised mean differences (SMDs) and 95% confidence intervals (CI) for comparisons using a random-effects model. Sensitivity analyses were carried out for subjects with/without dementia and by age matching between study groups, as both strongly influence CBF. Meta-analyses were conducted using the Cochrane Collaboration's Review Manager (Revman Version 5.3). We assessed for heterogeneity by calculating the I^2 statistic and publication bias using a funnel plot.

Results

A total of 2843 publications were initially identified, of which 75 were potentially eligible and were selected for

further review. We ultimately included 38 articles and excluded (Figure 1): conference abstracts (6), those where we were unable to access the full text (6) or that had no analysable data (18), duplicate publications including the same participant population (3) and studies of severe carotid stenosis or occlusion (4). Note that although presence of arterial diseases was an inclusion criterion of Second Manifestations of ARTerial disease-magnetic resonance (SMART-MR) study, carotid arterial stenosis or occlusion was not one of the criteria: here patients with carotid artery stenosis were included, but they only represented a small proportion of participants, thus we included the study[10] in our review. The 38 studies included a total of 4006 participants: 4/38 were longitudinal and 34/38 were cross-sectional.

Some papers are from the same studies: van der Veen et al.[10] and Bisschops et al.[11] from the SMART-MR study; ten Dam et al.[12] and van Es et al.[13] from the Prospective Study of the Elderly at Risk (PROSPER) trial; Vernooij et al.[14] and Claus et al.[15] from the Rotterdam Scan Study. We were careful to count each participant only once in any analysis.

Characteristics of included studies

Cross-sectional studies. Thirty-four cross-sectional studies were included (Table 1). 24/34 were suitable for meta-analysis. 6/24 studies used patients with dementia plus WMH as disease groups. Of these six studies, two included Alzheimer's disease (AD),[16,17] the other four focused on vascular dementia including subcortical vascular dementia,[18] multi-infarct dementia (MID),[19,20] and Binswanger's disease (BD).[5] AD diagnosis used the criteria of the National Institute of Neurological

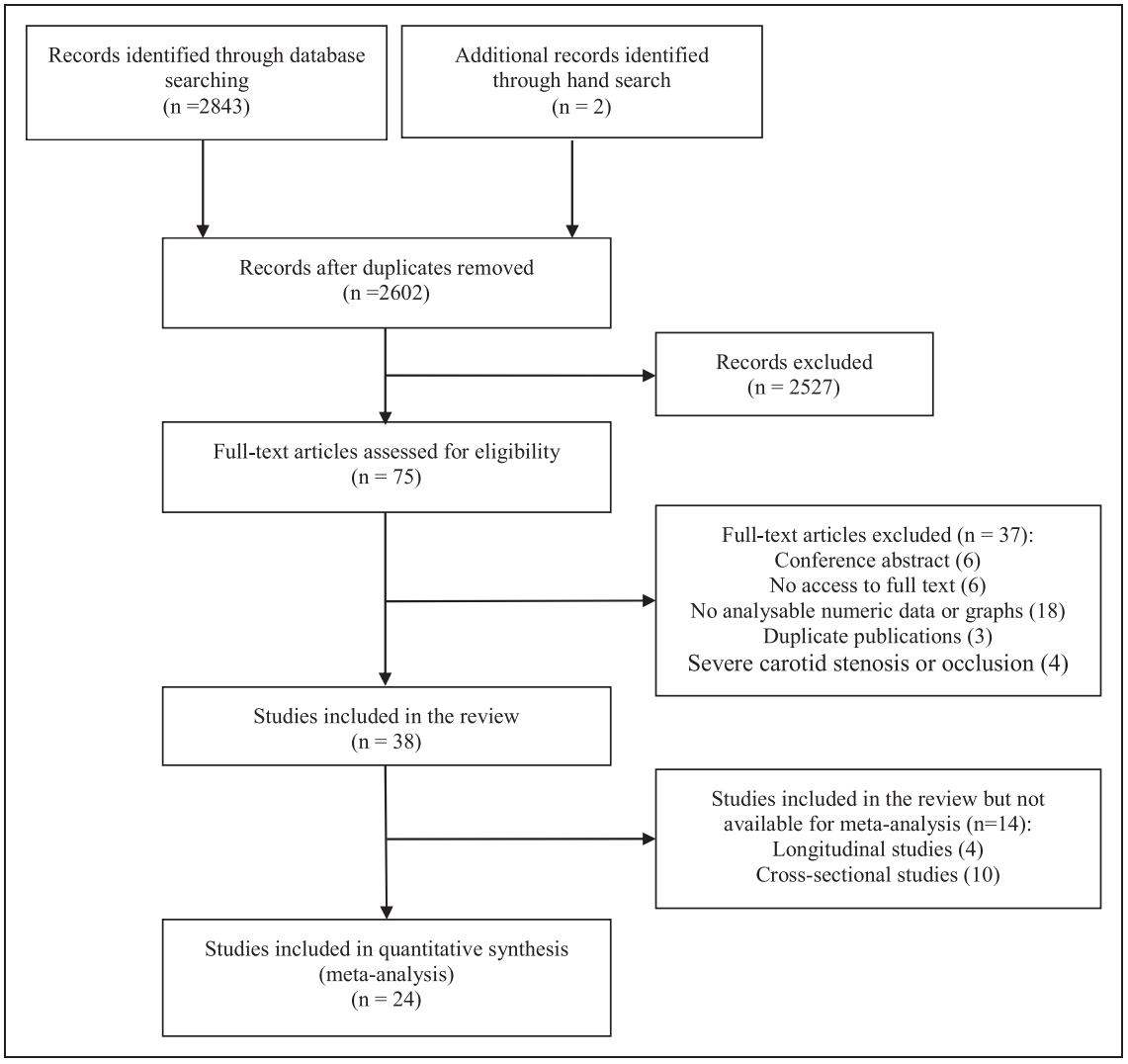

Figure 1. PRISMA flow diagram of literature search.

Table 1. Characteristics of all included studies.

Study	Sample size	Participants	(Baseline) Age (years, mean ± S.D.)	Methods of measuring CBF	CBF units
Longitudinal studies (4)					
Bernbaum et al.[43]	40	High risk TIA or minor ischemic stroke	61.0 ± 11.0	DCS PWI	ml/100 g/min
van der Veen et al.[10]	575	Manifest arterial diseases[a]	57.0 ± 10.0	Phase-contrast MRI	ml/100 ml/min
Kraut et al.[44]	74	Progressive WMH	70.0 ± 6.9	PET	Not shown
		Stable WMH	67.1 ± 7.0		
ten Dam et al.[12]	390	History of vascular disease or were at increased vascular risk	75.0 ± 3.2	Phase-contrast MRI	ml/min
Cross-sectional studies (34)					
Cognitive impairment/dementia (6)					
Kimura et al.[16]	98	Late-onset AD with WMH	78.6 ± 5.1	SPECT	ml/100 g/min
		AD without WMH	77.4 ± 5.0		
Schuff 2009[18]	26	Subcortical vascular dementia	77.0 ± 8.0	ASL	ml/100 g/min
		Cognitively normal	73.0 ± 8.0		
Ibayashi 2000[5]	15	Dementia of BD	60.0 ± 2.0	PET	ml/100 ml/min
		Age-matched hypertensive controls	59.0 ± 2.0		
Yamaji 1997[17]	32	AD with WMH	71.6 ± 3.1	PET	ml/100 ml/min
		AD without WMH	71.0 ± 4.3		
Kawamura et al.[19]	40	MID	64.4 ± 10.2	Xenon CT	ml/100 g/min
		No WMH	67.2 ± 10.5		
Kobari et al.[20]	20	MID	68.1 ± 12.0	Xenon CT	ml/100 g/min
		Neurologically normal controls	52.3 ± 5.7		
No cognitive impairment (18)					
Wagner et al.[45]	36	Extensive WMH	71.0	ASL	ml/100 g/min
		No or mild WMH	67.0		
Fu et al.[33]	56	WMH Grade 3[b]	68.1 ± 8.1	Xenon CT	ml/100 g/min
		WMH Grade 2	68.9 ± 7.7		
		WMH Grade 1	64.5 ± 5.8		
		WMH Grade 0	65.3 ± 6.3		
Nezu et al.[21]	18	Lacunar stroke with severe WMHs	76.0	PET	ml/100 g/min
		Lacunar stroke with mild WMH	74.0		
Huynh et al.[36]	35	TIA with moderate to severe WMH	77.1 ± 6.0	CT perfusion	ml/100 g/min
		TIA with mild WMH	62.6 ± 16.3		
De Bastos-Leite et al.[34]	21	WMH Grade 3[b]	77.7 ± 5.7	ASL	ml/100 ml/min
		WMH Grade 2	74.4 ± 4.6		
		WMH Grade 1	74.0 ± 5.0		
Zheng et al.[22]	35	Asymptomatic WMH	69.7 ± 8.9	SPECT	ml/g/min
		No WMH	67.1 ± 6.9		
Ramli et al.[23]	42	Leukoaraiosis on CT	70.19	CT perfusion	ml/100 g/min
		No leukoaraiosis on CT	69.86		
Kimura et al.[32]	20	Depression (remission) with WMH	78.5 ± 5.1	SPECT	ml/100 g/min
			77.4 ± 5.0		

(continued)

Table 1. Continued

Study	Sample size	Participants	(Baseline) Age (years, mean ± S.D.)	Methods of measuring CBF	CBF units
		Depression (remission) without WMH			
Cui et al.[24]	98	WMH	70.0	TCD, SPECT	cm/s
		No WMH	66.0		
O'Sullivan et al.[25]	36	WMH	68.9 ± 9.2	PET	ml/100 g/min
		No WMH	72.7 ± 7.7		
Yao et al.[26]	10	Extensive WMH	75.0 ± 5.0	Xenon CT	ml/100 g/min
		No WMH	72.0 ± 5.0		
Markus et al.[27]	17	Leukoaraiosis	63.3 ± 12.3	MRI contrast	ml/100 g/min
		No leukoaraiosis	68.3 ± 7.3		
Oishi and Mochizuki[28]	45	WMH	66.8 ± 8.4	Xenon CT	ml/100 g/min
		No WMH	65.1 ± 8.5		
Hatazawa et al.[29]	33	Asymptomatic WMH	71.3 ± 8.6	PET	ml/100 ml/min
		No WMH	68.5 ± 10.2		
Miyazawa et al.[35]	135	WMH Grade IV[c]	71.90 ± 8.17	Xenon CT	ml/100 g/min
		WMH Grade III	69.00 ± 8.08		
		WMH Grade II	67.30 ± 9.87		
		WMH Grade I	64.20 ± 5.55		
		WMH Grade 0	57.3 ± 12.0		
Kuwabara et al.[6]	24	Hypertensive with moderate to severe leukoaraiosis[c]	67.0 ± 9.0	PET	ml/100 ml/min
		Hypertensive with negative to mild leukoaraiosis	54.0 ± 7.0		
		Normotensive control	60.0 ± 12.0		
Kobayashi et al.[30]	246	Apparent PVWMH	67.0 ± 6.1	Xenon CT	ml/100 g/min
		No or mild PVWMH	60.0 ± 8.2		
Fazekas et al.[31]	23	WMH	58.8 ± 5.3	Xenon CT	ml/100 g/min
		No WMH	58.2 ± 2.8		
Studies only showing correlation coefficients (10)					
Crane et al.[47]	26	Mild to severe WMH	73.3 ± 8.8	ASL	ml/100 g/min
Alosco et al.[40]	69	Heart failure with WMH	68.55 ± 8.07	Ultrasound Doppler	cm/s
Heliopoulos et al.[38]	52	Hypertension with WMH	71.4 ± 4.5	Ultrasound Doppler	cm/s
van Es et al.[13]	447	Cerebrovascular risk factors without major neurological deficits	75.0 ± 3.0	Phase-contrast MRI	ml/min, ml/100 ml/min
Vernooij et al.[14]	892	Population-based	67.5 ± 5.5	Phase-contrast MRI	ml/100 g/min
Bisschops et al.[42]	228	Manifest arterial diseases[a]	59.0	Phase-contrast MRI	ml/min
Tzourio et al.[37]	628	Population-based	68.9 ± 2.9	Ultrasound Doppler	m/s
Ott et al.[41]	40	Mixed dementia	72.8 ± 8.7	SPECT	%rCBF relative to cerebellum
Claus et al.[46]	60	Non-demented WMH	65.0–85.0[d]	SPECT	%rCBF relative to cerebellum
Isaka et al.[39]	28	Cerebrovascular risk factors without neurological deficits	67.8	Xenon CT	ml/100 ml/min

S.D.: standard deviation; CBF: cerebral blood flow; TIA: transient ischemic attack; DCS-PWI: dynamic susceptibility contrast perfusion-weighted imaging; MRI: magnetic resonance imaging; AD: Alzheimer's disease; MID: multi-infarct dementia; BD: Binswanger's disease; WMH: white matter hyperintensity; SPECT: single-photon emission computed tomography; ASL: arterial spin labelling MRI; PET: positron emission tomography; TCD: transcranial Doppler; CT: computed tomography; PVWMH: periventricular white matter hyperintensity; rCBF: regional cerebral blood flow. [a]Includes manifest coronary artery disease, cerebrovascular disease, peripheral arterial disease or an abdominal aortic aneurysm. [b]Fazekas WMH score. [c]Self-designed scoring system for WMH. [d]Age range.

and Communicative Disorders and Stroke, and the Alzheimer's disease and Related Disorders Association (NINCDS/ADRDA) for probable AD. Vascular dementia diagnosis varied: CT/MRI evidence, DSM-III-R criteria,[5,19,20] Hachinski ischaemia scores[19] and the criteria of the State of California Alzheimer's Disease Diagnostic and Treatment Centres.[18] In the 18/24 studies of non-demented subjects, 11 compared CBF between subjects having WMHs and normal controls with no or mild WMHs,[21–31] one study performed the comparison between patients with depression (DSM-IV criteria) plus WMHs vs no WMHs,[32] and the other four papers examined the differences in CBF across grades of WMH severity.[6,33–35] Of these four studies, two used Fazekas WMH rating scores,[6,35] the other two used a self-designed rating systems similar to Fazekas's method.[33,34] Two studies recruited patients with acute ischemic symptoms: in Nezu et al.,[21] patients presented with minor ischemic stroke and brain scans were performed at least 3 weeks after onset; Huynh et al. only included TIA patients and brain scans were done acutely.[36]

In the other 10/34 studies which only reported association analysis, two were population-based studies,[14,37] the other nine hospital-based studies included patients with cerebrovascular risk factors,[13,38,39] heart failure,[40] dementia[41] and manifest arterial diseases.[42]

Longitudinal studies. Four longitudinal prospective studies, including 1079 participants, were included (Table 1). Three were hospital-based[10,12,43] and one from a population-based aging study.[44] Among these four studies, Bernbaum et al. recruited participants who presented acute minor stroke symptoms or transient ischemic attack (TIA) and had baseline MRI within 48 h after the onset.[43] The other three studies did not include acute patients. The follow-up durations ranged from 1.5 to 7.7 years. Kraut et al. compared the patterns of long-term CBF change in patients with progressive WMHs to those with stable WMHs,[44] whereas the other three studies performed regression analyses between CBF and WMH data without subdividing patient groups.[10,12,43]

Quality assessment. The average study quality score was 6/9. Scores were mainly lost for not reporting the drop-outs (25/38), no adjustment or matching for risk factors (including age) (17/38), not reporting expertise of image observers (20/38) and not using blinding (25/38) (Supplementary Figure S1).

Assessment of CBF measurement methods. Three studies used phase-contrast MRI,[10,12–14,42] seven used positron emission tomography (PET),[5,6,17,21,25,29,44] six used single-photon emission computerised tomography,[15,16,22,24,32,41] two used MRI contrast,[27,43] two used arterial spin labelling (ASL)-MRI,[18,45] nine used Xenon-CT[19,20,26,28,30,31,33,35,39] and two used CT perfusion[23,36] to assess CBF. Four studies measured CBFv in the middle cerebral arteries using transcranial Doppler ultrasound.[24,37,38,40]

Meta-analysis of differences in CBF by WMH burden

Meta-analysis using SMD in CBF was only possible for 24 cross-sectional studies. Twenty-two brain regions were extracted, but sufficient data were available from only 11 regions which were used by at least three studies and were selected for the primary meta-analysis. These included: global brain mean CBF, basal ganglia, cortical grey matter (total, frontal, temporal, parietal and occipital grey matter) and white matter (total, frontal and occipital white matter, centrum semiovale). Most data were available for grey matter; few studies provided white matter data.

Patients with more severe WMH had lower CBF than patients with mild WMH, globally and in most grey and white matter regions (e.g. mean global CBF: SMD −0.71, 95% CI −1.12, −0.30; total grey matter: SMD −0.50, 95% CI −0.97, −0.03; total white matter: SMD −1.16, 95% CI −1.08, −0.53; see Figure 2a and b), except in basal ganglia (SMD −1.25, 95% CI −2.53, 0.30) and occipital white matter (SMD −0.45, 95% CI −0.96, 0.05) where the difference in CBF did not reach significance. No studies in the meta-analysis separated normal appearing white matter (NAWM) and WMH. However, there was heterogeneity between studies for most of these comparisons (Figure 2a and b) that was not due to publication bias (funnel plot, Supplementary Figure S2). One study found that CBF in patients with lacunar lesions was lower than in those without, however, the result was not adjusted for WMH volume and could not be meta-analysed.[30]

Sensitivity analysis of dementia and age. We repeated the meta-analyses after excluding studies that included patients with dementia and then further excluded studies without age-matching. In most grey and white matter regions, the differences in CBF between subjects with high and low WMH burdens attenuated and were no longer significant, except for mean global brain CBF and centrum semiovale. Most of the trends in the comparisons were still the same, apart from temporal grey matter (Figure 3).

Only one study, Ibayashi et al., used hypertensive but neurologically normal patients as the control group, and found lower CBF in patients with Binswanger's dementia compared to the control group;[5] none of the other studies matched or adjusted

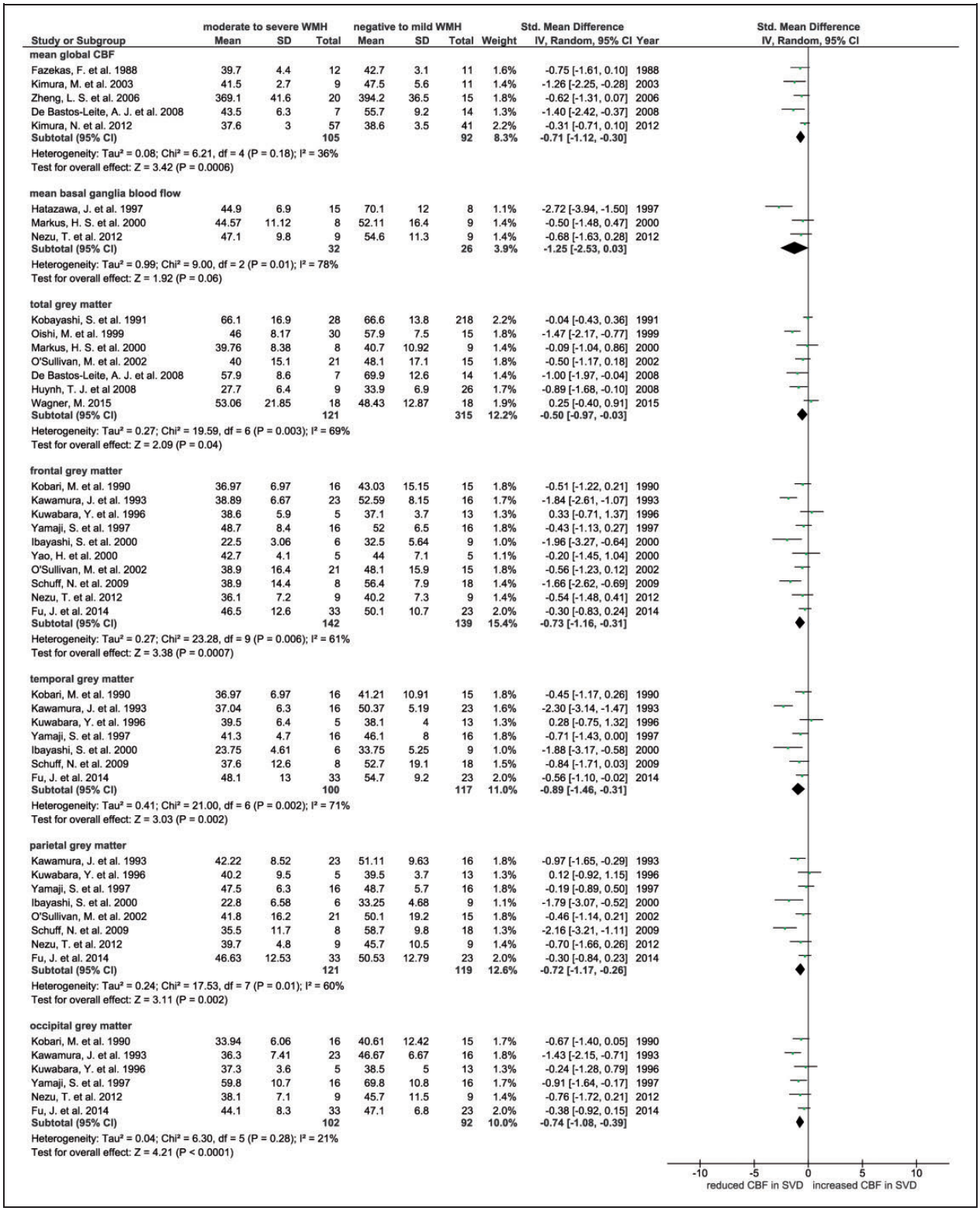

Figure 2. (a) Forest plot showing standard mean differences in global and grey matter CBF in patients with WMH in dementia and non-dementia studies. CBF in different brain regions was analysed in subgroups. (b) Forest plot showing standard mean differences in white matter CBF in patients with WMH in dementia and non-dementia studies. CBF in different brain regions was analysed in subgroups. CBF: cerebral blood flow; WMH: white matter hyperintensity.

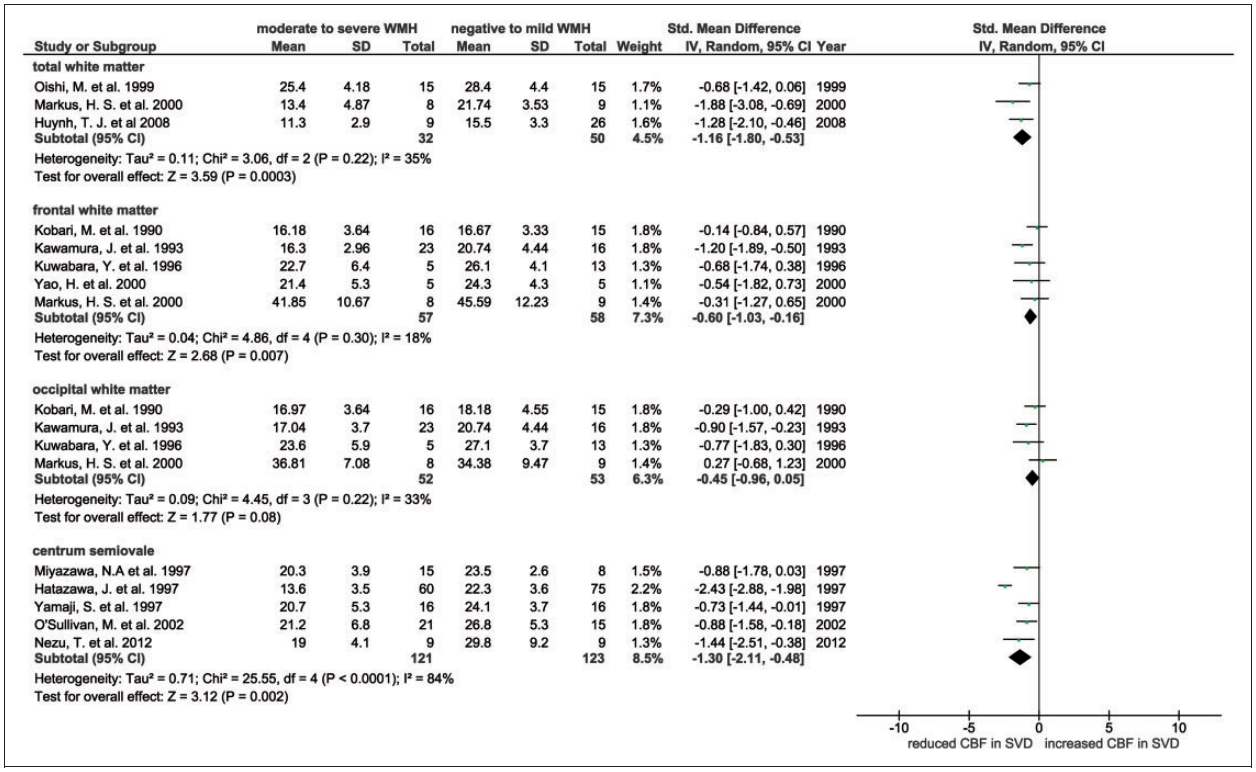

Figure 2. Continued.

for vascular risk factors. Therefore, we were not able to do a sensitivity analysis for vascular risk factors. Hypertension is significantly more prevalent in patients with more severe WMH.

Cross-sectional studies that provided data on associations between CBF and SVD features

Among the 10 cross-sectional papers which only performed association analysis, three studies did not find association between CBF and WMH burden.[39,41,46] Four studies reported that CBF was negatively related to WMH severity.[11,13,14,47] Negative correlation between WMH features and CBFv was found in three studies, of which one assessed CBFv in internal carotid arteries,[38] and the other two in middle cerebral arteries.[37,40] Among all 10 studies, six adjusted for covariates such as age, gender and other vascular risk factors (Table 2).[11,37,40,46–48]

Longitudinal studies

In longitudinal studies, the largest study (575 subjects), van der Veen et al., found that high WMH volume at baseline was significantly associated with falling CBF over 3.9 years follow-up.[10] ten Dam et al. demonstrated in 390 subjects that a decline in global CBF over 2.75 years was associated with a progression in periventricular WMH (PVWMH) but not in deep WMH (DWMH).[12] A small study ($n = 40$) found low CBF in regions that developed WMH over 1.5 years follow-up (Table 3).[43] In contrast to the other findings of falling CBF over time, Kraut et al. demonstrated in 74 subjects that CBF increased in some brain areas (right inferior temporal gyrus, right anterior cingulate and the left superior temporal gyrus) over 7.7 years in patients with progressive WMH.[44] Falling CBF was observed more in the posterior regions including right inferior parietal lobule and right occipital pole but was not specifically associated with WMH change.

Discussion

WMHs are often considered to be a consequence of chronic hypoperfusion. However, while our review of all available published and some unpublished data show that high WMH load is associated with lower CBF, they do not strongly support causation. In cross-sectional studies, low CBF was observed in most of the patients with more WMHs. However the association was damped after removing non-age matched subjects and those with dementia, which suggests that the underlying association is between reduced CBF and age or dementia rather than just WMH. One

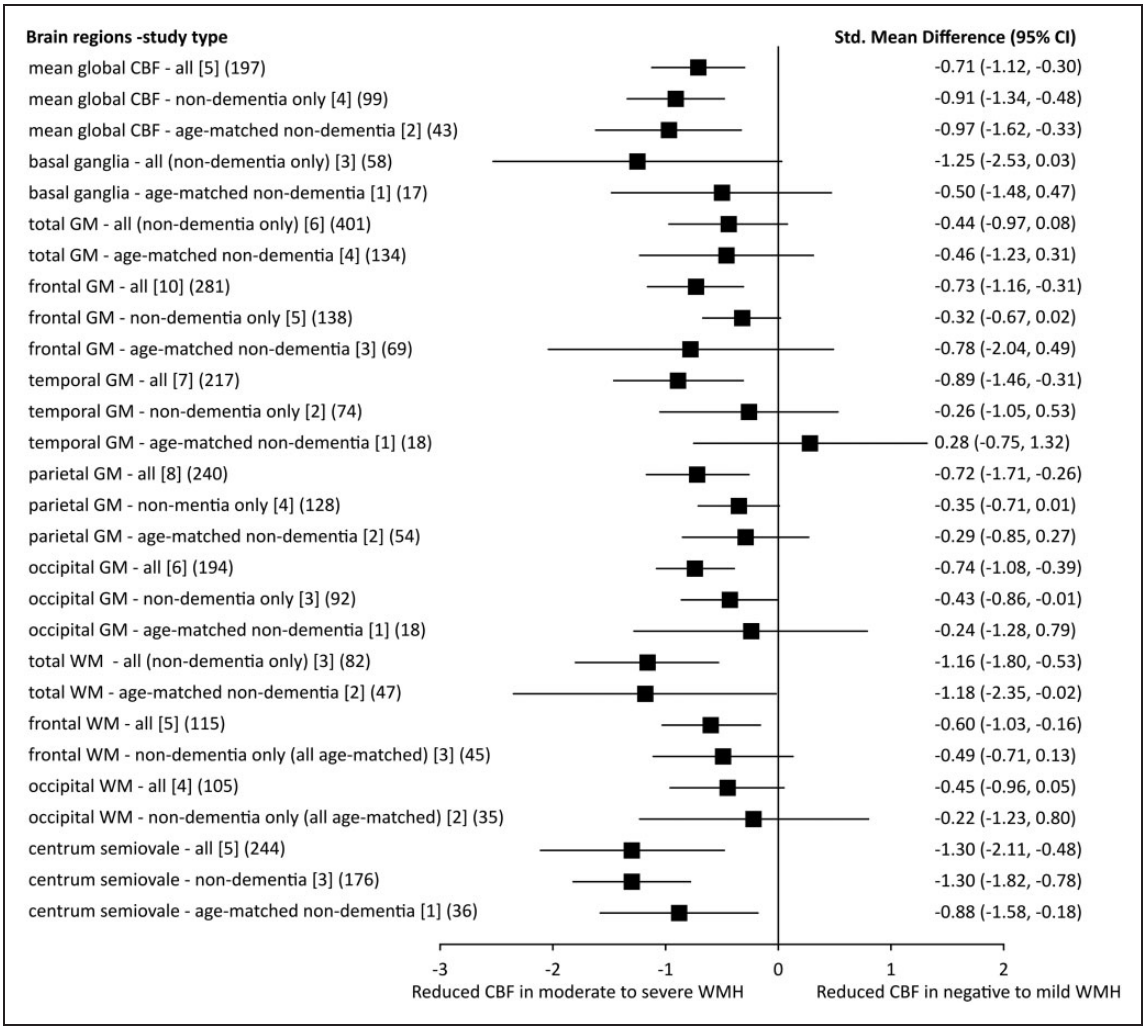

Figure 3. Sensitivity analysis: SMDs of CBF in different brain areas in patients with moderate to severe WMH against those with negative to mild WMH. In each brain area, we showed the SMD of CBF in all studies, after excluding dementia studies and furthermore excluding studies without age-matching [number of studies] (number of participants).
SMD: standard mean difference; CBF: cerebral blood flow; GM: grey matter; WM: white matter; WMH: white matter hyperintensity; CI: confidence interval.

longitudinal study ($n = 575$) also showed a correlation between high baseline WMH volume and decrease in CBF over time, questioning whether a CBF decline causes the tissue loss or vice versa.[10]

The strengths of this systematic review include the use of well-established guidelines for meta-analysis, cautious exclusion of duplicate data, thorough analysis of different study types and sensitivity analysis of clinically important subgroups. Some studies provided more than one comparison but we avoided double-counting the total number of participants. We used every piece of data we could obtain. Studies that recruited subjects with AD, heart failure and depression but compared CBF between patients with and without SVD were also included. Moreover, we included papers in non-English languages, including three papers in Chinese. As most studies measured regional CBF in different brain areas, we carefully chose regions that were mentioned by at least three studies to obtain robust SMDs in meta-analyses.

There are some limitations of the review which in most part reflect the limitation of the literature. First, there are differences between studies in terms of study design and imaging methods which we tried to harmonise to enable comparisons. Longitudinal studies were rare. Data for white matter regions such as centrum semiovale or immediate periventricular white matter were limited or lacking. CBF was obtained by different techniques and varied by technique. However, it is important to note that meta-analysis compares the magnitude of association within one study with that within the others, rather than making direct

Table 2. Results of association-only cross-sectional studies.

Study	Sample size	Statistical method	Results			
			Variables	Coefficients	*P* Values	Adjusted for other variables
Crane et al.[47]	26	Partial correlation (post hoc test)	Mean CBF in cluster (LAP, SC, accumbens, AC and OF) and Fazekas score	Rho = −0.55	0.006	Age, gender
			Mean CBF in cluster (LAI and OF) and Fazekas score	Rho = −0.49	0.015	
			Mean CBF in cluster (LOF and FP) and Fazekas score	Rho = −0.56	0.005	
Alosco et al.[40]	69	Multivariable hierarchical regression	CBFv and WMH volume	$\beta = -0.34$	0.02	Age, gender, premorbid intelligence, depressive symptoms, BMI, hypertension, diabetes, thyroid abnormalities, intracranial volume
Heliopoulos et al.[38]	52	Spearman rank-order correlation	CCA-PSV and WMH score	$r = -0.256$	0.067	No
			CCA-EDV and WMH score	$r = -0.205$	0.144	
			CCA-MFV and WMH score	$r = -0.134$	0.342	
			ICA-PSV and WMH score	$r = -0.135$	0.341	
			ICA-EDV and WMH score	$r = -0.324$	0.019	
			ICA-MFV and WMH score	$r = -0.363$	0.008	
van Es et al.[13]	447	Linear regression model	tCBF and WMH volume	$r = -0.069$	0.148	No
			TCBF and WMH volume	$r = -0.106$	0.044	
Vernooij et al.[14]	892	Linear regression model	WMH volume and tCBF	0.03[a]	NS	Age, gender
			WMH volume and TCBF	0.07[b]	Significant	
Bisschops et al.[42]	282	Linear regression model	WMH score and tCBF	−1.0[c]	0.041	Age, gender, IMT, hypertension
Tzourio et al.[37]	628	Multiple logistic regression	Quartiles of mean CBFv and WMH	OR = 1.4 (1st quartile)	0.22	Age, gender, BMI, hypertension, diabetes, hematocrit, IMT
				OR = 1.6 (2nd quartile)	0.11	
				OR = 2.3 (3rd quartile)	0.006	
Ott et al.[41]	40	Spearman rank-order correlation	Perfusion score and PVWMH score	$r = -0.17$	0.3	No
			Perfusion score and SCWMH score	$r = -0.13$	0.42	
Claus et al.[46]	60	Multiple linear regression model	CBF and grades of severity of WMH	−1.7[d] (Frontal lobe)	NS	Age, gender, type of SPET camera and ventricle-to-brain ratio
				0.4[d] (Parietal lobe)	NS	
				1.2[d] (Temporo-parietal area)	NS	
				−0.4[d] (Temporal lobe)	NS	
Isaka et al.[39]	28	Spearman rank-order correlation	PVWMH score and baseline CBF	$r = -0.364$	NS	No

LAP: left anterior putamen; SC: subcallosal; AC: anterior caudate; OF: orbital frontal; LAI: left anterior insula; LOF: left orbital; FP: frontal pole; CBFv: cerebral blood flow velocity (measured by Ultrasound Doppler); WMH: white matter hyperintensity; BMI: body mass index; CCA: common carotid artery; ICA: internal carotid artery; PSV: peak systolic velocity; EDV: end-diastolic velocity; MFV: mean-flow velocity; tCBF: total cerebral blow flow in ml/min; TCBF: cerebral blood flow per 100 mL brain volume; total brain perfusion: tCBF divided by brain volume; S.D.: standard deviation; lnWMH: natural log transformed white matter hyperintensity volume; IMT: intima media thickness; OR: odds ratio; PVWMH: periventricular white matter hyperintensity; SCWMH: subcortical white matter hyperintensity; NS: not significant; SPET: single-positron emission tomography. [a]Difference in lnWMH volume per S.D. increase in tCBF. [b]Difference in lnWMH volume per S.D. decrease in TCBF. [c]Difference in WMH per 100 ml/min increase in tCBF. [d]Difference in % CBF between persons with no/slight WMH and persons with moderate/severe WMH.

Table 3. Results of longitudinal studies.

		Bernbaum et al.[43]	van der Veen et al.[10]	Kraut et al.[44,a]	ten Dam et al.[12]
Sample size		40	575	74	390
Follow-up time (years)		1.5	3.9	7.7	2.75
CBF	At baseline	16.0 ± 0.2[b] (ml/100 g/min)	52.3 ± 9.8 (ml/100 ml/min)	NA	520.0 ± 88.0 (ml/min)
	At follow-up	NA	NA		504.0 ± 92.0 (ml/min)
WMH (ml)	At baseline	9.21 ± 11.87	2.86 ± 5.44		5.27 ± 9.60
	At follow-up	11.96 ± 13.16	3.74 ± 7.66		7.48 ± 11.70
Association analysis					
bCBF and bWMH volume	Coefficient	NA	NA	NA	TWMH: OR = 1.02 [95%CI: 0.86, 1.21] PVWMH: OR = 1.03 [95%CI: 0.87, 1.21] TWMH: OR = 0.88 [95%CI: 0.74, 1.06]
	P value				NS
bCBF and ΔWMH volume	Coefficient	OR = 0.61 [95%CI: 0.57, 0.65]	PVWMH: B[c] = 0.00 [95%CI: −0.06, 0.05] DWMH: B[c] = 0.04 [95%CI: −0.04, 0.12]		NA
	P value	<0.001	NS		
bWMH volume and ΔCBF	Coefficient	NA	PVWMH: B[d] = −0.61 [95%CI: −1.32, 0.10] DWMH: B[d] = −0.92 [95%CI: −1.56, −0.28]		NA
	P value		PVWMH: NS DWMH: <0.05		
ΔWMH volume and ΔCBF	Coefficient	NA	$r = -0.37$		TWMH: OR = 1.17 [95%CI: 0.84, 1.46] PVWMH: OR = 1.32 [95%CI: 1.06, 1.66] DWMH: OR = 1.00 [95%CI: 0.79, 1.25]
	P value		NS		TWMH: NS PVWMH: 0.015 DWMH: NS
Adjusted for other variables		Age, sex, diabetes, hypertension	Age, sex, follow-up periods, baseline WMHs, cardiovascular risk factors, IMT, carotid stenosis > 50%, non lacunes		Age, sex, baseline atrophy, treatment allocation, baseline CBF

Note: CBF value and WMH volume at both baseline and follow-up, and results of association analysis in longitudinal studies. CBF: cerebral blood flow; WMH: white matter hyperintensity; PVWMH: periventricular white matter hyperintensity; DWMH: deep white matter hyperintensity; TWMH: total white matter hyperintensity; bCBF: baseline CBF; bWMH: baseline white matter hyperintensity; ΔWMH: change of white matter hyperintensity; ΔCBF: change of cerebral blood flow; OR: odds ratio; CI: confidence interval; NA: not available; NS: not significant; IMT: intima media thickness. [a]No numeric data were available from this paper as statistical parametric mapping methods were used as the image analysis tool. [b]CBF of tissues which was normal appearing white matter at baseline but became WMH at follow-up. [c]% change in PVWMH or DWHMs-natural log transformed (% intracranial volume, ICV) per decrease in baseline CBF. [d]Absolute change in CBF per % ICV PVWMH or DWMH (natural log transformed) at baseline.

comparisons of CBF between studies. There are also differences in patient populations: most studies chose patients without neurological symptoms or from community-based populations, whereas three studies recruited patients with acute onset of TIA or minor stroke. Two studies used acute brain MRI as baseline imaging.[36,43] Image analysis methods differed and few if any studies differentiated normal tissue from WMH in the ROIs, thus including more tissue affected by lesions in subjects with high WMH burdens than with few WMH – an obvious confound if measuring CBF. Second, as some studies divided subjects into different severity groups, we converted them into pair-wise comparisons in the form of low WMHs versus high WMHs. Therefore, it is possible that disease groups in the original pair-wise studies might include some patients with mild lesions. Third, the sample sizes of the studies included in meta-analyses were small – the whole analysis of 24 studies included 1161 patients (mean 48/study or 24/group). Only a few studies used age-matched controls. Patients with more severe WMHs were in general significantly older than those who had mild or no WMH, introducing an obvious confound; we addressed this in sensitivity analyses but these were underpowered for meta-regression. In addition, only one study matched for important confounders like vascular risk factors so that sensitivity analysis for risk factors was not possible, and of course hypertension was generally more prevalent in severe WMH groups. Moreover, data for other imaging changes like lacunes or lacunar lesions are lacking.[30]

The meta-analysis demonstrated that CBF measured concurrently was significantly lower in patients with more severe WMH. Cross-sectional studies which only did regression/correlation analyses also showed an association between high WMH burden and low CBF. However, the differences between groups in most brain regions were largely attenuated by excluding dementia and non-age-matched studies, except global mean CBF and CBF in centrum semiovale which remained significant and the point estimate did not move. These results suggest that disease severity and age confound the relationship between WMH and CBF, which was again supported by results from longitudinal studies showing that high burden of WMH predated falling CBF.[10] Additionally, in regression/correlation-only cross-sectional studies where a negative association between WMH and CBF was found, the correlation tends to be significant in more severe patients.[37]

These results indicate that the reduced CBF in patients with WMH might reflect a reduction in the blood supply required by the tissue, due to reduced neuronal activity, or atrophy with fewer cells. As most included studies recorded CBF in cortical grey matter, these associations between reduced CBF and cortical atrophy should not be overlooked. Cortical atrophy is known to occur with the aging process. Results from a large cohort study demonstrated that baseline brain atrophy predicted decline in total CBF over time.[49] There are many imaging studies reporting an association between cortical atrophy and WMH severity.[50] However, there is little information about cortical volume from included studies. Although data for white matter are limited, CBF in frontal and occipital white matter regions changed in the similar way as in grey matter. Results in DWMH and in PVWM differed: a longitudinal study showed that decreasing CBF over time was related to progression of PVWMH rather than to that of DWMH,[12] which is in agreement with a cross-sectional study showing depressed CBF only in NAWM in periventricular regions.[25] The contradictory results from white matter indicate that there might be differential vulnerability for DWMH and PVWMH as these two brain areas are on different sections of the arteriolar tree.[25] However, such a suggestion is not supported by available data – studies indicate that PVWMH and DWMH are on a continuum in terms of location.[51]

The limitation of resting CBF is that it only provides information of a cut-off time point at which CBF might still to be relatively preserved or compensated especially in the early stage of disease.[52] One of the included studies showed a reduced CBF response to hypercapnia in non-demented hypertensive patients with leukoaraiosis while resting CBF was shown to be unaffected.[6] Reduced cerebral vascular reactivity (CVR) represents the dilatory ability of brain vessels, has been suggested as an alternative mechanism of SVD. Risk factors such as hypertension alter the structure of penetrating arterioles by promoting lipohyalinosis and vessel wall thickening, which has led to the suggestion that cerebral arterioles might become stiffer and thus cause a decrease in vasodilatory capacity. Evidences from other studies also suggest that the reduction in CVR might play a critical role in the disease process of SVD.[53] Further studies are required to investigate how blood flow responsiveness (not just resting CBF) varies across different tissues (NAWM, WMHs and grey matter), and how it changes across the course of the disease.

In conclusion, despite large heterogeneities across included studies and the cross-sectional nature of most studies, this systematic review showed that CBF was negatively related to WMH severity. Our results suggest that hypoperfusion in the whole brain and low cortical blood flow is more likely a consequence of WMH than the cause. However, whether WMH is due to focal ischemia in particular white matter tissues and whether development of PVWMHs and DWMHs differs in mechanisms still remain unanswered. This

systematic review emphasises that more data are needed for white matter, especially separate data for NAWM and WMH. Future studies should obtain longitudinal data from white matter as well as grey matter, have larger sample sizes, include appropriate control groups, stratify by and adjust for important cofounders such as age, important risk factors like hypertension, clinical diagnosis (including the type of dementia if relevant), by different features and severities of SVD and by cognitive status. In addition, if studying patients with acute stroke, it would be better to avoid the acute phase after stroke for imaging assessments to avoid effects of the acute stroke interfering with the study of WMH. Moreover, investigation of alternative mechanisms such as impaired CVR and effects of blood–brain barrier changes should be pursued in parallel with CBF measurement to provide new perspectives on treatment for SVD.

Dedication

This paper is dedicated to the memory of Dr Anton J M de Craen who is sorely missed.

Funding

The author(s) disclosed receipt of the following financial support for the research, authorship, and/or publication of this article: Y.S. is funded by China Scholarships Council. M.J.T. is funded by NHS Lothian Research and Development Office. A.J.M.D.C. was and M.A.VB. is an investigator of PROSPER study which was sponsored by an investigator-initiated grant from Bristol Myers-Squibb (Princeton, NJ). J.M.W. was supported by the Scottish Funding Council and Chief Scientist Office through the Scottish Imaging Network A Platform for Scientific Excellence (SINAPSE), the Wellcome Trust funding for SJM and the Medical Research Council through the Centre for Cognitive Ageing and Cognitive Epidemiology (CCACE). The authors hold the data independently of funders.

Acknowledgements

We thank Dr Francesca Chappell and Dr Emily Sena for providing advice on statistical analysis.

Declaration of conflicting interests

The author(s) declared no potential conflicts of interest with respect to the research, authorship, and/or publication of this article.

Authors' contributions

S.D.M. and J.M.W. conceived the idea of the study. Y.S. and J.M.W. designed the study. Y.S. did the data search and extracted data and statistical analyses. A.J.M.D.C. (now deceased), M.A.VB. and M.I.G. provided unpublished data for two longitudinal studies. J.M.W. cross-checked the data. Y.S. drafted the report and designed the tables and figures. J.M.W., M.J.T., S.M., I.M., A.J.M.D.C., M.A.VB. and M.I.G. revised the report. All authors approved the manuscript. We regret to report the sudden death of A.J.M.D.C. who is sorely missed and to whom this paper is dedicated.

Supplementary material

Supplementary material for this paper can be found at http://jcbfm.sagepub.com/content/by/supplementary-data

References

1. Wardlaw JM, Smith EE, Biessels GJ, et al. Neuroimaging standards for research into small vessel disease and its contribution to ageing and neurodegeneration. *Lancet Neurol* 2013; 12: 822–838.
2. Jeerakathil T, Wolf PA, Beiser A, et al. Stroke risk profile predicts white matter hyperintensity volume: The Framingham Study. *Stroke* 2004; 35: 1857–1861.
3. Yata K and Tomimoto H. Chronic cerebral hypoperfusion and dementia. *Neurol Clin Neurosci* 2014; 2: 129–134.
4. Potter GM, Doubal FN, Jackson CA, et al. Lack of association of white matter lesions with ipsilateral carotid artery stenosis. *Cerebrovasc Dis* 2012; 33: 378–384.
5. Ibayashi S, Nagao T, Kuwabara Y, et al. Mechanism for decreased cortical oxygen metabolism in patients with leukoaraiosis: Is disconnection the answer? *J Stroke Cerebrovasc Dis* 2000; 9: 22–26.
6. Kuwabara Y, Ichiya Y, Sasaki M, et al. Cerebral blood flow and vascular response to hypercapnia in hypertensive patients with leukoaraiosis. *Ann Nucl Med* 1996; 10: 293–298.
7. Stroup DF, Berlin JA, Morton SC, et al. Meta-analysis of observational studies in epidemiology: A proposal for reporting. Meta-analysis Of Observational Studies in Epidemiology (MOOSE) group. *JAMA* 2000; 283: 2008–2012.
8. Wardlaw JM, Smith EE, Biessels GJ, et al. Neuroimaging standards for research into small vessel disease and its contribution to ageing and neurodegeneration. *Lancet Neurol* 2013; 12: 822–838.
9. Bailey EL, Smith C, Sudlow CL, et al. Pathology of lacunar ischemic stroke in humans – A systematic review. *Brain Pathol* 2012; 22: 583–591.
10. van der Veen PH, Muller M, Vincken KL, et al. Longitudinal relationship between cerebral small-vessel disease and cerebral blood flow: The second manifestations of arterial disease-magnetic resonance study. *Stroke* 2015; 46: 1233–1238.
11. Bisschops RHC, Van Der Graaf Y, Mali WPTM, et al. High total cerebral blood flow is associated with a decrease of white matter lesions. *J Neurol* 2004; 251: 1481–1485.
12. ten Dam VH, Van Den Heuvel DMJ, De Craen AJM, et al. Decline in total cerebral blood flow is linked with increase in periventricular but not deep white matter hyperintensities. *Radiology* 2007; 243: 198–203.
13. van Es AC, van der Grond J, ten Dam VH, et al. Associations between total cerebral blood flow and age related changes of the brain. *PLoS One* 2010; 5: e9825.

14. Vernooij MW, van der Lugt A, Ikram MA, et al. Total cerebral blood flow and total brain perfusion in the general population: the Rotterdam Scan Study. *J Cereb Blood Flow Metab* 2008; 28: 412–419.
15. Claus JJ, Breteler MM, Hasan D, et al. Vascular risk factors, atherosclerosis, cerebral white matter lesions and cerebral perfusion in a population-based study. *Eur J Nucl Med* 1996; 23: 675–682.
16. Kimura N, Nakama H, Nakamura K, et al. Effect of white matter lesions on brain perfusion in Alzheimer's disease. *Dement Geriatr Cogn Disord* 2012; 34: 256–261.
17. Yamaji S, Ishii K, Sasaki M, et al. Changes in cerebral blood flow and oxygen metabolism related to magnetic resonance imaging white matter hyperintensities in Alzheimer's disease. *J Nucl Med* 1997; 38: 1471–1474.
18. Schuff N, Matsumoto S, Kmiecik J, et al. Cerebral blood flow in ischemic vascular dementia and Alzheimer's disease, measured by arterial spin-labeling magnetic resonance imaging. *Alzheimers Dement* 2009; 5: 454–462.
19. Kawamura J, Meyer JS, Ichijo M, et al. Correlations of leuko-araiosis with cerebral atrophy and perfusion in elderly normal subjects and demented patients. *J Neurol Neurosurg Psychiatry* 1993; 56: 182–187.
20. Kobari M, Meyer JS, Ichijo M, et al. Leukoaraiosis: Correlation of MR and CT findings with blood flow, atrophy, and cognition. *AJNR Am J Neuroradiol* 1990; 11: 273–281.
21. Nezu T, Yokota C, Uehara T, et al. Preserved acetazolamide reactivity in lacunar patients with severe white-matter lesions: 15O-labeled gas and H_2O positron emission tomography studies. *J Cereb Blood Flow Metab* 2012; 32: 844–850.
22. Zheng LS, Xu J and Wang JP. Quantitative evaluation of regional cerebral blood flow in patients with silent Leukoaraiosis [Chinese]. *Chin J Clin Rehabil* 2006; 10: 80–82.
23. Ramli N, Ho KL, Nawawi O, et al. CT perfusion as a useful tool in the evaluation of leuko-araiosis. *Biomed Imag Interv J* 2006; 2: e16.
24. Cui BW, Qi X and Guo HZ. Comparative study on the cerebral hemodynamics changes between Leukoaraiosis and Binswanger disease [Chinese]. *Chin J Clin Rehabil* 2003; 7: 3460–3461.
25. O'Sullivan M, Lythgoe DJ, Pereira AC, et al. Patterns of cerebral blood flow reduction in patients with ischemic leukoaraiosis. *Neurology* 2002; 59: 321–326.
26. Yao H, Yuzuriha T, Fukuda K, et al. Cerebral blood flow in nondemented elderly subjects with extensive deep white matter lesions on magnetic resonance imaging. *J Stroke Cerebrovasc Dis* 2000; 9: 172–175.
27. Markus HS, Lythgoe DJ, Ostegaard L, et al. Reduced cerebral blood flow in white matter in ischaemic leukoaraiosis demonstrated using quantitative exogenous contrast based perfusion MRI. *J Neurol Neurosurg Psychiatry* 2000; 69: 48–53.
28. Oishi M and Mochizuki Y. Differences in regional cerebral blood flow in two types of leuko-araiosis. *J Neurol Sci* 1999; 164: 129–133.
29. Hatazawa J, Shimosegawa E, Satoh T, et al. Subcortical hypoperfusion associated with asymptomatic white matter lesions on magnetic resonance imaging. *Stroke* 1997; 28: 1944–1947.
30. Kobayashi S, Okada K and Yamashita K. Incidence of silent lacunar lesion in normal adults and its relation to cerebral blood flow and risk factors. *Stroke* 1991; 22: 1379–1383.
31. Fazekas F, Niederkorn K, Schmidt R, et al. White matter signal abnormalities in normal individuals: Correlation with carotid ultrasonography, cerebral blood flow measurements, and cerebrovascular risk factors. *Stroke* 1988; 19: 1285–1288.
32. Kimura M, Shimoda K, Mizumura S, et al. Regional cerebral blood flow in vascular depression assessed by 123I-IMP SPECT. *J Nippon Med Sch* 2003; 70: 321–326.
33. Fu J, Tang J, Han J, et al. The reduction of regional cerebral blood flow in normal-appearing white matter is associated with the severity of white matter lesions in elderly: A Xeon-CT study. *PLoS ONE* 2014; 9: e112832.
34. De Bastos-Leite AJ, Kuijer JPA, Rombouts SARB, et al. Cerebral blood flow by using pulsed arterial spin-labeling in elderly subjects with white matter hyperintensities. *AJNR Am J Neuroradiol* 2008; 29: 1296–1301.
35. Miyazawa N, Satoh T, Hashizume K, et al. Xenon contrast CT-CBF measurements in high-intensity foci on T2-weighted MR images in centrum semiovale of asymptomatic individuals. *Stroke* 1997; 28: 984–987.
36. Huynh TJ, Murphy B, Pettersen JA, et al. CT perfusion quantification of small-vessel ischemic severity. *AJNR Am J Neuroradiol* 2008; 29: 1831–1836.
37. Tzourio C, Levy C, Dufouil C, et al. Low cerebral blood flow velocity and risk of white matter hyperintensities. *Ann Neurol* 2001; 49: 411–414.
38. Heliopoulos I, Artemis D, Vadikolias K, et al. Association of ultrasonographic parameters with subclinical white-matter hyperintensities in hypertensive patients. *Cardiovasc Psychiatry Neurol* 2012; 2012: 616572.
39. Isaka Y, Okamoto M, Ashida K, et al. Decreased cerebrovascular dilatory capacity in subjects with asymptomatic periventricular hyperintensities. *Stroke* 1994; 25: 375–381.
40. Alosco ML, Brickman AM, Spitznagel MB, et al. Cerebral perfusion is associated with white matter hyperintensities in older adults with heart failure. *Congest Heart Fail* 2013; 19: E29–E34.
41. Ott BR, Faberman RS, Noto RB, et al. A SPECT imaging study of MRI white matter hyperintensity in patients with degenerative dementia. *Dement Geriatr Cogn Disord* 1997; 8: 348–354.
42. Bisschops RH, van der Graaf Y, Mali WP, et al. High total cerebral blood flow is associated with a decrease of white matter lesions. *J Neurol* 2004; 251: 1481–1485.
43. Bernbaum M, Menon BK, Fick G, et al. Reduced blood flow in normal white matter predicts development of leukoaraiosis. *J Cereb Blood Flow Metab* 2015; 35: 1610–1615.
44. Kraut MA, Beason-Held LL, Elkins WD, et al. The impact of magnetic resonance imaging-detected white matter hyperintensities on longitudinal changes in

regional cerebral blood flow. *J Cereb Blood Flow Metab* 2008; 28: 190–197.
45. Wagner M, Helfrich M, Volz S, et al. Quantitative T2, T2*, and T2′ MR imaging in patients with ischemic leukoaraiosis might detect microstructural changes and cortical hypoxia. *Neuroradiology* 2015; 57: 1023–1030.
46. Claus JJ, Breteler MMB, Hasan D, et al. Vascular risk factors, atherosclerosis, cerebral white matter lesions and cerebral perfusion in a population-based study. *Eur J Nucl Med* 1996; 23: 675–682.
47. Crane DE, Black SE, Ganda A, et al. Grey matter blood flow and volume are reduced in association with white matter hyperintensity lesion burden: A cross-sectional MRI study. *Front Aging Neurosci* 2015; 7: 131.
48. Vernooij MW, Van Der Lugt A, Ikram MA, et al. Total cerebral blood flow and total brain perfusion in the general population: The Rotterdam Scan Study. *J Cereb Blood Flow Metab* 2008; 28: 412–419.
49. Zonneveld HI, Loehrer EA, Hofman A, et al. The bidirectional association between reduced cerebral blood flow and brain atrophy in the general population. *J Cereb Blood Flow Metab* 2015; 35: 1882–1887.
50. Schmidt R, Ropele S, Enzinger C, et al. White matter lesion progression, brain atrophy, and cognitive decline: The Austrian Stroke Prevention Study. *Ann Neurol* 2005; 58: 610–616.
51. Ryu WS, Woo SH, Schellingerhout D, et al. Grading and interpretation of white matter hyperintensities using statistical maps. *Stroke* 2014; 45: 3567–3575.
52. Østergaard L, Engedal TS, Moreton F, et al. Cerebral small vessel disease: Capillary pathways to stroke and cognitive decline. *J Cereb Blood Flow Metab* 2016; 2: 302–325.
53. Liem MK, Lesnik Oberstein SA, Haan J, et al. Cerebrovascular reactivity is a main determinant of white matter hyperintensity progression in CADASIL. *AJNR Am J Neuroradiol* 2009; 30: 1244–1247.

SVN Stroke and Vascular Neurology

Update on cerebral small vessel disease: a dynamic whole-brain disease

Yulu Shi,[1,2] Joanna M Wardlaw[1]

To cite: Shi Y, Wardlaw JM. Update on cerebral small vessel disease: a dynamic whole-brain disease. *Stroke and Vascular Neurology* 2016;**1**:e000035. doi:10.1136/svn-2016-000035

Received 26 July 2016
Revised 5 September 2016
Accepted 7 September 2016

[1]Centre for Clinical Brain Sciences, University of Edinburgh, Edinburgh, UK
[2]Department of Neurology, Zhongnan Hospital, Wuhan University, Wuhan, China

Correspondence to
Professor Joanna M Wardlaw;
Joanna.Wardlaw@ed.ac.uk

ABSTRACT

Cerebral small vessel disease (CSVD) is a very common neurological disease in older people. It causes stroke and dementia, mood disturbance and gait problems. Since it is difficult to visualise CSVD pathologies in vivo, the diagnosis of CSVD has relied on imaging findings including white matter hyperintensities, lacunar ischaemic stroke, lacunes, microbleeds, visible perivascular spaces and many haemorrhagic strokes. However, variations in the use of definition and terms of these features have probably caused confusion and difficulties in interpreting results of previous studies. A standardised use of terms should be encouraged in CSVD research. These CSVD features have long been regarded as different lesions, but emerging evidence has indicated that they might share some common intrinsic microvascular pathologies and therefore, owing to its diffuse nature, CSVD should be regarded as a 'whole-brain disease'. Single antiplatelet (for acute lacunar ischaemic stroke) and management of traditional risk factors still remain the most important therapeutic and preventive approach, due to limited understanding of pathophysiology in CSVD. Increasing evidence suggests that new studies should consider drugs that target endothelium and blood–brain barrier to prevent and treat CSVD. Epidemiology of CSVD might differ in Asian compared with Western populations (where most results and guidelines about CSVD and stroke originate), but more community-based data and clear stratification of stroke types are required to address this.

INTRODUCTION

The term 'cerebral small vessel disease (CSVD)' refers to a syndrome of clinical and imaging findings that are thought to result from pathologies in perforating cerebral arterioles, capillaries and venules. CSVD causes up to 45% of dementia, and accounts for about 20% of all stroke worldwide, 25% of ischaemic (or lacunar strokes), of whom about 20% are left disabled.[1] Cognitive impairment, depression and gait problems are also frequently seen in patients with CSVD. The prevalence of lacunar stroke may be higher in patients in China where recent studies have suggested that lacunar infarction accounts for 38–46% of ischaemic stroke.[2 3]

Generally, including in this review, CSVD is used to describe a series of imaging changes in the white matter and subcortical grey matter, including recent small subcortical infarct, lacunes, white matter hyperintensities (WMHs), prominent perivascular spaces (PVS), cerebral microbleeds (CMBs) and atrophy.[4] Usually, recent small subcortical infarcts cause acute stroke symptoms, whereas other CSVD lesions are clinically more insidious and thus referred to as 'silent' lesions. However, the definitions and terms of these lesions have varied greatly among studies. For example, a recent review identified 159 different names for recent small subcortical infarcts, but these names like 'lacunar infarct' were also frequently used to describe lacunes[4 5] that were not necessarily related to symptoms and might have been due to haemorrhage. The substantial variation in the use of these terms has probably contributed to confusion and difficulties in interpreting previous research. Therefore, in 2013, an expert workgroup on CSVD proposed a list of standard terms to help avoid confusion and suggests that CSVD researchers should be encouraged to apply these terms in future studies.[4] We will also use these terms in this review.

The different features of CSVD have long been regarded as different types of tissue changes. However, recent studies show that these features are correlated, are more likely to share common diffuse intrinsic small vessel pathologies, and are probably also more 'dynamic' than previously thought. Advances in imaging techniques have brought new insights into mechanisms of CSVD. In this review, we will summarise findings in recent clinical studies on CSVD, discuss CSVD mechanisms and explore emerging prevention and treatment options.

Clinical lacunar stroke

A lacunar clinical syndrome could be due to either ischaemia or a small haemorrhage.[6] Many haemorrhagic strokes in older people are also due to CSVD pathology.[1] In this

review, we will focus mainly on ischaemic CSVD. Lacunar ischaemic stroke is defined as a stroke that is attributable to a recent small infarct <1.5 (or some say 2) cm diameter in the white matter, basal ganglia, pons or brainstem, and is consistent with a lacunar clinical syndrome.[7] It is commonly attributed to an abnormality in a single small deep perforating (or lenticulostriate) artery. On MRI, an acute lacunar infarct is shown as hyperintense on diffusion-weighted imaging (DWI), hypointense on an apparent diffusion coefficient map, hyperintense on T2-weighted and fluid-attenuated inversion recovery (FLAIR), hypointense on T1 and hypoattenuated on CT (figure 1). It can be rounded, ovoid or tubular.[4] Generally, the Oxfordshire Community Stroke Project (OCSP) classification, which uses only clinical features to diagnose the stroke subtype, can predict correctly the size and location of a recent brain infarct on imaging in 75–80% of patients with stroke.[8] However, up to 20% of acute lacunar infarcts can present with cortical symptoms, and conversely cortical infarcts can present with lacunar syndromes.[9] One explanation is that lacunar infarcts closer to the cortex are more likely to cause cortical symptoms.[9] Therefore, in studies where stroke diagnosis relied mainly on the clinical presentations, this 'mismatch' may have added 'noise'. Thus, in epidemiology, mechanistic studies or clinical trials, it is important to verify stroke lesions using sensitive imaging wherever possible.

However, even with sensitive imaging like DWI, about 30% of patients with clinically definite stroke did not show any recent ischaemic change on MRI;[10] when followed up for a year, the DWI-negative patients had just as much recurrent stroke, dependency and cognitive impairment as the DWI-positive patients. Therefore, negative DWI/MRI cannot exclude stroke diagnosis. Rapid access to scanning after stroke onset can increase the chance of positive findings.[11] It is also noteworthy that DWI-positive lesions can be clinically 'silent', for example, (1) as a second silent acute infarct in patients presenting with stroke due to another acute symptomatic infarct, or (2) in patients with acute haemorrhagic stroke, and (3) in patients with severe WMHs who did not have any overt stroke symptoms.[12]

In some clinical stroke classifications such as the Trial of Org 10172 in Acute Stroke Treatment (TOAST) or the ASCO (A: atherosclerosis; S: small-vessel disease; C: cardiac pathology; O: other causes), another term 'small vessel/artery disease' rather than 'lacunar stroke' is used to represent a stroke that is supposed to be due to a small artery occlusion. However, these classifications use risk factors to decide the stroke subtype, not just the clinical presentation, so as to distinguish 'small vessel/artery disease' from strokes caused by large artery atherosclerosis, cardiac emboli or other unknown reasons. However, a small embolus, or atheroma in the middle cerebral artery (MCA) or perforating arterioles can all

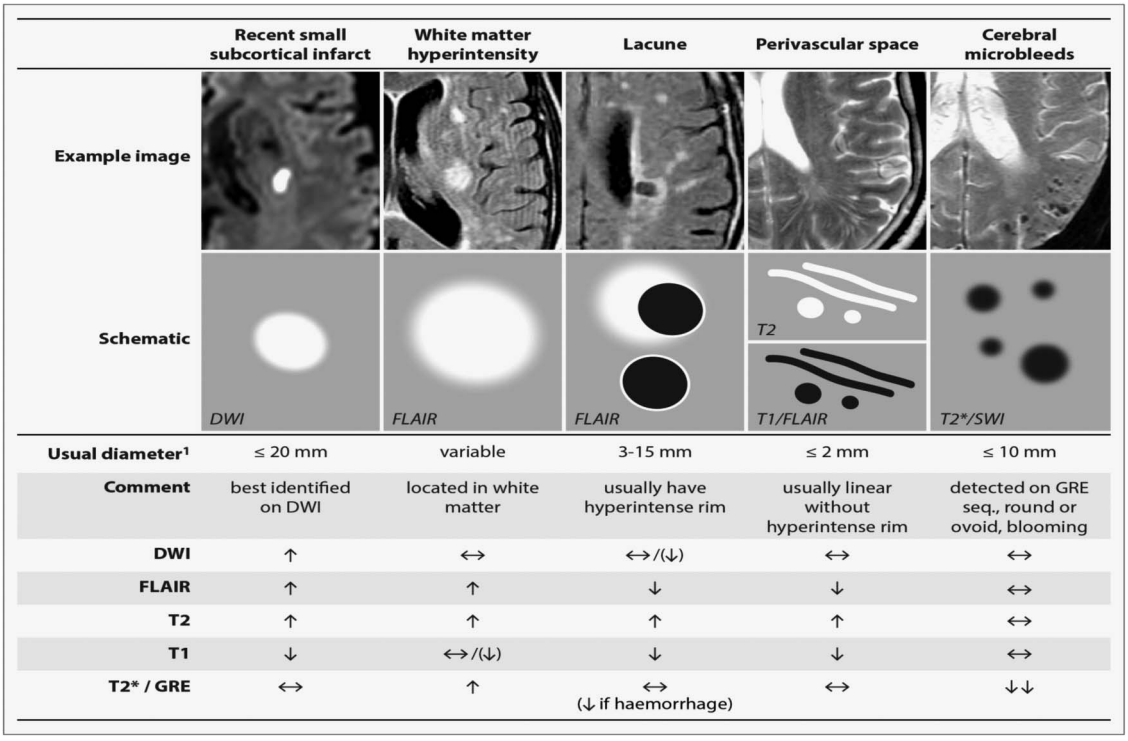

	Recent small subcortical infarct	White matter hyperintensity	Lacune	Perivascular space	Cerebral microbleeds
Usual diameter[1]	≤ 20 mm	variable	3-15 mm	≤ 2 mm	≤ 10 mm
Comment	best identified on DWI	located in white matter	usually have hyperintense rim	usually linear without hyperintense rim	detected on GRE seq., round or ovoid, blooming
DWI	↑	↔	↔/(↓)	↔	↔
FLAIR	↑	↑	↓	↓	↔
T2	↑	↑	↑	↑	↔
T1	↓	↔/(↓)	↓	↓	↔
T2* / GRE	↔	↑	↔ (↓ if haemorrhage)	↔	↓↓

Figure 1 STRIVE, STandards for Reporting and Imaging of Small Vessel Disease: example findings (upper), schematic representation (middle) and a summary of imaging characteristics (lower) of MRI features for changes related to small vessel disease.[4] DWI, diffusion-weighted imaging; FLAIR, fluid-attenuated inversion recovery; SWI, susceptibility-weighted imaging; GRE, gradient-recalled echo.

block the perforating arteriole, and any of these can cause a lacunar ischaemic stroke (see figure 2). Therefore, it might be better to focus on the clinical presentation to assign the stroke syndrome and separately focus on the risk factors for patient management.

Risk factors and causes of lacunar infarcts

Four possible main aetiologies for lacunar ischaemic stroke have been proposed (figure 2): atheroma of parent arteries (usually MCA) or perforating arterioles, embolism from the heart or carotid arteries, and intrinsic small vessel disease (lipohyalinosis or fibrinoid necrosis). Atheroma in MCA appears to cause <20% of lacunar ischaemic stroke. In the Warfarin Aspirin Symptomatic Intracranial Disease (WASID) trial, only 11% (38/347) of all patients with stroke were lacunar type,[13] which is surprising if MCA stenosis is supposed to be a common cause of lacunar stroke. A recent study also did not find any association between lacunar stroke and MCA stenosis.[14] A systematic review of Asian studies showed that parent artery atherosclerosis accounted for 20% of single lacunar infarcts in anterior circulation territory; however, these hospital-based studies were rather small (n=71–118) and some were even retrospective.[15] Larger and tubular lacunar infarcts might be more likely to be caused by proximal artery diseases.[16] However, the results of both our study and the Secondary Prevention of Small Subcortical Stokes Trial (SPS3) suggest that it is not possible to identify the cause of a particular recent lacunar ischaemic stroke based on its size, shape or location.[17 18]

Evidence for embolism as a common cause for lacunar ischaemic stroke is limited. Presence of cardioembolic sources was found significantly less often in lacunar than in non-lacunar ischaemic stroke.[19 20] Few if any associations were found between ipsilateral carotid stenosis and lacunar ischaemic stroke or other features of CSVD.[21 22] In primate models, <6% of emboli injected into carotid arteries entered the lenticulostriate arteries, while the majority entered the cortical arteries.[23] Lacunar ischaemic strokes in the basal ganglia were marginally more often associated with embolism than those in the centrum semiovale (11% vs 3%, respectively), but the overall rate of known embolic sources in symptomatic lacunar ischaemic stroke was very low (11%).[18]

Intrinsic small vessel pathologies remain the most common cause of lacunar ischaemic stroke, although the underlying mechanism is unclear. Fisher attributed the lipohyalinosis in small arteries to hypertension. However, the diagnosis and treatment of hypertension were less good when Fisher was working in the 1950s and 1960s and he may have seen some particularly severe cases of hypertension. Now, epidemiology data show that hypertension is equally common in non-lacunar as in lacunar ischaemic stroke;[19] and many patients with lacunar stroke are normotensive. Similarly, other traditional risk factors like diabetes mellitus,

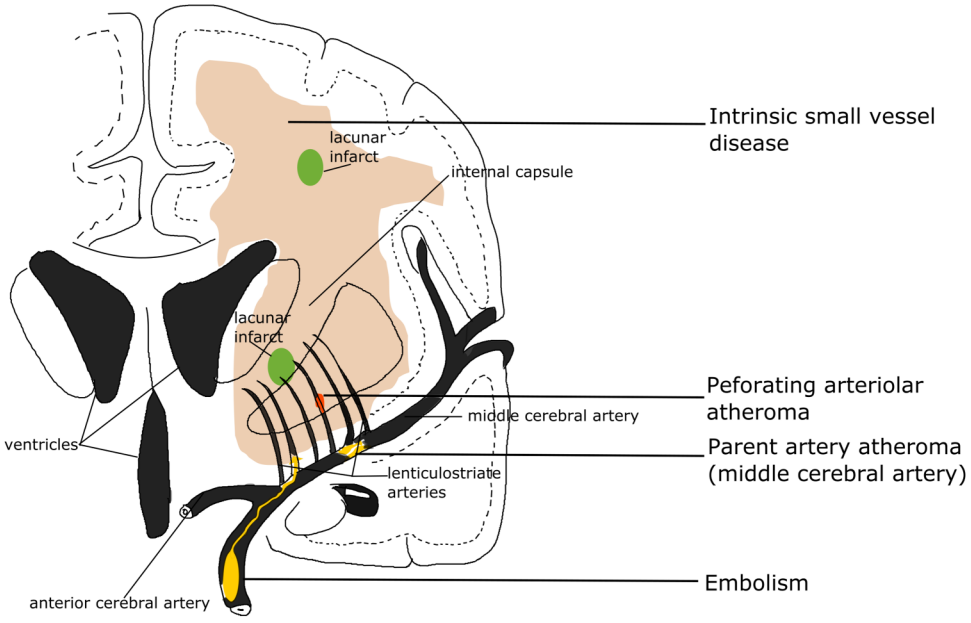

Figure 2 Four possible mechanisms that cause a lacunar infarct (from bottom to top): (A) an embolus from the big arteries or cardiac sources goes up to MCA and ends up entering and occluding lenticulostriate arteries, resulting in a lacunar lesion in basal ganglia; (B) if the atheroma in the parent artery (ie, MCA) is positioned at the opening of its penetrating branches, it could lead to an acute occlusion of one or several penetrating arteries, hence causing a lacunar infarct; (C) a lacunar infarct could also be due to atheroma in the perforating artery if an acute occlusion happens; (D) intrinsic small vessel disease may lead to diffused disrupted blood–brain barrier. If this happens at an arteriolar level, plasma fluid components would enter and deposit in the vessel wall, resulting in narrowing of the arteriolar lumen, vessel wall thickening and eventually a secondary luminal occlusion and traditional infarct. MCA, middle cerebral arteries.

hypercholesterolaemia and smoking were as frequent in lacunar stroke as in other ischaemic strokes.[24] Risk factor profiles of lacunar stroke seemed different in China, but it might be too early to say so. The Beijing stroke registry (n=1184) showed a higher proportion of hypertension in lacunar (acute stroke symptoms+subcortical lesion <2 cm diameter on acute CT/MRI) than in non-lacunar stroke after adjusting for age and gender.[3] Some other studies had similar findings, but the stroke diagnosis varied: in some studies, the differentiation between lacunar stroke and 'large artery atherosclerosis' stroke relied only on lesion size, and clinical classification included risk factors.[25 26] Additionally, most studies were hospital-based. Hence, population scale data on lacunar stroke are lacking. It is important to distinguish lacunar stroke from other subtypes because of the mechanism, hence prevention and treatment might differ. More data and careful separation of lacunar stroke from other subtypes are required in future studies.

Clinically 'Silent' CSVD

White matter hyperintensities

WMH of presumed vascular origin are very common in older individuals and regarded as typical signs of CSVD. Symptoms of WMH develop insidiously, such as cognitive impairment, dementia and depression,[1] but it almost triples the risk of stroke, doubles the risk of dementia and increases the risk of death.[27]

WMHs are usually symmetrically and bilaterally distributed in the white matter including the pons and brain stem, and also occur in deep grey matter. They appear hyperintense to the normal brain on T2 or FLAIR MRI (figure 1), and can be patchy or confluent depending on their stage in development and severity.

Owing to limited pathology studies, the underlying pathology of WMH remains imprecise. Demyelination, loss of oligodendrocytes and axonal damage were often reported. Diffusion tensor imaging studies provided indirect evidence for axonal damage and impaired white matter integrity in WMH.[28] Indeed, recent evidence indicates that WMHs are rather heterogeneous, perhaps reflecting different disease stages. Reduced density of glia and vacuolation were observed in severe WMH suggesting end stage disease.[29] Autopsy MRI studies also found oedema that suggests leakage of fluid from an impaired blood–brain barrier (BBB) in and around WMH.[30 31] Although these 'white' lesions have until now been treated as if they were all the same, different degrees of 'whiteness' might indicate different 'stages of formation'—some very white WMHs are probably at the end stage of disease and irreversible once demyelination or axonal damage has happened; some perhaps less white lesions might be reversible if they are mainly interstitial fluid (ISF) imbalances before permanent tissue damage has occurred. These observations remain to be confirmed in larger studies. These microstructural changes happen in WMH, and are also present in normal appearing white matter (NAWM).[32 33] The white matter integrity in NAWM declines with increasing closeness to the edge of WMH[32] and with more severe WMH.[34]

Multiple mechanisms underlying WMH such as incomplete infarct, chronic hypoperfusion and venous collagenous have been proposed, but evidence for each is limited. In a pathology study (n=15), no incomplete infarct was found in WMH.[29] Though many cross-sectional studies have found low cerebral blood flow (CBF) to be associated with higher WMH burden, the causality between low CBF and WMH is unclear.[35] A longitudinal study (n=575) showed that more severe baseline WMH predated CBF decline over time rather than falling CBF predating WMH progression.[36] In a post-mortem study, some non-inflammatory, periventricular venulopathy was observed in periventricular WMH, suggesting that venous collagenosis might cause tissue damage by vasogenic oedema and impede ISF circulation.[31] However, this theory remains to be confirmed in in vivo studies. Impaired BBB was noted in WMH areas in autopsies,[29 30] which was corroborated by studies using cerebrospinal fluid (CSF)/plasma albumin ratio[37] and MRI.[38–41] It is hypothesised that the disrupted BBB would result in leakage of fluid, plasma components and cells and eventually lead to perivascular inflammation, demyelination and gliosis. Indeed, the formation of WMH is likely to be multifactorial. Hypoperfusion, venous pathologies and BBB impairment might all play critical roles in WMH initiation or progression and interact with each other, but which one is the key initial factor remains unknown.

Lacunes

The term 'lacune' was used by Fisher to describe a small fluid cavity in the brain which he thought was a healed lacunar infarct. Therefore, in CSVD research, it is very common that terms like 'lacunar infarction', 'lacunar stroke' and 'silent brain infarct' were used to refer to the CSF-filled cavities on brain MRI or autopsy.[42] In fact, lacunes are not always 'ischaemic'. They can also be the residual lesion of a small haemorrhage[43] (figure 3). Also, it is common that many non-cavitated lacunar ischaemic strokes were not counted as 'lacunar infarcts'. Therefore, in order to avoid more confusion, the term 'lacune of presumed vascular origin' was proposed to replace 'lacune' and the term 'lacunar infarct' should NOT be used to describe 'lacunes' any more.

Lacunes of presumed vascular origin are round or ovoid, subcortical, fluid-filled cavities with a diameter of 3–15 mm. These can occur without any prior symptoms, but can also result from a previous acute small subcortical infarct or haemorrhage[4] (figure 1). PVS could also mimic lacunes when they are more than 3 mm in diameter.[44] Large PVS might have also been miscounted as lacunes in many studies.[42] Lacunes usually present as a hypointense 'hole' on FLAIR surrounded by a hyperintense rim which can help its differentiation from PVS. However, the rim can be absent in some cases and PVS

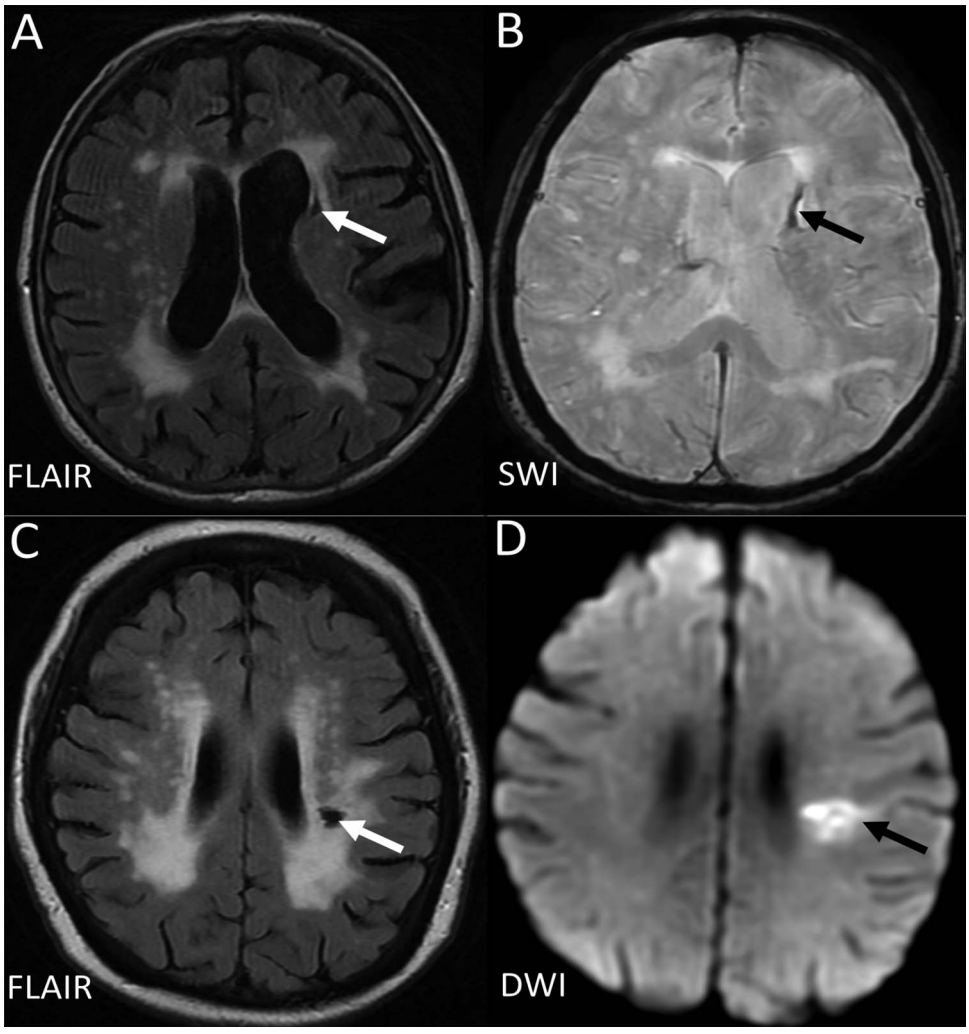

Figure 3 Example of MRIs of a lacune from a haemorrhagic source (A,B), and from a lacunar infarct (C, D). D (the DWI) is from the acute presentation (i.e. within a few days of the stroke), and C (the FlAIR) is weeks to months later when the lesion has cavitated. DWI, diffusion-weighted imaging; FLAIR, fluid-attenuated inversion recovery; SWI, susceptibility-weighted imaging.

within extensive WMH areas may appear as if surrounded by hyperintensities, so the insistence on a rim to differentiate lacunes from PVS is not helpful in practice. Nonetheless, it is important to distinguish between lacunes and PVS if possible, on size at least, because they represent different pathologies as well as differ in clinical associations and implications.

Although many lacunes might have lacked acute symptoms, when present in larger numbers they are associated with dementia, cognitive impairment, gait disturbance and increased risk of stroke.[5 45 46] In the general elderly population, the prevalence of lacunes ranges from 8% to 28% (mean age=50–75 years).[5] A systematic review suggests that silent brain infarcts (another term sometimes used for lacune) are more prevalent in the Asian than in the non-Asian population.[47] However, it is noteworthy that most of these Asian studies were hospital-based, whereas all non-Asian studies were community-based; therefore, more relevant comparisons are needed to determine if the prevalence of lacunes and other CSVD features does differ between world regions and ethnic groups.

Perivascular spaces

PVS are the extension of subarachnoid spaces that surround cerebral microvessels.[48] They are fluid-filled spaces that follow the course of a vessel through the brain parenchyma.[48] PVS are usually microscopic and not detected on CT or conventional MRIs. When enlarged, PVS are commonly seen as hyperintense on T2 MRI, either punctuate with a diameter <3 mm if imaged perpendicular to the course of the vessel, or linear if imaged parallel to the course of the vessel[49] (figure 1). PVS are most frequent in the inferior parts of the basal ganglia and centrum semiovale but can also occur in the brainstem. Though 3 mm has generally been considered as the cut-off diameter for distinguishing PVS from lacunes,[44] occasional PVS could be larger and even cause a mass effect.[4] PVS usually do not have a hyperintense rim on T2-weighted or FLAIR unless passing through a WMH area, which can help the discrimination between PVS and lacunes.

Whether PVS should be regarded as 'lesions' is still controversial, as their clinical significance remains

unclear. Although a few PVS can be normal,[50] numbers of PVS increased with advancing age and other features of CSVD.[51–54] In some studies, more PVS were associated with increased risk of dementia or worse cognitive function or hypertension.[44 55 56] The mechanisms underlying enlarged PVS are not well understood. In normal ageing and other neurological diseases like multiple sclerosis, PVS are associated with inflammatory markers.[57] In CSVD, it might be a sign of impaired BBB.[39] There is also a hypothesis that visible PVS are associated with a blockage of drainage of ISF,[58] which might be attributed to increased vessel stiffness, as arterial pulsatility is thought to be a key driver of ISF drainage.[59] They may also be a key conduit for drainage of brain interstitial metabolic products that occurs during sleep.[60]

Cerebral microbleeds

CMBs are regarded as small round and homogeneous foci of hypointensity on T2-weighted (gradient echo) MRI and susceptibility-weighted imaging (figure 1). In the very few studies of radiological–pathological correlation, perivascular hemosiderin-laden macrophages were found to underlie most of the CMBs shown on MRI. Other possible pathologies include old haematomas, intact erythrocytes and, very rarely, vascular pseudocalcification, microaneurysm and distended dissected vessels.[61] Lipofibrohyalinosis and amyloid angiopathy are the most common vascular findings in relation to CMB. These two vasculopathies are thought to have different patterns of CMB distribution: CMBs in the basal ganglia, thalamus, brainstem and cerebellum are typically attributed to lipofibrohyalinosis, whereas amyloid angiopathy is more associated with lobar CMBs.[62] However, some studies suggest that there may be more overlap and larger studies are awaited to confirm the specificity of CMB distribution for particular pathologies.

Most CMBs are asymptomatic; they can be found in healthy adults but are more often a marker of vascular risk factor exposure or amyloid deposition.[63] In addition to its potential association with stroke, CMBs also contribute to cognitive impairment and dementia, and to transient neurological deficits.[64] The prevalence of CMBs detected in community-dwelling participants in the Rotterdam Scan study (n=3979, mean age=60.3 years) and AGES-Reykjavik study (n=1962, mean age=76 years) was 11.1–15.3%[65 66] and increased with age.[66] In patients with ischaemic stroke and non-traumatic intracerebral haemorrhage, the prevalence of CMBs could be as high as 33.5–67.5%.[63] It seems that CMBs may be more common in the Asian than in the non-Asian population. However, the differences might be due to a higher proportion of hypertensive patients recruited in these Asian studies or more hospital-based than community studies.

It is unclear whether CMBs increase the risk of haemorrhage in patients receiving antiplatelet or anticoagulant or thrombolytic therapy and further discussion is outside the ischaemic focus of this review. We refer the reader to recent reviews on this topic[63 67] and note that randomised trials are needed to answer these questions.

Risk factors and causes of 'silent' CSVD

Increasing age is significantly associated with CSVD features; thus, age has to be controlled for while interpreting relevant studies. Modifiable risk factors including hypertension, hypercholesterolaemia, smoking and diabetes mellitus are also thought to be key risk factors in the pathogenesis of CSVD, particularly hypertension. However, the relationship between these risk factors and CSVD is complex. Lipohyalinosis, the typical vascular changes of CSVD, has long been thought to result from hypertension. The theory is supported by clinical evidence showing that hypertension is more prevalent in patients with WMH and that higher blood pressure was associated with more severe WMH.[68] A recent study shows that vascular risk factors and large artery disease explained only 2% of the variance in WMH, leaving 98% of the variance unexplained, providing further evidence that WMHs are mostly non-atheromatous.[69] This finding may give a clue as to why risk factor modifications so far have very limited effects on preventing WMH progression. Other important risk factors for CSVD include other high-risk lifestyles: lack of exercise, poor diet and smoking. High salt intake is associated with more severe WMH through causing high blood pressure, as well as by having direct effects on the endothelium.[70] Current smoking is also an independent predictor of WMH progression[71] and is associated with a high burden of combined CSVD features.[72] Lack of exercise is a risk factor for having more WMH in later life, although it is not clear if active exercise programmes reduce WMH risk.[73]

CSVD as a 'whole-brain disease'

Common small vessel pathologies and BBB impairment were found in clinically evident and covert CSVD features, suggesting that CSVD should be regarded as a whole-brain disease rather than be treated separately as individual conditions. Small penetrating vessels and the endothelium, which forms the BBB, are diffuse in the brain. Various studies also demonstrate that all these CSVD features were associated with each other: patients with small vessel stroke (TOAST classification) or lacunar stroke (OCSP classification) had more WMH than those who had other stroke subtypes;[74 75] more than 90% of incident lacunes appeared at the edge of WMH or had a partial overlap with WMH in 365 patients with Cerebral Autosomal-Dominant Arteriopathy with Subcortical Infarcts and Leukoencephalopathy (CADASIL);[76] visible PVS were frequently seen in patients with lacunar stroke, WMH and lacunes; CMBs were also associated with WMH and lacunar stroke.[63] When counting the presence of any CSVD as the total CSVD score, patients with lacunar stroke had a

significantly higher CSVD burden than those with cortical stroke.[72]

Why do some CSVD lesions cause stroke while others are 'silent'? One explanation is the locations of lesions. A study using probability mapping shows that lesions presenting with stroke were predominantly located in or near the primary motor and sensory tracts, whereas silent lesions were mostly in the basal ganglia and centrum semiovale away from these main tracts.[77] Another explanation could be the levels of vessels where the vascular pathologies happened. In general, disrupted BBB would enable plasma fluid components and blood cells to enter the vessel wall, leading to disintegration of the vessel wall and fibrin deposition. If this happens at arterioles where there is smooth muscle, the components deposited in the arteriolar wall could result in dilation and narrowing of the vessel lumen and vessel wall thickening, which would eventually precipitate inflammation, platelet adhesion, luminal occlusion and thus traditional infarct. However, at the capillary level where there is no smooth muscle between the epithelium and brain tissue, the leaky BBB would cause direct damage in the tissue, such as oedema and demyelination in white matter tracts. Further studies to assess changes over time in lesion development and symptoms are required to find out the reasons.

CSVD as a 'dynamic disease'

There is increasing evidence showing that CSVD is more dynamic than originally thought. Lesions progress over time and the long-term outcome and impact on brain damage vary. Cavitation is not the only fate of acute lacunar ischaemic stroke.[78] An acute lacunar ischaemic stroke can also disappear or resemble a WMH (figure 4). In a prospective study (n=90), definite cavitation (ie, that looked like a lacune) was only present in 20% of patients, and was marginally associated with increasing time from stroke onset to follow-up scans. A large proportion of lacunar lesions remained looking like WMH. Thus, only calculating cavitated lacunes could lead to a large underestimation of lacunar ischaemic stroke burden. Similarly, WMH burden is likely to be overestimated without previous scans of index stroke lesions.

The evolution of WMH also varies. The single strongest predictor of WMH progression is high baseline WMH,[79 80] with little progression in punctate WMH but rapid progression in confluent WMHs.[81] The Austrian Stroke Prevention Study, a community-based study,

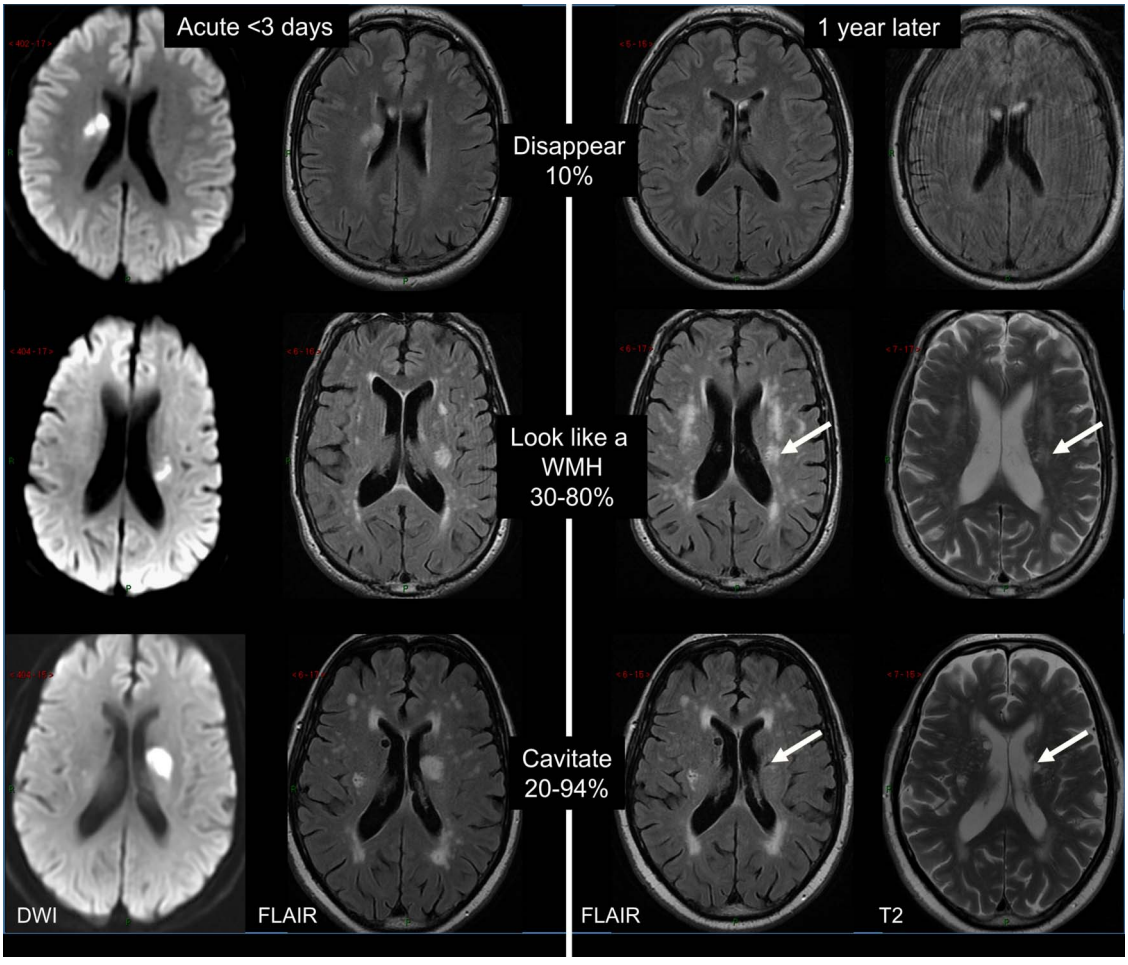

Figure 4 Long-term appearances of lacunar infarcts (arrows: old stroke lesion on the follow-up scans). DWI, diffusion-weighted imaging; FLAIR, fluid-attenuated inversion recovery; WMH, white matter hyperintensity.

reported WMH progression in about 18% of participants with vascular risk factors.[79] WMH can also cavitate to take on the appearance of lacunes and they can also disappear—these dynamic features are only now being realised. Though early microstructural impairment could be detected in NAWM contouring WMH, not all NAWM will eventually develop into WMH.[82] The level of NAWM deterioration was also strongly associated with WMH severity, regardless of distance from the WMH.[32]

The variance in long-term changes of CSVD lesions might reflect different pathologies underlying the similar appearance on imaging, for example, reversible lacunar ischaemic stroke lesions versus those that cavitated, or NAWM in patients with mild WMH versus in extensive WMH. Serial imaging studies using advanced techniques like cerebral vascular reactivity, BBB and CBF imaging and use of higher fields, for example, 7 tesla MRI might help differentiate these changes.[83]

Treatments for CSVD

Management of traditional risk factors is still the main approach for treating or preventing CSVD, despite the fact that most of these treatments have not yet shown ideal effects on long-term outcome. Antihypertensive treatment produced contradictory results: it reduced WMH progression in some observational studies[84] but showed little or no effects in randomised controlled trials.[85 86] Although hypertension has been reported to be highly associated with CSVD, other factors may be involved or be influenced by genetic factors,[87] yet more evidences are required. Likewise, most lipid-lowering treatment had neutral results in preventing WMH, like pravastatin.[88] Post hoc analysis of a 2-year follow-up study from Hong Kong showed that statins might be able to delay WMH progression in patients with severe baseline WMH.[89] Statins might also have other therapeutic effects including anti-inflammatory and proendothelial activities.[90] Likewise, subgroup analysis of the VITAmins TO Prevent Stroke (VITATOPS) MRI substudy shows that vitamin B supplementation may reduce WMH progression in patients with severe baseline CSVD.[91]

Studies of treatment specifically targeting lacunar stroke are limited.[90] Apart from the SPS3 trial, there are very few clinical trials of antiplatelets where the results were reported by stroke subtype, and, except trials of cilostazol[92 93] which has weak antiplatelet effects,[94] are especially scarce in Asian populations. Although some trials reported the proportion of lacunar stroke in their study population, the diagnostic criteria varied considerably and the results were not always reported by subgroup. A systematic review of randomised trials found that any single antiplatelet appeared beneficial for secondary prevention of lacunar stroke,[95] but the SPS3 trial showed that long-term dual antiplatelet treatment doubled the risk of bleeding without reducing the risk of stroke recurrence in patients with recent lacunar stroke. Also, blood pressure lowering did not show significant reduction in recurrent lacunar stroke in the SPS3 trial, although it was consistent with a modest benefit.[96]

Prevention and treatment of CSVD in the future should consider targeting the BBB, brain endothelium and microvascular function. There are multiple potential endothelial targets, such as the nitric oxide/cyclic guanylate monophosphate (cGMP) system and prostacyclin/cyclic AMP (cAMP) system.[90] Therefore, interventions that could induce cAMP or cGMP or reduce their degradation appear promising. There are several licensed drugs that have these properties like some nitric oxide donors and phosphodiesterases-5 inhibitors,[90] while others are still in development. More experimental studies should be encouraged. However, in the meantime, management of these traditional risk factors according to guidelines should still be encouraged except to avoid long-term dual antiplatelet drugs.

In conclusion, CSVD is not just a collection of individual brain lesions, but is both a 'dynamic' and 'whole-brain' disease. All CSVD subtypes might share some common intrinsic CSVD aetiologies. Some pathological changes at the early stage of the disease could be reversible, but will gradually worsen and become irreversible as the damage in vessels and tissues accumulates. Modification of traditional risk factors and a healthy lifestyle are currently the most important prophylactic and therapeutic approaches for CSVD indefinitely and until more specific treatments are available. Apart from the trials of cilostazol which have mostly been conducted in China or Japan, in general, large clinical trials of CSVD treatments targeting the Asian population are lacking, especially in lacunar stroke. Community-based studies of CSVD prevalence and progression are also needed to determine if prevalence genuinely differs in different world regions or ethnic groups. Future studies in CSVDs should stratify by stroke subtype and by MRI diagnosis and measure risk factors carefully. Clinical trials and experimental studies targeting endothelium and BBB integrity should be pursued.

Contributors This paper is based on a lecture given by JMW at the Chinese Stroke Association Inaugural Conference in 2015, Beijing. YS drafted the review which was then amended and approved by JMW.

Funding YS is supported by the China Scholarships Council. The work described in this paper was supported by the Wellcome Trust (WT088134/Z/09/A), the MRC, the Scottish Chief Scientist Office (CZB/4/281), Chest Heart Stroke Scotland, the UK HTA, etc.

Competing interests None declared.

Provenance and peer review Commissioned; externally peer reviewed.

Data sharing statement No additional data are available.

REFERENCES

1. Pantoni L. Cerebral small vessel disease: from pathogenesis and clinical characteristics to therapeutic challenges. *Lancet Neurol* 2010;9:689–701.

2. Tsai CF, Thomas B, Sudlow CL. Epidemiology of stroke and its subtypes in Chinese vs white populations: a systematic review. *Neurology* 2013;81:264–72.
3. Fang XH, Wang WH, Zhang XQ, *et al*. Incidence and survival of symptomatic lacunar infarction in a Beijing population: a 6-year prospective study. *Eur J Neurol* 2012;19:1114–20.
4. Wardlaw JM, Smith EE, Biessels GJ, *et al*. Neuroimaging standards for research into small vessel disease and its contribution to ageing and neurodegeneration. *Lancet Neurol* 2013;12:822–38.
5. Vermeer SE, Longstreth WT Jr, Koudstaal PJ. Silent brain infarcts: a systematic review. *Lancet Neurol* 2007;6:611–19.
6. Mori E, Tabuchi M, Yamadori A. Lacunar syndrome due to intracerebral hemorrhage. *Stroke* 1985;16:454–9.
7. Wardlaw JM, Smith C, Dichgans M. Mechanisms of sporadic cerebral small vessel disease: insights from neuroimaging. *Lancet Neurol* 2013;12:483–97.
8. Mead GE, Lewis SC, Wardlaw JM, *et al*. How well does the Oxfordshire community stroke project classification predict the site and size of the infarct on brain imaging? *J Neurol Neurosurg Psychiatr* 2000;68:558–62.
9. Potter G, Doubal F, Jackson C, *et al*. Associations of clinical stroke misclassification ('clinical-imaging dissociation') in acute ischemic stroke. *Cerebrovasc Dis* 2010;29:395–402.
10. Makin SD, Doubal FN, Dennis MS, *et al*. Clinically confirmed stroke with negative diffusion-weighted imaging magnetic resonance imaging: longitudinal study of clinical outcomes, stroke recurrence, and systematic review. *Stroke* 2015;46:3142–8.
11. Doubal FN, Dennis MS, Wardlaw JM. Characteristics of patients with minor ischaemic strokes and negative MRI: a cross-sectional study. *J Neurol Neurosurg Psychiatr* 2011;82:540–2.
12. Kimberly WT, Gilson A, Rost NS, *et al*. Silent ischemic infarcts are associated with hemorrhage burden in cerebral amyloid angiopathy. *Neurology* 2009;72:1230–5.
13. Khan A, Kasner SE, Lynn MJ, *et al*. Risk factors and outcome of patients with symptomatic intracranial stenosis presenting with lacunar stroke. *Stroke* 2012;43:1230–3.
14. Wardlaw JM, Doubal FN, Eadie E, *et al*. Little association between intracranial arterial stenosis and lacunar stroke. *Cerebrovasc Dis* 2011;31:12–18.
15. Kim JS, Yoon Y. Single subcortical infarction associated with parental arterial disease: important yet neglected sub-type of atherothrombotic stroke. *Int J Stroke* 2013;8:197–203.
16. de Jong G, Kessels F, Lodder J. Two types of lacunar infarcts: further arguments from a study on prognosis. *Stroke* 2002;33:2072–6.
17. Asdaghi N, Pearce LA, Nakajima M, *et al*. Clinical correlates of infarct shape and volume in lacunar strokes: the Secondary Prevention of Small Subcortical Strokes trial. *Stroke* 2014;45:2952–8.
18. Del Bene A, Makin SD, Doubal FN, *et al*. Variation in risk factors for recent small subcortical infarcts with infarct size, shape, and location. *Stroke* 2013;44:3000–6.
19. Jackson CA, Hutchison A, Dennis MS, *et al*. Differing risk factor profiles of ischemic stroke subtypes: evidence for a distinct lacunar arteriopathy? *Stroke* 2010;41:624–9.
20. Lodder J, Bamford JM, Sandercock PA, *et al*. Are hypertension or cardiac embolism likely causes of lacunar infarction? *Stroke* 1990;21:375–81.
21. Potter GM, Doubal FN, Jackson CA, *et al*. Lack of association of white matter lesions with ipsilateral carotid artery stenosis. *Cerebrovasc Dis* 2012;33:378–84.
22. Kwon HM, Lynn MJ, Turan TN, *et al*. Frequency, risk factors, and outcome of coexistent small vessel disease and intracranial arterial stenosis: results from the Stenting and Aggressive Medical Management for Preventing Recurrent Stroke in Intracranial Stenosis (SAMMPRIS) Trial. *JAMA Neurol* 2016;73:36–42.
23. Macdonald RL, Kowalczuk A, Johns L. Emboli enter penetrating arteries of monkey brain in relation to their size. *Stroke* 1995;26:1247–50; discussion 1250–1.
24. Jackson C, Sudlow C. Are lacunar strokes really different? A systematic review of differences in risk factor profiles between lacunar and nonlacunar infarcts. *Stroke* 2005;36:891–901.
25. Zhang B, Zhang W, Li X, *et al*. Admission markers predict lacunar and non-lacunar stroke in young patients. *Thromb Res* 2011;128:14–17.
26. Lv P, Jin H, Liu Y, *et al*. Comparison of risk factor between lacunar stroke and large artery atherosclerosis stroke: a cross-sectional study in China. *PLoS ONE* 2016;11:e0149605.
27. Debette S, Markus HS. The clinical importance of white matter hyperintensities on brain magnetic resonance imaging: systematic review and meta-analysis. *BMJ* 2010;341:c3666.
28. Madden DJ, Bennett IJ, Burzynska A, *et al*. Diffusion tensor imaging of cerebral white matter integrity in cognitive aging. *Biochim Biophys Acta* 2012;1822:386–400.
29. Munoz DG, Hastak SM, Harper B, *et al*. Pathologic correlates of increased signals of the centrum ovale on magnetic resonance imaging. *Arch Neurol* 1993;50:492–7.
30. Feigin I, Popoff N. Neuropathological changes late in cerebral edema: the relationship to trauma, hypertensive disease and Binswanger's encephalopathy. *J Neuropathol Exp Neurol* 1963;22:500–11.
31. Black S, Gao F, Bilbao J. Understanding white matter disease: imaging-pathological correlations in vascular cognitive impairment. *Stroke* 2009;40:S48–52.
32. Maniega SM, Valdes Hernandez MC, Clayden JD, *et al*. White matter hyperintensities and normal-appearing white matter integrity in the aging brain. *Neurobiol Aging* 2015;36:909–18.
33. Bastin ME, Clayden JD, Pattie A, *et al*. Diffusion tensor and magnetization transfer MRI measurements of periventricular white matter hyperintensities in old age. *Neurobiol Aging* 2009;30:125–36.
34. Maillard P, Fletcher E, Lockhart SN, *et al*. White matter hyperintensities and their penumbra lie along a continuum of injury in the aging brain. *Stroke* 2014;45:1721–6.
35. Shi Y, Thrippleton MJ, Makin SD, *et al*. Cerebral blood flow in small vessel disease: a systematic review and meta-analysis. *J Cereb Blood Flow Metab* 2016. Published online first: 5 Aug 2016 doi:10.1177/0271678X16662891.
36. van der Veen PH, Muller M, Vincken KL, *et al*. Longitudinal relationship between cerebral small-vessel disease and cerebral blood flow: the second manifestations of arterial disease-magnetic resonance study. *Stroke* 2015;46:1233–8.
37. Farrall AJ, Wardlaw JM. Blood-brain barrier: ageing and microvascular disease–systematic review and meta-analysis. *Neurobiol Aging* 2009;30:337–52.
38. Wardlaw JM, Doubal FN, Valdes-Hernandez M, *et al*. Blood-brain barrier permeability and long-term clinical and imaging outcomes in cerebral small vessel disease. *Stroke* 2013;44:525–7.
39. Wardlaw JM, Doubal F, Armitage P, *et al*. Lacunar stroke is associated with diffuse blood-brain barrier dysfunction. *Ann Neurol* 2009;65:194–202.
40. Topakian R, Barrick TR, Howe FA, *et al*. Blood-brain barrier permeability is increased in normal-appearing white matter in patients with lacunar stroke and leucoaraiosis. *J Neurol Neurosurg Psychiatr* 2010;81:192–7.
41. Taheri S, Gasparovic C, Huisa BN, *et al*. Blood-brain barrier permeability abnormalities in vascular cognitive impairment. *Stroke* 2011;42:2158–63.
42. Potter GM, Marlborough FJ, Wardlaw JM. Wide variation in definition, detection, and description of lacunar lesions on imaging. *Stroke* 2011;42:359–66.
43. Franke CL, van Swieten JC, van Gijn J. Residual lesions on computed tomography after intracerebral hemorrhage. *Stroke* 1991;22:1530–3.
44. Hernandez Mdel C, Piper RJ, Wang X, *et al*. Towards the automatic computational assessment of enlarged perivascular spaces on brain magnetic resonance images: a systematic review. *J Magn Reson Imaging* 2013;38:774–85.
45. Snowdon DA, Greiner LH, Mortimer JA, *et al*. Brain infarction and the clinical expression of Alzheimer disease. The Nun Study. *JAMA* 1997;277:813–17.
46. Vermeer SE, Prins ND, den Heijer T, *et al*. Silent brain infarcts and the risk of dementia and cognitive decline. *N Engl J Med* 2003;348:1215–22.
47. Fanning JP, Wong AA, Fraser JF. The epidemiology of silent brain infarction: a systematic review of population-based cohorts. *BMC Med* 2014;12:119.
48. Braffman BH, Zimmerman RA, Trojanowski JQ, *et al*. Brain MR. pathologic correlation with gross and histopathology. 1. Lacunar infarction and Virchow-Robin spaces. *AJR Am J Roentgenol* 1988;151:551–8.
49. Potter GM, Chappell FM, Morris Z, *et al*. Cerebral perivascular spaces visible on magnetic resonance imaging: development of a qualitative rating scale and its observer reliability. *Cerebrovasc Dis* 2015;39:224–31.
50. Groeschel S, Chong WK, Surtees R, *et al*. Virchow-Robin spaces on magnetic resonance images: normative data, their dilatation, and a review of the literature. *Neuroradiology* 2006;48:745–54.
51. Zhu YC, Tzourio C, Soumare A, *et al*. Severity of dilated Virchow-Robin spaces is associated with age, blood pressure, and MRI markers of small vessel disease: a population-based study. *Stroke* 2010;41:2483–90.
52. Heier LA, Bauer CJ, Schwartz L, *et al*. Large Virchow-Robin spaces: MR-clinical correlation. *AJNR Am J Neuroradiol* 1989;10:929–36.

53. Potter GM, Doubal FN, Jackson CA, *et al*. Enlarged perivascular spaces and cerebral small vessel disease. *Int J Stroke* 2015;10:376–81.
54. Doubal FN, MacLullich AM, Ferguson KJ, *et al*. Enlarged perivascular spaces on MRI are a feature of cerebral small vessel disease. *Stroke* 2010;41:450–4.
55. Zhu YC, Dufouil C, Soumare A, *et al*. High degree of dilated Virchow-Robin spaces on MRI is associated with increased risk of dementia. *J Alzheimers Dis* 2010;22:663–72.
56. Maclullich AM, Wardlaw JM, Ferguson KJ, *et al*. Enlarged perivascular spaces are associated with cognitive function in healthy elderly men. *J Neurol Neurosurg Psychiatr* 2004;75:1519–23.
57. Wuerfel J, Haertle M, Waiczies H, *et al*. Perivascular spaces—MRI marker of inflammatory activity in the brain? *Brain* 2008;131:2332–40.
58. Weller RO, Djuanda E, Yow HY, *et al*. Lymphatic drainage of the brain and the pathophysiology of neurological disease. *Acta Neuropathol* 2009;117:1–14.
59. Iliff JJ, Wang M, Zeppenfeld DM, *et al*. Cerebral arterial pulsation drives paravascular CSF-interstitial fluid exchange in the murine brain. *J Neurosci* 2013;33:18190–9.
60. Xie L, Kang H, Xu Q, *et al*. Sleep drives metabolite clearance from the adult brain. *Science* 2013;342:373–7.
61. Shoamanesh A, Kwok CS, Benavente O. Cerebral microbleeds: histopathological correlation of neuroimaging. *Cerebrovasc Dis* 2011;32:528–34.
62. Greenberg SM, Vernooij MW, Cordonnier C, *et al*. Cerebral microbleeds: a guide to detection and interpretation. *Lancet Neurol* 2009;8:165–74.
63. Cordonnier C, Al-Shahi Salman R, Wardlaw J. Spontaneous brain microbleeds: systematic review, subgroup analyses and standards for study design and reporting. *Brain* 2007;130:1988–2003.
64. Martinez-Ramirez S, Greenberg SM, Viswanathan A. Cerebral microbleeds: overview and implications in cognitive impairment. *Alzheimers Res Ther* 2014;6:33.
65. Sveinbjornsdottir S, Sigurdsson S, Aspelund T, *et al*. Cerebral microbleeds in the population based AGES-Reykjavik study: prevalence and location. *J Neurol Neurosurg Psychiatr* 2008;79:1002–6.
66. Poels MM, Vernooij MW, Ikram MA, *et al*. Prevalence and risk factors of cerebral microbleeds: an update of the Rotterdam scan study. *Stroke* 2010;41:S103–6.
67. Kakar P, Charidimou A, Werring DJ. Cerebral microbleeds: a new dilemma in stroke medicine. *JRSM Cardiovasc Dis* 2012;1:22.
68. van Dijk EJ, Breteler MM, Schmidt R, *et al*. The association between blood pressure, hypertension, and cerebral white matter lesions: cardiovascular determinants of dementia study. *Hypertension* 2004;44:625–30.
69. Wardlaw JM, Allerhand M, Doubal FN, *et al*. Vascular risk factors, large-artery atheroma, and brain white matter hyperintensities. *Neurology* 2014;82:1331–8.
70. Ihara M, Yamamoto Y. Emerging evidence for pathogenesis of sporadic cerebral small vessel disease. *Stroke* 2016;47:554–60.
71. van Dijk EJ, Prins ND, Vrooman HA, *et al*. Progression of cerebral small vessel disease in relation to risk factors and cognitive consequences: Rotterdam Scan study. *Stroke* 2008;39:2712–19.
72. Staals J, Makin SD, Doubal FN, *et al*. Stroke subtype, vascular risk factors, and total MRI brain small-vessel disease burden. *Neurology* 2014;83:1228–34.
73. Gow AJ, Bastin ME, Munoz Maniega S, *et al*. Neuroprotective lifestyles and the aging brain: activity, atrophy, and white matter integrity. *Neurology* 2012;79:1802–8.
74. Rost NS, Rahman RM, Biffi A, *et al*. White matter hyperintensity volume is increased in small vessel stroke subtypes. *Neurology* 2010;75:1670–7.
75. Wardlaw JM, Lewis SC, Keir SL, *et al*. Cerebral microbleeds are associated with lacunar stroke defined clinically and radiologically, independently of white matter lesions. *Stroke* 2006;37:2633–6.
76. Duering M, Csanadi E, Gesierich B, *et al*. Incident lacunes preferentially localized to the edge of white matter hyperintensities: insights into the pathophysiology of cerebral small vessel disease. *Brain* 2013;136:2717–26.
77. Valdes Hernandez Mdel C, Maconick LC, Munoz Maniega S, *et al*. A comparison of location of acute symptomatic vs. 'silent' small vessel lesions. *Int J Stroke* 2015;10:1044–50.
78. Potter GM, Doubal FN, Jackson CA, *et al*. Counting cavitating lacunes underestimates the burden of lacunar infarction. *Stroke* 2010;41:267–72.
79. Schmidt R, Enzinger C, Ropele S, *et al*. Progression of cerebral white matter lesions: 6-year results of the Austrian Stroke Prevention Study. *Lancet* 2003;361:2046–8.
80. Gouw AA, van der Flier WM, Fazekas F, *et al*. Progression of white matter hyperintensities and incidence of new lacunes over a 3-year period: the Leukoaraiosis and Disability study. *Stroke* 2008;39:1414–20.
81. Schmidt R, Seiler S, Loitfelder M. Longitudinal change of small-vessel disease-related brain abnormalities. *J Cereb Blood Flow Metab* 2016;36:26–39.
82. Munoz Maniega S, Chappell FM, Valdes Hernandez MC, *et al*. Integrity of normal-appearing white matter: influence of age, visible lesion burden and hypertension in patients with small-vessel disease. *J Cereb Blood Flow Metab* 2016. Published Online First: 1 Mar 2016 doi: 10.1177/0271678X16635657.
83. Bouvy WH, Biessels GJ, Kuijf HJ, *et al*. Visualization of perivascular spaces and perforating arteries with 7 T magnetic resonance imaging. *Invest Radiol* 2014;49:307–13.
84. Dufouil C, de Kersaint-Gilly A, Besancon V, *et al*. Longitudinal study of blood pressure and white matter hyperintensities: the EVA MRI Cohort. *Neurology* 2001;56:921–6.
85. Dufouil C, Chalmers J, Coskun O, *et al*. Effects of blood pressure lowering on cerebral white matter hyperintensities in patients with stroke: the PROGRESS (Perindopril Protection Against Recurrent Stroke Study) Magnetic Resonance Imaging Substudy. *Circulation* 2005;112:1644–50.
86. Weber R, Weimar C, Blatchford J, *et al*. Telmisartan on top of antihypertensive treatment does not prevent progression of cerebral white matter lesions in the prevention regimen for effectively avoiding second strokes (PRoFESS) MRI substudy. *Stroke* 2012;43:2336–42.
87. Turner ST, Fornage M, Jack CR Jr, *et al*. Genomic susceptibility loci for brain atrophy in hypertensive sibships from the GENOA study. *Hypertension* 2005;45:793–8.
88. ten Dam VH, van den Heuvel DM, van Buchem MA, *et al*. Effect of pravastatin on cerebral infarcts and white matter lesions. *Neurology* 2005;64:1807–9.
89. Mok VC, Lam WW, Fan YH, *et al*. Effects of statins on the progression of cerebral white matter lesion: post hoc analysis of the ROCAS (Regression of Cerebral Artery Stenosis) study. *J Neurol* 2009;256:750–7.
90. Bath PM, Wardlaw JM. Pharmacological treatment and prevention of cerebral small vessel disease: a review of potential interventions. *Int J Stroke* 2015;10:469–78.
91. Cavalieri M, Schmidt R, Chen C, *et al*. B vitamins and magnetic resonance imaging-detected ischemic brain lesions in patients with recent transient ischemic attack or stroke: the VITAmins TO Prevent Stroke (VITATOPS) MRI-substudy. *Stroke* 2012;43:3266–70.
92. Shinohara Y, Katayama Y, Uchiyama S, *et al*. Cilostazol for prevention of secondary stroke (CSPS 2): an aspirin-controlled, double-blind, randomised non-inferiority trial. *Lancet Neurol* 2010;9:959–68.
93. Huang Y, Cheng Y, Wu J, *et al*. Cilostazol as an alternative to aspirin after ischaemic stroke: a randomised, double-blind, pilot study. *Lancet Neurol* 2008;7:494–9.
94. Comerota AJ. Effect on platelet function of cilostazol, clopidogrel, and aspirin, each alone or in combination. *Atheroscler Suppl* 2005;6:13–19.
95. Kwok CS, Shoamanesh A, Copley HC, *et al*. Efficacy of antiplatelet therapy in secondary prevention following lacunar stroke: pooled analysis of randomized trials. *Stroke* 2015;46:1014–23.
96. Group SPSS, Benavente OR, Coffey CS, *et al*. Blood-pressure targets in patients with recent lacunar stroke: the SPS3 randomised trial. *Lancet* 2013;382:507–15.

Clinical Science (2018) **132** 157–171
https://doi.org/10.1042/CS20171280

PORTLAND PRESS

Research Article

Intracranial pulsatility in patients with cerebral small vessel disease: a systematic review

Yulu Shi[1,2], Michael J. Thrippleton[1,2], Ian Marshall[1,2] and Joanna M. Wardlaw[1,2,3]

[1]Brain Research Imaging Centre, Centre for Clinical Brain Sciences, University of Edinburgh, Edinburgh, U.K.; [2]UK Dementia Research Institute at The University of Edinburgh, Edinburgh Medical School, 47 Little France Crescent, Edinburgh EH16 4TJ, U.K.; [3]Centre for Cognitive Ageing and Cognitive Epidemiology, University of Edinburgh, Edinburgh, U.K.

Correspondence: Joanna M. Wardlaw (Joanna.Wardlaw@ed.ac.uk)

Growing evidence suggests that increased intracranial pulsatility is associated with cerebral small vessel disease (SVD). We systematically reviewed papers that assessed intracranial pulsatility in subjects with SVD. We included 27 cross-sectional studies (n=3356): 20 used Doppler ultrasound and 7 used phase-contrast MRI. Most studies measured pulsatility in the internal carotid or middle cerebral arteries (ICA, MCA), whereas few assessed veins or cerebrospinal fluid (CSF). Methods to reduce bias and risk factor adjustment were poorly reported. Substantial variation between studies in assessment of SVD and of pulsatility indices precluded a formal meta-analysis. Eight studies compared pulsatility by SVD severity (n=26–159, median = 74.5): arterial pulsatility index was generally higher in more severe SVD (e.g. MCA: standardized mean difference = 3.24, 95% confidence interval [2.40, 4.07]), although most did not match for age. Seventeen studies (n=9–700; median = 110) performed regression or correlation analysis, of which most showed that increased pulsatility was associated with SVD after adjustment for age. In conclusion, most studies support a cross-sectional association between higher pulsatility in large intracranial arteries and SVD. Future studies should minimize bias, adjust for potential confounders, include pulsatility in veins and CSF, and examine longitudinal relationship between pulsatility and SVD. Agreement on reliable measures of intracranial pulsatility would be helpful.

Introduction

Cerebral small vessel disease (SVD) is responsible for up to 45% of dementia and approximately 20% of all stroke worldwide [1,2]. SVD is mainly diagnosed on brain imaging, based on various features such as white matter hyperintensities (WMH), perivascular space (PVS), microbleeds, lacunes, and recent small subcortical (lacunar) infarcts. Although each individual imaging feature might represent different underlying tissue changes, evidence from autopsy and clinical studies indicate that these features are all related to pathologies in brain small vessels [2]. For example, though white matter changes could be seen in other conditions such as multiple sclerosis, WMH of presumed vascular origin are the most typical and known SVD changes. They are usually symmetrically and bilaterally distributed in subcortical areas, and various theories have been proposed to explain the small vessel pathology and how this affects the brain [2].

Ageing and hypertension are important risk factors for SVD [3], both of which are associated with loss of elasticity in the arterial walls. Growing evidence has shown a relationship between increased aortic pulsatility and lacunar infarcts or WMH volume [4,5]. It is hypothesized that the stiffened vessel walls would be less able to dampen the systemic arterial pressure pulse via the *Windkessel* effect, leading to high pulsatility being transmitted into the brain and causing or exacerbating small vessel damage, such as endothelial dysfunction and blood–brain barrier (BBB) impairment [6].

Cerebrovascular pulsatility is also an important driving force of the cerebrospinal fluid (CSF)–interstitial fluid (ISF) exchange via the glymphatic system in the perivascular spaces, which is essential for clearing metabolic and other waste products from the brain [7,8]. Altered pulsatility and

Received: 14 August 2017
Revised: 20 November 2017
Accepted: 07 December 2017

Accepted Manuscript Online: 11 December 2017
Version of Record published: 16 January 2018

Clinical Science (2018) **132** 157–171
https://doi.org/10.1042/CS20171280

abnormality in the PVS might cause or accelerate glymphatic dysfunction and aggregation of waste products such as Aβ, other proteins or cell debris, which is related to age-related neurodegenerative diseases and SVD [8]. Thus, for several reasons, increased intracranial pulsatility might be an important underlying mechanism of SVD. However, so far very few clinical studies have assessed pulsatility directly in the intracranial vessels [9,10].

Doppler ultrasound and magnetic resonance imaging (MRI) are two main techniques that could measure intracranial pulsatility. Doppler ultrasound measures real-time blood flow velocity in the large arteries, mainly internal carotid arteries (ICA) and middle cerebral arteries (MCA). Pulsatility is generally calculated using Gosling's equation (pulsatility index, PI = (peak systolic velocity − peak diastolic velocity)/mean velocity)). Phase-contrast MRI can quantify fluid velocity and flow in the intracranial arteries, veins, and CSF. It has mostly been used in disorders such as hydrocephalus that present with abnormal CSF dynamics [11] with few studies in SVD. Some MRI studies used a similar equation (flow was used instead of velocity) to calculate the pulsatility in the vessels, but indices reported for CSF pulsatility vary [9,10]. It is unclear which measures are most relevant and reliable for quantifying intracranial pulsatility in patients with SVD.

Furthermore it is unclear if high pulsatility and SVD were both simply the result of exposure to vascular risk factors, since some studies did not adjust for age or important risk factors when assessing the relationship between intracranial pulsatility and SVD [9]. Also, WMH are commonly used by studies to represent SVD burden [12-14], and it is unknown whether high pulsatility was also related to other features of SVD, such as lacunar stroke or PVS.

In order to provide a complete summary of all knowledge to date on intracranial pulsatility in SVD patients, we systematically reviewed papers that measured cerebral pulsatility in SVD with a view to performing a meta-analysis. We aimed to determine if there was an association between intracranial pulsatility and SVD, the magnitude of any association, whether pulsatility predicted SVD progression longitudinally, and if any individual SVD features were more strongly associated with pulsatility than others.

Methods

We performed this review according to the MOOSE guidelines for meta-analysis of observational studies [15]. We conducted a literature search of Ovid MEDLINE and Embase from 1946 up to April 2017 using the Ovid Web Gateway. We searched terms related to pulsatility and SVD in all contents of the papers using the strategy: "Pulsatility" or "Resistance" or "Velocity" or "cerebrospinal fluid pulsatility" or "Phase-contrast MRI" and "Cerebral small vessel disease" or "White matter hyperintensities" or "Leukoaraiosis". English and non-English literatures were sought. Additional records were identified by hand from relevant reviews, primary papers, and from the authors' publication lists. We defined SVD features according to the STRIVE Guideline [16].

Eligibility criteria

We included papers that reported primary results of studies that fulfilled all the following criteria: (1) recruited participants with SVD features; (2) assessed resting-state intracranial pulsatility (including ICA) using any imaging technique; (3) assessed the relationship between intracranial pulsatility and SVD. We only included studies that focused on sporadic SVD in this review as the mechanisms for hereditary SVDs might differ. We excluded review papers, abstracts, and papers that used pharmacological, CO_2 or other stimulus without providing pre-stimulus data.

Data extraction

We extracted data on participant characteristics, study design, MRI or Doppler technicalities, location, and type of pulsatility indices assessed. For studies that compared pulsatility between groups and reported means and standard deviations, we extracted the results of the comparisons from text or tables where available, or from graphs where necessary; for those that performed association analysis such as correlation or regression models, we extracted the statistical methods, coefficients, *P* values, and confounding factors or co-variates (if any) that were adjusted for. For studies that performed both non-adjusted and adjusted analysis, we only included the adjusted results. We assessed the study quality using a checklist that includes factors such as study population and methods for bias controlling (Supplementary Table S1).

Statistical analysis

We displayed the results of comparisons between groups using forest plots in the Cochrane Collaboration's Review Manager (Revman Version 5.3) and used standardised mean difference (SMD) to represent the difference between groups. We did not include data from studies that did not provide standard deviations (s.d.), because the SMD is inestimable without s.d.. In this review, we were not able to perform robust meta-analyses because of the limited data and

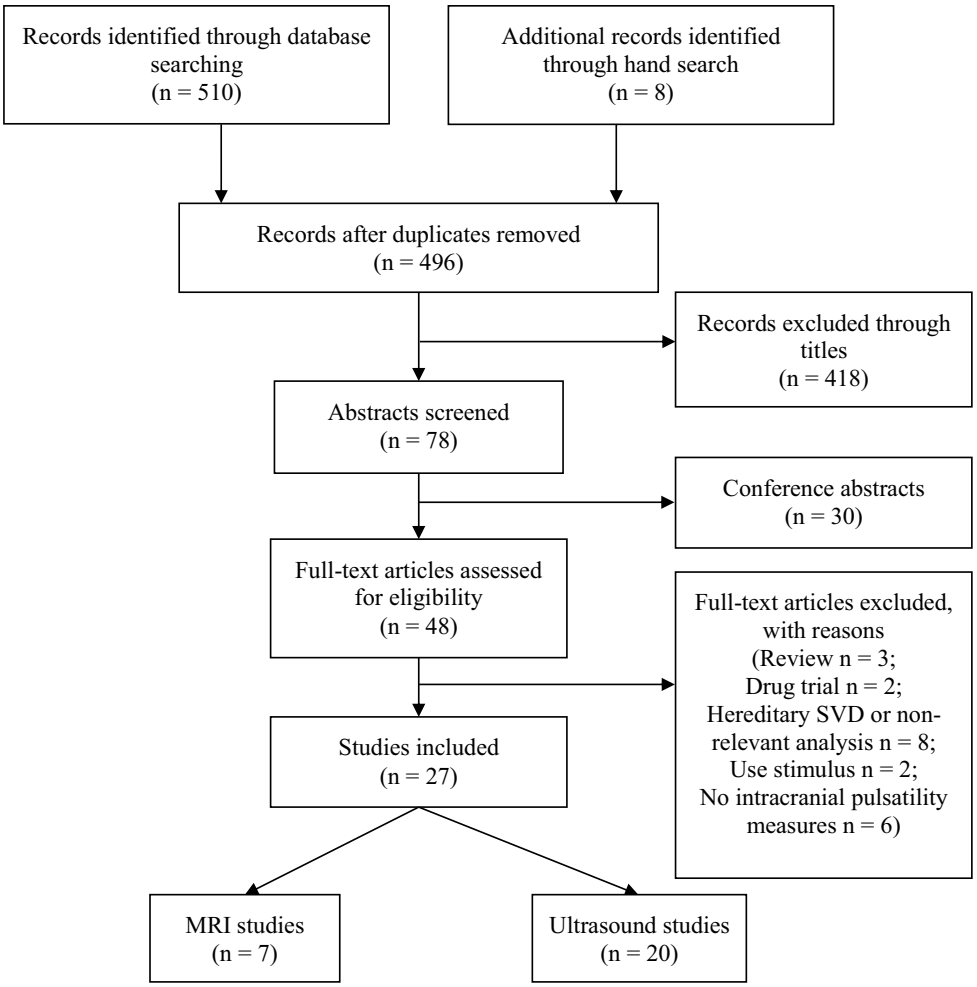

Figure 1. PRISMA flow diagram of literature search and its results

the large heterogeneity in study population and pulsatility measures. Therefore, in the forest plot we did not calculate overall effect sizes. For studies that divided patients into more than two grades of WMH severity, we combined the means and s.d.s of PI from patients who had similar severity of SVD to create a single pair-wise comparison using formulae from the Cochrane handbook (Supplementary Equation S1) [17]. For example, we created new groups "mild WMHs" by combining groups of Fazekas score 0 to 1, and "severe WMHs" from Fazekas score 2 to 3.

Results

The search strategy identified 518 papers, of which 48 were potentially eligible and 27 were ultimately selected for further review (Figure 1). We excluded reviews (3), drug trials without providing baseline information on pulsatility and SVD (2), hereditary SVD study or non-relevant analysis (8), studies that used stimulus only (2) or did not assess intracranial pulsatility (6). One MRI study compared CSF pulsatility between patients with late-life depression and age-matched healthy volunteers, but we included the results in the forest plot because patients had higher WMH burden than the healthy volunteers and late-onset depression is associated with SVD [18].

Characteristics of included studies

Twenty-seven studies (n=3356) were included, of which 20 used ultrasound [12,14,19-36] and 7 used MRI to measure pulsatility [9,10,13,18,37-39], 26/27 were cross-sectional and one was a clinical trial of cilostazol [35] from which we only extracted the data obtained at baseline.

Clinical Science (2018) **132** 157–171
https://doi.org/10.1042/CS20171280

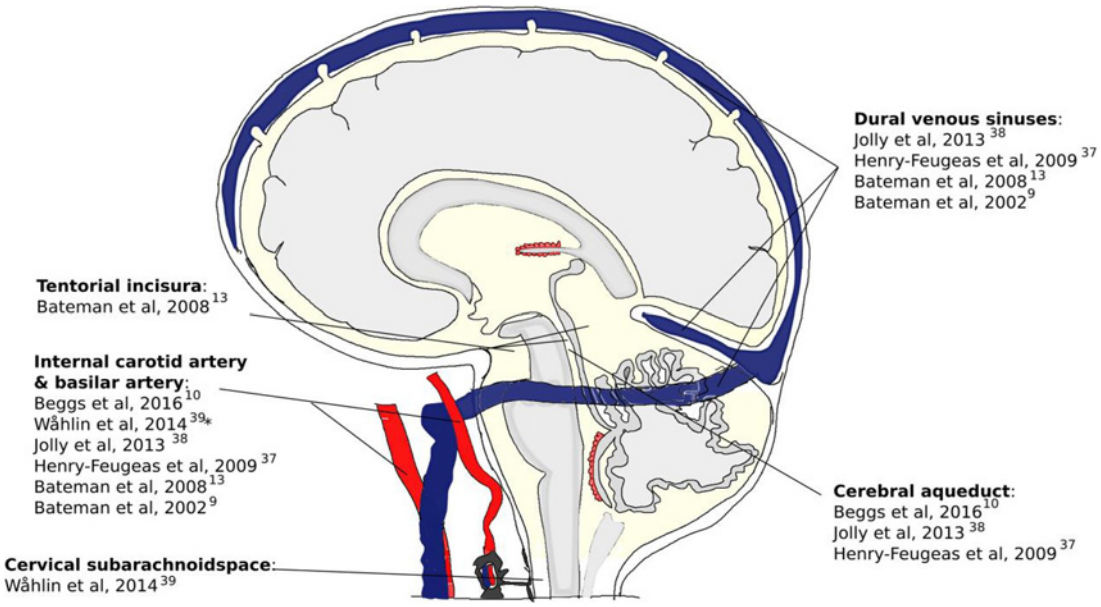

Figure 2. Regions of interest for flow measurement used in phase-contrast MRI studies included in this review.
*Anders Wåhlin et al. [39] selected the vertebral arteries instead of the basilar artery.

Doppler ultrasound studies

Table 1 summarises patient characteristics from 20 ultrasound studies (n=2935) with sample sizes ranging from 9 to 700 (median = 107). Fourteen used WMH (if MRI used for structural brain imaging) or white matter hypoattenuation (if CT used) to represent SVD burden. Two studies included patients with stroke: one compared pulsatility between lacunar and non-lacunar ischaemic stroke [25], and one compared pulsatility between patients with lacunar stroke (according to Trial of ORG 1072 in Acute Stroke Treatment (TOAST) classification) and age- and sex-matched healthy controls [32]. One study included patients with multi-infarct dementia [22] and one recruited patients with cerebral amyloid angiopathy (CAA) [31] (Table 1).

Three studies assessed pulsatility in the ICA (cervical), seventeen in the MCA, one in the basilar artery, one in the posterior cerebral artery (PCA), and one in the central retinal artery. Most studies calculated PI using Gosling's equation. One study measured brain tissue pulsatile movement [20].

MRI studies

Patient characteristics and scanner information of seven MRI studies (n=421, range 35–101, median = 51) are shown in Table 2. Three studies recruited patients with dementia or cognitive impairment, including idiopathic dementia [9], Alzheimer's disease [13], vascular dementia [13], and mild cognitive impairment [37]. Only one reported the diagnosis criteria for Alzheimer's disease and vascular dementia [13]. One study recruited patients with late onset major depressive disorder [18]. Three studies recruited healthy volunteers (age range: 43–82, 18–75, and 62–82 years) [10,38,39] (Table 2).

All seven studies used phase-contrast MRI. Four studies used 1.5 Tesla and three used 3 Tesla scanners. All studies used retrospective gated phase-contrast MRI: four used peripheral pulse- and two used electrocardiogram (ECG)-gating; four studies reported the numbers of time points measured per cardiac cycle, among which three used 32 whereas one used 16 time points (Table 2).

There were large differences between studies as to where flow was measured. Figure 2 shows the regions of interests used in these studies. Six included the ICA(s) [9,10,13,37-39]; in posterior circulation five chose the basilar artery [9,10,13,37,38] and one selected the vertebral arteries [39]; four studied pulsatility in the venous sinuses [9,13,37,38]; six measured CSF flow, among which one selected the cervical subarachnoid spaces [39], one selected tentorial incisura [13], and four measured the cerebral aqueduct [10,18,37,38]. In total, three studies measured flow or pulsatility across the cerebral arteries, veins, and the CSF system concurrently [13,18,37] (Figure 2).

Table 1 Patient characteristics of ultrasound studies

First author	Year	Subjects/Disease	Sample size	Group	Age ± s.d.(years)	Vessels of interest
Jordi Sanahuja [30]	2016	Type 2 diabetes	202	Higher SVD score (*n*=21)		MCA
				Lower SVD score (*n*=181)		
Oscar H. Del Brutto [33]	2015	Community	70	Mild WMH (*n*=42)	72.2 ± 5.5	MCA, vertebral artery
					77.4 ± 7.34	
Abbas Ghorbani [34]	2015	Patients who had SVD on imaging	104	Patients who had WMH or lacunar infarct on MRI	68.4	MCA
				Patients who had no lesion on MRI	62.6	
Monika Turk [21]	2014	Leukoraiosis	96	Leukoaraiosis (*n*=52)	54.9 ± 8.3	ICA
				Age and sex-matched healthy volunteers (*n*=44)	52.39 ± 7.34	
Benjamin S. Aribisala [12]	2014	Lothian birth cohort 1936	700	–	70	ICA
Redouane Ternifi [20]	2014	Healthy volunteers	9	–	70.56 ± 5.46	Brain tissue displacement
Joao Sargento-Freitas [29]	2014	Patients who visited neurosonology lab	439	–	63.47 ± 14.94	MCA
Sushmita Purkayastha [28]	2014	Patients with vascular risk factors	48	–	75±7	MCA
Sang Won Han [35]	2014	Lacunar stroke	130	–	64.7	MCA
Alastain J.S. Webb [27]	2012	TIA or minor stroke	110	Fazekas 3 (*n*=25)	74.9 ± 7.9	MCA
				Fazekas 2 (*n*=24)	68.5 ± 11	
				Fazekas 1 (*n*=21)	66.5 ± 12	
				Fazekas 0 (*n*=30)	53 ± 15	
Vincent Mok [26]	2012	Community	205	With severe WMH	74 ± 6	MCA
				without severe WMH	69 ± 6	
Ioannis Heliopoulos [14]	2012	Hypertensive patients	52	–	71.4 ± 4.5	MCA
Kerstin Bettermann [36]	2012	Patients with WMH	26	Patients with WMH	63.5 ± 11.25	MCA
				Control without WMH	55.07 ± 7.91	
Iria Rodriguez [25]	2010	Ischaemic stroke	186	Lacunar (*n*=35)	69.7 ± 10.8	MCA
				Non-lacunar (*n*=151)	71.6 ± 8.1	
Tomotaka Tanaka [19]	2009	Diabetic patients	122	Hypertensive (*n*=43)	66.9 ± 9.8	ICA
				Non-hypertensive (*n*=79)	62.0 ± 11.0	
Eric E. Smith [31]	2008	CAA	20	CAA (*n*=11)	73.5 ± 7.4	Basilar artery
				Healthy volunteers (*n*=9)	70.9 ± 7.9	
Chelsea S. Kidwell [23]	2001	Retrospective review in patients who had both TCD and MRI	55	–	62 (range 28–98)	MCA
Rosa M. Sánchez-Pérez [24]	2003	Patients (>60 years) who visited neurological department for minor symptoms	116	–	74.44 ± 6.35	MCA
Masahiko Hiroki [32]	2002	Stroke	167	Small vessel disease (TOAST) (*n*=103)	70.9 ± 9.0	Central retinal artery
				Age and sex-matched controls (*n*=64)	69.7 ± 8.8	
Stefan Biedert [22]	1995	Dementia	78	Multi-infarct dementia (*n*=19)	Age range 60–69 for all	MCA, basilar artery
				AD (*n*=23)		
				Age-matched healthy volunteers (*n*=36)		

Abbreviations: AD, Alzheimer's disease; CAA, cerebral amyloid angiopathy; ICA, internal carotid artery; MCA, middle cerebral artery; MRI, magnetic resonance imaging; SVD, small vessel disease; TCD, transcranial Doppler; TIA, transient ischaemic attack; WMH: white matter hyperintensities.

Clinical Science (2018) **132** 157–171
https://doi.org/10.1042/CS20171280

Table 2 Patient characteristics and scanner information of MRI studies

First author	Year	Subjects/ Disease	Sample size	Groups	Age (years)	Scanner and sequences	T_E/T_R (ms)	Venc	Time points in a cardiac cycle
Clive B. Beggs [10]	2016	Healthy volunteers	101	–	44.7 ± 17.8 (range 18–75)	GE 3 Tesla; Retrospectively peripheral pulse-gated 2-D phase contrast cine sequences	7.9/40	20 cm/s aqueduct	32
Anders Wåhlin [39]	2014	Healthy volunteers	37	–	71 ± 6	Philips 3 Tesla; Retrospectively peripheral pulse or ECG-gated 2-D phase contrast cine sequences	6–11/10–16	70 cm/s for arteries and 7 cm/s for CSF	32
Todd A.D. Jolly [38]	2013	Healthy volunteers	35	–	65.67 ± 9.31 (range 43–82)	Siemens 3 Tesla; Retrospectively ECG-gated 2-D phase contrast cine sequences	6.9/26.5	Arteries 75 cm/s, veins 40 cm/s, CSF 22 cm/s	Not mentioned
Marie C. Henry-Feugeas [37]	2009	Mild cognitive impairment	71	Significant WHM (*n*=42)	74 ± 5	GE 1.5 Tesla; Retrospectively ECG-gated 2-D phase contrast cine sequences	7.6–9.9/20–23	Not mentioned	16
				No significant WHM (*n*=29)	69 ± 5				
Grant A. Bateman [13]	2008	Senile dementia	48	AD (*n*=12)	76 ± 4	Siemens 1.5 Tesla; Retrospectively ECG-gated 2-D phase contrast cine sequences	7/29	Arteries 75 cm/s, veins 40 cm/s, CSF 10 cm/s	Not mentioned
				Vascular dementia (*n*=12)	70 ± 11				
				Normal aging (*n*=12)	70 ± 5				
				Normal young (*n*=12)	25 ± 12				
Josephine H. Naish [18]	2006	Late onset major depressive disorder	51	Responders to anti-depressant monotherapy (*n*=21)	71.0 ± 6.54	Philips 1.5 Tesla; Retrospectively peripheral pulse-gated 2-D phase contrast cine sequences	7–8.2/14–15 ms	Not mentioned	16
				Non-responders (*n*=8)	75.2 ± 6.18				
				Age-matched control (*n*=22)	72.9 ± 5.38				
				Young (*n*=19)	27.5 ± 4.4				

Continued over

Table 2 Patient characteristics and scanner information of MRI studies (Continued)

First author	Year	Subjects/ Disease	Sample size	Groups	Age (years)	Scanner and sequences	T_E/T_R (ms)	Venc	Time points in a cardiac cycle
Grant A. Bateman [9]	2002	Idiopathic dementia	78	Fazekas 0 (n=10)	71 ± 8	1.5 Tesla; Retrospectively ECG-gated 2-D phase contrast cine sequences	7/29 ms	Not mentioned	Not mentioned
				Fazekas 1 (n=18)	75 ± 8				
				Fazekas 2 (n=24)	76 ± 7				
				Fazekas 3 (n=8)	77 ± 8				
				Healthy controls (n=18)	42 ± 17				

Abbreviations: AD, Alzheimer's disease; CSF, cerebrospinal fluid; ECG, electrocardiogram; T_E, Echo time; T_R, repetition time; Venc, velocity encoding parameter; WMH, white matter hyperintensities.

Quality assessment

The average quality score of 27 studies was 6.85/10. 26/27 studies were prospective. However, seven studies did not report participants' demographic information or general health condition. Only about half of the studies adjusted or matched for risk factors (15/27) or reported the expertise of observers of structural MRI (15/27). Less than half of the studies reported dropout (12/27) or use of blinding in structural image analysis (11/27) (Supplementary Figure S1).

Result of comparisons of pulsatility measures

Doppler ultrasound studies

Three studies (n=356, median = 96) compared arterial PI between patients with different WMH severities. One study examined the ICA, one chose MCA, and one chose both MCA and basilar artery. PI was generally higher in patients with more severe WMH in the ICA [21], MCA [22,26], and the basilar artery [22] (e.g. in MCA: SMD = 3.24, 95% confidence interval (CI) [2.4, 4.07]), although the result for ICA did not reach statistical significance (SMD = 0.38, 95% CI [−0.02, 0.79] [21]). 2/3 of the studies were age-matched [21,22], one of which also matched for gender [21] (Figure 3A).

Two studies looked at other SVD features. One study (n=167) showed that patients with lacunar stroke (TOAST) had higher PI in the central retinal artery compared with age- and sex-matched heathy controls (SMD = 0.35, 95% CI [0.03, 0.66]) [32] (Figure 3B). One study of CAA (n=20) found that patients with CAA had a significantly higher PI in PCA than non-age-matched healthy elderly controls (SMD = 1.07, 95% CI [0.12, 2.03]) [31] (Figure 3C).

MRI studies

Three phase-contrast MRI studies (n=124, median = 50) performed comparisons of cerebrovascular or CSF pulsatility between patients with different WMH severities. None of these studies corrected for age. The indices for pulsatility included PI, stroke volume, and delay between waveform peaks. The trend in all the comparisons is that higher arterial or venous PI (e.g. arterial PI: SMD = 0.93, 95% CI [0.40, 1.47] [9]), larger arterial or venous or CSF stroke volume (e.g. CSF stroke volume: SMD = 1.58, 95% CI [0.64, 2.52] [13]) was associated with more WMH, although some results did not reach a statistical significance (e.g. venous PI: SMD = 0.18, 95% CI [−0.33, 0.69] [9]) (Figure 3D).

Two studies (n=110) calculated the delay between waveform systolic peaks. There was no significant difference in arterial-venous (n=60, SMD = 0.95% CI [−0.51, 0.51]) [13] or arterial-aqueduct peak delays (n=51, SMD = 0.49, 95% CI [−0.07, 1.06]) [18] between different severities of WMH (Figure 3E).

Results of studies that performed regression or correlation analysis

Table 3 summarises studies that performed regression or correlation analysis, including 13 Doppler ultrasound (n=9–700, median = 116) and three MRI studies (n=35–100, median = 37). 14/16 studies adjusted for co-variates, of which 12 included age. No studies adjusted for blood pressure although five considered history of hypertension.

Clinical Science (2018) **132** 157–171
https://doi.org/10.1042/CS20171280

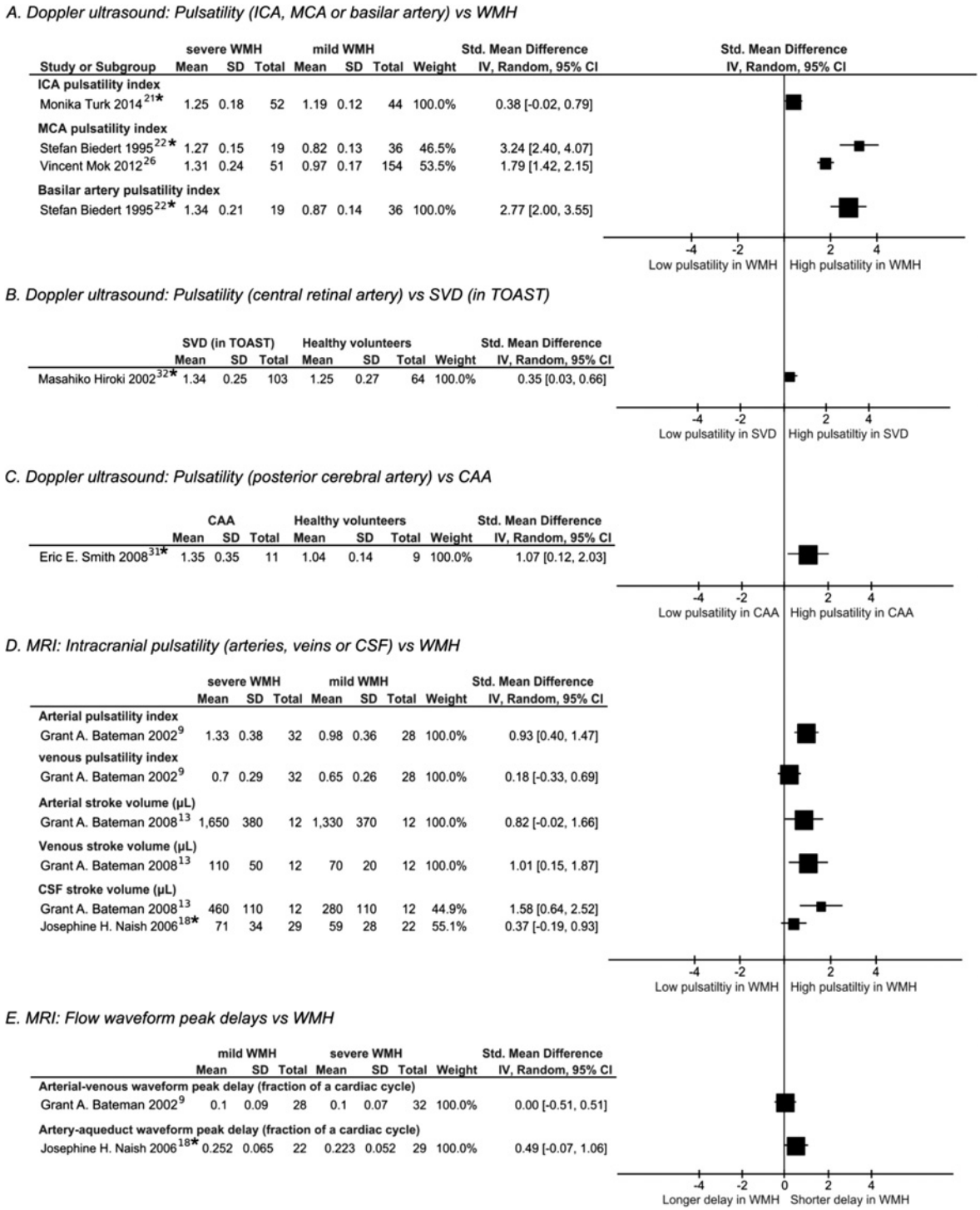

Figure 3. Forest plots of studies that compared pulsatility (using Doppler ultrasound or MRI) between SVD and control groups; *indicates studies that matched for age

(**A**–**C**): Pulsatility was measured by Doppler ultrasound. (A) Comparison of vascular pulsatility between patients with severe and mild white matter hyperintensities (WMH). (B) Comparison of central retinal artery pulsatility between patients with SVD-stroke (TOAST classification) and healthy volunteers. (C) Comparison of posterior cerebral artery pulsatility between patients with cerebral amyloid angiopathy (CAA) and healthy volunteers. (**D** and **E**): Pulsatility was measured by phase-contrast MRI. (D) Comparison of vascular or CSF pulsatility between patients with severe and mild WMH. (E) Comparison of flow waveform peak delays between patients with severe and mild WMH. It is worth noting that, in forest plot (E), shorter peak delay is suggested by the authors to represent higher intracranial stiffness.

Table 3 Results of correlation analyses in MRI and ultrasound studies

First author	Year	Sample size	Correlation or regression models	Variables (*y*∼*x*)	Coefficient	*P* value	Adjustment for confounding factors
Ultrasound studies							
ICA							
Benjamin S. Aribisala [12]	2014	700	Multiple variable regression	WMH volume ∼ ICA PI	β = 0.09	0.016	Age, sex, ICV, HBp history
Tomotaka Tanaka [19]	2009	122	Multivariate regression analysis	WMH volume ∼ ICA PI	not shown	>0.05	Age
MCA							
Oscar H. Del Brutto [33]	2015	70	Generalised linear model	WMH severity ∼ MCA PI	β = 0.065, 95% CI[−0.084, 0.177]	0.474	Age, sex, the cardiovascular health status
				WMH severity ∼ vertebral artery	β = 0.066, 95% CI [−0.024, 0.156]	0.146	
Joao Sargento-Freitas [29]	2014	439	Multiple ordinal regression	DWMH score ∼ MCA PI	OR 17.994, 95% CI [6.875, 47.11]	<0.001	Age, sex, HBp history, DM, smoking, dyslipidaemia, coronariopathy, heart failure, obesity, peripheral artery disease, alcoholism, IMT
				PVH score ∼ MCA PI	OR 5.739, 95% CI [2.288, 14.397]	<0.001	
				Basal ganglia score ∼ MCA PI	OR 11.844, 95% CI [4.486, 31.268]	<0.001	
Sang Won Han [35]	2014	130	Pearson correlation	WMH volume ∼ MCA PI	*R*=0.195	0.026	No
Sushmita Purkayastha [28]	2014	48	Multivariable linear regression	WMH/ICV ∼ MCA PI	OR 1.25, 95% CI [0.14, 2.09]	<0.01	Age, sex, race, DM, HBp
Alastain J. S. Webb [27]	2012	110	Ordinal regression	WMH score ∼ MCA PI	β = 4.33	*P*=0.037	Age, sex, physiology
Vincent Mok [26]	2012	159*	Multiple logistic regression	Severe WMH (vs without severe WMH) ∼ MCA PI	OR = 1.33, 95% CI [1.04,1.70] per 0.1 increase in PI	<0.01	Age
Ioannis Heliopoulos [14]	2012	52	Multivariable regression	WMH score ∼ MCA PI	β = 0.262	*P*=0.025	Age, sex, BMI, HBp, DM, hyperlipidaemia, smoking
Iria Rodriguez [25]	2010	186	Multivariate logistic analysis	Lacunar infarct (vs non-lacunar) ∼ MCA PI	OR = 8.13, 95% CI [1.17, 56.27]	0.034	Previous ranking score, WMH, retinal microangiopathy
Rosa M. Sánchez-Pérez [24]	2003	116	Multiple linear regression	Leukoaraiosis severity score ∼ MCA PI	β = −0.108	0.353	Age, sex, vascular risk factors, cognitive performance, blood flow velocity in MCA
Chelsea S. Kidwell [23]	2001	55	Multivariate regression	WMH score ∼ MCA PI	0.71	*P*<0.05	Age, sex, HBp, coronary artery disease
Brain tissue pulsatility							
Redouane Ternifi [20]	2014	9	Non-parametric spearman correlation	WMH volume ∼ Max BTD	ρ = −0.86	<0.001	No
				WMH volume ∼ Mean BTD	ρ = −0.72	<0.001	No
MRI studies							
Clive B. Beggs [10]	2016	101	Multiple linear regression	total WMH volume ∼ CSF peak negative velocity	β = −124.903	*P*=0.041	Age
Anders Wåhlin [39]	2014	37	Ordinary linear regression	Total brain volume ∼ arterial PI	β = −0.42	*P*<0.01	Age, ICV, arterial net flow
				Total brain volume ∼ CSF flow volume pulsatility	β = −0.44	*P*<0.01	Age, ICV, arterial net flow

Continued over

Clinical Science (2018) **132** 157–171
https://doi.org/10.1042/CS20171280

Table 3 Results of correlation analyses in MRI and ultrasound studies (Continued)

First author	Year	Sample size	Correlation or regression models	Variables ($y \sim x$)	Coefficient	*P* value	Adjustment for confounding factors
Todd A.D Jolly [38]	2013	35	Partial correlation	WMH volume ~ pulse wave amplitude in arteries or venous sinuses	not shown	$P>0.05$	Age
				WMH volume ~ pulse width in arteries or sinuses	not shown	$P>0.05$	Age
				WMH volume ~ PI in arteries or venous sinuses	not shown	$P>0.05$	Age

Abbreviations: BMI, body mass index; BTD, brain tissue displacement; CI, confidence interval; CSF, cerebrospinal fluid; DM, diabetes mellitus; DWI, diffusion-weighted imaging; DWMH, deep white matter hyperintensities; HBp, hypertension; ICA, internal carotid artery; ICV, intracranial volume; IMT, intima-media thickness; MCA, middle cerebral artery; OR, odds ratio; PI, pulsatility index; PVH, periventricular white matter hyperintensities; SD, standard deviation; WMH, white matter hyperintensities.
*The original sample size of this study [26] was 205 but only 159 participants were included in the analysis.

Eight studies used visual rating scores to assess SVD burden, whereas the other eight measured WMH or brain volume, among which one used manual ROIs [38], one used semi-automated [10] and six used automated masks. Only 2/6 of the papers using automated masks reported that the masks were manually checked [35,39].

Doppler ultrasound studies

Two studies measured ICA and eleven measured MCA. Most studies (apart from two [19,24]) reported a significant association between increased ICA or MCA PI and more WMH after adjustment for age. One (n=186) found that higher MCA PI was predictive of having a lacunar infarct (vs other types of infarct) [25]. One paper (n=159) mentioned that they did not find significant associations between MCA PI and microbleeds or lacunes, although no detailed information was provided [26].

One study (n=9) found that higher brain tissue displacement, which was used for representing brain tissue pulsatility, was significantly correlated with larger WMH volume, however it did not adjust for any co-variates [20] (Table 3).

MRI studies

All three MRI studies adjusted for age. Two assessed WMH volume showing that increased WMH volume was significantly associated with higher CSF systolic peak velocity in one study (n=101, $\beta = -124.903$, P=0.041) [10], but not with arterial or venous pulsatility (pulse amplitude, pulse width or PI) in the other (n=35) [38].

One study (n=37) found that increased arterial PI and cervical CSF pulsatility were associated with smaller brain volume in healthy volunteers [39] (Table 3).

Discussion

We identified 27 studies that assessed intracranial pulsatility in relation to SVD features including 3356 subjects. Most studies found a significant association between increased intracranial pulsatility and SVD. However, these studies showed considerable heterogeneity with regard to participants' clinical characteristics, adjustment for co-variates, image acquisitions and processing, vessels or regions of interest studied, and pulsatility measures used. About half of the studies gave little detail on control of bias, such as use of blinding. We were not able to perform a formal meta-analyse due to the substantial heterogeneities and limited data, although we were able to calculate summary statistics for WMH and pulsatility for some studies.

The limitations of the literature include that SVD features differed or were assessed differently across studies. Most studies used WMH volume or semi-quantitative score to represent SVD burden. Only half of the papers reported the expertise of the observers doing the SVD rating. Semi-quantitative scales and volumes of WMH were shown to be closely correlated and nearly equivalent in estimating WMH burden [40,41]. However, volumetric methods might be more sensitive in detecting subtle WMH differences [42] and may require smaller sample sizes in longitudinal studies [43], but are more difficult to undertake and require more resources than visual rating in a large-scale study

with follow-ups. Many studies used automated approaches to measure WMH volume but very few reported whether the WMH masks were manually checked, but failure to check increases errors. So far there is no automated method that can identify WMH without any manual input [44]. Two studies used recent small subcortical (lacunar) ischaemic stroke as the SVD feature: one referred to subcortical infarct on imaging whereas one used the definition of "small vessel disease" in the TOAST classification. Although there is overlap between the two definitions, they are different: "small vessel disease" in TOAST involves clinical features and consideration of vascular risk factors and does not necessarily need imaging evidence [45]. Studies that assessed pulsatility in relation to other SVD features including lacunes [26], microbleeds [26], or atrophy [39] were scant and lacked details of analysis. So far no clinical studies have reported the relationship between cerebrovascular pulsatility and PVS visibility. Enlarged PVS is one of the most consistent imaging findings of SVD, but the underlying pathophysiology remains unknown. Increasing evidence suggest that altered cerebrovascular pulsatility might affect the ISF–CSF exchange and impede the clearance of toxic solutes through the perivascular glymphatic system, which might possibly result in enlarged PVS [7,46]. Thus future SVD studies should consider including PVS especially when investigating the role of cerebrovascular pulsatility in SVD.

A third of papers provided little detail on patients' demographic or health characteristics. Age and blood pressure are thought to influence intracranial pulsatility [47,48] and are also important risk factors of SVD [2] and should be adjusted for in relevant studies. Most studies that performed correlation or regression analysis have adjusted for age, but in studies that performed comparisons of WMH, patients with more severe WMH were significantly older than those with mild WMH [9,27,36,37]. Blood pressure also changes with age, but very few studies accounted for blood pressure in their analyses although some included history of hypertension as a co-variate.

Indices used to represent pulsatility also varied. Most studies focused on the ICA or MCA. When calculating vascular PI, both MRI and ultrasound studies applied Gosling's equation. However, some MRI scanners only collected flow values at 16 time points in the cardiac cycle [18,37], meaning that low temporal resolution might affect the accuracy of the PI value as the peak flow might have been missed. In studies that used Doppler ultrasound, another source of variability is inherent when using the technique, including the dependency on the skills of ultrasound technicians and the positioning of the probe. Although the reliability of Gosling's PI in representing vascular resistance has been questioned [49], there is evidence that ICA and MCA PI are well correlated with cerebrovascular reactivity measured using CO_2 stimulus or invasive monitoring [50,51]. One study used a novel ultrasound technique to measure brain tissue pulsatile movement, but it only had nine participants and the validity still needs to be tested [20].

Apart from including large arteries, four MRI studies also considered pulsatility in veins and CSF. As the volume inside the cranium is fixed, the venous system and CSF are also important components in compensating for arterial pressure [52]. Two studies calculated venous PI [9,38] and one measured venous stroke volume [13]. CSF pulsatility assessment varied in terms of both locations and indices. There is so far no accepted definition of pulsatility in CSF, although stroke volume seemed to be the most used. Future studies need to test the reliability of different measures and also select ones that provide more relevant measurements about pulsatility. In addition, one MRI study measured the delay between arterial peak and venous sinus peak [13] whereas another looked at the delay between arterial blood and aqueduct CSF pulsations [18]. These two measures also might be non-comparable, as it is suggested that CSF pulse through the aqueduct is associated with capillary expansion whereas the venous pulse at neck level relates more directly to the arterial expansion [52]. So far no studies have measured pulsatility in vessels more downstream than MCA or PCA due to the limitations of the methodology, such as the spatial resolution or the sequences of the MRI scanner. Future SVD studies could consider techniques such as 4D phase-contrast MRI or 7-T MRI which enables flow assessment in multiple vessels including perforating arteries [53,54], or blood-oxygenation-level-dependent MRI or ultra-fast magnetic resonance encephalography which could measure pulsatility in brain tissues [55,56].

Despite these heterogeneities, in general, most cross-sectional studies found that arterial or venous pulsatility was associated with worse SVD, although the relationship could be confounded by risk factors, particularly age and blood pressure. For ICA, one community based-study (n=700) with all participants aged 70 years that adjusted for age and other medical co-variates, found increased ICA PI to be independently associated with larger WMH volume [12], whereas in another study of diabetic patients (n=122) the significance of the association disappeared after adjustment for age [19]. The relationship between increased MCA PI and WMH or lacunar infarct was found in most studies after adjustment for confounding factors. We are unable to draw conclusions on the relationship between CSF pulsatility and WMH because of different indices and locations used by each study, but the trend seems to be that larger CSF stroke volume is related to more WMH. It was also impossible to conclude if any specific SVD features are more associated with pulsatility due to the very limited data on any features other than WMH.

This is the first paper to comprehensively summarize studies that measured intracranial pulsatility in relation to SVD. The strengths included a systematic search including papers in non-English languages and a careful assessment

Clinical Science (2018) **132** 157–171
https://doi.org/10.1042/CS20171280

of all included studies. However, we were not able to perform a meta-analysis due to many sources of heterogeneity, or to pool the results of association analyses as regression analyses were performed differently in each study.

In conclusion, most of the data support a cross-sectional association between SVD and higher pulsatility in large intracranial arteries such as MCA and ICA, although whether a specific SVD feature is more related to high intracranial pulsatility remains unknown, and it is not known if high pulsatility leads to more WMH or the opposite. Therefore, methodologically robust longitudinal studies are required to help establish cause and effect, such as measuring both WMH and intracranial pulsatility at baseline and follow-up. The sample size and follow-up duration of the longitudinal study might partly depend on the baseline WMH burden and which method of WMH estimation is used (visual rating or volumetric quantification), since baseline WMH burden is an important predictor for WMH progression and should be accounted for in the study design and analysis [57]. Ultimately, randomized clinical trials of agents to reduce vessel stiffness will be required to determine if reduction in pulsatility (as a measure of stiffness) prevents SVD progression. Doppler ultrasound might be affordable and easy to use when measuring pulsatility, but it has only limited access to individual vessels and requires experienced technicians. MRI techniques enable assessment of pulsatility in multiple and smaller vessels and in different types of brain tissues, which therefore should be encouraged in future studies. Agreement on reliable measures of intracranial pulsatility is also needed to allow for better comparison between studies, especially for CSF pulsatility. Future studies should clearly define participants' clinical features, use blinding, improve expertise in SVD assessment, and adjust for relevant co-variates.

Clinical perspectives

- Increasing evidence suggest that high intracranial pulsatility might be an underlying mechanism of small vessel disease (SVD).
- Most studies support a cross-sectional association between higher pulsatility in large intracranial arteries and white matter hyperintensities, but there are substantial variations between studies in pulsatility indices, and there is lack of longitudinal data and studies on other important SVD features such as perivascular spaces.
- Our results suggest that increased intracranial pulsatility might play an important role in the pathophysiology of SVD. However, future studies should minimize bias, adjust for potential confounders, include pulsatility in veins and CSF, and examine longitudinal relationship between pulsatility and SVD.

Author Contribution

Y.S. conceived the idea of the study and did the data search, extraction, and statistical analyses. M.J.T. cross-checked the search strategy. Y.S. drafted the report which was then revised by M.J.T., I.M., and J.M.W. All authors approved the manuscript.

Funding

The author(s) disclosed receipt of the following financial support for the research, authorship, and/or publication of this article: Y.S. is funded by China Scholarships Council. M.J.T is funded by NHS Lothian Research and Development Office. We acknowledge support from the Scottish Funding Council and Chief Scientist Office through the Scottish Imaging Network A Platform for Scientific Excellence (SINAPSE), the Medical Research Council through the Centre for Cognitive Ageing and Cognitive Epidemiology (CCACE), the Fondation Leducq Network for the Study of Perivascular Spaces in Small Vessel Disease (ref. no. 16 CVD 05) and European Union Horizon 2020, PHC-03-15, project No 666881, 'SVDs@Target'. The work is that of the authors and does not reflect the views of the funders.

Competing interests

The authors declare that there are no competing interests associated with the manuscript.

Abbreviations

CAA, cerebral amyloid angiopathy; CI, confidence interval; CSF, cerebrospinal fluid; CT, computed tomography; ECG, electrocardiogram; ICA, internal carotid artery; MCA, middle cerebral artery; MOOSE, meta-analysis of observational studies in

epidemiology; MRI, magnetic resonance imaging; PI, pulsatility index; PVS, perivascular space; SMD, standardised mean difference; STRIVE, Standards for Reporting Vascular changes on nEuroimaging; SVD, small vessel disease; TOAST, according to Trial of ORG 1072 in Acute Stroke Treatment; WMH, white matter hyperintensities.

References

1 Gorelick, P.B., Scuteri, A., Black, S.E., Decarli, C., Greenberg, S.M., Iadecola, C. et al. (2011) Vascular contributions to cognitive impairment and dementia: a statement for healthcare professionals from the american heart association/american stroke association. *Stroke* **42**, 2672–2713, https://doi.org/10.1161/STR.0b013e3182299496
2 Wardlaw, J.M., Smith, C. and Dichgans, M. (2013) Mechanisms of sporadic cerebral small vessel disease: insights from neuroimaging. *Lancet Neurol.* **12**, 483–497, https://doi.org/10.1016/S1474-4422(13)70060-7
3 Shi, Y. and Wardlaw, J. (2016) Update on cerebral small vessel disease: a dynamic whole-brain disease. *Stroke Vasc. Neurol.* **2**, 83–92, https://doi.org/10.1136/svn-2016-000035
4 Mitchell, G.F., van Buchem, M.A., Sigurdsson, S., Gotal, J.D., Jonsdottir, M.K., Kjartansson, O. et al. (2011) Arterial stiffness, pressure and flow pulsatility and brain structure and function: the Age, Gene/Environment Susceptibility–Reykjavik study. *Brain* **134**, 3398–3407, https://doi.org/10.1093/brain/awr253
5 Poels, M.M., Zaccai, K., Verwoert, G.C., Vernooij, M.W., Hofman, A., van der Lugt, A. et al. (2012) Arterial stiffness and cerebral small vessel disease: the Rotterdam Scan Study. *Stroke* **43**, 2637–2642, https://doi.org/10.1161/STROKEAHA.111.642264
6 Mitchell, G.F. (2008) Effects of central arterial aging on the structure and function of the peripheral vasculature: implications for end-organ damage. *J. Appl. Physiol. (1985)* **105**, 1652–1660, https://doi.org/10.1152/japplphysiol.90549.2008
7 Iliff, J.J., Wang, M., Zeppenfeld, D.M., Venkataraman, A., Plog, B.A., Liao, Y. et al. (2013) Cerebral arterial pulsation drives paravascular CSF-interstitial fluid exchange in the murine brain. *J. Neurosci.* **33**, 18190–18199, https://doi.org/10.1523/JNEUROSCI.1592-13.2013
8 Mestre, H., Kostrikov, S., Mehta, R.I. and Nedergaard, M. (2017) Perivascular spaces, glymphatic dysfunction, and small vessel disease. *Clin. Sci.* **131**, 2257–2274, https://doi.org/10.1042/CS20160381
9 Bateman, G.A. (2002) Pulse-wave encephalopathy: a comparative study of the hydrodynamics of leukoaraiosis and normal-pressure hydrocephalus. *Neuroradiology* **44**, 740–748, https://doi.org/10.1007/s00234-002-0812-0
10 Beggs, C.B., Magnano, C., Shepherd, S.J., Belov, P., Ramasamy, D.P., Hagemeier, J. et al. (2016) Dirty-appearing white matter in the brain is associated with altered cerebrospinal fluid pulsatility and hypertension in individuals without neurologic disease. *J. Neuroimaging* **26**, 136–143, https://doi.org/10.1111/jon.12249
11 Battal, B., Kocaoglu, M., Bulakbasi, N., Husmen, G., Tuba Sanal, H. and Tayfun, C. (2011) Cerebrospinal fluid flow imaging by using phase-contrast MR technique. *Br. J. Radiol.* **84**, 758–765, https://doi.org/10.1259/bjr/66206791
12 Aribisala, B.S., Morris, Z., Eadie, E., Thomas, A., Gow, A., Valdes Hernandez, M.C. et al. (2014) Blood pressure, internal carotid artery flow parameters, and age-related white matter hyperintensities. *Hypertension* **63**, 1011–1018, https://doi.org/10.1161/HYPERTENSIONAHA.113.02735
13 Bateman, G.A., Levi, C.R., Schofield, P., Wang, Y. and Lovett, E.C. (2008) The venous manifestations of pulse wave encephalopathy: windkessel dysfunction in normal aging and senile dementia. *Neuroradiology* **50**, 491–497, https://doi.org/10.1007/s00234-008-0374-x
14 Heliopoulos, I., Artemis, D., Vadikolias, K., Tripsianis, G., Piperidou, C. and Tsivgoulis, G. (2012) Association of ultrasonographic parameters with subclinical white-matter hyperintensities in hypertensive patients. *Cardiovasc. Psychiatry Neurol.* **2012**, 616572, https://doi.org/10.1155/2012/616572
15 Stroup, D.F., Berlin, J.A., Morton, S.C., Olkin, I., Williamson, G.D., Rennie, D. et al. (2000) Meta-analysis of observational studies in epidemiology: a proposal for reporting. Meta-analysis Of Observational Studies in Epidemiology (MOOSE) group. *JAMA* **283**, 2008–2012, https://doi.org/10.1001/jama.283.15.2008
16 Wardlaw, J.M., Smith, E.E., Biessels, G.J., Cordonnier, C., Fazekas, F., Frayne, R. et al. (2013) Neuroimaging standards for research into small vessel disease and its contribution to ageing and neurodegeneration. *Lancet Neurol.* **12**, 822–838, https://doi.org/10.1016/S1474-4422(13)70124-8
17 Higgins, J. and Green, S. (eds) (2011) *Cochrane Handbook for Systematic Reviews of Interventions Version 5.1.0 [updated March 2011]*, The Cochrane Collaboration, Available from http://www.handbook.cochrane.org
18 Naish, J.H., Baldwin, R.C., Patankar, T., Jeffries, S., Burns, A.S., Taylor, C.J. et al. (2006) Abnormalities of CSF flow patterns in the cerebral aqueduct in treatment-resistant late-life depression: a potential biomarker of microvascular angiopathy. *Magn. Reson. Med.* **56**, 509–516, https://doi.org/10.1002/mrm.20999
19 Tanaka, T., Shimizu, T. and Fukuhara, T. (2009) The relationship between leukoaraiosis volume and parameters of carotid artery duplex ultrasonographic scanning in asymptomatic diabetic patients. *Comput. Med. Imaging Graph.* **33**, 489–493, https://doi.org/10.1016/j.compmedimag.2009.04.007
20 Ternifi, R., Cazals, X., Desmidt, T., Andersson, F., Camus, V., Cottier, J.P. et al. (2014) Ultrasound measurements of brain tissue pulsatility correlate with the volume of MRI white-matter hyperintensity. *J. Cereb. Blood Flow Metab.* **34**, 942–944, https://doi.org/10.1038/jcbfm.2014.58
21 Turk, M., Zupan, M., Zaletel, M., Zvan, B. and Oblak, J.P. (2015) Carotid arterial hemodynamic in ischemic levkoaraiosis suggests hypoperfusion mechanism. *Eur. Neurol.* **73**, 310–315, https://doi.org/10.1159/000381706
22 Biedert, S., Forstl, H. and Hewer, W. (1995) Multiinfarct dementia vs Alzheimer's disease: Sonographic criteria. *Angiology* **46**, 129–135, https://doi.org/10.1177/000331979504600206
23 Kidwell, C.S., El-Saden, S., Livshits, Z., Martin, N.A., Glenn, T.C. and Saver, J.L. (2001) Transcranial doppler pulsatility indices as a measure of diffuse small-vessel disease. *J. Neuroimaging* **11**, 229–235, https://doi.org/10.1111/j.1552-6569.2001.tb00039.x

Clinical Science (2018) **132** 157–171
https://doi.org/10.1042/CS20171280

24 Sanchez-Perez, R.M., Hernandez-Lorido, R., Castano, P., Diaz-Marin, C., Carneado-Ruiz, J. and Molto-Jorda, J. (2003) Evaluation of hemodynamic parameters by transcranial Doppler in patients with leukoaraiosis. [Spanish]. *Rev. Neurol.* **37**, 301–311

25 Rodriguez, I., Lema, I., Blanco, M., Rodriguez-Yanez, M., Leira, R. and Castillo, J. (2010) Vascular retinal, neuroimaging and ultrasonographic markers of lacunar infarcts. *Int. J. Stroke* **5**, 360–366, https://doi.org/10.1111/j.1747-4949.2010.00462.x

26 Mok, V., Ding, D., Fu, J., Xiong, Y., Chu, W.W.C., Wang, D. et al. (2012) Transcranial doppler ultrasound for screening cerebral small vessel disease: A community study. *Stroke* **43**, 2791–2793, https://doi.org/10.1161/STROKEAHA.112.665711

27 Webb, A.J.S., Simoni, M., Mazzucco, S., Kuker, W., Schulz, U. and Rothwell, P.M. (2012) Increased cerebral arterial pulsatility in patients with leukoaraiosis: arterial stiffness enhances transmission of aortic pulsatility. *Stroke* **43**, 2631–2636, https://doi.org/10.1161/STROKEAHA.112.655837

28 Purkayastha, S., Fadar, O., Mehregan, A., Salat, D.H., Moscufo, N., Meier, D.S. et al. (2014) Impaired cerebrovascular hemodynamics are associated with cerebral white matter damage. *J. Cereb. Blood Flow Metab.* **34**, 228–234, https://doi.org/10.1038/jcbfm.2013.180

29 Sargento-Freitas, J., Felix-Morais, R., Ribeiro, J., Gouveia, A., Nunes, C., Duque, C. et al. (2014) Different locations but common associations in subcortical hypodensities of presumed vascular origin: Cross-sectional study on clinical and neurosonologic correlates. *BMC Neurology* **14**, 24, https://doi.org/10.1186/1471-2377-14-24

30 Sanahuja, J., Alonso, N., Diez, J., Ortega, E., Rubinat, E., Traveset, A. et al. (2016) Increased burden of cerebral small vessel disease in patients with type 2 diabetes and retinopathy. *Diabetes Care* **39**, 1614–1620, https://doi.org/10.2337/dc15-2671

31 Smith, E.E., Vijayappa, M., Lima, F., Delgado, P., Wendell, L., Rosand, J. et al. (2008) Impaired visual evoked flow velocity response in cerebral amyloid angiopathy. *Neurology* **71**, 1424–1430, https://doi.org/10.1212/01.wnl.0000327887.64299.a4

32 Hiroki, M., Miyashita, K., Yoshida, H., Hirai, S. and Fukuyama, H. (2003) Central retinal artery Doppler flow parameters reflect the severity of cerebral small-vessel disease. *Stroke* **34**, e92–4, https://doi.org/10.1161/01.STR.0000075768.91709.E4

33 Del Brutto, O.H., Mera, R.M., De La Luz Andrade, M., Castillo, P.R., Zambrano, M. and Nader, J.A. (2015) Disappointing reliability of pulsatility indices to identify candidates for magnetic resonance imaging screening in population-based studies assessing prevalence of cerebral small vessel disease. *J. Neurosci. Rural Prac.* **6**, 336–338, https://doi.org/10.4103/0976-3147.158760

34 Ghorbani, A., Ahmadi, M.J. and Shemshaki, H. (2015) The value of transcranial Doppler derived pulsatility index for diagnosing cerebral small-vessel disease. *Adv. Biomed. Res.* **4**, 54, https://doi.org/10.4103/2277-9175.151574

35 Han, S.W., Song, T.J., Bushnell, C.D., Lee, S.S., Kim, S.H., Lee, J.H. et al. (2014) Cilostazol decreases cerebral arterial pulsatility in patients with mild white matter hyperintensities: Subgroup analysis from the effect of cilostazol in acute lacunar infarction based on pulsatility index of transcranial doppler (ECLIPse) study. *Cerebrovasc. Dis.* **38**, 197–203, https://doi.org/10.1159/000365840

36 Bettermann, K., Slocomb, J.E., Shivkumar, V. and Lott, MEJ (2012) Retinal vasoreactivity as a marker for chronic ischemic white matter disease? *J. Neurol. Sci.* **322**, 206–210, https://doi.org/10.1016/j.jns.2012.05.041

37 Henry-Feugeas, M.C., Roy, C., Baron, G. and Schouman-Claeys, E. (2009) Leukoaraiosis and pulse-wave encephalopathy: Observations with phase-contrast MRI in mild cognitive impairment. *J. Neuroradiology* **36**, 212–218, https://doi.org/10.1016/j.neurad.2009.01.003

38 Jolly, TAD, Bateman, G.A., Levi, C.R., Parsons, M.W., Michie, P.T. and Karayanidis, F. (2013) Early detection of microstructural white matter changes associated with arterial pulsatility. *Front. Human Neurosci.* **7**, 782, https://doi.org/10.3389/fnhum.2013.00782

39 Wahlin, A., Ambarki, K., Birgander, R., Malm, J. and Eklund, A. (2014) Intracranial pulsatility is associated with regional brain volume in elderly individuals. *Neurobiol. Aging* **35**, 365–372, https://doi.org/10.1016/j.neurobiolaging.2013.08.026

40 Valdes Hernandez Mdel, C., Morris, Z., Dickie, D.A., Royle, N.A., Munoz Maniega, S., Aribisala, B.S. et al. (2013) Close correlation between quantitative and qualitative assessments of white matter lesions. *Neuroepidemiology* **40**, 13–22, https://doi.org/10.1159/000341859

41 Oboudiyat, C., Garderner, H., Marquez, C., Elkind, M., Sacco, R., DeCarli, C. et al. (2014) Comparing Semi-quantitative and Volumetric Measurements of MRI White Matter Hyperintensities: The Northern Manhattan Study. *Neurology* **82**, Supplement S62.007

42 van Straaten, E.C., Fazekas, F., Rostrup, E., Scheltens, P., Schmidt, R., Pantoni, L. et al. (2006) Impact of white matter hyperintensities scoring method on correlations with clinical data: the LADIS study. *Stroke* **37**, 836–840, https://doi.org/10.1161/01.STR.0000202585.26325.74

43 Chappell, F.M., Del Carmen Valdes Hernandez, M., Makin, S.D., Shuler, K., Sakka, E., Dennis, M.S. et al. (2017) Sample size considerations for trials using cerebral white matter hyperintensity progression as an intermediate outcome at 1 year after mild stroke: results of a prospective cohort study. *Trials* **18**, 78, https://doi.org/10.1186/s13063-017-1825-7

44 Wardlaw, J.M., Valdes Hernandez, M.C. and Munoz-Maniega, S. (2015) What are white matter hyperintensities made of? Relevance to vascular cognitive impairment. *J. Am. Heart Assoc.* **4**, 001140, https://doi.org/10.1161/JAHA.114.001140

45 Adams, Jr, H.P., Bendixen, B.H., Kappelle, L.J., Biller, J., Love, B.B., Gordon, D.L. et al. (1993) Classification of subtype of acute ischemic stroke. Definitions for use in a multicenter clinical trial. TOAST. Trial of Org 10172 in Acute Stroke Treatment. *Stroke* **24**, 35–41, https://doi.org/10.1161/01.STR.24.1.35

46 Weller, R.O., Djuanda, E., Yow, H.Y. and Carare, R.O. (2009) Lymphatic drainage of the brain and the pathophysiology of neurological disease. *Acta Neuropathol.* **117**, 1–14, https://doi.org/10.1007/s00401-008-0457-0

47 Stoquart-ElSankari, S., Baledent, O., Gondry-Jouet, C., Makki, M., Godefroy, O. and Meyer, M.E. (2007) Aging effects on cerebral blood and cerebrospinal fluid flows. *J. Cereb. Blood Flow Metab.* **27**, 1563–1572, https://doi.org/10.1038/sj.jcbfm.9600462

48 Wagshul, M.E., Eide, P.K. and Madsen, J.R. (2011) The pulsating brain: a review of experimental and clinical studies of intracranial pulsatility. *Fluids Barriers CNS* **8**, 5, https://doi.org/10.1186/2045-8118-8-5

49 Michel, E. and Zernikow, B. (1998) Gosling's Doppler pulsatility index revisited. *Ultrasound Med. Biol.* **24**, 597–599, https://doi.org/10.1016/S0301-5629(98)00024-6

50 Czosnyka, M., Richards, H.K., Whitehouse, H.E. and Pickard, J.D. (1996) Relationship between transcranial Doppler-determined pulsatility index and cerebrovascular resistance: an experimental study. *J. Neurosurg.* **84**, 79–84, https://doi.org/10.3171/jns.1996.84.1.0079

51 Beasley, M.G., Blau, J.N. and Gosling, R.G. (1979) Changes in internal carotid artery flow velocities with cerebral vasodilation and constriction. *Stroke* **10**, 331–335, https://doi.org/10.1161/01.STR.10.3.331

52 Stivaros, S.M. and Jackson, A. (2007) Changing concepts of cerebrospinal fluid hydrodynamics: role of phase-contrast magnetic resonance imaging and implications for cerebral microvascular disease. *Neurotherapeutics* **4**, 511–522, https://doi.org/10.1016/j.nurt.2007.04.007

53 Rivera-Rivera, L.A., Turski, P., Johnson, K.M., Hoffman, C., Berman, S.E., Kilgas, P. et al. (2016) 4D flow MRI for intracranial hemodynamics assessment in Alzheimer's disease. *J. Cereb. Blood Flow Metab.* **36**, 1718–1730, https://doi.org/10.1177/0271678X15617171

54 Bouvy, W.H., Geurts, L.J., Kuijf, H.J., Luijten, P.R., Kappelle, L.J., Biessels, G.J. et al. (2016) Assessment of blood flow velocity and pulsatility in cerebral perforating arteries with 7-T quantitative flow MRI. *NMR Biomed.* **29**, 1295–1304, https://doi.org/10.1002/nbm.3306

55 Kiviniemi, V., Wang, X., Korhonen, V., Keinanen, T., Tuovinen, T., Autio, J. et al. (2016) Ultra-fast magnetic resonance encephalography of physiological brain activity - Glymphatic pulsation mechanisms? *J. Cereb. Blood Flow Metab.* **36**, 1033–1045, https://doi.org/10.1177/0271678X15622047

56 Makedonov, I., Black, S.E. and Macintosh, B.J. (2013) BOLD fMRI in the white matter as a marker of aging and small vessel disease. *PLoS One* **8**, e67652, https://doi.org/10.1371/journal.pone.0067652

57 Gouw, A.A., van der Flier, W.M., Fazekas, F., van Straaten, E.C., Pantoni, L., Poggesi, A. et al. (2008) Progression of white matter hyperintensities and incidence of new lacunes over a 3-year period: the Leukoaraiosis and Disability study. *Stroke* **39**, 1414–1420, https://doi.org/10.1161/STROKEAHA.107.498535

Page Proof Instructions and Queries

Journal Title: International Journal of Stroke (WSO)

Article Number: 730740

Thank you for choosing to publish with us. This is your final opportunity to ensure your article will be accurate at publication. Please review your proof carefully and respond to the queries using the circled tools in the image below, which are available **by clicking "Comment"** from the right-side menu in Adobe Reader DC.*

Please use *only* the tools circled in the image, as edits via other tools/methods can be lost during file conversion. For comments, questions, or formatting requests, please use T. Please do *not* use comment bubbles/sticky notes.

*If you do not see these tools, please ensure you have opened this file with Adobe Reader DC, available for free at get.adobe.com/reader or by going to Help > Check for Updates within other versions of Reader. For more detailed instructions, please see us.sagepub.com/ReaderXProofs.

No.	Query
	Please confirm that all author information, including names, affiliations, sequence, and contact details, is correct.
	Please review the entire document for typographical errors, mathematical errors, and any other necessary corrections; check headings, tables, and figures.
	Please confirm that the Funding and Conflict of Interest statements are accurate.
	Please ensure that you have obtained and enclosed all necessary permissions for the reproduction of artistic works, (e.g. illustrations, photographs, charts, maps, other visual material, etc.) not owned by yourself. Please refer to your publishing agreement for further information.
	Please note that this proof represents your final opportunity to review your article prior to publication, so please do send all of your changes now.
AQ: 1	Journal style is to list all authors when there are six or fewer; when seven or more, first three should be listed and then 'etal.' should be added. In this article's reference list, there are already some references with three authors and etal. Can you please confirm that all these references have seven or more authors and not six or fewer? If six or fewer, please list all the authors with an 'and' before the last author.

International Journal of Stroke
WSO

International Journal of Stroke
0(0) 1–12

DOI: 10.1177/1747493017730740
journals.sagepub.com/home/wso
SAGE

Cerebrovascular reactivity measurement in cerebral small vessel disease: Rationale and reproducibility of a protocol for MRI acquisition and image processing

Michael J Thrippleton[1], Yulu Shi[1], Gordon Blair[1], Iona Hamilton[1], Gordon Waiter[2], Christian Schwarzbauer[3], Cyril Pernet[1], Peter JD Andrews[4], Ian Marshall[1], Fergus Doubal[1] and Joanna M Wardlaw[1]

Abstract

Background: Impaired autoregulation may contribute to the pathogenesis of cerebral small vessel disease. Reliable protocols for measuring microvascular reactivity are required to test this hypothesis and for providing secondary endpoints in clinical trials.

Aims: To develop and assess a protocol for acquisition and processing of cerebrovascular reactivity by MRI, in subcortical tissue of patients with small vessel disease and minor stroke.

Methods: We recruited 15 healthy volunteers, testing paradigms using 1- and 3-min 6% CO_2 challenges with repeat scanning, and 15 patients with history of minor stroke. We developed a protocol to measure cerebrovascular reactivity and delay times, assessing tolerability and reproducibility in grey and white matter areas.

Results: The 3-min paradigm yielded more reproducible data than the 1-min paradigm (CV respectively: 7.9–15.4% and 11.7–70.2% for cerebrovascular reactivity in grey matter), and was less reproducible in white matter (16.1–24.4% and 27.5–141.0%). Tolerability was similar for the two paradigms, but mean cerebrovascular reactivity and cerebrovascular reactivity delay were significantly higher for the 3-min paradigm in most regions. Patient tolerability was high with no evidence of greater failure rate (1/15 patients vs. 2/15 volunteers withdrew at the first visit). Grey matter cerebrovascular reactivity was lower in patients than in volunteers (0.110–0.234 vs. 0.172–0.313%/mmHg; $p < 0.05$ in 6/8 regions), as was the white matter cerebrovascular reactivity delay (16.2–43.9 vs. 31.1–47.9 s; $p < 0.05$ in 4/8 regions).

Conclusions: An effective and well-tolerated protocol for measurement of cerebrovascular reactivity was developed for use in ongoing and future trials to investigate small vessel disease pathophysiology and to measure treatment effects.

Keywords

Cerebrovascular reactivity, cerebral small vessel disease, magnetic resonance imaging, stroke

Received: 17 January 2017; accepted: 2 July 2017

Introduction

Cerebral small vessel disease (SVD) accounts for 20–25% of strokes and increases the risk of cognitive impairment, disability, and dementia. The pathogenesis is poorly understood but there is evidence of a role for increased vessel stiffness;[1,2] it is hypothesized that affected arterioles do not vasodilate efficiently in response to demand for increased blood flow, leading to secondary ischemic damage.[3] Impaired cerebrovascular reactivity (CVR) has been reported in Alzheimer's

[1]Neuroimaging Sciences, University of Edinburgh, Edinburgh, UK
[2]Aberdeen Biomedical Imaging Centre, University of Aberdeen, Aberdeen, UK
[3]Faculty of Applied Sciences & Mechatronics, Munich University of Applied Sciences, Munich, Germany
[4]Centre for Clinical Brain Sciences, University of Edinburgh, Edinburgh, UK

Corresponding author:
Joanna M Wardlaw, Centre for Clinical Brain Science, University of Edinburgh, 49 Little France Crescent, Edinburgh EH16 4SB, UK.
Email: joanna.wardlaw@ed.ac.uk

dementia[4] and cerebral amyloid angiopathy.[5] As a result, there is growing interest in endothelial dysfunction as a therapeutic target for treating SVD and clinical trials of licensed drugs with relevant modes of action (e.g. Cilostazol and isosorbide mononitrate; https://clinicaltrials.gov/ct2/show/NCT02481323) and antihypertensive drugs have recently commenced at our center and elsewhere.

Clinically feasible and reliable non-invasive methods for assessing microvessel reactivity would provide mechanistic insight and secondary endpoints in trials of drugs to prevent and reverse SVD. Transcranial Doppler ultrasound combined with a hypercapnic or pharmacologic challenge is well-established, and has been used to show reduced CVR in age-matched subjects with white matter hyperintensities (WMH) and similar vascular risk factors,[6] but only provides information on blood flow in a chosen large artery. In contrast, MRI permits CVR measurement throughout the brain using blood oxygenation level dependent (BOLD) imaging or arterial spin labelling (ASL) in response to a respiratory challenge. However, although CVR MRI has been widely used to study large artery diseases such as Moyamoya and carotid stenosis,[7,8] the technique has infrequently been applied in the study of SVD.[9–14] Although the aims, methods, and findings of these studies were varied, Uh et al.[14] reported a reduction in CVR both in WMH compared with normal-appearing WM (NAWM) and in the NAWM of subjects with greater WMH burden. This suggests a potentially valuable role for CVR measurement as a secondary endpoint in clinical trials of drugs for SVD prevention and reversal.

The aim of our work was to develop and pilot a robust, reliable, and well-tolerated protocol for reproducible and tolerable measurement of CVR in patients presenting with minor ischemic stroke, with emphasis on measurements in subcortical regions of the brain. The minor stroke population allows both assessment of CVR in relation to stroke etiology (SVD versus large artery disease) and CVR in relation to specific SVD radiological features, which while more common in SVD stroke are prevalent in stroke patients regardless of stroke etiology.[15,16] We tested two different hypercapnia paradigms with BOLD MRI, with repeat scanning to measure reproducibility, and recorded tolerability and symptoms associated with the procedures. In addition, we developed an image analysis protocol for measuring CVR in multiple grey matter (GM) and white matter (WM) brain areas relevant to SVD, including subcortical GM, deep WM, and periventricular regions, deriving CVR and CVR delay values for both healthy volunteers and patients.

Methods

Participants

We recruited healthy volunteers, who were asked to attend two CVR scanning sessions, and patients with a history of minor stroke, who were invited to a single scanning session. The study was conducted following Research Ethics Committee approvals (ref. 14/HV/0001 and 14/EM/1126) and according to the principles expressed in the Declaration of Helsinki. All subjects gave written informed consent.

Healthy volunteers were recruited from the surrounding area, excluding any potential participants having cardiovascular or respiratory illness, hypertension, migraine, anxiety disorders, and panic attacks; we also excluded those with a known family history of intracranial aneurysm, subarachnoid hemorrhage, arteriovenous malformation as well as those with contraindications to MRI.

Patients were recruited from the in- and out-patient stroke service as described previously.[17,18] We recruited patients presenting with a new clinical diagnosis of minor ischemic stroke, i.e. that was non-disabling, and also from our register of patients with a clinical diagnosis of minor non-disabling ischemic stroke in the past five years. ''Non-disabling'' was defined as not requiring assistance in activities of daily living. We included those with diabetes, hypertension, and other vascular risk factors as long as these were well controlled. We excluded patients with unstable hypertension, unstable diabetes, other neurological disorders, significant cardiac or respiratory illness or other life threatening medical conditions. We also excluded patients unable to give consent, with contraindications to MRI, and who had hemorrhagic stroke (but not hemorrhagic transformation of an infarct).

Participants were administered CO_2 in medical air at a concentration of 6% via a disposable anesthetic face mask (Intersurgical, Wokingham, UK) for a test period prior to entering the scanner in order to familiarize them with the respiratory challenge and related equipment, and to monitor them for anxiety and other symptoms. Anecdotally, it has been reported that a 4% CO_2 gas mixture is noticeably better tolerated compared with 6% CO_2, though a smaller vasodilatory effect is expected. Therefore, we used simple randomization to allocate the first 10 patients to either 4% CO_2 or 6% CO_2 to assess the impact on procedure tolerability and aid in the planning of future studies; patients but not researchers were blinded to CO_2 concentration.

Magnetic resonance imaging

During CVR MRI, subjects wore a unidirectional breathing circuit (Figure 1) designed by the University

Figure 1. (a) CVR MRI breathing circuit, designed by the University of Aberdeen and Intersurgical (Wokingham, UK). Red and blue arrows indicate the flow of inhaled and exhaled gas respectively. 1 = oxygen tubing for gas delivery; 2 = open-ended reservoir tube; 3 = anaesthetic face mask; 4,5 = one-way valve; 6 = exit port for exhaled gas; 7 = gas sampling line. (b) Photograph showing subject positioned in the head coil with the breathing circuit and patient monitoring equipment in place.

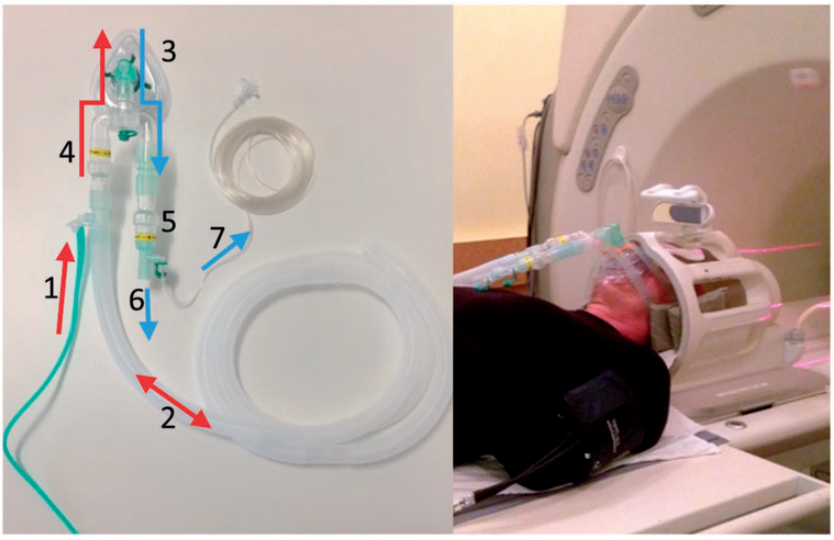

of Aberdeen and Intersurgical (Wokingham, UK; product code: 2013018) that enabled administration of air or a gas mixture containing 4 or 6% carbon dioxide; the circuit was open to room air via a length of anesthetic breathing circuit (with a volume greater than tidal volume (350 ml)) that served as a gas reservoir and ensured participant safety when the cylinder gas flow rate was insufficient or turned off. To ensure that accurate concentrations of CO_2 were administered, two cylinders of certified, medical grade gas mixtures were used, containing 6% CO_2, 21% O_2, 73% N_2, and 4% CO_2, 21% O_2, 75% N_2, respectively (BOC Special Products, UK). The CO_2 gas mixture was administered to volunteers using both a "1-min" (four 1-min blocks of air alternated with three 1-min blocks of CO_2)[19] and a "3-min" (three 2-min blocks of air interleaved with two 3-min blocks of CO_2)[20] paradigm; as the results showed improved reproducibility with the latter, the 3-min paradigm alone was used for patient CVR scans. We measured vital signs (peripheral oxygen saturation, blood pressure, heart rate, end-tidal CO_2 (ETCO2), and respiratory rate) using a CD-3A CO_2 sensor (AEI Technologies, Pittsburgh, USA) and MR patient monitors (Millennia 3155A and Magnitude 3150 MRI; Invivo, Best, The Netherlands). Gas cylinders and CO_2 sensors were positioned in the MR control room; tubes and sample lines entered the scanner room via a waveguide.

Magnetic resonance imaging was acquired with a 1.5 Tesla MRI scanner (Signa HDxt, General Electric, Milwaukee, WI) using an 8-channel phased-array head coil. BOLD images were acquired every 3 s during the CVR scan using axial single-shot gradient echo echo-planar imaging (GE-EPI; TR/TE = 3000/45 ms, 90° flip angle, 25.6 × 25.6 cm field of view (FoV), 64 × 64 acquisition matrix, 36 × 4 mm contiguous slices), including eight dummy scans prior to the start of the gas paradigm.

For minor stroke patients, axial T2-weighted (T2W; TR/TE = 7000/90 ms, 24 × 24 cm FoV, Propeller acquisition with matrix size 384, 1.5 signal averages, 36 × 4 mm contiguous slices), axial fluid-attenuated inversion recovery (FLAIR; TR/TE/TI = 8000/100/2000, 24 × 24 cm FoV, 320 × 256 acquisition matrix, 36 × 4 mm contiguous slices), gradient echo (GRE; TR/TE = 900/15 ms, 20° flip angle, 24 × 24 cm FoV, 384 × 256 acquisition matrix, 36 × 4 mm contiguous slices) and 3D T1-weighted imaging (T1W; inversion recovery-prepared spoiled gradient echo (SPGR), sagittal acquisition, TR/TE/TI = 9.6/4.0/500 ms, 8° flip angle, 25.6 × 25.6 cm FoV, 192 × 192 acquisition matrix, 160 × 1.3 mm slices). For healthy volunteers, T2W and T1W structural images only were obtained using similar parameters.

Participants were asked to rate the tolerability of the CVR procedure on a four-point scale ("intolerable," "not very tolerable," "tolerable," or "very tolerable") and healthy volunteers were asked which of the two paradigms was more tolerable.

Image processing and analysis

End-tidal CO_2. $ETCO_2$ values were obtained using the Millenia monitor with 1-s temporal resolution and stored digitally. For patients and a subset of the volunteers, CO_2 waveforms generated by the CD-3A sensor were recorded digitally with a sampling rate of $20.s^{-1}$; these were converted to $ETCO_2$ profiles using in-house Matlab code for identifying peaks in CO_2 concentration corresponding to end-tidal values (MathWorks, Inc., MA, USA), which were temporally aligned with the Millenia $ETCO_2$ profile. The CD-3A sensor was calibrated prior to each scan using room air and the certified gas mixtures, and readings from this device were used for determining CVR in patients; since most of the volunteers were measured using the Millenia monitor, $ETCO_2$ readings were calibrated against the CD-3A device in a subset of volunteers so that data for patients and volunteers could be compared.

CVR. A range of parameters and quantification methods have been proposed for CVR measurement, including linear regression with[21] and without[19] a tissue-dependent delay, parameterization of the ETCO2-BOLD response curve,[22] frequency-domain analysis,[23] and fitting the signal response using a non-linear model.[24] We chose to use linear regression with a variable CVR delay, since this method is relatively computationally efficient and there is good evidence for a tissue-dependent delay in the BOLD response to CO_2.[21] The BOLD signal was regressed with an intercept against ETCO2 and scan number (to account for linear signal drift). The CVR (units %/mmHg) is the regression coefficient corresponding to the $ETCO_2$ regressor, with the latter shifted by the delay that minimizes the residual sum of squares, and is expressed as a percentage of the mean signal during the first 45 s of the paradigm. CVR and CVR delay were calculated in a voxel-wise manner to generate parameter maps using the mean signal for each ROI. CVR delay values were adjusted by +4 s to account for the time delay between exhalation and detection of CO_2 concentration changes.

Image pre-processing. MR images were converted from DICOM to NIFTI format using SPM8 (Wellcome Department of Imaging Neuroscience, London, UK); BOLD dummy scans recorded prior to the start of the paradigm were discarded and the remaining volumes were spatially aligned to the mean volume using the two-pass procedure in SPM8. T1W images were co-registered to the T2W images using rigid-body registration and the transformation between the T2W and mean BOLD image spaces was determined (FSL FLIRT[25]).

Regions of interest. The contrast-to-noise ratio of the BOLD signal for individual voxels is generally small, resulting in somewhat noisy parameter maps, particularly in the WM.[23] Many studies have employed automatically generated tissue masks as regions of interest (ROIs) to increase the contrast-to-noise ratio and improve the model fitting, though such an approach does not provide regional information and assumes a global CVR delay. We therefore selected an intermediate approach, using ROIs to reduce the influence of noise[21] while retaining region- and tissue-specific information. Sixteen ROIs were chosen to sample WM and subcortical GM brain areas affected by SVD in addition to two cortical GM ROIs (Figure 2). First, an axial slice intersecting the basal ganglia was chosen and ROIs covering the caudate heads, thalamus, and putamen were drawn. A second slice superior to the basal ganglia showing the lateral ventricles was chosen for WM (periventricular, frontal and posterior) and cortical GM (frontal and parietal lobe) ROIs. Finally, a slice superior to the lateral ventricles was selected and ROIs covering the centrum semiovale were drawn. For each slice, the ROIs were extended to cover the same regions or structures on a neighboring slice to increase the signal-to-noise ratio (for frontal and posterior WM ROIs, three neighboring slices were used). For patients, stroke lesions (as identified on the FLAIR image) were excluded from the ROIs. Finally, the ROIs were overlaid on the co-registered CVR maps; voxels covering midline hyperintensities on the CVR maps corresponding to blooming around the large veins and venous sinuses were excluded to reduce the influence of large vessels.

Statistical analysis

Descriptive statistics in the text are presented as mean ± standard deviation. Differences within and between the participant groups were tested in Matlab using the *t*-test, assuming unequal variance for unpaired data and with $p < 0.05$ (two-sided) as the significance threshold. Reproducibility was measured using variance component analysis in Matlab (*anovan* function) and illustrated using Bland–Altman plots.[26] The standard deviations resulting from this procedure are presented as coefficients of variation (CVs), i.e. normalized to the mean (averaged first over both visits and then over subjects).

Results

Compliance, tolerability, and symptoms

Among the 15 healthy volunteers (mean age 33.8 ± 9.5, range 22–50 years; 27% female), CVR scans were obtained in 13/15. Two subjects withdrew before data were collected (one tolerated the pre-scan CO_2 test run

Figure 2. (a) Regions of interest for a healthy volunteer, (b) CVR magnitude (%/mmHg) and (c) CVR delay (s) parameters maps at the slice level shown by the right hand image in (a); both parameter maps were generated using BOLD data smoothed using a 4 mm full width at half maximum Gaussian kernel (note that ROI data were generated from unsmoothed data). (d–e) BOLD MRI signal (dotted line) and model fit (solid line) for the (d) right putamen and (e) right centrum semiovale ROIs. The signal drift visible in (d–e) is accounted for by a term in the model.

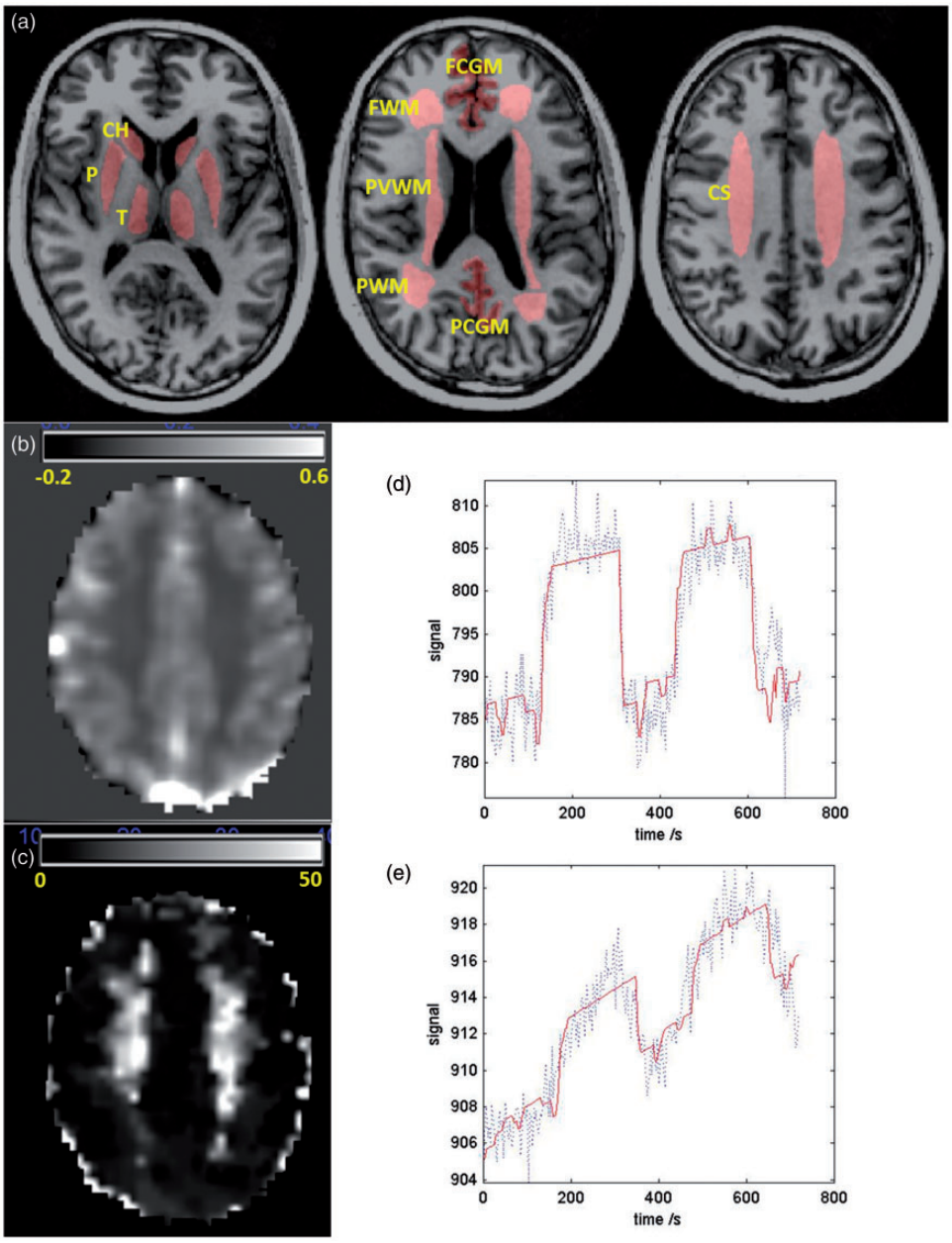

but experienced claustrophobia shortly after entering the scanner and a second experienced anxiety during the pre-scan CO_2 test run); 11 of the 13 volunteers scanned agreed to be scanned on a second occasion (one had left the area, a second was excluded due to anxiety during the first visit); one of the repeat scans was halted due to sustained tachycardia that was likely caused by anxiety exacerbated by head cold symptoms (the subject had rated the first scan ''very tolerable''). Two scans were interrupted due to scanner failure; at two of the visits, the start time was not recorded, providing CVR but not CVR delay values. Most of the

CVR scans (11/15 for visit 1, 9/12 for visit 2) were rated as either "tolerable" or "very tolerable" (Figure 3).

Volunteers had a range of previously described hypercapnia-related symptoms: respiratory symptoms (variously reported as shortness of breath, breathing resistance etc.; $n = 12$ of 24 CVR scanning sessions initiated), anxiety ($n = 2$), and temporary nausea, paraesthesia, confusion and blurred vision ($n = 1$). Three participants had transient tachycardia apparent from physiological monitoring data. No symptoms were reported following 10 of the scans. One subject reported the 3-min paradigm as more tolerable, while two subjects preferred the 1-min paradigm and one subject chose a different paradigm at either visit; the remainder had no preference.

Among the 15 patients (mean age 66.4 ± 8.1, range 53–77 years; 20 % female), 14/15 completed CVR scanning, compared with 13/15 for the volunteers (one subject tolerated the hypercapnic challenge outside the scanner but was unable to tolerate MRI due to claustrophobia), all of whom rated the procedure as "tolerable" or "very tolerable" (Figure 3). Five patients reported no hypercapnia symptoms, while others reported respiratory symptoms ($n = 9$), anxiety ($n = 1$) and paraesthesia ($n = 1$). Tolerability was similar among the 10 patients randomized to different CO_2 concentrations: patients administered 4% CO_2 rated the scans as very tolerable ($n = 2$), tolerable ($n = 2$) or intolerable ($n = 1$; experienced claustrophobia as noted above), while those administered 6% CO_2 rated the scans as either very tolerable ($n = 4$) or tolerable ($n = 1$). Since similar CVR values were observed (Figure 4(e) and (f)) with greater changes in $ETCO_2$ for 6% versus 4% CO_2 administration (12.8 ± 3.7 vs. 8.0 ± 1.0 mmHg, $p < 0.01$), the higher CO_2 concentration was used for subsequent patient scans.

Patients had a range of radiological SVD features including lacunes (60%), cerebral microbleeds (6.7%), enlarged perivascular spaces (PVS; basal ganglia PVS scores: 1 (40%), 2 (40%), 3 (20%); centrum semiovale PVS scores: 0 (0%), 1 (33.3%), 2 (6.7%), 3 (46.7%), 4 (13.3%)), and WMH (perventricular Fazekas scores: 0 (6.7%), 1 (60%), 2 (33.3%); deep WM Fazekas scores: 0 (13.3%), 1 (66.7%), 2 (20%)).

Comparison of paradigms and reproducibility in healthy volunteers

CVR and CVR delay measurements for each ROI are shown in Table 1 and Figure 4(a) and (b). Average CVR was significantly greater for the 3-min versus the 1-min paradigm for all ROIs (0.041–0.313 vs. 0.021–0.251%/mmHg respectively, $p < 0.05$); the average CVR delay was similar in most GM ROIs, but was longer for the 3-min paradigm in WM ROIs. Inter-visit coefficients of variation (CV; Table 2) were lower for the 3-min paradigm in most ROIs (7.9–15.4% vs. 11.7–70.2% respectively for CVR in GM). Large or negative variance estimates were found in some ROIs for the 1-min paradigm; inspection of the Bland–Altman plots (Supplementary Figures 1 to 4) and individual model fits showed these data to be affected by outliers caused by the periodicity of the 1-min paradigm; as illustrated in Supplementary Figure 5, the algorithm fits some noisy data by reversing the sign of the fitted CVR while increasing the CVR delay by 60 s. This effect was not seen for the 3-min paradigm due to the lower frequency of the stimulus.

Regional CVR in healthy volunteers and patients

Table 1 and Figure 4(c) and (d) compare CVR and CVR delays obtained in volunteers and patients,

Figure 3. Tolerability of CVR scanning for healthy volunteers and patients. Charts indicate the tolerability ratings given at each visit by participants.

Figure 4. Mean (a) CVR and (b) CVR delay values in healthy volunteers for the 1-min and 3-min CO_2 paradigms, averaged first over visits and secondly over subjects. (c–d) compare mean (c) CVR and (d) CVR delay values for healthy volunteers and patients, obtained using the 3-min gas paradigm. (e–f) compare mean (e) CVR and (f) CVR delay for patients scanned using 4% ($n = 4$) and 6% ($n = 10$) CO_2 gas mixtures. "*" indicates a significant difference ($p < 0.05$) between paradigms, between patients and volunteers, or between CO_2 concentrations; error bars indicate the standard deviation after averaging over visits (part (a) only).

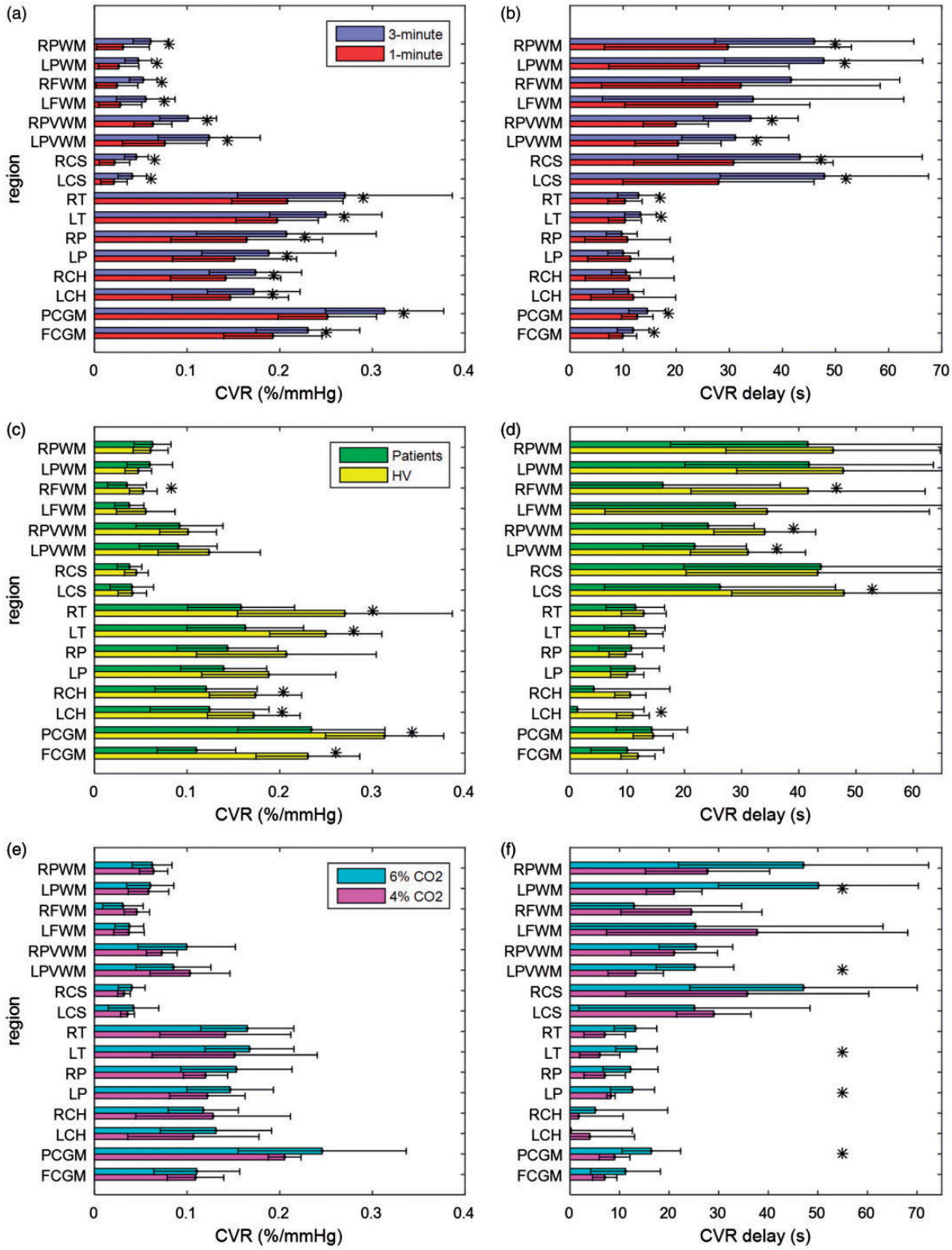

Table 1. Mean CVR and CVR delay measurements in healthy volunteers and patients

	CVR (%/mmHg)			CVR Delay (s)		
	Healthy volunteers		Patients	Healthy volunteers		Patients
region	1 min	3 min	3 min	1 min	3 min	3 min
FCGM	0.193 (0.053)	0.230[a] (0.056)	0.110[b] (0.042)	9.9 (2.6)	11.9[a] (3.0)	10.0 (6.4)
PCGM	0.251 (0.053)	0.313[a] (0.064)	0.234[b] (0.079)	12.7 (3.0)	14.5[a] (3.5)	14.3 (6.2)
LCH	0.147 (0.063)	0.172[a] (0.050)	0.124[b] (0.064)	11.9 (8.0)	11.0 (2.9)	1.3[b] (11.7)
RCH	0.142 (0.060)	0.174[a] (0.050)	0.120[b] (0.055)	11.2 (8.4)	10.5 (2.7)	4.1 (13.3)
LP	0.151 (0.067)	0.188[a] (0.072)	0.139 (0.046)	11.4 (8.0)	10.0 (2.9)	11.4 (4.3)
RP	0.164 (0.082)	0.207[a] (0.097)	0.144 (0.054)	10.8 (8.0)	9.7 (2.9)	10.7 (5.7)
LT	0.197 (0.045)	0.250[a] (0.061)	0.163[b] (0.063)	10.3 (3.1)	13.3[a] (3.0)	11.3 (5.3)
RT	0.208 (0.060)	0.270[a] (0.116)	0.158[b] (0.058)	10.3 (3.2)	12.9[a] (3.9)	11.4 (5.1)
LCS	0.021 (0.014)	0.041[a] (0.015)	0.040 (0.024)	28.0 (18.0)	47.9[a] (19.6)	26.2[b] (20.2)
RCS	0.022 (0.016)	0.045[a] (0.013)	0.038 (0.013)	30.8 (18.8)	43.3[a] (23.0)	43.9 (23.9)
LPVWM	0.076 (0.046)	0.124[a] (0.055)	0.090 (0.042)	20.3 (8.1)	31.1[a] (10.1)	21.8[b] (9.0)
RPVWM	0.063 (0.020)	0.101[a] (0.031)	0.092 (0.047)	19.9 (6.1)	34.0[a] (8.9)	24.1[b] (8.1)
LFWM	0.028 (0.023)	0.055[a] (0.032)	0.038 (0.016)	27.7 (17.4)	34.5 (28.4)	28.9 (36.3)
RFWM	0.024 (0.023)	0.053[a] (0.015)	0.035[b] (0.021)	32.2 (26.2)	41.6 (20.5)	16.2[b] (20.5)
LPWM	0.026 (0.022)	0.047[a] (0.014)	0.060 (0.025)	24.3 (17.0)	47.8[a] (18.6)	41.8 (21.7)
RPWM	0.031 (0.028)	0.061[a] (0.019)	0.063 (0.020)	29.7 (23.3)	46.0[a] (18.7)	41.6 (24.0)

Note: Healthy volunteer measurements were first averaged over both scans.
[a]Indicates a significant difference between 1-min and 3-min paradigms.
[b]Indicates a significant difference between patients and healthy volunteers (3-min paradigm; $p < 0.05$).
RPWM/LPWM: right/left posterior WM; RFWM/LFWM: right/left frontal WM; RPVWM/LPVWM: right/left periventricular WM; RCS/LCS: right/left centrum semiovale; RT/LT: right/left thalamus; RP/LP: right/left putamen; RCH/LCH: right/left caudate head; PCGM: posterior cortical GM; FCGM: frontal cortical GM.

measured using the same 3-min CO_2 paradigm. Mean CVR was higher for healthy volunteers in most GM ROIs (0.172–0.313 vs. 0.110–0.234%/mmHg); CVR was lower in WM regions, where mean values were similar for volunteers and patients (0.035–0.124%/mmHg). The CVR delay was similar for patients and volunteers in GM (1.3–14.5 s); in some WM ROIs, the CVR delay was significantly greater for healthy volunteers than for patients (16.2–43.9 vs. 31.1–47.9 s).

Discussion

Several cerebrovascular vasodilatory stimuli and paradigms have been presented in the literature but rarely tested in our patient population. Our first aim was therefore to select a suitable stimulus for studies of cerebral SVD and minor stroke. A range of methods have been proposed, including simple respiratory challenges such as breath-holding and hyperventilation, pharmacologic stimuli such as acetazolamide, inspired gas challenges, and automated systems for targeting precise changes in end-tidal gas concentration. We selected a hypercapnic challenge because CO_2 is endogenous, simple to administer and measure using widely available equipment, and safe to inhale at low concentrations. A fixed-inspired CO_2 challenge was chosen as a compromise between experimental precision and ease of implementation for use in multicenter clinical studies: unlike an acetazolamide injection, a CO_2 stimulus is easily administered and quickly reversed; hyperventilation and breath-hold challenges require less equipment but rely on a higher degree of

Table 2. Coefficients of variation (%) resulting from variance component analysis of healthy volunteer data for both CO_2 paradigms

	CV_{CVR} (%)				$CV_{CVR\ Delay}$ (%)			
	1 min		3 min		1 min		3 min	
region	Subject	Visit	Subject	Visit	Subject	Visit	Subject	Visit
FCGM	28.1	15.1	21.5	10.7	23.6	20.8	25.2	16.1
PCGM	16.8	17.1	15.2	15.4	16.1	23.1	5.3	30.9
LCH	29.0	49.6	27.6	7.9	-	120.7	23.2	23.6
RCH	-	70.2	27.6	8.7	-	128.6	20.6	25.1
LP	26.0	51.9	31.1	13.6	-	126.4	27.6	16.0
RP	36.5	52.4	39.5	8.7	-	126.0	32.2	7.3
LT	20.9	17.6	22.0	9.3	28.5	18.6	20.7	15.7
RT	30.3	11.7	40.5	11.2	24.3	26.8	25.3	19.8
LCS	69.0	34.0	31.0	18.3	71.5	19.9	31.0	25.2
RCS	53.7	67.4	25.0	17.5	51.4	37.1	47.8	19.5
LPVWM	58.8	31.7	47.0	18.3	32.3	17.1	24.0	23.0
RPVWM	25.7	27.5	26.0	16.1	14.4	32.2	24.9	10.5
LFWM	17.6	113.9	46.6	17.4	32.4	63.3	66.3	42.9
RFWM	-	141.0	21.2	22.3	46.1	75.0	33.1	35.4
LPWM	-	125.1	25.2	24.4	38.8	61.6	22.1	37.7
RPWM	85.0	38.5	23.2	22.2	66.2	18.6	32.3	25.9

Note: The ANOVA procedure yielded negative variance component estimates in some ROIs for the 1-min paradigm; these values, which may be caused by outliers as described in the text, are not shown and are indicated by "-".
RPWM/LPWM: right/left posterior WM; RFWM/LFWM: right/left frontal WM; RPVWM/LPVWM: right/left periventricular WM; RCS/LCS: right/left centrum semiovale; RT/LT: right/left thalamus; RP/LP: right/left putamen; RCH/LCH: right/left caudate head; PCGM: posterior cortical GM; FCGM: frontal cortical GM.

participant cooperation, and with breath holding it is difficult to monitor the participant's physiological parameters non-invasively. The benefits and drawbacks of different CVR challenges,[24,25] and other practical aspects of CVR measurement in clinical research,[27] have been discussed in detail elsewhere. We chose to use a 6% CO_2 concentration in medical air since we measured similar CVR values and tolerability with greater $ETCO_2$ and signal changes with this gas mixture in a randomized comparison with 4% CO_2. Carbogen (CO_2 and O_2 with no nitrogen) gas mixtures have also been used for measuring CVR but the effects on the BOLD signal via changes in CBF and other mechanisms are more complex.[28] The experiments performed here could also be performed using a computerized system for prospective targeting of $ETCO_2$ values, subject to sufficient patient cooperation, availability of specialized equipment and provided a calibration step is performed before CVR scanning; such an approach should result in a more reproducible stimulus with better correspondence between $ETCO_2$ and arterial $PaCO_2$.[29]

Comparing two previously published hypercapnia paradigms, we found the paradigm based on 3-min CO_2 spells to be more reliable than a 1-min paradigm for measuring CVR and the CVR delay. This is partly because more signal is collected during the 3-min paradigm (12 min vs. 7 min total duration). Another factor is the longer repetition period of the 3-min paradigm, which reduces the likelihood of selecting the "wrong" minima as illustrated in Supplementary Figure 5. Such errors were observed in a small number of cases only

due to the use of pre-scan $ETCO_2$ data, which negates the periodicity of the paradigm; such errors could be further suppressed by further constraining the permitted delay values, but this would potentially bias the results, particularly in regions, voxels, or patients with slow CVR response (the group of greatest interest) and appropriate arbitrary limits would be difficult to determine a-priori without further knowledge of human cerebrovascular biology. We also found that CVR and the CVR delay were on average greater for the 3-min paradigm, with the difference more pronounced in WM ROIs. This observation suggests that the linear regression model is an incomplete description of the BOLD response to changes in $ETCO_2$. Improved fitting will likely result from convolving the $ETCO_2$ regressor with an impulse response function[21] or by permitting multiple (e.g. fast and slow) components to the response in any given tissue. However, the ideal approach is yet to be determined and the inclusion of additional fitting parameters would increase the computational burden and likely reduce the precision of other parameters. Further investigation is required to determine the optimal approach and care should be taken when comparing CVR values between studies. In general, data were more reproducible for GM than WM ROIs, which is expected due to the greater CBF in GM. The tolerability was similar for the two paradigms tested. Healthy volunteers had a similar rate of hypercapnia-related symptoms to patients but, on average, found the CVR procedure less tolerable compared with patients; this may be due to the administration of two CVR paradigms per session in volunteers, or due to healthy volunteers being less accustomed than patients to medical procedures. Encouragingly, all patients who underwent CVR scanning described the experience as either ''tolerable'' or ''very tolerable.'' In an analysis of 434 CVR scans across multiple patient groups, Spano et al.[30] also reported a high success rate for examinations using a prospective $ETCO_2$ targeting approach, with CVR maps generated for 83.9% of scans.

There are limited data on the reproducibility of BOLD CVR in the literature. Goode et al.,[31] using 10% CO_2 (9 min paradigm duration at 1.5T) reported coefficients of variation for CVR of around 25% in whole-brain GM and WM regions,[31] comparable to our findings. Kassner et al.[32] reported higher reproducibility (6.8% and 9.9% in GM and WM, respectively, at 1.5T) using a paradigm of around 12-min duration,[32] attributing this to more precise control of the $ETCO_2$ stimulus through use of a rebreathing circuit; the use of whole-brain ROIs and a constant CVR delay would also likely influence their findings.

The voxel-wise BOLD signal response to hypercapnia typically has low contrast-to-noise ratio, particularly in the WM, resulting in noisy parameter maps. As a result, several previous studies have used whole-brain tissue masks, but this precludes region-specific information needed for studies of SVD, which primarily affects periventricular WM, deep WM, and subcortical GM. We therefore selected an intermediate approach, averaging signal over ROIs to reduce parameter uncertainty while retaining region-specific information. This approach also permits manual exclusion of the large draining veins and sinuses, which have a significant influence on the signal in surrounding voxels due to the ''blooming'' effect. Despite this approach, reproducibility was lower in ROIs with low CVR; use of higher field MRI (e.g. 3T) should in principle permit increased reproducibility in these regions.

In common with previous volunteer studies, we found CVR to be greater in GM than in WM. Few if any studies have specifically measured subcortical GM CVR, which we found to be comparable to that in cortical GM. CVR values measured using the 1-min CO_2 challenge in GM and WM had similar magnitude to those reported by Thomas et al.[21] using the same paradigm. Within the WM, CVR was greater in periventricular ROIs than in the deep WM areas, which may be due to inclusion in the ROI of the draining veins surrounding the lateral ventricles (it being very difficult to ensure that no draining veins have been included). Also, in agreement with Thomas et al., we report a delay of approximately 20 s between the BOLD responses in GM and WM; this difference was greater still using the 3-min paradigm. Sam et al.[13] also observed differences between GM and WM in addition to reporting data for WMH, which were found to have reduced CVR and increased delay compared with normal-appearing WM. It is noted that the speed and magnitude of the WM response could be influenced by a steal effect by the faster-responding GM in addition to differences in intrinsic tissue properties such as cerebral blood volume and vasodilatory function.[33]

BOLD CVR was on average greater in healthy volunteers than in patients for most ROIs. Since the primary purpose of this work was to develop and assess protocols, the groups were not matched for age or vascular risk factors. However, the difference is consistent with the expected reduction in vasoreactivity both with ageing[34,35] (patients were older than the healthy volunteers) and cerebrovascular disease.[6,14] More surprisingly, the CVR delay was shorter for patients in most ROIs. Thomas et al. also reported a longer CVR delay in young versus older participants, though neither group comprised patients.

Other aspects of the BOLD CVR examination protocol, not addressed in this work, should also be considered for CVR studies in SVD. While a field strength of 1.5 T, as used in this work, has the benefit

of wide availability in clinical settings, 3T scanning would likely increase reproducibility as a result of higher signal- and contrast-to-noise ratio for BOLD MRI; adverse susceptibility effects including blooming artefacts around the large veins are also greater at 3 T, but this can be mitigated by increasing bandwidth and reducing voxel size, which will also reduce partial volume effects on CVR values, particularly in small structures and lesions. We also did not address the optimization of MR acquisition parameters, using, as in most CVR studies, "standard" BOLD fMRI values for the echo time and repetition time. The choice of echo time affects the signal-to-noise ratio, sensitivity to deoxyhaemoglobin, and other aspects of the acquisition protocol. Ravi et al.[36] proposed the use of a shorter echo time to suppress negative CVR values that were attributed by the authors to displacement of CSF by dilated vessels. Finally, the increasing availability of simultaneous multislice and other parallel imaging techniques on commercial MR scanners will facilitate higher spatial and/or temporal resolution in future studies.[37] The "HARNESS" (Harmonising Brain Imaging Methods for Vascular Contributions to Neurodegeneration) collaboration, currently in progress, and ongoing discussions within the wider CVR community, should result in further recommendations and guidance relevant to the conduct of CVR experiments in SVD research.

In conclusion, the protocol described herein will permit further investigation of the relationship between cerebral SVD burden and subcortical CVR in cross-sectional studies of patients presenting with minor ischemic stroke, cognitive impairment, and CADASIL (INVESTIGATE-SVDs: ISRCTN1051422). Since the progression of WM changes visible by structural MRI is typically slow,[38] this protocol will also be used to provide intermediary end-points in clinical trials of drugs to prevent and reverse SVD (LACI-1: ISRCTN12580546, TREAT-SVDs: NCT03082014).

Acknowledgements

We thank K. Shuler and the radiography staff for providing expert research support.

Authors' contributions

MJT: volunteer recruitment, experimental design, data collection, data analysis, statistics, manuscript preparation. GB: patient recruitment, data collection, data management, manuscript preparation. FD: recruitment, data collection, study design, supervision, manuscript preparation. IH: data collection, study coordination, manuscript preparation. CP: advice regarding data analysis, manuscript preparation. PJDA: advice on breathing circuits, monitors and physiology; manuscript preparation. GW: advice regarding experimental set up and design, manuscript preparation. CS: advice regarding experimental set up and design, manuscript preparation. IM: study design, manuscript preparation. YS: data collection, image analysis, manuscript preparation. JMW: conception, funding, study design, supervision, manuscript preparation.

Declaration of conflicting interests

The author(s) declared no potential conflicts of interest with respect to the research, authorship, and/or publication of this article.

Funding

The author(s) disclosed receipt of the following financial support for the research, authorship, and/or publication of this article: This work was funded primarily by the Chief Scientist Office of Scotland (grant ETM/326) and the Wellcome Trust-University of Edinburgh Institutional Strategic Support Fund. Support was also received from: NHS Lothian Research and Development Office (MJT), the China Scholarships Council/University of Edinburgh (YS), the Scottish Imaging Network: A Platform for Scientific Excellence ("SINAPSE," funded by the Scottish Funding Council and the Chief Scientist Office of Scotland; GB, radiography staff), the Alzheimer's Society (grant ref AS-PG-14-033; GB), the European Union Horizon 2020, "SVDs@target" (grant No 666881; GB), The Stroke Association Garfield Weston Foundation Senior Lectureship (FD), NHS Research fellowship (FD) and the Medical Research Council (FD).

References

1. Deplanque D, Lavallee PC, Labreuche J, et al. Cerebral and extracerebral vasoreactivity in symptomatic lacunar stroke patients: a case-control study. *Int J Stroke* 2013; 8: 413–421 [AQ1].
2. Stevenson SF, Doubal FN, Shuler K and Wardlaw JM. A systematic review of dynamic cerebral and peripheral endothelial function in lacunar stroke versus controls. *Stroke* 2010; 41: e434–e442.
3. Fernando MS, Simpson JE, Matthews F, et al. White matter lesions in an unselected cohort of the elderly: molecular pathology suggests origin from chronic hypoperfusion injury. *Stroke* 2006; 37: 1391–1398.
4. Cantin S, Villien M, Moreaud O, et al. Impaired cerebral vasoreactivity to CO2 in Alzheimer's disease using BOLD fMRI. *Neuroimage* 2011; 58: 579–587.
5. Dumas A, Dierksen GA, Gurol ME, et al. Functional magnetic resonance imaging detection of vascular reactivity in cerebral amyloid angiopathy. *Ann Neurol* 2012; 72: 76–81.
6. Zupan M, Sabovic M, Zaletel M, Popovic KS and Zvan B. The presence of cerebral and/or systemic endothelial dysfunction in patients with leukoaraiosis – a case control pilot study. *BMC Neurol* 2015; 15: 158.
7. Han JS, Mikulis DJ, Mardimae A, et al. Measurement of cerebrovascular reactivity in pediatric patients with cerebral vasculopathy using blood oxygen level-dependent MRI. *Stroke* 2011; 42: 1261–1269.
8. Lythgoe DJ, Williams SC, Cullinane M and Markus HS. Mapping of cerebrovascular reactivity using BOLD

magnetic resonance imaging. *Magn Reson Imag* 1999; 17: 495–502.
9. Blair GW, Doubal FN, Thrippleton MJ, Marshall I and Wardlaw JM. Magnetic resonance imaging for assessment of cerebrovascular reactivity in cerebral small vessel disease: a systematic review. *J Cereb Blood Flow Metab* 2016; 36: 833–841.
10. Conijn MM, Hoogduin JM, van der Graaf Y, Hendrikse J, Luijten PR and Geerlings MI. Microbleeds, lacunar infarcts, white matter lesions and cerebrovascular reactivity – a 7 T study. *Neuroimage* 2012; 59: 950–956.
11. Gauthier CJ, Lefort M, Mekary S, et al. Hearts and minds: linking vascular rigidity and aerobic fitness with cognitive aging. *Neurobiol Aging* 2015; 36: 304–314.
12. Hund-Georgiadis M, Zysset S, Naganawa S, Norris DG and Von Cramon DY. Determination of cerebrovascular reactivity by means of FMRI signal changes in cerebral microangiopathy: a correlation with morphological abnormalities. *Cerebrovasc Dis* 2003; 16: 158–165.
13. Sam K, Conklin J, Holmes KR, et al. Impaired dynamic cerebrovascular response to hypercapnia predicts development of white matter hyperintensities. *Neuroimage Clin* 2016; 11: 796–801.
14. Uh J, Yezhuvath U, Cheng Y and Lu H. In vivo vascular hallmarks of diffuse leukoaraiosis. *J Magn Reson Imag* 2010; 32: 184–190.
15. Rost NS, Rahman RM, Biffi A, et al. White matter hyperintensity volume is increased in small vessel stroke subtypes. *Neurology* 2010; 75: 1670–1677.
16. Staals J, Makin SD, Doubal FN, Dennis MS and Wardlaw JM. Stroke subtype, vascular risk factors, and total MRI brain small-vessel disease burden. *Neurology* 2014; 83: 1228–1234.
17. Heye AK, Thrippleton MJ, Armitage PA, et al. Tracer kinetic modelling for DCE-MRI quantification of subtle blood-brain barrier permeability. *Neuroimage* 2016; 125: 446–455.
18. Wardlaw JM, Doubal F, Armitage P, et al. Lacunar stroke is associated with diffuse blood-brain barrier dysfunction. *Ann Neurol* 2009; 65: 194–202.
19. Yezhuvath US, Lewis-Amezcua K, Varghese R, Xiao G and Lu H. On the assessment of cerebrovascular reactivity using hypercapnia BOLD MRI. *NMR Biomed* 2009; 22: 779–786.
20. Shen Y, Pu IM, Ahearn T, Clemence M and Schwarzbauer C. Quantification of venous vessel size in human brain in response to hypercapnia and hyperoxia using magnetic resonance imaging. *Magn Reson Med* 2013; 69: 1541–1552.
21. Thomas BP, Liu P, Park DC, van Osch MJ and Lu H. Cerebrovascular reactivity in the brain white matter: magnitude, temporal characteristics, and age effects. *J Cereb Blood Flow Metab* 2014; 34: 242–247.
22. Bhogal AA, Siero JC, Fisher JA, et al. Investigating the non-linearity of the BOLD cerebrovascular reactivity response to targeted hypo/hypercapnia at 7T. *Neuroimage* 2014; 98: 296–305.
23. Blockley NP, Driver ID, Francis ST, Fisher JA and Gowland PA. An improved method for acquiring cerebrovascular reactivity maps. *Magn Reson Med* 2011; 65: 1278–1286.
24. Ziyeh S, Rick J, Reinhard M, Hetzel A, Mader I and Speck O. Blood oxygen level-dependent MRI of cerebral CO2 reactivity in severe carotid stenosis and occlusion. *Stroke* 2005; 36: 751–756.
25. Jenkinson M, Bannister P, Brady M and Smith S. Improved optimization for the robust and accurate linear registration and motion correction of brain images. *Neuroimage* 2002; 17: 825–841.
26. Bland JM and Altman DG. Statistical methods for assessing agreement between two methods of clinical measurement. *Lancet* 1986; 1: 307–310.
27. Moreton FC, Dani KA, Goutcher C, O'Hare K and Muir KW. Respiratory challenge MRI: practical aspects. *Neuroimage Clin* 2016; 11: 667–677.
28. Hare HV, Germuska M, Kelly ME and Bulte DP. Comparison of CO2 in air versus carbogen for the measurement of cerebrovascular reactivity with magnetic resonance imaging. *J Cereb Blood Flow Metab* 2013; 33: 1799–1805.
29. Ainslie PN and Duffin J. Integration of cerebrovascular CO2 reactivity and chemoreflex control of breathing: mechanisms of regulation, measurement, and interpretation. *Am J Physiol Regul Integr Comp Physiol* 2009; 296: R1473–R1495.
30. Spano VR, Mandell DM, Poublanc J, et al. CO2 blood oxygen level-dependent MR mapping of cerebrovascular reserve in a clinical population: safety, tolerability, and technical feasibility. *Radiology* 2013; 266: 592–598.
31. Goode S, Altaf N, Dineen RA, Krishnan S and Auer D. Intraplaque haemorrhage mimicking carotid pseudoaneurysm on magnetic resonance angiography. *Br J Radiol* 2007; 80: e271–e274.
32. Kassner A, Winter JD, Poublanc J, Mikulis DJ and Crawley AP. Blood-oxygen level dependent MRI measures of cerebrovascular reactivity using a controlled respiratory challenge: reproducibility and gender differences. *J Magn Reson Imag* 2010; 31: 298–304.
33. Mandell DM, Han JS, Poublanc J, et al. Selective reduction of blood flow to white matter during hypercapnia corresponds with leukoaraiosis. *Stroke* 2008; 39: 1993–1998.
34. Lu H, Xu F, Rodrigue KM, et al. Alterations in cerebral metabolic rate and blood supply across the adult lifespan. *Cereb cortex* 2011; 21: 1426–1434.
35. Reich T and Rusinek H. Cerebral cortical and white matter reactivity to carbon-dioxide. *Stroke* 1989; 20: 453–457.
36. Ravi H, Thomas BP, Peng SL, Liu H and Lu H. On the optimization of imaging protocol for the mapping of cerebrovascular reactivity. *J Magn Reson Imag* 2016; 43: 661–668.
37. Ravi H, Liu P, Peng SL, Liu H and Lu H. Simultaneous multi-slice (SMS) acquisition enhances the sensitivity of hemodynamic mapping using gas challenges. *NMR Biomed* 2016; 29: 1511–1518.
38. Schmidt R, Seiler S and Loitfelder M. Longitudinal change of small-vessel disease-related brain abnormalities. *J Cereb Blood Flow Metab* 2016; 36: 26–39.

International Journal of Stroke
WSO

International Journal of Stroke
0(0) 1–9

DOI: 10.1177/1747493017731947
journals.sagepub.com/home/wso
SAGE

Preventing cognitive decline and dementia from cerebral small vessel disease: The LACI-1 Trial. Protocol and statistical analysis plan of a phase IIa dose escalation trial testing tolerability, safety and effect on intermediary endpoints of isosorbide mononitrate and cilostazol, separately and in combination

Gordon W Blair[1,2,3], Jason P Appleton[4], Zhe Kang Law[4,5], Fergus Doubal[1,2,3], Katie Flaherty[4], Richard Dooley[4], Kirsten Shuler[1,2,3], Carla Richardson[4], Iona Hamilton[1,2,3], Yulu Shi[1,2,3], Michael Stringer[1,2,3], Julia Boyd[6], Michael J Thrippleton[1,2,3], Nikola Sprigg[4], Philip M Bath[4] and Joanna M Wardlaw[1,2,3]

Abstract

Rationale: The pathophysiology of most lacunar stroke, a form of small vessel disease, is thought to differ from large artery atherothrombo- or cardio-embolic stroke. Licensed drugs, isosorbide mononitrate and cilostazol, have promising mechanisms of action to support their testing to prevent stroke recurrence, cognitive impairment, or radiological progression after lacunar stroke.

Aim: LACI-1 will assess the tolerability, safety, and efficacy, by dose, of isosorbide mononitrate and cilostazol, alone and in combination, in patients with ischemic lacunar stroke.

Sample size: A sample of 60 provides 80+% power (significance 0.05) to detect a difference of 35% (90% versus 55%) between those reaching target dose on one versus both drugs.

Methods and design: LACI-1 is a phase IIa partial factorial, dose-escalation, prospective, randomized, open label, blinded endpoint trial. Participants are randomized to isosorbide mononitrate and/or cilostazol for 11 weeks with dose escalation to target as tolerated in two centers (Edinburgh, Nottingham). At three visits, tolerability, safety, blood pressure, pulse wave velocity, and platelet function are assessed, plus magnetic resonance imaging to assess cerebrovascular reactivity in a subgroup.

Study outcomes: Primary: proportion of patients completing study achieving target maximum dose.

Secondary: symptoms whilst taking medications; safety (hemorrhage, recurrent vascular events, falls); blood pressure, platelet function, arterial stiffness, and cerebrovascular reactivity.

Discussion: This study will inform the design of a larger phase III trial of isosorbide mononitrate and cilostazol in lacunar stroke, whilst providing data on the drugs' effects on vascular and platelet function.

[1]Centre for Clinical Brain Sciences, University of Edinburgh, Edinburgh, UK
[2]Edinburgh Dementia Research Centre in the UK Dementia Research Institute, University of Edinburgh, Edinburgh, UK
[3]Fondation Leducq Network for the Study of Perivascular Spaces in Small Vessel Disease, University of Edinburgh, Edinburgh, UK
[4]Stroke Trials Unit, Division of Clinical Neuroscience, University of Nottingham, Nottingham, UK
[5]Department of Medicine, National University of Malaysia, Kuala Lumpur, Malaysia
[6]Edinburgh Clinical Trial's Unit, Western General Hospital, Edinburgh, UK

Corresponding author:
Joanna M Wardlaw, Centre for Clinical Brain Sciences, University of Edinburgh, Chancellor's Building, 49 Little France Crescent, Edinburgh EH16 4SB, UK.
Email: joanna.wardlaw@ed.ac.uk

Trial registration: ISRCTN (ISRCTN12580546) and EudraCT (2015-001953-33).

Keywords
Lacunar stroke, small vessel disease, cilostazol, isosorbide mononitrate, endothelium, blood–brain barrier, white matter hyperintensities, cerebrovascular reactivity

Received: 30 May 2017; accepted: 14 August 2017

Introduction and rationale

Cerebral small vessel disease (SVD) is a common disorder that affects small perforating arterioles in the brain's deep white and gray matter.[1] It causes 25% of ischemic strokes (''lacunar'' stroke), intracerebral hemorrhage, vascular and many mixed dementias, gait and bladder dysfunction.[1,2] Cardioembolism and atherothromboembolism are uncommon in lacunar stroke and SVD, respectively. Although the pathophysiology remains poorly understood, endothelial dysfunction,[1,3,4] inflammation,[3,5] blood–brain barrier failure,[6] and impaired vasoreactivity[4,7] have been demonstrated.

There is no specific secondary prevention for lacunar stroke, SVD-associated dementia, or progression of SVD lesions on neuroimaging.[1] We recently summarized available drugs with potentially relevant actions and identified two agents that seemed worthy of further testing: isosorbide mononitrate (ISMN) and cilostazol.[8]

ISMN, a nitric oxide (NO) donor, is commonly used in angina. NO levels are reduced in acute, [9] chronic[10] and possibly in lacunar stroke.[11] NO has many potentially beneficial effects for SVD including improved vasoreactivity, neuroprotection, and anti-inflammatory effects.[8] In the Efficacy of Nitric Oxide in Stroke (ENOS) trial, the NO donor glyceryl trinitrate administered within 6 h of all types of stroke, improved cognitive test scores at 90 days.[12] However, there are few data on ISMN in lacunar stroke in part because ischemic heart disease, for which ISMN is licensed, is relatively infrequent in those with SVD.[13]

Cilostazol is a phosphodiesterase 3′ inhibitor,[8] mainly used for peripheral vascular disease in Europe and North America,[14] but more widely used for cerebrovascular disease prevention in Asia-Pacific countries. Cilostazol has mild antiplatelet effects plus several potentially beneficial effects for SVD including improved blood–brain barrier integrity, vasodilatory and anti-proliferative activity, improves oligodendrocyte maturation and hence myelination,[15] and reduces white cell chemotaxis.[8] In models, it improved motor and cognitive function, and reduced infarct volume[16] and in human lacunar stroke it improved middle cerebral artery pulsatility index.[17] Over 6000 patients, many with lacunar stroke, have been included in trials of cilostazol in secondary stroke prevention mostly in Asia-Pacific countries (Figure 1); a meta-analysis of these suggested that cilostazol reduces recurrent stroke.[18–21]

There is little experience of ISMN in lacunar stroke, cilostazol is rarely used for stroke prevention in Europe or the Americas. There are no data on the effects of cilostazol when combined with ISMN yet the effects are potentially synergistic.[8]

Therefore, the Lacunar Intervention Trial-1 (LACI-1) will test ISMN and cilostazol, alone and combined, in patients with lacunar ischemic stroke, to assess their tolerability, safety, and efficacy on mechanistic endpoints including cerebrovascular reactivity assessed using magnetic resonance imaging (MRI). Treatment will be given in addition to current guideline-based post-stroke secondary prevention. LACI-1 will inform the design of a larger trial to test ISMN and cilostazol effects on recurrent vascular events, cognition, disability, death, and SVD lesion progression on MRI (LACI-2). LACI-1 was designed through a UK National Institute for Health Research Stroke Research Network Expert Writing Group.

Methods

Design

Phase IIa, partial factorial, dose-escalation, prospective, randomized, open label, blinded endpoint (PROBE) trial conducted in two UK centers (Edinburgh, Nottingham).

Participants are randomized in a 1:1:1:1 ratio into four groups: cilostazol alone; ISMN alone; cilostazol and ISMN combined, started immediately (with ISMN given first); and cilostazol and ISMN combined, start delayed for three weeks (cilostazol first) (Figure 2). The delayed start group also provides a ''no drug'' comparison group during the first three weeks.

Participants take trial medication for 11 weeks. The dose is increased, in weekly increments over two to three weeks as tolerated, sustained until eight weeks post-randomization, then decreased gradually over two weeks and stopped (Supplementary Information

Figure 1. Meta-analysis of trials of cilostazol for secondary stroke prevention.[31–35]

Study	Lacunar proportion	Cilostazol group events	Cilostazol group size	Control group events	Control group size	Weight	Odds Ratio	95% Confidence Interval
Nakamura[31]	47%	2	38	3	38	1.3%	0.67	(0.12-3.77)
CAIST[32]	55%	5	231	9	227	3.4%	0.55	(0.19-1.60)
CSPS 2[33]	65%	82	1337	119	1335	54.0%	0.69	(0.52-0.90)
TOHOKU (Shimizu)[34]	67%	5	251	6	256	2.9%	0.85	(0.26-2.75)
CSPS[35]	75%	34	533	64	534	25.0%	0.53	(0.36-0.79)
Total		128	2390	201	2390		0.64	(0.51-0.79)

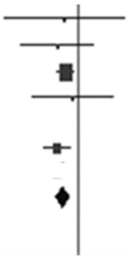

Heterogeneity: Tau2=0.00;Chi2=1.41, df=4(P=0.84);I2=0%
Test for overall effect: Z=4.13(P<0.0001)

Favours Cilostazol Favours Control

gives medication by study week). The escalating dose is designed to reduce potential adverse effects following initiation of cilostazol and is standard for ISMN. Gradual dose reduction aims to prevent large hemodynamic changes on cessation of medication.

Patient population

Inclusion:

1. Mild symptomatic ischemic lacunar stroke in the past four years, compatible with a clinical lacunar stroke syndrome, with brain MRI or CT scanning showing a symptomatic small subcortical (lacunar) infarct (<20 mm), or if no recent relevant infarct is visible, that excluded other cause for symptoms. Clinical or imaging evidence of a prior non-lacunar stroke is not an exclusion as long as the randomizing clinician is confident that the non-lacunar stroke is not responsible for the index lacunar stroke symptoms.
2. Age ≥ 35 years.
3. Independent in activities of daily living (modified Rankin Scale of ≤ 2) and able to give informed consent.

Exclusion:

1. Other significant neurological illness since the incident stroke.
2. Age < 35 years.
3. Montreal Cognitive Assessment (MoCA) < 20.
4. Requiring assistance with activities of daily living (modified Rankin Scale ≥ 3).
5. Active cardiac disease.
6. Carotid stenosis > 50% (NASCET criteria) on the side of the symptomatic stroke lesion requiring urgent intervention. Note: successfully treated carotid artery stenosis may be included.
7. Definite indication for, or contraindication to, cilostazol or ISMN.
8. Unable to swallow.
9. Bleeding tendency.
10. Unlikely to comply with trial medication based on past history or lifestyle.
11. Planned surgery during the trial period.
12. History of intracranial hemorrhage (but not asymptomatic hemorrhagic transformation of an infarct).
13. Other life threatening illness.
14. History of drug overdose, attempted suicide or significant active mental illness.
15. Pregnant or breastfeeding women.
16. Women of childbearing age not taking contraception.
17. Use of prohibited medications (anticoagulants, phosphodiesterase 5′ inhibitors, macrolides, ketoconazole, itraconazole, omeprazole).
18. Creatinine clearance < 25 ml/min.
19. Hepatic impairment.
20. Current enrolment in another Clinical Trial of Investigational Medicinal Product (CTIMP).

Randomization

Baseline information is entered on a password-protected website (https://nottingham.ac.uk/~nszwww/prev-svd/). Once checked and complete, a computer algorithm randomizes participants at a 1:1:1:1 ratio to a study group. Randomization is minimized on age ≤/>70 years, SVD severity on brain scanning (SVD score ≤/>2),[22] systolic blood pressure ≤/>140 mmHg and time after stroke ≤/>100 days.

Figure 2. Flow chart of study procedures.

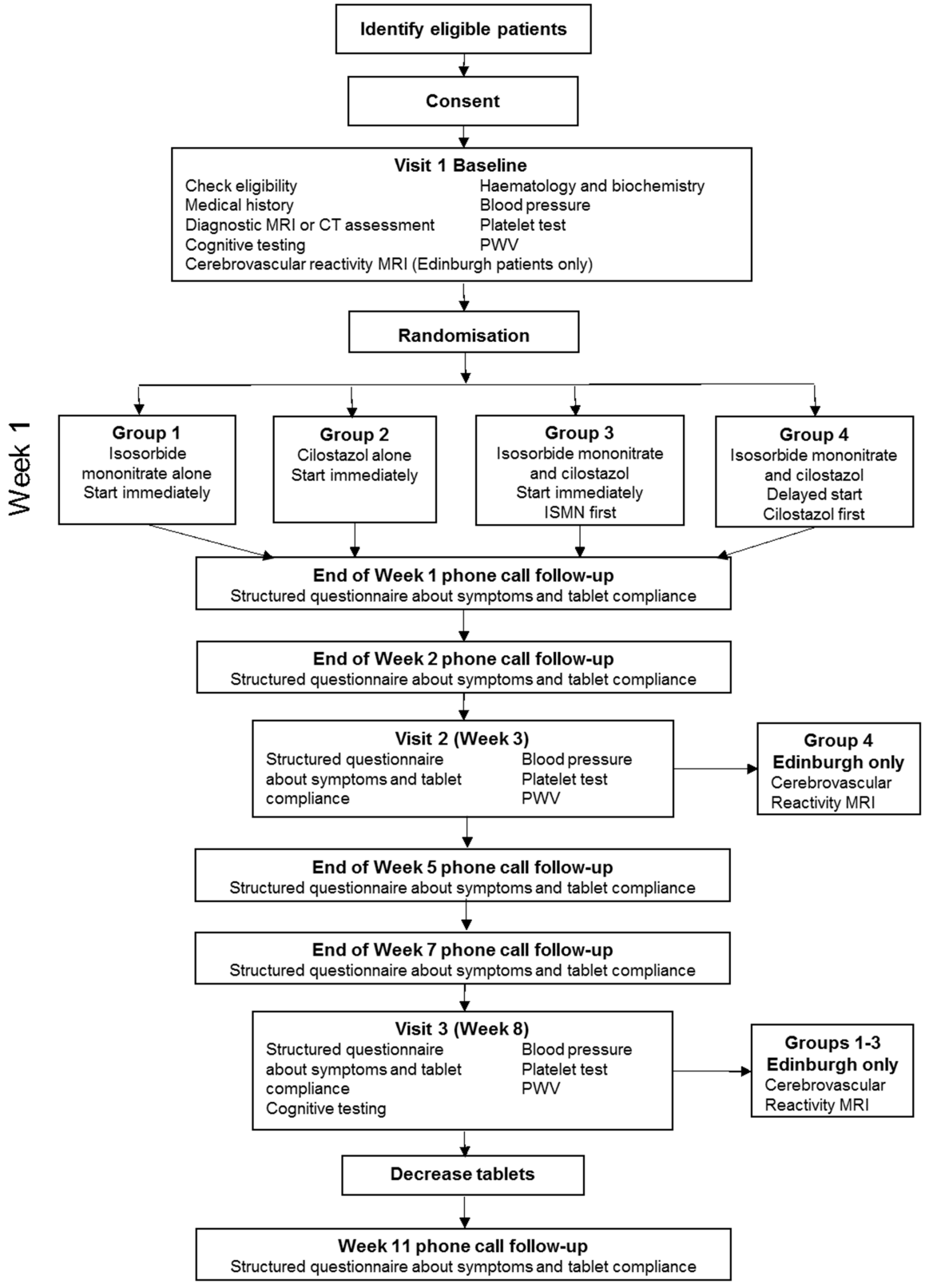

Intervention

The starting dose for cilostazol is 50 mg twice daily, increasing to 100 mg twice daily (target dose). The starting dose of ISMN is 25 mg once daily increasing to 25 mg twice daily (target dose). Participants allocated to both drugs aim to attain the same target doses as for the drugs alone (dose schedules in Supplementary Information). Unused tablets are returned to Pharmacy for counting and destruction at the end of the 11-week period.

Primary outcome

The proportion of participants achieving target dose assessed by alternate weeks structured questionnaire, supplemented by diary and Pharmacy tablet count.

Secondary outcomes

1. Symptoms (headache, nausea, diarrhea, vomiting, bleeding) recorded by structured questionnaire.
2. Safety (systemic or intracranial bleeding, recurrent vascular events, death).
3. Blood pressure.
4. Platelet function (P-selectin flow cytometry).[23]
5. Systemic arterial stiffness (pulse wave velocity and pulse wave analysis using the SphygmoCor tonometry device).
6. In a subgroup recruited in Edinburgh, cerebrovascular reactivity (CVR)[7] in white matter and cerebrospinal fluid and blood pulsatility, assessed using MRI. Acquisition details are provided in the Supplementary Information.

Blinding

The processing and analysis of CVR, platelet function, pulse wave velocity, blood pressure, and all tablet counts, study questionnaires and compliance data will be performed blind to treatment allocation. Apart from the study research fellow and research nurse, other staff performing the above assessments will not be aware of the treatment allocation, particularly during image analysis, blood tests and follow-up data analysis. When talking to participants, the tablets will only be referred to as ''A'' or ''B'' to facilitate patients' understanding of procedures.

Data monitoring committee

An independent data monitoring committee (DMC) is established, chair Prof. Colin Baigent (Oxford).

Sample size

A sample size of 55 provides 80% power (significance 0.05) to detect a difference of 90% versus 55% (i.e. an absolute difference of 35%) between those reaching target doses on one drug versus both drugs; i.e. we expect that 35% fewer patients will tolerate both versus one of the two drugs and the sample size is set to be able to detect that difference. For CVR, lacunar stroke patients have impaired middle cerebral artery vasoreactivity on transcranial Doppler ultrasound with an effect size of 25%, standard deviation (SD) of 40%.[4] Little data exist on CVR measured by blood oxygen level dependent (BOLD) MRI in lacunar stroke.[7] The 40-participant sample in Edinburgh will allow detection of a relative difference in CVR of 25% (4% versus 3% signal; with estimated common SD of 40%) between no treatment and target dose of both drugs, significance 0.05 and power 0.80.

Allowing for losses, 60 participants will be recruited in total.

Analyses

Image processing. Structural MR images will be scored for SVD lesion burden using validated scales[24] and processed to generate tissue segmentation maps using validated software.[25] CVR (% signal change/mmHg change in end-tidal CO_2) will be determined by multiple linear regression of the BOLD MRI signal time course, with the end-tidal CO_2 and time (to account for scanner drift) as regressors, for specific tissue regions for comparison of trial drugs and doses.

Statistical. We will compare cilostazol versus none, ISMN versus none, and cilostazol and ISMN given immediately versus both given after a delay (the delayed start provides a drug-free control period; having two groups that both get both drugs compares drug initiation with one versus the other drug). We will compare symptoms, blood pressure, arterial stiffness, platelet function, and CVR by treatment allocation. The primary outcome (proportion of participants achieving target dose) will be assessed using binary logistic regression with adjustment for minimization factors; age, SVD score, systolic blood pressure, and time from stroke to randomization (days). The secondary outcomes will be assessed using binary logistic regression for binary variables, multiple linear regression for continuous variables and Cox proportional hazards regression for variables which have a time-until-event component. As data are collected over an 11-week period, time trends will also be examined.

Data tables and figures summarizing the main planned comparisons are provided in the Supplementary Information.

Figure 3. Mechanistic endpoints (intermediary outcomes) assessing brain and systemic vascular function in response to cilostazol and isosorbide mononitrate. (a) Brain—CVR MRI scans. The dark blue areas indicate the least reactive tissues, and the bright red areas are the most reactive tissues. (b) Carotid and vertebral arteries—phase contrast MRI scan, which also measures intracranial arterial, venous sinus and CSF flow. (c) Systemic arteries—aortic and radial artery pressure waveforms and pulse wave velocity. (d) Platelet function is assessed with P-selectin flow cytometry.

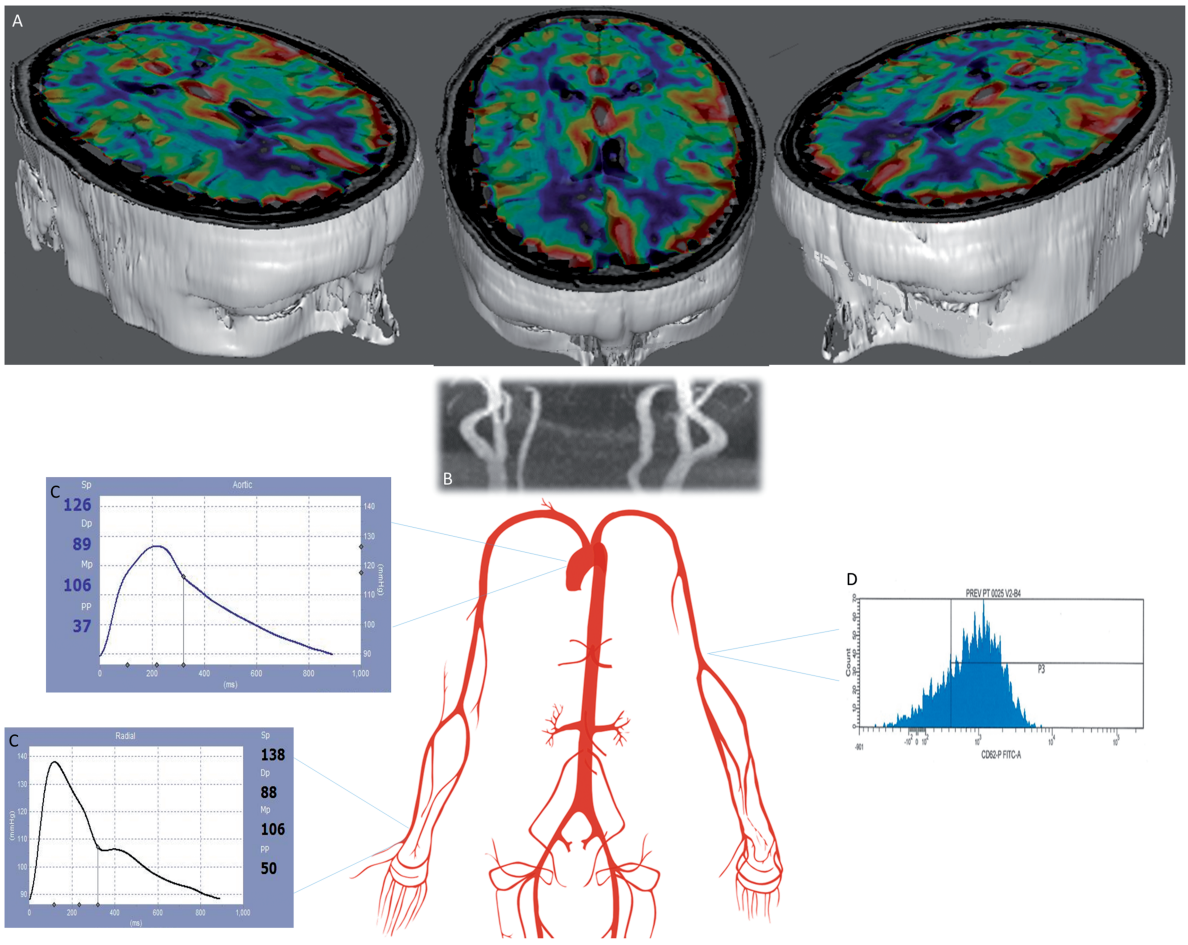

Study organization and funding

The study is funded by The Alzheimer's Society and will be performed in the Centre for Clinical Brain Sciences and Edinburgh Clinical Trials Unit, University of Edinburgh and the Stroke Trials Unit, Division of Clinical Neuroscience, University of Nottingham.

Discussion

Intensive assessment

LACI-1 follows participants intensively over 11 weeks including 3 research clinic visits (to assess BP, platelet function, arterial stiffness, CVR, and symptoms) and 5 telephone follow-ups (to assess side-effects and guide dose escalation). The intense follow-up provides data on dose escalation and safety to inform a future larger, pragmatic, phase III trial with less frequent follow-up.

PROBE design

The PROBE design blinds the main study outcomes whilst maintaining feasibility of dose escalation. A double-blind design proved to be impractical as there is no matching placebo for either study drug. Furthermore, masking by over-encapsulation was impractical and prohibitively expensive when combined with dose escalation. Complicated arrangements for dispensing multiple bottles of study drug, with different dose combinations, were required, with high risk of reduced compliance, confusion, and incorrect medication. The PROBE design is well established[26] and the

study has been designed and staffed appropriately to maintain investigator blinding at the point of outcome assessment.

Factorial design

The factorial design compares each drug to no drug and also combination therapy to no therapy. The ''delayed start'' group provides a modified ''no-drug'' control group as these participants do not receive medication for the first three weeks after randomization so are not on any medication at the second visit (week 3). They start medication following the week 3 visit, creating a more efficient design, as all participants receive study drug and tests the effect of which drug is commenced first in the combination groups (Supplementary Information). Randomization using minimization increases statistical power.

Dose escalation

The common side-effects of both study drugs (ISMN: headache; cilostazol: headache, palpitations) are usually encountered soon after starting the medication. Slow dose escalation at treatment initiation is widely used to lessen these side-effects. However, evidence for this comes from a single non-randomized study[27] and personal experience. Dose escalation of dipyridamole, a phosphodiesterase 5′ inhibitor with a similar pharmacodynamics profile to cilostazol, did not reduce headache in a blinded randomized comparison.[28] LACI-1 will provide objective evidence on the frequency of common inception side-effects to inform a larger pragmatic trial at up to 20 sites to select the regimen that best balances simplicity with tolerability and compliance.

Mechanistic endpoints

Stroke recurrence, whilst a significant problem following lacunar stroke, occurs relatively infrequently and late, whilst radiological progression of SVD is relatively slow.[29] Hence large trials with long follow-up periods are required to detect treatment effects. To enhance information on pharmacological effects of cilostazol and ISMN at these doses, we will use mechanistic vascular function endpoints (Figure 3): changes in CVR measured using hypercapnic challenge BOLD MRI scans,[7] and changes in arterial, venous, and cerebrospinal fluid flow characteristics measured using phase-contrast MRI; improvement in systemic vascular stiffness using pulse wave velocity (SphygmoCor tonometry device); and alteration in platelet function will test effects on platelet activation and provide safety data.[30]

Bleeding

Cilostazol (but not ISMN) has a low risk of bleeding, a potential interaction with the background antiplatelet medication that patients will be taking. One of the aims of LACI-1 is to assess whether bleeding is enhanced when patients take these combinations of antiplatelet agents.

Summary and conclusions

LACI-1 will provide data on tolerability, safety and surrogate efficacy markers for cilostazol and ISMN in patients with lacunar stroke, and will inform the design of a larger pragmatic phase III study.

Declaration of conflicting interests

The author(s) declared no potential conflicts of interest with respect to the research, authorship, and/or publication of this article.

Funding

The author(s) disclosed receipt of the following financial support for the research, authorship, and/or publication of this article: LACI-1 is funded by the Alzheimer's Society (Ref: 252 (AS-PG-14-033)). Additional support is provided by the European Union Horizon 2020 project No. 666881, 'SVDs@Target' (GWB, MS), the Stroke Association Princess Margaret Research Development Fellowship scheme (GWB), the Stroke Association Garfield Weston Foundation Senior Clinical Lectureship (FND), NHS Research Scotland (FND), the China Scholarships Council/University of Edinburgh (YS), NHS Lothian Research and Development Office (MJT) and the Scottish Funding Council through the Scottish Imaging Network, A Platform for Scientific Excellence (SINAPSE) Collaboration. Funding is gratefully acknowledged from the Fondation Leducq (ref no. 16 CVD 05) and Edinburgh and Lothians Health Foundation. JPA is supported, in part, by the National Institutes of Health Research (NIHR) HTA TARDIS and BHF RIGHT-2 trials. ZKL and KF are supported, in part, by the NIHR HTA TICH-2 trial. RD is supported, in part, by the HTA TARDIS trial. CR is supported through the NIHR Clinical Research network (CRN) East Midlands. PMB is Stroke Association Professor of Stroke Medicine, and is a NIHR Senior Investigator. LACI-1 was adopted by the NIHR CRN.

Authors' contributions

Gordon W Blair participated in study design, study set-up, manuscript preparation, and figures. Jason P Appleton participated in study design, study set-up, and manuscript preparation. Zhe Kang Law contributed in study set-up and preparation. Fergus Doubal contributed study design, supervision, study set-up and manuscript preparation. Katie Flaherty contributed for study design, statistics and manuscript preparation. Richard Dooley contributed for study design, randomization algorithm and manuscript

preparation. Kirsten Shuler and Carla Richardson participated in trial management, study set-up and manuscript preparation. Iona Hamilton contributed for study set-up, imaging protocol and manuscript preparation. Yulu Shi and Michael Stringer participated in study set-up and manuscript preparation. Julia Boyd has done the trial management and manuscript preparation. Michael J Thrippleton has participated in manuscript preparation, study design, and imaging protocol. Nikola Sprigg designed the study and supervised the manuscript preparation. Philip M Bath contributed for conception, study design, supervision, and manuscript preparation. Joanna M Wardlaw contributed for conception, funding, study design, supervision, and manuscript preparation.

References

1. Wardlaw JM, Smith C and Dichgans M. Mechanisms of sporadic cerebral small vessel disease: insights from neuroimaging. *Lancet Neurol* 2013; 12: 483–497.
2. Debette S and Markus HS. The clinical importance of white matter hyperintensities on brain magnetic resonance imaging: systematic review and meta-analysis. *Br Med J* 2010; 341: c3666.
3. Wiseman S, Marlborough F, Doubal F, Webb DJ and Wardlaw J. Blood markers of coagulation, fibrinolysis, endothelial dysfunction and inflammation in lacunar stroke versus non-lacunar stroke and non-stroke: systematic review and meta-analysis. *Cerebrovasc Dis* 2014; 37: 64–75.
4. Stevenson SF, Doubal FN, Shuler K and Wardlaw JM. A systematic review of dynamic cerebral and peripheral endothelial function in lacunar stroke versus controls. *Stroke* 2010; 41: e434–e42.
5. Bailey EL, Smith C, Sudlow CLM and Wardlaw JM. Pathology of lacunar ischaemic stroke in humans – a systematic review. *Brain Pathol* 2012; 22: 583–591.
6. Wardlaw JM, Makin S, Hernández MCV, et al. Blood–brain barrier failure as a core mechanism in cerebral small vessel disease and dementia: evidence from a cohort study. *Alzheimer's Dementia* 2017; 13: 634–643.
7. Blair G, Doubal FN, Thrippleton MJ, Marshall I and Wardlaw JM. Magnetic resonance imaging for assessment of cerebrovascular reactivity in cerebral small vessel disease. A systematic review. *J Cereb Blood Flow Metab* 2016; 36: 833–841.
8. Bath PM and Wardlaw JM. Pharmacological treatment and prevention of cerebral small vessel disease: a review of potential interventions. *Int J Stroke* 2015; 10: 469–478.
9. Rashid PA, Whitehurst A, Lawson N and Bath PM. Plasma nitric oxide (nitrate/nitrite) levels in acute stroke and their relationship with severity and outcome. *J Stroke Cerebrovasc Dis* 2003; 12: 82–87.
10. Ferlito S, Gallina M, Pitari G and Bianchi A. Nitric oxide plasma levels in patients with chronic and acute cerebrovascular disorders. *Panminerva Med* 1998; 40: 51–54.
11. Hassan A, Hunt BJ, O'Sullivan M, et al. Markers of endothelial dysfunction in lacunar infarction and ischaemic leukoaraiosis. *Brain* 2003; 126: 424–432.
12. Woodhouse L, Scutt P, Krishnan K, et al. Effect of hyperacute administration (within 6 hours) of transdermal glyceryl trinitrate, a nitric oxide donor, on outcome after stroke: subgroup analysis of the efficacy of nitric oxide in stroke (ENOS) trial. *Stroke* 2015; 46: 3194–3201.
13. Jackson CA, Hutchison A, Dennis MS, et al. Differing risk factor profiles of ischemic stroke subtypes: evidence for a distinct lacunar arteriopathy? *Stroke* 2010; 41: 624–629.
14. Bedenis R, Stewart M, Cleanthis M, et al. Cilostazol for intermittent claudication. *Cochrane Database Syst Rev* 2014. Issue 10. Art. No.: CD003748. DOI: 10.1002/14651858.CD003748.pub4.
15. Miyamoto N, Pham L-DD, Hayakawa K, et al. Age-related decline in oligodendrogenesis retards white matter repair in mice. *Stroke* 2013; 44: 2573–2578.
16. Omote Y, Deguchi K, Tian F, et al. Clinical and pathological improvement in stroke-prone spontaneous hypertensive rats related to the pleiotropic effect of cilostazol. *Stroke* 2012; 43: 1639–1646.
17. Han SW, Lee SS, Kim SH, et al. Effect of cilostazol in acute lacunar infarction based on pulsatility index of transcranial Doppler (ECLIPse): a multicenter, randomized, double-blind, placebo-controlled trial. *Eur Neurol* 2012; 69: 33–40.
18. Uchiyama S, Demaerschalk BM, Goto S, et al. Stroke prevention by cilostazol in patients with atherothrombosis: meta-analysis of placebo-controlled randomized trials. *J Stroke Cerebrovasc Dis* 2009; 18: 482–490.
19. Kamal AK, Naqvi I, Husain MR and Khealani BA. Cilostazol versus aspirin for secondary prevention of vascular events after stroke of arterial origin. *Cochrane Database Syst Rev* 2011; (1): CD008076.
20. DiNicolantonio JJ, Lavie CJ, Fares H, et al. Meta-analysis of cilostazol versus aspirin for the secondary prevention of stroke. *Am J Cardiol* 2013; 112: 1230–1234.
21. Shi L, Pu J, Xu L, Malaguit J, Zhang J and Chen S. The efficacy and safety of cilostazol for the secondary prevention of ischemic stroke in acute and chronic phases in Asian population- an updated meta-analysis. *BMC Neurol* 2014; 14: 1–10.
22. Klarenbeek P, van Oostenbrugge RJ, Rouhl RP, Knottnerus IL and Staals J. Ambulatory blood pressure in patients with lacunar stroke: association with total MRI burden of cerebral small vessel disease. *Stroke* 2013; 44: 2995–2999.
23. Fox SC, May JA, Shah A, Neubert U and Heptinstall S. Measurement of platelet P-selectin for remote testing of platelet function during treatment with clopidogrel and/or aspirin. *Platelets* 2009; 20: 250–259.
24. Wardlaw JM, Smith EE, Biessels GJ, et al. Neuroimaging standards for research into small vessel disease and its contribution to ageing and neurodegeneration: a united approach. *Lancet Neurol* 2013; 12: 822–838.
25. Valdés Hernández M, Armitage P, Thrippleton MJ, et al. Rationale, design and methodology of the image analysis protocol for studies of patients with cerebral small vessel disease and mild stroke. *Brain Behav* 2015; DOI: 10.1002/brb3.415.

26. Hansson L, Hedner T and Dahlöf B. Prospective randomized open blinded end-point (PROBE) study. A novel design for intervention trials. *Blood Pressure* 1992; 1: 113–119.
27. Nishiyama K, Seyama H, Okano H, et al. Escalation regimen of cilostazol for acute brain infarction. *Internal Med* 2011; 50: 1559–1563.
28. de Vos-Koppelaar NC, Kerkhoff H, de Vogel EM, Zock E and Dieleman HG. The effect of a slower than standard dose escalation scheme for dipyridamole on headaches in secondary prevention therapy of strokes: a randomized, open-label trial (DOSE). *Cerebrovasc Dis* 2014; 37: 285–289.
29. Schmidt R, Scheltens P, Erkinjuntti T, et al. White matter lesion progression: a surrogate endpoint for trials in cerebral small-vessel disease. *Neurology* 2004; 63: 139–144.
30. Sprigg N, Gray LJ, England T, et al. A randomised controlled trial of triple antiplatelet therapy (aspirin, clopidogrel and dipyridamole) in the secondary prevention of stroke: safety, tolerability and feasibility. *PLoS ONE* 2008; 3: e2852.
31. Nakamura T, Tsuruta S and Uchiyama S. Cilostazol combined with aspirin prevents early neurological deterioration in patients with acute ischemic stroke: a pilot study. *J Neurol Sci* 2012; 313: 22–26.
32. Lee YS, Bae HJ, Kang DW, et al. Cilostazol in Acute Ischemic Stroke Treatment (CAIST Trial): a randomized double-blind non-inferiority trial. *Cerebrovasc Dis* 2011; 32: 65–71.
33. Shinohara Y, Katayama Y, Uchiyama S, et al. Cilostazol for prevention of secondary stroke (CSPS 2): an aspirin-controlled, double-blind, randomised non-inferiority trial. *Lancet Neurol* 2010; 9: 959–968.
34. Shimizu H, Tominaga T, Ogawa A, et al. Cilostazol for the prevention of acute progressing stroke: a multicenter, randomized controlled trial. *J Stroke Cerebrovasc Dis* 2013; 22: 449–456.
35. Gotoh F, Tohgi H, Hirai S, et al. Cilostazol stroke prevention study: a placebo-controlled double-blind trial for secondary prevention of cerebral infarction. *J Stroke Cerebrovasc Dis* 2000; 9: 147–157.